

UNIVERSITY OF
BIRMINGHAM

EFFECT OF UNDER SLEEPER PADS ON RAILWAY TRACK SUBGRADE

by

RAFAEL S. KAMALOV

A thesis submitted to the University of Birmingham for the degree of

DOCTOR OF PHILOSOPHY

Department of Civil Engineering

School of Engineering

College of Engineering and Physical Science

The University of Birmingham

June 2020

UNIVERSITY OF
BIRMINGHAM

University of Birmingham Research Archive

e-theses repository

This unpublished thesis/dissertation is copyright of the author and/or third parties. The intellectual property rights of the author or third parties in respect of this work are as defined by The Copyright Designs and Patents Act 1988 or as modified by any successor legislation.

Any use made of information contained in this thesis/dissertation must be in accordance with that legislation and must be properly acknowledged. Further distribution or reproduction in any format is prohibited without the permission of the copyright holder.

ABSTRACT

The subgrade layer is designed to provide a stable foundation and carry the load of an entire railway track structure. The migration of fine particles from the cohesive subgrade layer into the overlying ballast is a common and significant problem in the railway industry. Under repeated loading the ballast voids become filled with subgrade cohesive material that reduces the ballast's permeability, which then further increases the chances of problems such as mud pumping and subgrade deformation. This research work studied the effect of the under-sleeper pads (the USPs) on subgrade deformation, stiffness and erodibility. Four cohesive soils were tested in a small-scale cyclic test. The effects of the moisture content and the strength of the subgrade were investigated. The whole system has been subjected to repeated loading over 200,000 cycles under conditions simulating a railway. To validate the data received from the small-scale test, several tests were run on a large-scale apparatus . Laboratory testing has been carried out employing a set-up resembling a railway cross-section. The received data enabled analysis of the trends in the permanent and cyclic subgrade deformations. The amount of eroded soil, the stiffness and strength of the soil (before and after the test), and the development of pore water pressure were investigated. The results show that applying the USP has an overall beneficial effect on the subgrade layer, reducing the level of permanent deformation and reducing the amount of eroded soil. The large-scale tests showed similar trends in terms of permanent deformation and soil stiffness, which suggested that the small-scale test results correlate well with railway track conditions.

DEDICATION

To our dreams, goals, and willpower

ACKNOWLEGMENTS

I am very grateful to my supervisors, Dr Gurmel Ghataora and Dr Michael Burrow, for their constant supervision, support, encouragement, enthusiasm, and very patient guidance throughout the research. This work would not have been possible without the Global Education Programme and I am sincerely grateful. I would like to express my thanks to the staff of the Civil Engineering laboratory at the University of Birmingham for their help, assistance, basically for making my days in the lab much more exciting. A special thank you goes to our amazing community of the University of Birmingham including staff, students, societies and clubs, and to my Uni friends Raid, Giulio, Andrea, Carlo, Dennis, Sheima, Ryan, Rachel, Simon, Valeria, Tassin, Ermano, Guilia, Carlos, Nadia, Omar, Esdras, Abby, Chris, Will, Kat for making my PhD journey so amazing and wonderful. Many thanks are due to Mrs Janet Hingley for kindly proofreading my thesis. And of course, to my parents and family for their unconditional love and support.

Table of Contents

List of Figures vii

List of Tables ix

ABBREVIATIONS x

Chapter 1 INTRODUCTION 1

1.1 Background and problem definition 1

1.2 Aim and Objectives of the research 3

1.3 Novelty of the research 4

1.4 Thesis layout 5

Chapter 2 LITERATURE REVIEW 8

2.1 Background information 8

2.2 Ballasted track structure 10

2.2.1 Rails 10

2.2.2 Sleepers 11

2.2.3 Ballast 12

2.2.5 Subgrade 13

2.2.6 Transition layer 14

2.2.7 Geosynthetics 15

2.2.8 Under sleeper pads 17

2.3 Types of subgrade failure 20

2.3.1 Massive shear failure 21

2.3.2 Progressive shear failure 21

2.3.3 Excessive plastic deformation 22

2.3.4 Attrition and mud pumping 24

2.4 Track forces 24

2.4.1 Static and dynamic loads 25

2.4.2 Behaviour of subgrade soil under repeated loading 28

2.4.3 Calculating dynamic loads 29

2.4.4 Track stiffness 30

2.4.5 Frequency of load applications 32

2.5 Ballast fouling 33

2.5.1 Types of ballast fouling 33

2.5.2 Effect of ballast fouling on drainage characteristics 35

2.5.3 Methods of measuring the level of ballast fouling 36

2.6 Attrition and mud pumping 39

2.6.1 Mechanism of mud pumping 40

2.6.2 Development of pore water pressure 43

2.6.3 Soil strength in cyclic loading 47

2.6.4 Mud pumping enhanced by localised concentration of cyclic stress/strain 48

2.7 Remediation solutions 49

2.7.1 Sand layer 50

2.7.2 Geotextiles 51

2.8 Previously investigated soils 54

2.9 Summary 57

Chapter 3 METHODOLOGY 58
3.1 Introduction 58
3.2 The laboratory work programme 59
3.3 Tested materials 62
3.3.1 Ballast 62
3.3.2 Under sleeper pad (the USP) 63
3.3.3 Geotextile 63
3.3.4 Subgrade soil 64
3.4 Soil classification tests 65
3.4.1 Atterberg limits 66
3.4.2 Particles' size distribution 68
3.4.3. Specific gravity 69
3.4.4. Compaction test (y_d/OMC) 69
3.4.5 Shear strength of the tested soils 71
3.4.6 Consolidation test 74
3.4.7 Permeability test 76
3.4.8 Organic content test 77
3.4.9 Void ratio 79
3.4.10 Discussion 79
3.5 Determination of soil erodibility 82
3.5.1 Crumb test 85
3.5.2 Hole erosion test 87
3.5.3 Results and Discussion 91
3.6 Small-scale test 93
3.6.1 Determination criteria of remediation solutions 94
3.6.2 Cyclic loading machine 95
3.6.3 Instrumentation 96
3.6.4 Test variables 100
3.6.5 Investigation procedure 101
3.6.6 Data analysis 107
3.7 Large-scale test 110
3.7.1 General information 110
3.7.2. Tested Materials 111
3.8 Contact area between ballast and a sleeper 114
3.9 Summary 116
Chapter 4 RESULTS AND DISCUSSION 117
4.1 Introduction 117
4.2 Permanent deformation, the small-scale test 119
4.2.1 Subgrade permanent deformation, saturated/unsaturated conditions 119
4.2.2 Subgrade permanent deformation, effect of soil type 122
4.2.3 Subgrade permanent deformation, with/without the USP 124
4.2.5 Subgrade permanent deformation. Summary 130
4.3 Stiffness 132
4.3.2 Stiffness, subgrade soil, London clay 138
4.3.3 Stiffness, subgrade soil, china clay 140
4.3.4 Stiffness, subgrade soil, a mix of china clay and 5%bentonite 142
4.3.5 Discussion 144
4.4 Pore water pressure 146
4.4.1 Development of pore water pressure at OMC 80% 147

4.4.2 Development of pore water pressure, OMC 100% 149
4.4.3 Development of pore water pressure, OMC 120% 151
4.4.4 Summary 154
4.5 Analysis of results of the small-scale tests 155
4.5.1 Relationship between liquidity index and subgrade strength 155
4.5.2 Relationship between liquidity index and eroded soil 159
4.5.3 Relationships between stiffness and deformation 166
4.5.4 Discussion 168
Chapter 5 CONCLUSIONS AND RECOMMENDATIONS 170
5.1 Summary 170
5.2 Conclusions 171
5.3 Recommendations for further research works 174
REFERENCE LIST 176
APPENDIX 184

List of Figures

FIGURE 1.1 THESIS STRUCTURE 7
FIGURE 2.1 MUD PUMPING 8
FIGURE 2.2 RAILWAY TRACK STRUCTURE (SELIG AND WATERS, 1994) 10
FIGURE 2.3 A) GEOTEXTILE; B) GEOMEMBRANE; C) GEOGRID; D) GEOCOMPOSITE 17
FIGURE 2.4 A SAMPLE OF USP 18
FIGURE 2.5 LOAD DISTRIBUTION WITH AND WITHOUT THE USP 20
FIGURE 2.6 MASSIVE SHEAR FAILURE (SELIG AND WATERS,1994) 21
FIGURE 2.7 PROGRESSIVE SHEAR FAILURE (SELIG AND WATERS, 1994) 22
FIGURE 2.8 EXCESSIVE SUBGRADE PLASTIC DEFORMATION (LI AND SELIG, 1994) 23
FIGURE 2.9 DYNAMIC AND STATIC WHEEL LOADS (SELIG AND WATERS, 1994) 26
FIGURE 2.10 LOAD DISTRIBUTION (SELIG AND WATERS, 1994) 27
FIGURE 2.11 THE CONTACT PRESSURE UNDER SLEEPER/BALLAST (SHENTON, 1975) 28
FIGURE 2.12 STRESS-STRAIN CURVE BEHAVIOUR (SELIG AND WATERS, 1995) 29
FIGURE 2.13 BALLAST BREAKAGE 34
FIGURE 2.14 SUBGRADE ATTRITION AND FOULING BALLAST (TENNAKOON ET AL., 2014) 35
FIGURE 2.15 BEARING CAPACITY/VCI BALLAST (TENNAKOON ET AL., 2014) 39
FIGURE 2.16 PUMPING MECHANISM (TAKATOSHI, 1976) 40
FIGURE 2.17 FORMATION OF THE SLURRY (GHATAORA ET AL., 2006) 42
FIGURE 2.18 MUD PUMPING MECHANISM (RAYMOND, 1999) 43
FIGURE 2.19 SATURATED AND UNSATURATED SOIL PARTICLES 43
FIGURE 2.20 STRESS/STRAIN CONCENTRATION UNDER SLEEPERS AT RAIL JOINTS 49
FIGURE 2.21 PLASTICITY CHART OF PREVIOUSLY INVESTIGATED SOILS 56
FIGURE 2.22 PLASTICITY CHART OF PREVIOUSLY INVESTIGATED SOILS 56
FIGURE 3.1 BALLAST PARTICLE SIZE DISTRIBUTION, (BS1377: PART 2, 1990) 63
FIGURE 3.2 CASAGRANDE PLASTICITY CHART (AFTER BARNES, 2016) 67
FIGURE 3.3 PARTICLE SIZE DISTRIBUTION 68
FIGURE 3.4 COMPACTION CURVE OF ETRURIA MARL 70
FIGURE 3.5 COMPACTION CURVE OF LONDON CLAY 71
FIGURE 3.6 COMPACTION CURVES OF CHINA CLAY AND 5% BENTONITE MIX 71
FIGURE 3.7 RELATIONSHIP BETWEEN MOISTURE CONTENT/SHEAR STRENGTH, EM 73
FIGURE 3.8 RELATIONSHIP BETWEEN MOISTURE CONTENT/SHEAR STRENGTH, LC 73
FIGURE 3.9 RELATIONSHIP BETWEEN MOISTURE CONTENT/ SHEAR STRENGTH, CC 74
FIGURE 3.10 RELATIONSHIP BETWEEN MOISTURE CONTENT/SHEAR STRENGTH, CCB 74
FIGURE 3.11 CLAY ACTIVITY IN EMBANKMENTS FAILED BY PIPING (RESÉNDIZ, 1977) 84
FIGURE 3.12 SOIL DISPERSION CHART (PERRY AND POSTOL, 1977) 85
FIGURE 3.13 SCHEMATIC DIAGRAM OF HOLE EROSION TEST (WALENNA ET AL., 2019) 89
FIGURE 3.14 HOLE EROSION TEST APPARATUS 90
FIGURE 3.15 SPECIMEN OF ETRURIA MARL DURING HET 91
FIGURE 3.16 CRUMB TEST, SPECIMENS OF TESTED SOILS 92
FIGURE 3.17 LAYOUT OF THE SMALL-SCALE TEST (GHATAORA ET. AL. 2006) 94
FIGURE 3.18 THE SMALL-SCALE TEST APPARATUS 95
FIGURE 3.19 PRESSURE CALIBRATION CURVE AND MERCURY PRESSURE SYSTEM 99
FIGURE 3.20 THE SMALL-SCALE TEST 103
FIGURE 3.21 CALCULATION OF CONE RESISTANCE 105
FIGURE 3.22 THE LARGE-SCALE TEST, PERMANENT DEFORMATION INVESTIGATION 112
FIGURE 3.23 THE LARGE-SCALE TEST, THE UNIVERSITY OF BIRMINGHAM 113
FIGURE 3.24 THE CONTACT AREA BETWEEN BALLAST AND THE USP, THE PRINT 115
FIGURE 4.1 PERMANENT DEFORMATION, SATURATED/UNSATURATED CONDITION, EM 120
FIGURE 4.2 PERMANENT DEFORMATION, SATURATED/UNSATURATED CONDITION, LC 120
FIGURE 4.3 PERMANENT DEFORMATION, SATURATED/UNSATURATED CONDITION, CC 121
FIGURE 4.4 PERMANENT DEFORMATION, SATURATED/UNSATURATED CONDITION, CC 121
FIGURE 4.5 PERMANENT DEFORMATION, EFFECT OF SOIL TYPE, OMC 80% 123

FIGURE 4.6 PERMANENT DEFORMATION, EFFECT OF SOIL TYPE, OMC 100% 123
FIGURE 4.7 PERMANENT DEFORMATION, EFFECT OF SOIL TYPE, OMC 120% 124
FIGURE 4.8 PERMANENT DEFORMATION, WITH/WITHOUT THE USP, EM 126
FIGURE 4.9 PERMANENT DEFORMATION, WITH/WITHOUT THE USP, LC 126
FIGURE 4.10 PERMANENT DEFORMATION, WITH/WITHOUT THE USP, CC 127
FIGURE 4.11 PERMANENT DEFORMATION, WITH/WITHOUT THE USP, CCB 127
FIGURE 4.12 PERMANENT DEFORMATION OF SUBGRADE LAYER, THE LARGE-SCALE TEST. 130
FIGURE 4.13 STIFFNESS OF THE UNDER-SLEEPER PADS (USP) 134
FIGURE 4.14 AN EXAMPLE OF FLUCTUATION OF STIFFNESS (ETRURIA MARL, RAW DATA).. 134
FIGURE 4.15 STIFFNESS OF UNSATURATED SUBGRADE, EM WITH/WITHOUT THE USP 136
FIGURE 4.16 STIFFNESS OF SATURATED SUBGRADE, EM WITH/WITHOUT THE USP 137
FIGURE 4.17 STIFFNESS AT STABILIZATION POINT, ETRURIA MARL 137
FIGURE 4.18 STIFFNESS OF UNSATURATED SUBGRADE, LC WITH/WITHOUT THE USP 139
FIGURE 4.19 STIFFNESS OF SATURATED SUBGRADE, LC WITH/WITHOUT THE USP 139
FIGURE 4.20 STIFFNESS AT STABILIZATION POINT, LONDON CLAY 140
FIGURE 4.21 STIFFNESS OF UNSATURATED SUBGRADE, CC WITH/WITHOUT THE USP 141
FIGURE 4.22 STIFFNESS OF SATURATED SUBGRADE, CC WITH/WITHOUT THE USP 141
FIGURE 4.23 STIFFNESS AT STABILIZATION POINT, CHINA CLAY 142
FIGURE 4.24 STIFFNESS OF UNSATURATED SUBGRADE, CCB WITH/ WITHOUT THE USP 143
FIGURE 4.25 STIFFNESS OF SATURATED SUBGRADE, CCB WITH/WITHOUT THE USP 143
FIGURE 4.26 STIFFNESS AT STABILIZATION POINT, CCB 144
FIGURE 4.27 DEVELOPMENT OF PORE WATER PRESSURE/ EM, OMC 80% 147
FIGURE 4.28 DEVELOPMENT OF PORE WATER PRESSURE/ LC, OMC 80% 148
FIGURE 4.29 DEVELOPMENT OF PORE WATER PRESSURE/ CC, OMC 80% 148
FIGURE 4.30 DEVELOPMENT OF PORE WATER PRESSURE/ CCB, OMC 80% 149
FIGURE 4.31 DEVELOPMENT OF PORE WATER PRESSURE/ EM, OMC 100% 150
FIGURE 4.32 DEVELOPMENT OF PORE WATER PRESSURE/ LC, OMC 100% 150
FIGURE 4.33 DEVELOPMENT OF PORE WATER PRESSURE/ CC, OMC 100% 151
FIGURE 4.34 DEVELOPMENT OF PORE WATER PRESSURE/ CCB, OMC 100% 151
FIGURE 4.35 DEVELOPMENT OF PORE WATER PRESSURE/ EM, OMC 120% 152
FIGURE 4.36 DEVELOPMENT OF PORE WATER PRESSURE/ LC, OMC 120% 153
FIGURE 4.37 DEVELOPMENT OF PORE WATER PRESSURE/ CC, OMC 120% 153
FIGURE 4.38 DEVELOPMENT OF PORE WATER PRESSURE/ CCB, OMC 120% 154
FIGURE 4.39 RELATIONSHIP BETWEEN SHEAR STRENGTH AND LIQUIDITY INDEX 156
FIGURE 4.40 RELATIONSHIP BETWEEN LIQUIDITY INDEX AND SUBGRADE DEFORMATION. 157
FIGURE 4.41 UNDRAINED SHEAR STRENGTH /MOISTURE CONTENT, EM 158
FIGURE 4.42 UNDRAINED SHEAR STRENGTH / MOISTURE CONTENT, LC 158
FIGURE 4.43 UNDRAINED SHEAR STRENGTH / MOISTURE CONTENT, CC 159
FIGURE 4.44 UNDRAINED SHEAR STRENGTH / MOISTURE CONTENT, CCB 159
FIGURE 4.45 RELATIONSHIP BETWEEN LI AND ERODED SOIL AFTER THE TEST 160
FIGURE 4.46 ERODABILITY OF ETRURIA MARL 161
FIGURE 4.47 ERODABILITY OF LONDON CLAY 161
FIGURE 4.48 ERODABILITY OF CHINA CLAY 162
FIGURE 4.49 ERODABILITY OF CCB 162
FIGURE 4.50 RELATIONSHIP BETWEEN LOOSENED SOIL AND SUBGRADE STRENGTH 165
FIGURE 4.51 RELATIONSHIP BETWEEN LOOSENED SOIL AND SUBGRADE SETTLEMENT 165
FIGURE 4.52 RELATIONSHIP BETWEEN ERODED SOIL AND SUBGRADE STIFFNESS 166
FIGURE 4.53 RELATIONSHIP BETWEEN SOIL STIFFNESS AND SUBGRADE DEFORMATION..... 167
FIGURE 4.54 RELATIONSHIP BETWEEN SOIL STRENGTH AND SUBGRADE STIFFNESS 167

List of Tables

TABLE 1. CHARACTERISTICS OF TYPICAL CARS AND LOCOMOTIVES (LI AND SELIG, 1998)..... 30
TABLE 2. SOURCES OF BALLAST FOULING (SELIG AND WATERS, 1994)..... 33
TABLE 3. BALLAST FOULING CATEGORIES (SELIG AND WATERS, 1994)..... 36
TABLE 4. LABORATORY-BASED STUDIES ON MIGRATION OF FINES..... 55
TABLE 5. THE LABORATORY WORK PROGRAMME..... 61
TABLE 6. BALLAST PARTICLE SIZE DISTRIBUTION LIMITS..... 62
TABLE 7. SUMMARY OF ATTERBERG LIMITS OF INVESTIGATED SOILS..... 67
TABLE 8. SPECIFIC GRAVITY (GS)..... 69
TABLE 9. UNDRAINED SHEAR STRENGTH OF CLAYS (BS EN ISO14688-2:2004)..... 72
TABLE 10. GENERAL VALUES OF MV (BARNES, 2001)..... 76
TABLE 11. COEFFICIENT OF PERMEABILITY VALUES..... 77
TABLE 12. RESULTS OF CONSOLIDATION TEST..... 77
TABLE 13. CLASSIFICATION OF SOILS WITH ORGANIC CONTENT..... 78
TABLE 14. ORGANIC CONTENT..... 78
TABLE 15. COMBINED DATA OF SPECIFIC GRAVITY AND VOID RATIO..... 79
TABLE 16. CRUMB TEST DISPERSION RESULTS, BS 1377-5:1990..... 92
TABLE 17. RESULTS OF HOLE EROSION TEST..... 93
TABLE 18 THE RAW DATA OF A CYCLIC LOAD TEST..... 108
TABLE 19 COMPILATION OF DATA..... 109
TABLE 20. MEASURED CONTACT AREA BETWEEN BALLAST AND SLEEPER (WITH/WITHOUT USP)..... 115
TABLE 21. STIFFNESS AT THE END OF THE TESTS..... 135
TABLE 22. MOISTURE CONTENT/ LIQUIDITY INDEX..... 156
TABLE 23. AMOUNT OF ERODED SOIL..... 163

ABBREVIATIONS

A	area
bs	ballast-subgrade
bsusp	ballast-subgrade-the USP
bsw	ballast-subgrade-water
bswusp	ballast-subgrade-water-the USP
c_u	undrained shear strength of the soil
c_v	coefficient of consolidation
d	Wheel diameter
E	Young's modulus
e	void ratio
e_0	initial void ratio
Δe	change in void ratio
f	frequency
G_s	specific gravity
h	depth of ballast
k	track stiffness
K	soil permeability
L	train length
LL	liquid limit
LI	liquidity index
LST	large-scale test
m_v	coefficient of compressibility

M_r	resilient modulus
N	number of repeated load applications
OMC	optimum moisture content
PI	plasticity index
PWP	pore water pressure
P	vertical force
Pd	design dynamic wheel load
Pdi	dynamic wheel load
Psi	static wheel load
q	deviator stress
SST	small-scale test
T_v	time factor of 90% consolidation
Ti	total traffic tonnage
Δu	change in pore water pressure
USP	under sleeper pad
w	moisture content
σ_c	Stress in the surrounding soil
σ_v	vertical stress
γ	unit weight of soil
γ_d	unit weight, dry
φ	angle of internal friction
V	train speed
ε_p	cumulative soil plastic strain (%)
ρ	cumulative soil plastic deformation

Chapter 1 INTRODUCTION

1.1 Background and problem definition

Railways play an important role in transport systems, providing the facility for people to travel and for industries to transport goods and commodities. According to Network Rail (2019) around 1.7 billion people travel annually in the UK and more than twenty billion net tonne kilometres were moved by railways in the year of 2018/2019. To provide satisfactory ride quality the railway track must be within a certain standard and level of alignment. The high performance of a railway track under repeated traffic loads depends on the quality of the railway's subgrade layer.

The main function of the railway subgrade layer is to provide a stable foundation and carry the load of the entire structure. Selig and Waters (1994) stated that the subgrade layer significantly influences the track performance, as it withstands traffic stresses that can extend up to five metres below the track. Thus, subgrade soils need to be strong enough to resist shear failure and excessive deformation. Subgrade soils are subjected to cyclic loading, resulting in local ballast/soil attrition. In the presence of water local erosion can take place at these locations of excessive pressure. Eroded soils form slurry and migrate upwards into the overlying ballast as the latter gradually presses into the subgrade. Rainfall or ground water may lead to an increase in slurry formation leading to the formation of "wet spots". The formation of slurry and its upward migration into the ballast is sometimes referred to as mud pumping. Such erosion can lead to localised excessive deformation; i.e. loss of line and level, which if left untreated may lead to derailment. The wet spots continue to increase in size until equilibrium conditions are reached. Coarse clays and silts are particularly susceptible to such erosion (Ghataora, 2006).

The earliest research studies which address the mud pumping problem date back to the middle of the 20th century (Yodel, 1957; Bell, 1978; Ayers, 1980; Hoare, 1982; Raymond, 1986). With the increase in the number of trains, their speed, and high axial loads, it has become a more common and significant issue for railways (Nguyen et al., 2019). Numerous issues related to the problem have been reported globally. In Australia, where the railways are important for moving freight and where the track infrastructure is the sixth largest in the world, along one single coastal line in New South Wales there were more than 300 mud pumping locations in 2019. The scale of the mud pumping problem can be very large; for example, along the Shanghai-Nanjing line (China) more than 300 km of the line was affected by mud pumping (Nguyen et al., 2019). In 2008, more than 800 wet spots were found on the Shuo-Huang line, China (Yu et al., 2016). Similar cases were reported in North America (Raymond, 1999; Sussman et al., 2012; Hendry et al., 2013). British railways comprise mostly of ballasted track built in the last century, typically before the 1960s, with a significant amount built before 1920. At that time the design of railway tracks was basic, when the ballast normally was placed over the subgrade soil, which makes them vulnerable to the mud pumping phenomenon (Duong et al., 2014). Because of its geology and climate, the problem of mud pumping is common in the UK and is frequently reported. For instance, around 25000 wet spots were identified at 238 sites on 25% of the area maintained by Carillion Rail in the UK in the year 2001, and that fact shows the scale of the subject. If this is regarded as typical of the network, then the scale of the problem is enormous (Ghataora et al., 2006; Hudson et al., 2016).

Relatively few studies have been carried out to analyse and solve the mud-pumping problem (Selig et al., 1994; Ghataora, 2006; Trinh et al., 2012; Duong, 2014; Chawla, 2016; Indraratna et al., 2019). Some researchers investigated the mud pumping problem in a pavement context (Hoare, 1982; Alobaidi 1994, 1996, 1998, 1999; Zhang, 2004). Different approaches were taken to study the issue. Some research works investigated the mechanism of mud pumping

(Ghataora, 2006; Duong, 2014;); while other researchers concentrated their effort on finding a solution to stop migration of fines and prevent mud pumping (Hoare, 1982; Alobaidi, 1994; Ghataora, 2006; Chawla, 2014). Several research works studied the formation of the interlayer, which is a mix of ballast and the subgrade material and occurs on the contact area between the subgrade. The interlayer usually occurs in railways where the ballast layer was placed directly on the cohesive subgrade without a transition sub-ballast layer; this was normal practice in the last century (Trinh et al., 2012; Cui et al., 2014; Duong et al., 2013, 2014). Although the magnitude of the problem is significant there is a lack of problem understanding and the available information is not sufficient.

1.2 Aim and Objectives of the research

The primary aim of this study was to develop a framework that describes the performance of railway track subgrade, its modes of failure and some appropriate methods for a remediation solution, in particular the effect of the USPs on cohesive subgrade soils.

To achieve the highlighted aim the following objectives of the research were defined:

- To undertake a comprehensive literature review on the behaviour of clayey soils subjected to cyclic loading, particularly in the context of railway track foundation subgrade. The literature review would also focus on modes of failure of railway subgrade including subgrade erosion (mud pumping) and methods of remediation.
- To investigate the erodibility of the selected cohesive soils and correlate their geotechnical characteristics and their erodibility.
- To investigate the effect of using the USPs on the response of subgrade soil when subjected to dynamic loading, through experimental work.

- To compare the small-scale test that was used for the bulk of the study with the large-scale test, and to validate the tests' results.
- To provide recommendations based on the findings of the conducted analysis.

1.3 Novelty of the research

The deterioration of railway track geometry and the condition of the subgrade layer are interconnected. The subgrade condition often depends on the stiffness of the soil. Several research studies have noted that a combination of factors such as repeated loading, a cohesive subgrade layer and freestanding water develop pore water pressure, which eventually leads to mud pumping (Raymond, 1986; Alobaidi and Hoare 1994; and Selig and Davis, 1994).

Geosynthetic materials such as geotextiles and the under-sleeper pads (the USPs) are often used in the railway industry to reduce the attrition of concrete sleepers and the ballast under cyclic loading from the train. The USPs are designed from resilient materials to increase the sleeper/ballast contact areas and mitigate vibrations from trains (Potocan and Dorfner, 2013). As a result, the highly concentrated stresses at the sleeper–ballast interface (from a hard concrete sleeper) is distributed over a wider area, which reduces the magnitude of the vertical stress, allowing for a more uniform distribution of stress, which in turn decreases overall deformation. The increased contact area of the ballast from the USPs at the sleeper–ballast interface reduces the induced stresses at the interface and at the particle–particle contact.

Although field investigations have showed that the use of the USPs could reduce the track misalignment, the available information is still limited (Baghsorkhi et al., 2017). Preliminary unpublished research at the University of Birmingham has indicated that the USPs may help to reduce the impact of dynamic loading on the subgrade and hence reduce the occurrence of mud pumping. There is no published research on the subject. More detailed analysis of the USPs'

influence on the dynamic response of the railway track structure is required. Thus, this study focussed on identifying the effect of using USPs on subgrade soil, particularly on the erosion of soils leading to mud pumping, subgrade stiffness and deformation. This research is laboratory-based experimental work which followed the research approaches that have been used previously at the University of Birmingham, where the problem of mud pumping in pavement and railway tracks was investigated (Hoare, 1982; Alobaidi, 1994; Ghataora, 2006). A major part of the research was done using a small-scale apparatus, designed to provide parameters essential to understand: the erosion and mud-pumping mechanisms; the distribution of the stress in railway track; the subgrade permanent deformation; as well as to study the development of pore water pressure, and the effect of the tested materials on the subgrade's performance. The main advantage of this test was the ability to change the tested materials and parameters relatively quickly.

1.4 Thesis layout

The thesis contains five chapters, the thesis structure is presented in Figure 1.1.

Chapter 1 the "Introduction" provides background information about the problem, the aim, and objectives of the research, as well as the novelty and thesis outline.

Chapter 2 summarises literature reviews of previously published works related to the studied problem. There is a limited number of works directly related to the subject of mud pumping and all of them are included and discussed. Other works that are important to support the topic are also included and discussed, including descriptions of railway tracks, load distributions, general erosion, and dispersion of cohesive soils.

Chapter 3 proposes the methodology and programme of the study. It outlines the research approach; providing a description of the materials used in the research. It includes a detailed

explanation of the conducted experimental tests; details of the engineering properties of the tested soils and materials used in the experiments; the efforts in the sample preparations; evaluations of the reliability and consistency of techniques employed; and errors inherent as well, as part of the thorough description of the test equipment and experimental set-up that was used to accomplish the research.

Chapter 4 presents the test results with discussion with regards to: the subgrade stiffness, permanent deformation, development of pore-water pressure and the effect of the USP on the subgrade performance.

Chapter 5 summarises the conclusions and recommendations of the uncovered aspects of the problem. Future works that could advance the understanding of the effect of the USPs on the railway track are suggested.

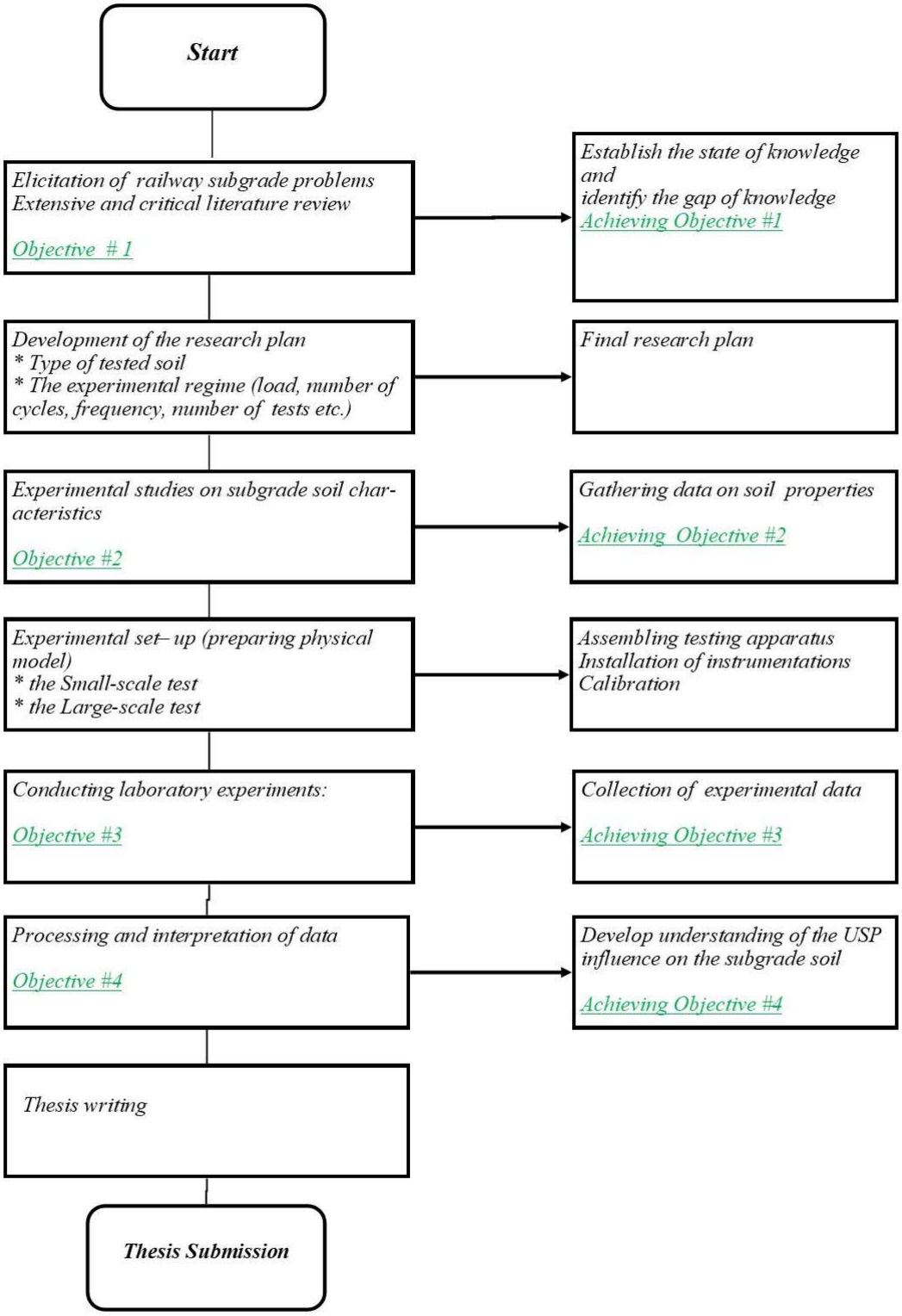


Figure 1.1 Thesis structure

Chapter 2 LITERATURE REVIEW

2.1 Background information

The UK superficial deposits refer to geological deposits typically of the Quaternary age, are mostly represented by cohesive soils, and large areas of clay and silt are common (Etruria marl, English china clay, Oxford, and London clays etc.). Construction of railway tracks on these soils potentially brings problems, such as differential settlement and mud pumping (Li and Selig, 1995; Brough et.al., 2003; Sanchez, 2014). The dynamic stress from passing trains liquefies the saturated cohesive subgrade soils and creates slurry (Figure 2.1). Migrated fine particles fill and block the upper layers of the sub-ballast and ballast. The slurry fills open voids and blocks the drainage system that deteriorates the operational condition of the railway track (Hudson et al., 2016).



Figure 2.1 Mud pumping (from https://railgallery.wongm.com/page/search/Mud/)

The placement of a sand layer between the ballast and subgrade layers has been proved as an efficient solution to stop subgrade fine particles' migration. It blocks clay fines whilst allowing for the dissipation of ground water away from the subgrade, which accordingly keeps the subgrade layer free of standing water, preventing the creation of slurry. However, there are

disadvantages of this method: the installation cost is high; it is also both technically challenging and time consuming to apply a layer of sand over a large area. As an alternative solution, geotextiles have become more popular. This solution offers a cheaper and faster alternative to the sand blanket and has become increasingly common over the last few decades (Ayers, 1984; Raymond 1986, Alobaidi, 1994; Ghataora, 2006; Chawla 2016; Nguyen et al., 2019). Although the geotextiles as a solution have been used since 1960s, they have only been used successfully to prevent migration of fines in the last 15-20 years and it is requiring further investigations. Another material, the USPs, have shown efficiency during the last 30 years in other applications. They give protection of the ballast surface from inter-particle abrasion and sleeper–ballast attrition (Witt et al., 2008; Schneider et al., 2011); improve lateral track stability (Lakusic et al., 2010); and reduce the variation of the stiffness of transition zones (Müller-Boruttau et al., 2001). However, the USPs as a relatively new material that were introduced to the industry just over 30 year ago are still relatively unknown. There is still limited available information about the influence of the USPs on the subgrade layer.

Although the level of the problem is significant, not many research works have been published describing the mud pumping phenomenon (Nguyen et al., 2019). The majority of the works have more practical applications for the railway industry demands, with little scientific analysis (Saxena, 1986; Raymond, 1999; Aw, 2007; Hudson, 2016). Information gleaned from the various literature was used to better define the problem, design the test programme, and analyse the findings. A literature review relating to the migration of fines from the subgrade to the ballast and use of the USPs is described in this chapter. The chapter is divided into sections as follows: ballasted track structure, types of subgrade failure, ballast fouling, attrition and mud pumping, remediation solutions, previously investigated soils, summary.

2.2 Ballasted track structure

The railway track must provide a safe and lasting support that can withstand traffic loads and any other environmental influences whilst retaining adequate vertical and horizontal alignment (Figure 2.2). The performance of the entire railway track system under the train's dynamic loading is a complex interaction of all the components. The performance of each of the components is critical to achieve a satisfactory support system. To achieve the optimum performance of the railway tracks, continuous and ongoing track maintenance works are required, which demand constant financial investments. The function and appearance of the different parts of the track structure as well the design loads will be described in the following section.

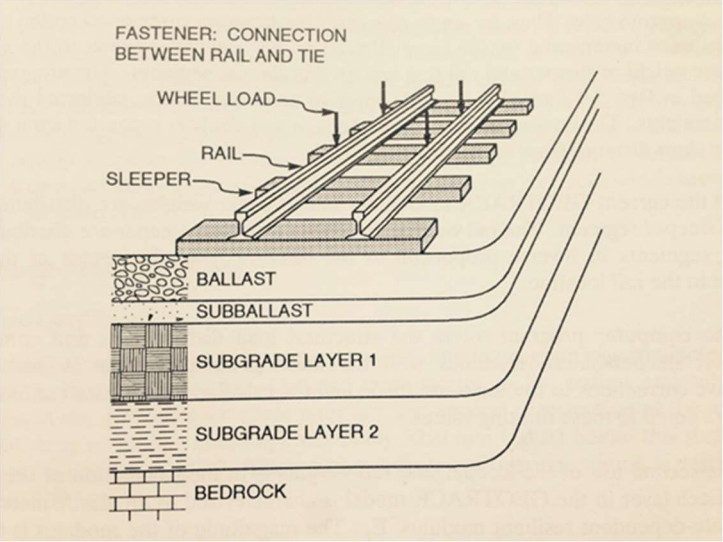


Figure 2.2 Railway track structure (Selig and Waters, 1994)

2.2.1 Rails

Rails are the longitudinal steel members that carry the load from the train wheels and transfer it down to the supports, the sleepers. Thus, the rails have to be of sufficient dimensions and

stiffness to withstand the traffic load without showing excessive deflection between the abutments (Selig and Waters, 1994). The separation between the inside faces of the rail head is 1435-1668 mm (RT/CE/S/006, 1998). Hay (1982) stated some essential characteristics of rails: such as while carrying the transferring load, rails should minimise the deflection, deliver a flat running surface for the wheels, allowing them to move smoothly; and resist fatigue cracking caused by cyclic loading. The condition and profile of the rails combined with the movement of the wheels can detrimentally influence the railway structure. Discontinuities along the track, caused by joints for example, can also result in increased stress on the ballast and subgrade (Mattsson, 2003).

2.2.2 Sleepers

Sleepers fix the spacing between the rails and the distribution of the dynamic load from the train to the underlying ballast (Selig and Waters, 1994). They hold the fastening system to maintain the proper track gauge. Anchoring the superstructure in the ballast, sleepers restrain rail movement in any direction (lateral, vertical, longitudinal). Sleepers are made of either timber, steel or concrete, with the latter becoming increasingly common as old railways are replaced. Concrete sleepers provide better support to the rails since they facilitate a more secure fastening system and are heavier than their wooden counterparts. On the other hand, sleepers made of wood are easier to handle and provide better resiliency. The sizes of sleepers are specified in the Railtrack Line Specification RT/CE/S/029 (2000), where the dimensions for a wooden sleeper are 250 × 150 × 2500 mm, width, thickness, and length respectively. The dimensions of concrete sleepers vary, but a commonly used sleeper in the UK is of the size 264 × 211 × 2515 mm. The weight of an average concrete sleeper is approximately 290 kg, compared to approximately 70 kg for a wooden sleeper.

2.2.3 Ballast

Ballast is the top layer of the railway structure located under the sleepers. It is angular, crushed, and uniformly graded (10-63 mm) granular materials, represented by igneous or metamorphic rocks, usually granite, basalt or limestone (RT/CE/S/006, 1998). The primary purpose of ballast is to carry the rail-sleeper assembly. It acts as a structural element, supporting and distributing loads to reduce the bearing pressure on the subgrade. Ballast distributes the load from the sleepers by transferring forces laterally, vertically, and longitudinally, and by doing so enables the track to stay within acceptable limits of displacement. It also serves as an anchor for the ties, which resist the vertical, lateral, and longitudinal forces applied. It facilitates storage of particles deriving from degraded ballast and enables fast dispersal of water, as well as facilitating the drainage of water away from the track (Selig and Waters, 1994). Ballast should be hard enough to withstand temperature changes and chemical attacks, with low absorption and free of cementing properties, it also ought to have high shear strength (Indraratna et al., 1998). The thickness of the ballast layer is normally in the range of 250-300 mm (RT/CE/S/006,1998). Over the years of operation and traffic loading, the ballast will be exposed to chemical and mechanical degradation, and the migration of particles from the underlying soil (Mattsson, 2003; Ghataora 2006). Therefore, the performance of the ballast cannot be expected to remain the same throughout the lifetime of a railway; although the type of material used, as well as sufficient maintenance, can delay the deterioration of the track. Ballast continues to be widely used because its installation and construction costs are generally low, and it lends itself easily to maintenance when required. While a ballasted track is the most common solution in the world, in some countries such as Germany and Japan and China ballast and ties are being replaced by slab tracks, which usually consist of a continuous concrete footing supporting the rails (Muramoto and Nakamura, 2011).

2.2.4 Sub-ballast

The sub-ballast is a layer of a processed sand-gravel mixture, that is placed between the ballast and the subgrade layers. According to the Rail Track Specification (RT/CE/S/033, 1998), the required particle size distribution is between 0.075-14 mm. The sub-ballast serves to aid the ballast in reducing pressures from the sleeper to the subgrade. Perhaps more importantly, it acts as a filter and minimizes the infiltration of the subgrade into the ballast and reduces upward migration of fine particles, which prevents degradation of the ballast by fouling. A track without sub-ballast typically requires more maintenance because of increased fouling (Duong, 2014). The sub-ballast layer also helps to insulate the subgrade from frost and provides water drainage. The thickness of the sub-ballast is in general around 150 mm; however, in the case of a soft subgrade layer, the thickness could be up to 300 mm (Raymond, 1986; Selig and Waters,1994).

2.2.5 Subgrade

The subgrade layer plays the role of the base layer and a platform for the railway structure. It is a main component of the superstructure's support resiliency and designed to provide a stable foundation and carry the load of the entire structure. Selig and Waters (1994) stated that the subgrade layer significantly influences the track performance, as it withstands traffic stresses that can extend up to five metres below the track. The physical characteristics of the subgrade soil play an important role. The elastic deflection of the rail under wheel loading depends on the subgrade soil's strength and stiffness. For instance, if the soil is soft and the moisture content is high, then there are possibilities of significant track settlement or mud pumping (Ayres, 1986; Brough and Ghataora, 2001; Sharpe et al., 2014), and as a result restriction of the applied load and train speed might be implemented. On the other hand, a stiff subgrade

layer provides higher bearing capacity, reduces track settlement and in general is more stable (Selig and Waters, 1994). According to Sadeghi (2007), who conducted a comparison test of degradation track models, the difference between the bearing capacity of good and poor-quality subgrades might be up to four times. There are two types of subgrade formations: natural soil formation and placed soil (fill). Placed soil is used either to raise the ground to the required level or to replace unsuitable existing soil. For economical and practical reasons, the most common approach is to use the *in situ* soil or other local soil as fill-subgrade (Selig and Waters, 1994). The existing ground should be used with as little disturbance as possible. The materials should be chosen based on those characteristics (Rushton and Ghataora, 2011). Negative aspects such as subgrade attrition, progressive settlement, progressive shear failure, and significant volume change must be avoided in order to maintain a stable platform (Selig and Waters,1994).

2.2.6 Transition layer

A layer of sand or geosynthetic material, which is placed between the subgrade and sub-ballast layers, is called a transitional layer. There are several functions of a transition layer: separation, filtration, reinforcement, and drainage. The functions are similar to the tasks that the sub-ballast layer fulfils (Selig and Waters,1994). The sand blanket layer acts as a self-filter, it blocks coarse aggregates and prevents penetration from the sub-base layer into the subgrade layer (Ayers, 1986). Although a sand layer is commonly used for filtering and reducing pressure on the subgrade, the method has disadvantages such as the installation process is time and recourses consuming, which increases the cost of the works (Ayres 1986; Ghataora et al., 2006; Sharpe et al., 2014). Installation of the sand blanket layer is technologically difficult. Therefore,

sometimes it is substituted by geosynthetics, which have economical and practical advantages and the use of geosynthetics is becoming more popular in the railway industry.

2.2.7 Geosynthetics

The use of geosynthetics is rapidly growing as the economical and practical advantages are being discovered and new products are being developed. The main functions for geosynthetics are separation, filtration, transmission, reinforcement, and protection. A separator is a material which when placed between two different soils prevents their intermixing under the action of repeated loading. The prime application is for roads and railways, where they are normally installed at the sub-base-subgrade interface. A filter is a material with adequately sized pores to allow water to pass through while soil particles remain. As a plastic material geosynthetics have many advantages, for example they will not corrode like metals. However, they can be subject to chemical attacks and will degrade in ultraviolet light. This is a problem during storage and installation when the materials are exposed to sunlight. There are different types of geosynthetics and each address specific purposes, they are explained below and presented in Figure 2.3

Geotextiles

Geotextiles are permeable materials that work as a separator between two subgrade and ballast layers. They prevent the penetration of the ballast or sub-ballast into the subgrade layer and can withstand local burst stresses; whereas the granular layer could be intermixed with the underlying subgrade cohesive soils (Duong, 2014; Sharpe et al., 2014; Chawla, 2016). The most important property when defining the separation capability of a geotextile is the apparent opening size (AOS). It indicates the largest particle that would pass through a geotextile. For a

fabric to perform well as a separator the AOS must be less than the largest soil particles, causing them to be blocked by the fabric. With the large particles blocked, the smaller particles will gradually be held within the soil, creating a filter zone adjacent to the fabric. In the case of a hard subgrade, where preventing attrition by the ballast is required, a geotextile would only provide temporary protection (Mattsson, 2003; Ghataora, 2006). Another sub-ballast function is to drain water from below, compensating for any excess pore water pressure in the subgrade caused by the repeated load. This is a permeability function, which the geotextile can initially perform well. However, if the subgrade is clay, or a material comprising clay as an abrasion product, then the pores can get clogged up by the fines and the permeability decreases or even ceases to exist (Section 2.7).

Geomembranes

Geomembranes are plastic sheets without holes, which prevent any fluids from passing through the material. The main functions are protection, separation, and reinforcement. They may have an uneven surface to create shearing resistance with the soil or to provide space for dispersal of water into the main draining system.

Geogrids

Geogrids are plastic sheets with holes forming a grid where the grid is often stretched in one direction. The main function is reinforcement. This aligns the long-chained polymer molecules and gives the grid a higher stiffness and strength. Tensile reinforcement is produced as the grid interlocks with the soil.

Geocomposites

To overcome the lack of ability to fulfil all the sub-ballast functions with a geofabric, geocomposite has been developed. A geocomposite is a combined product of two or more types of geosynthetics where each fulfils its own function. For example, a geocomposite made of a geofabric and a geogrid will provide both the separating function of the geofabric and the tensile reinforcement of the geogrid.

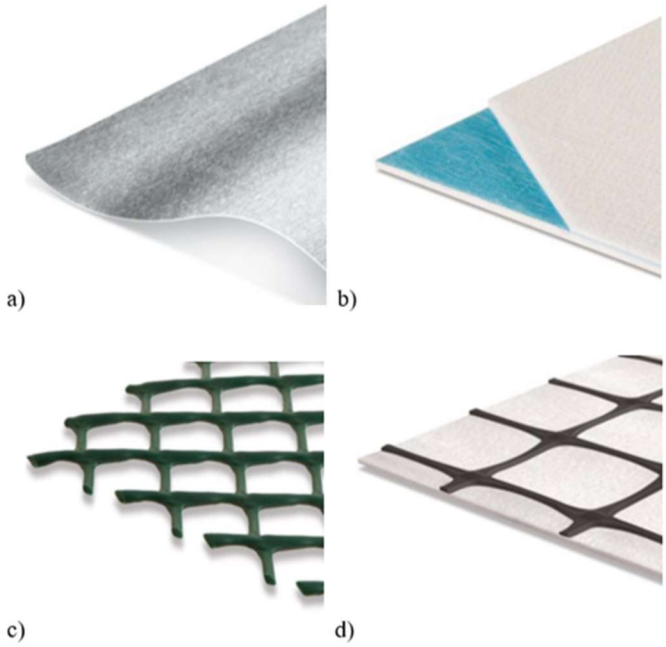


Figure 2.3 a) geotextile; b) geomembrane; c) geogrid; d) geocomposite (from: https://terram.com/products/)

2.2.8 Under sleeper pads

Under sleeper pads (the USPs) provide vibration protection, preserve the ballast under the tracks and improve track stability; to reduce life-cycle costs of track infrastructure by increasing longevity of track components, reducing rail corrugation and ballast thickness and minimising tamping frequency. The USPs reduce stresses on all track components and substructure due to a better load distribution over the track and its components both

longitudinally and transversely as a result the quality of railway track improves. They isolate vibrations and indirectly decrease noise. Applying the USPs under railway tracks allows the reduction of the thickness of the ballast layer and a reduction in the cost (International Union of Railways-UIC. Project USP, Summarising report; 2009).



Figure 2.4 A sample of USP (from: https://www.getzner.com/en/products/rail-products/sleeper-pads)

An under-sleeper pad is a 7-20-mm thick railway track component, placed below the sleeper, made of elastic and resilient materials, and possesses a foam structure (Figure 2.4). Materials with resilient properties that are often used are polyethylene, polyurethane rubber, and ethylene vinyl acetate (EVA) (Schneider et al., 2010). They are made of encapsulated air voids and normally consist of an elastic spring layer and a bonding layer. Their role is to improve interaction between these two railway track elements, the ballast, and the sleeper. The main parameter that characterises an under-sleeper pad is stiffness. Thompson et al. (1999), after studying dynamic stiffness of different materials, stated that the stiffness of the USPs could be divided into three groups of low, medium, and high stiffness at 35, 70 and 105 MN/m

respectively. Because of the deformation of the USPs at the contact point with the ballast, the resilient properties of the USP materials reduce the vertical stiffness of the track. The contact area between the sleepers and the ballast increases significantly; it depends on the stiffness of the under-sleeper pad's material and could be up to 36% (Sol-Sanchez et al., 2014). As a result, stress concentrations under the sleepers reduce with improvements of the stress distribution to the ballast layer (Dahlberg, 2010); which then reduces deterioration of the ballast layer and sleepers (Figure 2.5). This contributes to decrease the degradation rate of the track geometry (Bolmsvik, 2011). Previously conducted research works found that applying the USPs has advantages, such as protection of the ballast surface from inter-particle abrasion and sleeper–ballast attrition (Witt et al., 2008; Schneider et al., 2011). Installing the USPs improves lateral track stability due to the penetration of ballast into the elastic material (Lakusic et al., 2010). According to research works done by Müller-Boruttau et al. (2001) and Piaxao et al. (2014), the under-sleeper pads reduce variation of stiffness of transition zones (transitions between bridges and embankment, or locations between different track structures). Muller-Boruttau (2001) reported that misalignment of the track reduces when the USPs are installed. After conducting a UIC research project the effect of using the USPs was reported as positive and as having a beneficial influence. It also stated there was a shortage of available information, or was otherwise limited, and further detailed research works were required. It is not clear how these installed under sleeper pads influence the railway track's performance in the long term. It has not been investigated thoroughly and needs further investigations. There is also limited information on how different sleeper materials behave; for instance, the long-term settlement of wooden sleepers (Bolmsvik, 2011). The majority of the research works have investigated the dynamic behaviour of railway tracks with installed the USPs and have used numerical simulations and analysis (Lundqvist et al., 2006; Witt, 2008; Insa et al., 2013). Although the benefits of applying the USPs have been reported during the last 20 years, there is still a

shortage of guidance and standards; therefore, some railway networks do not implement under sleeper pads in the infrastructure. There is limited information about the effect of installed the USPs on the track settlement in the long term. There is no available information on the effect of the USPs on the development of pore-water pressure (PWP), which is a main factor in the creation of the mud pumping phenomenon (Alobaidi, 1994; Selig and Waters, 1994; Ghataora, 2006). Previously, no research work has been done in this regard. The present study proposes to investigate the effect of applying the USPs on track subgrade performance, as a potential remediation solution to minimize the mud pumping phenomenon.

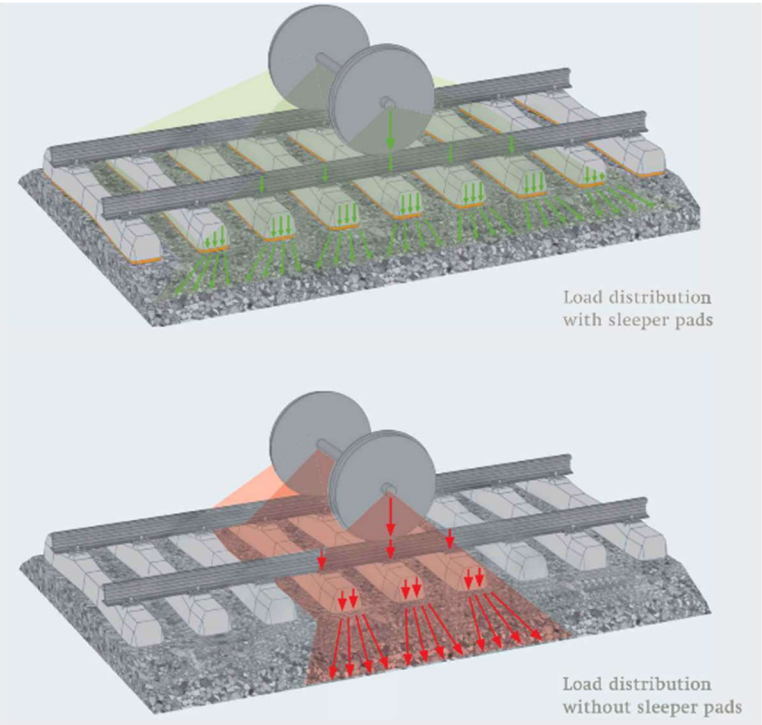


Figure 2.5 Load distribution with and without the USP (from https://www.getzner.com/en/products/rail-products/sleeper-pads)

2.3 Types of subgrade failure

The role of the subgrade layer is to distribute the load and provide reliable support to the entire railway structure. The filled and blocked ballast layer does not provide the required drainage,

which leads to subgrade problems. Failures such as massive and progressive shear failures, excessive settlement, subgrade attrition and mud pumping, swelling and shrinkage could occur. A description of some common subgrade failures is presented in this section.

2.3.1 Massive shear failure

This failure happens with an increase of water content and a reduction of the subgrade shear strength. Usually, massive subgrade failure occurs after flooding or heavy rainfall. It also could happen due to seepage of water through the slope and the reduction of the shear strength (Figure 2.6). The driving forces of massive shear failure are the weights of the trains and the track structure (Selig and Waters, 1994). This type of subgrade failure happens rarely in contrast with progressive failure, which requires a lower level of stresses. However, it is one of the most serious types of railway track failure.

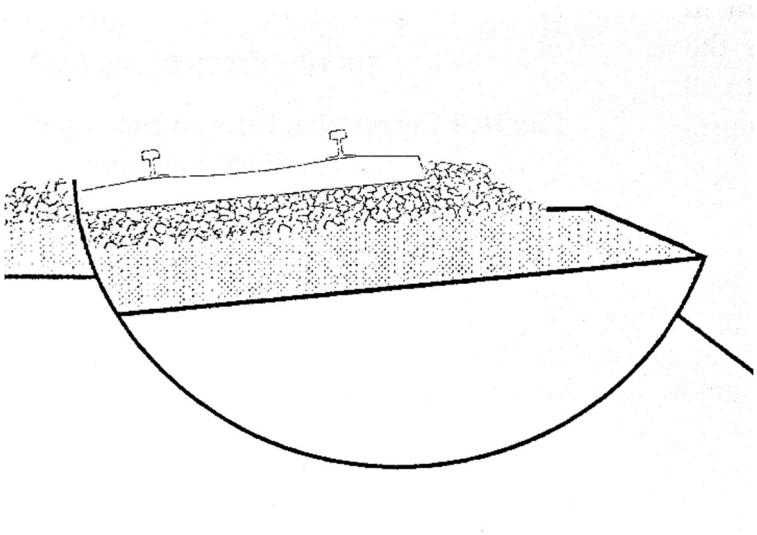


Figure 2.6 Massive shear failure (Selig and Waters,1994)

2.3.2 Progressive shear failure

Repeated load also could be a cause of progressive shear failure. According to Selig and Waters (1994), this failure happens most likely in the top of the subgrade where the traffic-induced

stresses are highest. Repeated loading pushes overstressed subgrade soil upwards and squeezes it to the sideway of the track, and that eventually causes the failure of the bearing capacity known as “cess heave” (Figure 2.7). The main consequence is the reduction of soil strength. In contrast to massive shear failure, this type of failure requires less applied stress. Progressive failure only occurs in fine grained materials exhibiting low values of internal friction.

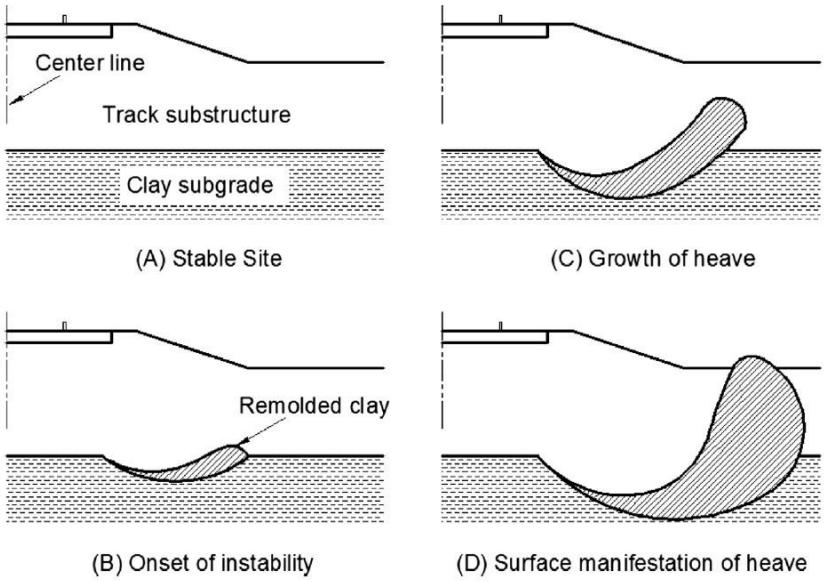


Figure 2.7 Progressive shear failure (Selig and Waters, 1994)

2.3.3 Excessive plastic deformation

Train operation could be seriously affected by excessive plastic settlement, which is another common failure that could happen under dynamic loading where a railway track is ballasted (Figure 2.8). The design of a railway track accepts a tolerable limit of settlement, and if the level of excessive plastic deformation is exceeded then the condition is considered as a failure. In theory, one single load does produce negligible plastic settlement; however, in the long term, cumulative plastic settlement becomes significant and could affect the railway track’s performance. This plastic settlement in general is not uniformly distributed along the track; consequently, often it could be a reason for the track’s geometry change. One of the solutions

to level and balance the track geometry is to add more ballast where it is required; however, that increases the thickness of the ballast and it cannot be added continuously to solve the issue. A cavity that occurs at the subgrade surface could provide a reservoir for water and would be a source of subgrade softening. The subgrade particles collected in the pocket eventually will change the geotechnical characteristics of the ballast and will cause deviations from ballast design standards.

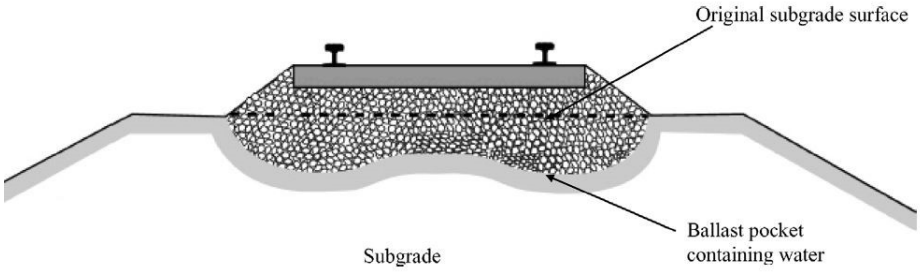


Figure 2.8 Excessive subgrade plastic deformation (Li and Selig, 1994)

The problem usually happens when there is a frost-susceptible fine grained and porous soil, pore water and sub-zero temperatures. Certain types of soils such as low plasticity clays, silts and silty-sands are more susceptible to facilitate water flow by capillary action. As a consequence, with the drop of temperature the collected water becomes ice. The volume increases when sub-zero temperatures freeze subgrade pore water and water into ice. With an increase of the temperature, the ice melts with a reduction of the initial volume. The change of the soil volume causes severe differential settlement that rapidly damages the rail track. The problem could be solved if the drainage system works properly, and water does not stand on the subgrade interface.

2.3.4 Attrition and mud pumping

Slurry formation and mud pumping is a combination of different adverse factors such as subgrade saturation, cohesive soils, and cyclic loading. The main factors that would lead to mud pumping are cyclic loading, free standing water, and cohesive subgrade soil (Alobaidi, 1996, Indraratna, 1997; Aw, 2007; Duong, 2014; Chawla, 2016). The mechanics of pumping could be described as the development of pore water pressure under the contact points of the ballast and the subgrade, and consequently, the subgrade surface at the contact areas softens and fine particles or flocs start to become free and move. Then under dynamic loading the pumping of fines occurs (Selig and Waters, 1995). Researched investigated mud problem in pavements had similar conclusion, for instance, Alobaidi and Hoare (1996, 1999) proposed that this phenomenon is mainly due to the water pressure developed at the interface between the sub-grade and sub-base layer of pavement. The amount of mud pumping increases with increases in the applied stress (Hoare, 1982; Glyn and Cochrane, 1987). The standing water accumulated on the surface of the subgrade layer plays a major role in the development of mud pumping (Bell, 1982; Glyn, 1987; Hoare, 1992; Alobaidi, 1994; Ghataora, 2006; Duong, 2014).

2.4 Track forces

The forces involved are divided into thermal, static, and dynamic forces. Thermal forces are those induced by temperature changes and the following expansion or contraction of the rails. The result can be track buckling in different directions. The dynamic variation has different sources, such as: 1) interactions between rail and vehicle; 2) wheel impact forces caused for example by rail joints and rail corrugations. These impact forces can be of high magnitudes and at the same time produce vibrations in the track structure. These vibrations have a

detrimental influence on the track structure by facilitating mechanisms such as subgrade pumping, ballast shoulder flow and powdering of ballast material.

2.4.1 Static and dynamic loads

The main force that acts on the ballast is the vertical force of a moving train and includes vertical wheel forces and uplift force. It consists of a static load (the weight of the train divided by the number of wheels and the track components such as the rail, sleepers, and the fastening system) and a dynamic load (wheel impact forces). According to Selig and Waters (1994), the static value ranges between 53 kN and 174 kN for light and heavy haul trains respectively (Figure 2.9).

One of the distinctive conditions concerning railways is that they are subjected to cyclic load. Cyclic load is considered as a series of dynamic loads, which is a single pulse. The term "cyclic" implies that the stress applied to the soil varies regularly in magnitude with time, whereas "repeated," allows changes in the load magnitude and frequency. For the traffic load applied to rail track structures "repeated" is a more accurate description and should generally be used. Based on the research conducted by the Federal Railway Administration in the US, the dynamic load could be two times higher than the static load when the speed is high, 128-176 km/h. At the same time, the dynamic and cyclic loads were in close agreement when the speed was low. The research investigated passengers and freight trains. The impact forces produce vibrations that accelerate the track settlement and degradation could be much larger than with static load.

The sources of vertical dynamic load variations are track geometry induced vehicle-rail interaction including rock, roll and bounce, and wheel impact forces from causes such as wheel flats, rail burns, rail corrugation and rail joints (Selig and Waters, 1994). According to

Steenbergen et al. (2015) the rate of load increase due to speed is much higher when wheel geometrical quality is poor. If the wheels have geometrical defects such as wheel flats and out-of-roundness, this causes an additional, dynamic component of the axle load. Youliang and Gaoxin (2016) stated that the lane position of trains, number of train carriages, and speed of trains affect the magnitude of the dynamic loading. According to Van Dyk (2016) there are dynamic wheel load factors apart from train speed, such as the wheel diameter, a dipped rail joint, the vehicle's mass, track stiffness, the track geometry, vehicle centre of gravity, and the age of the track.

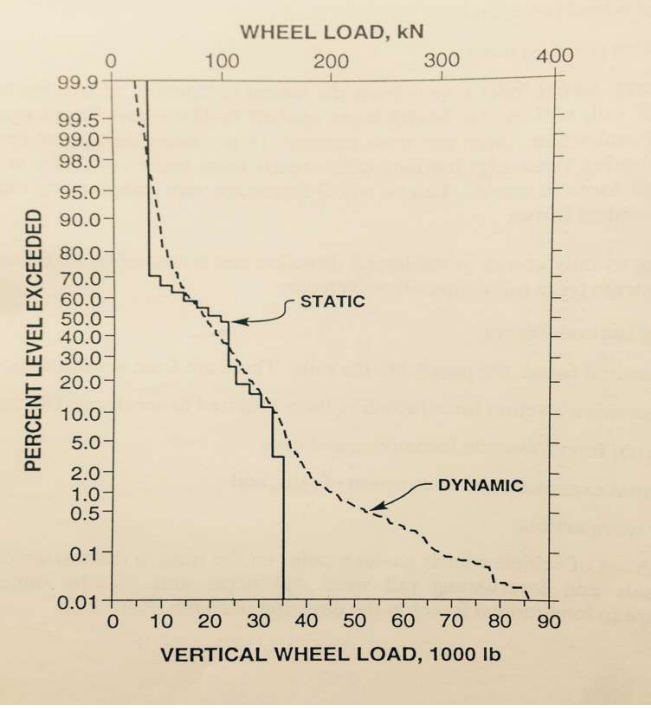


Figure 2.9 Dynamic and static wheel loads (Selig and Waters, 1994)

Figure 2.10 illustrates a typical load distribution along with the rail deflection and the way in which the rail tends to lift up near the contact points. The sleeper will be momentarily lifted by uplift forces if there is not sufficient counterbalance by the rail and sleeper weight. Once the

wheel moves forward the lifted sleeper is forced down, which, according to Selig and Waters (1994), is the reason for slurry formation and pumping action.

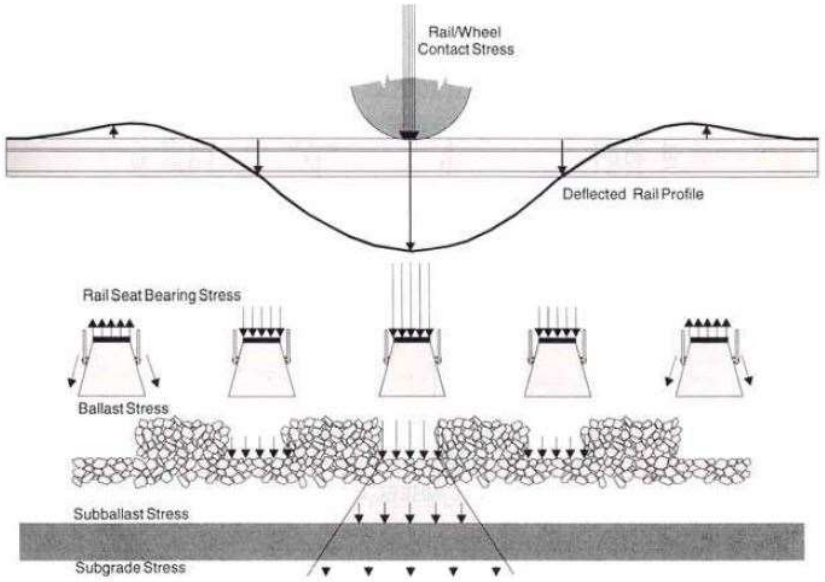


Figure 2.10 Load distribution (Selig and Waters, 1994)

Shenton (1975) studied stress distribution in practical tracks, to understand how the stress spreads at the interface of the sleeper and the ballast. The outcome was that a limited number of contact points between 100-200 distribute the stress, and the number of contact points was relatively small where the range of the ballast was between 25-50 mm. The contact pressure under the sleeper/ballast is illustrated in Figure 2.11. The maximum stress applied to the underlying ballast by the sleeper is under the wheel contact point.

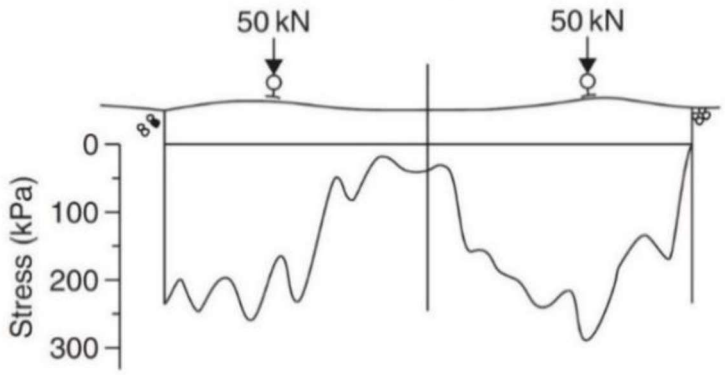


Figure 2.11 The contact pressure under sleeper/ballast (Shenton, 1975)

2.4.2 Behaviour of subgrade soil under repeated loading

The repeated load conditions cause non-linear behaviour of granular material, which is different compared to a monotonic load, when the force is increasing or decreasing, but always acts in the same direction. The soil strain quickly develops during the first load cycle and recovers only to a small extent during the unloading. Each cycle contributes to further plastic strain, but the growing will slow down with the increase of the number of cycles. The resilient modulus is a ratio of the repeated deviator stress over the strain. The term resilient or recoverable strain is often used in these contexts and represents the difference between the maximum strain under peak load and the permanent strain after unloading. Hence, the resilient strain decreases with the number of cycles (Mattsson, 2003; Ghataora, 2006). The resilient modulus of fine-grained soils depends on the geotechnical characteristics of the soil; the loading condition and the initial structure of the soil; the moisture content and dry density. The initial soil structure depends on the compacting method if the soil has been compacted. A cyclic triaxial test is a common technique to study the repeated load behaviour (Alobaidi, 1994, Indraratra, 1998; Suiker, 2005). The test provides a simplified approximation of the stress-strain conditions in the field, but the indication of the real behaviour is generally correct. The

stress-strain behaviour in a triaxial test under repeated load is presented in Figure 2.12. The stress difference (σ1-σ3) is cycled between zero and a value less than the strength of the soil, where σ1 and σ3 represents total principal stresses in different directions.

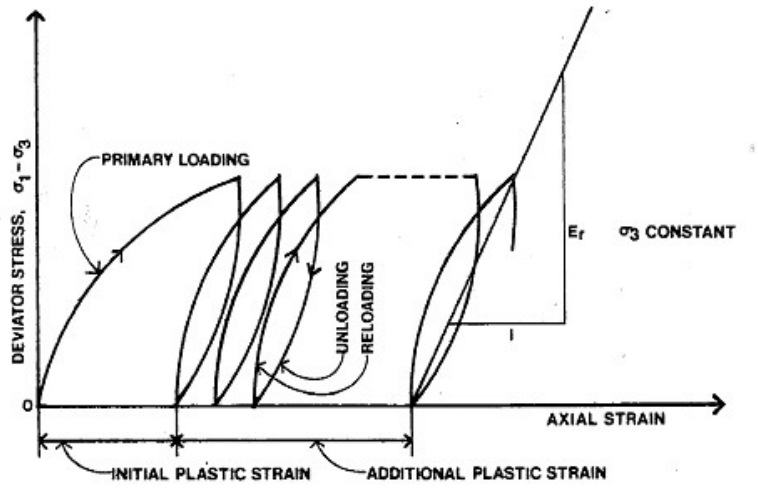


Figure 2.12 Stress-strain curve behaviour (Selig and Waters, 1995)

2.4.3 Calculating dynamic loads

A design method for calculating dynamic wheel loads was presented by Li and Selig (1998). The design parameters required for that calculation are the speed of the train, the static wheel loads and the tonnage (Equation 2.1).

$$P_{di} = \left(1 + \frac{0.0052\ V}{d}\right) P_{si}\ , \qquad \text{Equation 2.1}$$

Where:

P_{di} - dynamic wheel load

P_{si} - static wheel load

V - train speed (km/h)

d -wheel diameter (m)

Li and Selig (1998) summarised information about the common type of train locomotives and their physical dimensions (Table 1).

Table 1. Characteristics of typical cars and locomotives (Li and Selig, 1998)

Locomotive type	Wheel diameter (m)	Wheel loads (kN)	Axles per vehicle	Axle spacing (m)
125 tonnes	0.97	173	4	1.83
110 tonnes	0.91	160	4	1.78
100 tonnes	0.91	147	4	1.78
70 tonnes	0.84	125	4	1.73
Six axle locomotives	1.02	138	4	2.4
Four axle locomotives	1.02	142	4	2.84

The number of repeated load applications N_i is the ratio of the total traffic tonnage to wheel load and can be found using Equation 2.2.

$$N_i = \frac{T_i}{8 P_{si}}, \qquad \text{Equation 2.2}$$

2.4.4 Track stiffness

The stiffness of railway track has a major influence on its performance. To guarantee satisfactory quality the railway tracks the stiffness must lie within certain limits not only to control deflections, but also to maintain track geometry and ensure the longevity of track components. A track support that is too soft, or varies too widely over a short distance, may lead to excessive deformation and a rapid loss of geometry. A track support that is too stiff may result in damage to components such as rails and clips. The stiffness of material could be explained as the point load needed to cause a unit deflection (a Guide to Track Stiffness, 2016). Stiffness has units of force divided by deflection, kN/mm (Sussman, 2001).

Track modulus could be calculated by using different approaches; one of the most common is the Winkler method and was proposed by Crawford et al. (2001). In that approach, the track stiffness is a function of the vertical force (P) to the track stiffness (k) and could be defined as Equation 2.3; a vertical deflection (w) created by a vertical applied force directly related to the stiffness of the track (k).

$$k = \frac{P}{w} \qquad \text{Equation 2.3}$$

The track modulus (u) is then a function of the track stiffness (k) to the elastic modulus E and the rail moment of inertia (I).

$$u = \frac{k^{4/3}}{(64EI)^{1/3}} \qquad \text{Equation 2.4}$$

Cumulative plastic strain could be predicted using Li and Selig's (1996) model:

$$\varepsilon_p = AN^b \qquad \text{Equation 2.5}$$

where:

ε_p - cumulative soil plastic strain (%)

N - number of repeated load applications

A and b are parameters depending on soil type, soil properties and stress state

Coefficient A in Equation 2.5 is largely affected by the deviator stress and the soil influence, as represented by Equation 2.6:

$$A = a\left(\frac{\sigma_d}{\sigma_s}\right)^m, \qquad \text{Equation 2.6}$$

where σ_d -deviator stress $(\sigma_1 - \sigma_3)$; σ_s - the soil static strength; σ_1, σ_3 - total principal stresses in different directions. The relationship between A and variables σ_d and σ_s deepens in soils and is characterised by parameters a and m.

By combining Equations, 2.5 and 2.6 the model is described below:

$$\varepsilon_p = aN^b\left(\frac{\sigma_d}{\sigma_s}\right)^m \text{ and} \qquad \text{Equation 2.7}$$

$$\rho = \int_0^T \varepsilon_p dt \ , \qquad \text{Equation 2.8}$$

where T is the subgrade layer depth. Hence, the values of a, b and m need to be obtained to estimate the cumulative soil plastic deformation ρ, by Equation 2.8. Those parameters are usually estimated based on the type of the soil (Selig, 1996).

2.4.5 Frequency of load applications

The line speed can be translated to frequency of loading (Equation 2.9). Sunaga et al. (1990) suggested that the frequency, f (Hz) is connected to the train speed, V (km/h) and the length of railway carriage, L (m):

$$f = \frac{V}{3.6L} \qquad \text{Equation 2.9}$$

Fourier spectrums were produced, indicating a frequency peak between 1 and 2 Hz for a train speed of 97 km/h. The predominant frequency is considered to be in the range of 1 to 3 Hz. In earlier laboratory studies including cyclic load tests and mud pumping, different frequencies of the applied load were used, most of which ranged between 0.5 and 10 Hz. In the work done by Hoare (1982), the sensitivity of the test to changes in loading frequencies was investigated.

The results indicated that within the range tested in the study, the frequency does not affect the amount of pumping significantly (Nguyen, 2019), although the opposite opinion is common.

2.5 Ballast fouling

Fouling has a negative effect on ballast properties; it deteriorates the drainage and causes the ballast to hold water, reduces track resiliency, and decreases the bearing capacity. (Ghataora, 2006; Ngo, 2012; Ebrahimi, 2014). However, several research studies have shown that in dry conditions, coarse-grained fouling could increase the ballast strength; this is due to the charge of the physical characteristics (Indraratna, 2010; Ebrahimi et al., 2012).

2.5.1 Types of ballast fouling

Ballast is an essential element of railway track structure. One of its roles is to provide a reliable drainage pathway allowing rainwater to drain away quickly. However, the characteristics of ballast change with increases in the level of fouling; they no longer match the initial design parameters. Table 2 provides information about the type of fouling and its origin.

Table 2. Sources of ballast fouling (Selig and Waters, 1994)

Type of Fouling	Source of Ballast Fouling
Ballast breakdown	• Traffic damage (repeated loading; vibration; hydraulic action of slurry) • Tamping damage • Handling • Seasonal extreme weather temperatures (hot/cold) • Chemical wreathing
Infiltration from ballast surface	• Dust • Water borne • Dropped from train etc.
Subgrade infiltration	• Poor drainage • Saturation • Pumping action from underlying layer
Infiltration from underlying granular layers	• Old track bed breakdown • Migration of subgrade fine particles
Sleeper (tie) wear	• Attrition between sleeper and ballast due to lateral ballast

The most common type of ballast fouling could be grouped as intrusions from the surface of the railway track and includes debris from the surface, dust and sand (Figure 2.13). According to Selig and Davis (1999), ballast breakage is the cause of nearly 80% of the total amount of fouling. Under dynamic loading generated by a moving train, the ballast boulders are constantly subjected to some minor movements, so that with a large number of cycles the loading starts slowly to break the ballast and foul it. Ballast surface infiltration combines any waste and debris, accumulated transport dust, coal and iron ore fines that come from the surface of the railway track. These materials eventually block the ballast voids and reduce the drainage, creating ideal conditions for ballast contamination and mud. In the US and Australia, where the mining industry hugely relies on the railway infrastructure to carry the minerals, the source of ballast contamination is often surface dust finer than 0.075 mm.

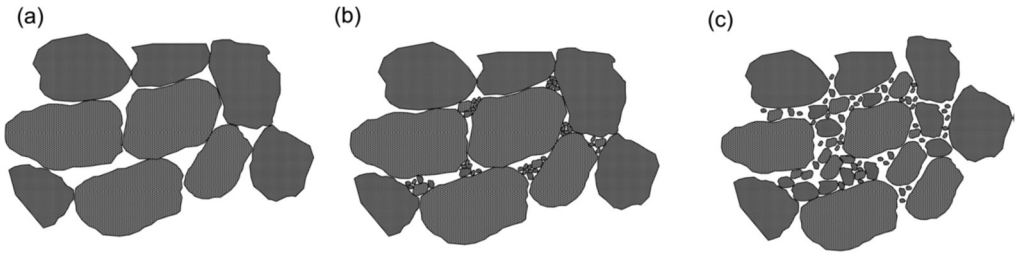


Figure 2.13 Ballast breakage a) clean ballast b) minor breakage c) major breakage

According to Selig and Waters (1994), the migration of fine particles from the subgrade to the overlaying ballast (Figure 2.14) is less common compared to other types of ballast fouling, such as infiltration from the ballast surface (coal dust or sand) and represents around 5% of the total fouling cases. The magnitude of the fine migrations largely depends on the geology and climate conditions of the region (Nguyen, 2019).

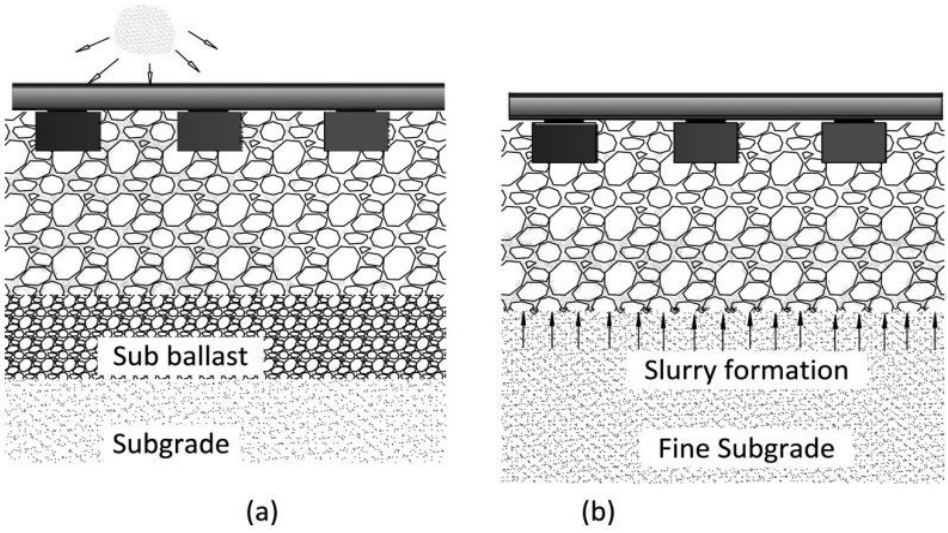


Figure 2.14 Subgrade attrition and fouling ballast (Tennakoon et al., 2014)

Mineralogy of fouling material depends on geographical location. For instance, in Australia the most common type of fouling is coal and iron ore; dust generated during transportation of mineral resources is a major source of fouling in up to 95% of all cases (Indraratna, 2000; Feldman and Nissen, 2002; Nguyen, 2019). A similar situation was seen in other regions of the world, in the US, China, and India (Selig et al., 1994). Whereas in the UK mud pumping and slurry formation are common causes of ballast fouling, due to geological factor where the top layers are often presented by cohesive soils. (Ghataora 2006, Hudson et al.2016, Nguen et al. 2019).

2.5.2 Effect of ballast fouling on drainage characteristics

Ballast is an essential part of a railway track; it helps to distribute carried load and large voids drain the water away. With an increase of fouling level, the fine particles start blocking the voids; gradually permeability of the ballast decreases, which leads to the effect of "standing water" and saturation of the subgrade layer. Then this results in the level of pore water pressure

increasing (Selig et al., 1993). With an increase of fouling materials, the permeability and hydraulic conductivity of the ballast decreases gradually (Selig et. al., 1993; Tennakoon et al., 2012; Danquah et al., 2014). This trend can be seen from Table 3 that represents the measured hydraulic conductivity of ballast specimens.

Table 3. Ballast fouling categories (Selig and Waters, 1994)

Fouling Category	Fouling Index	Hydraulic Conductivity, kh	
		(in/sec)	(mm/sec)
Clean	< 1	1-2	25-50
Moderately clean	1-9	0.1-1	2.5-25
Moderately fouled	10-19	0.06-0.1	1.5-2.5
Fouled	20-39	0.0002-0.06	0.005-1.5
Highly fouled	> 39	< 0.0002	< 0.005

2.5.3 Methods of measuring the level of ballast fouling

Different approaches could be used to measure the extent of fouling in ballast, they will be explained in the following section:

<u>The fouling index (FI) method</u>

The first method was defined by Selig and Waters (1994) and it is a summation of the percentage (by weight) passing through a 4.75-mm (No.4) sieve and a 0.075-mm (No. 200) sieve.

$$FI = P_4 + P_{200}$$

Equation 2.10

P_4 and P_{200} represent the number of ballast particles that could pass through sieve No. 4 (4.75 mm) and sieve No. 200 (0.075mm) respectively.

The percentage void contamination (PVC) method

Feldman and Nissen (2002) developed an alternative approach to measure the level of fouling:

$$\mathrm{PVC} = \frac{V_1}{V_2} \times 100\%$$

Equation 2.11

where V1 and V2 represent two volumes, the volume of the contaminated voids and the total volume of the ballast sample.

The void contamination index (VCI) test

$$\mathrm{VCI} = \frac{V_{f'}}{V_{\mathrm{vb}}} \times 100$$

Equation 2.12

The VCI is a modified version of the PVC (Equation 2.12), it allows the role of different fouling materials to be captured. The method considers the effect of the following parameters: e, Gs, particle size distribution of ballast and fouling materials. Therefore, the method gives a more realistic value of fouling, where $V_{f'}$ is the actual volume of the fouling material within the ballast voids (Tennakoon et al., 2014). Indraratna et al. (2011) concluded that the method was relatively easy to use, where the required parameters are the mass and specific gravity of ballast and fouling materials. However, it has one obvious disadvantage, that it always overestimates the degree of fouling. Therefore, a new modified approach was presented.

The $R_{b\text{-}f}$ method

A new parameter $R_{b\text{-}f}$ was introduced. The benefit of the method compared with others is the measurement time of the ballast fouling, which is faster and could be useful *in situ* for track engineers. The method is shown in Equation 2.13:

$$R_{b-f} = \frac{M_f \times \frac{G_{s-b}}{G_{s-f}}}{M_b} \times 100\%$$

Equation 2.13

The FI method is relatively simple to use and consider the weight of fines accumulated in the ballast. The FI method was proposed by Selig and Waters (1994), and considers four levels of ballast fouling (clean, moderately clean, moderately fouled and fouled); whereas PVC and VCI methods are more accurate and compare Gs, void ratio and the volume ratios. However, none of the methods considers the effect of plasticity and water content that certainly influences ballast behaviour; thus, resulting in a considerable limitation, especially when ballast is fouled by the subgrade mud pumping (Thanh, 2019). The $R_{b\text{-}f}$ method is quicker, more accurate and more attractive than the PVC method. To quickly estimate the condition of the ballast layer it is reasonable to use the fouling index (FI). The PVC method is time consuming and does not allow the consideration of the influence of the fouling particles' gradation, but does consider the parameter Gs, the specific gravity of the fouling materials. The Rb-f method is quick, and considers both specific gravity and gradation of fouling particles. While coarse-grained fouling can increase strength, clay fouling typically reduces shear strength (Indraratna et al., 2011b; Danesh et.al., 2018). The study conducted by Tennakoon et al., (2014) showed that when the void contamination index is above 25%, peak deviator stresses decrease significantly with the increase in fouling (Figure 2.15). For below 25% VCI there is a distinct drop in the post peak strength of the material. Formed abrasive slurry hastens the deterioration of the ballast layer, which eventually will lead to full ballast replacement (Tennakoon et al., 2014).

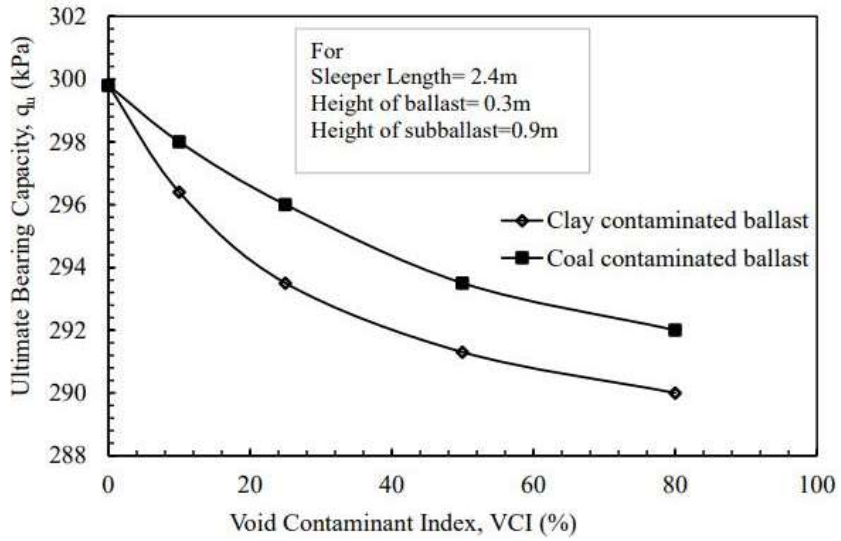


Figure 2.15 Bearing capacity/VCI ballast (Tennakoon et al., 2014)

2.6 Attrition and mud pumping

Although the mud pumping phenomenon seriously affects the safe operating of trains, and costs the railway industry significant maintenance funds annually, the subject has not been investigated thoroughly. There is a limited number of published research works available in open sources and only a few possible mud pumping mechanisms have been discussed (Nguyen, 2019). According to Selig and Waters (1994) mud pumping occurs when there is direct contact between the ballast and underlying cohesive subgrade soil at the contact points of the saturated subgrade soil and ballast material. The formed slurry pumps up and down under train cyclic loading, and within a certain period the slurry ejects up towards the track surface. Eventually, the trackside drainage is blocked by slurry and the deterioration process is further escalated. Created voids under the pumping sleeper make the actual geometry under the load of a train worse than at the unloaded state, which eventually exceeds the limits to meet the industry standards.

2.6.1 Mechanism of mud pumping

Takatoshi (1976) presented a suction driven model where mud pumping is directly related to movement of ties and a suction effect (Figure 2.19). Subgrade soils are often presented by cohesive soils that have low permeability characteristics. When the subgrade layer is in a saturated condition then constantly applied cyclic loading generates pore water pressure. The excess of it induced by cyclic loading could be higher by up to four times in contrast with that which is statically generated (O'Hara et al.,1981). Due to the small intervals between loading cycles, pore water pressure does not have sufficient time for dissipation; the pressure increases and sucks in the fine particles. Once the train has passed and the overall condition of the track is unloaded, the pore water pressure dissipates. This is the main driver of fines' migration, when within a period and with constant load repetition, mud pumping occurs.

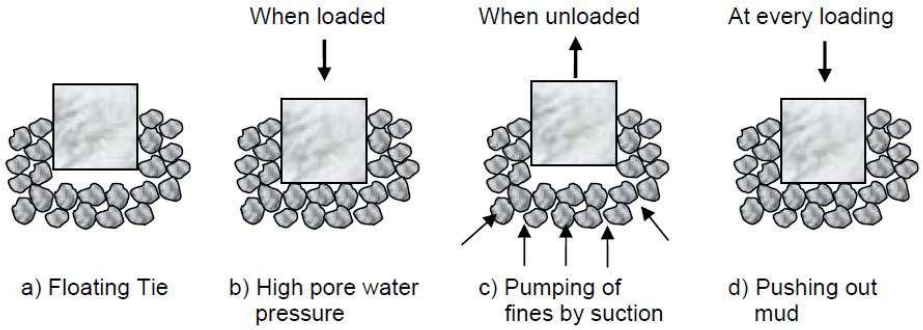


Figure 2.16 Pumping mechanism (Takatoshi, 1976)

The development of pore water pressure depends on the level of consolidation of cohesive soil (Duong, 2013). When cohesive soil is normally consolidated pore water pressure rises gradually; however, over-consolidated cohesive soils behave in a different way. At the beginning it would decline due to dilation of fine-grained soils, following this stage the excessive pore water pressure starts rising. Snaith and Bell (1978) suggested that under

dynamic loading particle contact pressure could be decreased because of the accumulated pore water pressure, to the extent that the soil structure would be damaged with potential freeing of soil particles or floss. Hoare (1982) conducted several experiments studying the mechanism of clay pumping. The conclusion was that the wetting of the subgrade surface with subsequent squeezing of fines through the transition layer was the main reason for mud pumping. The experiments were under partly drained conditions. Since the time of one cycle is too short, the drainage condition during a single cycle could be described as undrained. In that condition the pore water pressure does not have enough time to dissipate and that leads to further development of pressure. However, because the surface of the subgrade interacts with atmospheric pressure, the mean pore water pressure is expected to dissipate with time. The rate of dissipation depends on the permeability of the layers of the railway track. Hoare (1982) obtained a test result that could prove these allegations. He concluded that the drainage conditions at the surface and at the point of the transducers (a few millimetres below the subgrade surface) were different. Also, the dissipation of the pore water pressure at the subgrade surface was almost immediate; whereas at the position of the transducers it took up to 5 hours to dissipate the pressure. There was a big difference between contact stress and the maximum values of pore water pressure, 20 kPa and 1.5-3.5 kPa respectively. Much higher pressure would be expected if the transducers were placed close to the subbase-subgrade contacts. Another research study was conducted by Bell et al. (1982) where he measured pore water pressure development 3 mm below the surface of the subgrade, applying stress of 25-75 kPa. The rapid rise of the pore water pressure was reported from the beginning of the cyclic loading to reach a peak value between 16 and 88 kPa. The research outcomes of Bell and Hoare (1982) show similar trends in the increase of pore water pressure with the number of cycles, however the absolute values were very different. This could be explained by the fact that the applied stresses were different. Another reason could be the location of the transducers. Bell et

al. placed them nearer to the surface, which means the transducers were more affected by stress concentration. Saxena (1986) used a similar principle to that suggested by Hoare (1982): when subgrade fails under points of high stress concentration because of high pore-water pressure development under dynamic loading. In that research, the effect of the placing of geotextiles was investigated. He found that the mud pumping action greatly depends on small gaps under the contact points of the geotextile and the ballast. During the unloading stage of the cycle, geotextiles recover faster than the soil. This allows water and fine particles to infiltrate there. At the next unloading cycle, the mix of water and fine particles is sucked by the geotextile. The pore water pressure and the amount of retained fine particles will increase with the following cycles. The size of the gaps depends on the subgrade soil's characteristics, the characteristics of the geotextile, and the size of the contact area between them. The pumping was greater when the area of the gaps between the spheres (ballast) was large. Overall, the highlighted parameters have a big influence on the amount of pumping.

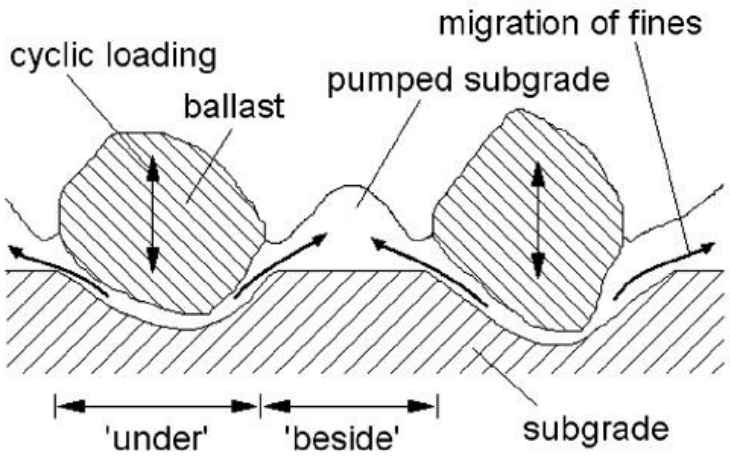


Figure 2.17 Formation of the slurry (Ghataora et al., 2006)

Raymond (1986, 1999) studied the effect of installing geotextiles on the maintenance of railway tracks in the US and Canada where the seasonal temperatures drop to sub-zero. The

observation showed that although the geotextiles had been placed during the previous season the ballast was filled by fine particles. The suggestion was that the seasonal fluctuation of subgrade temperatures leads to freezing and thawing cycles that could be a cause of fine particles' pumping (Figure 2.18).

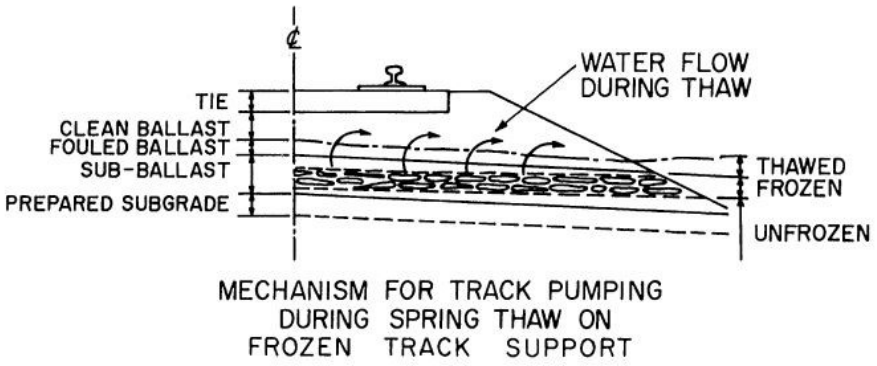


Figure 2.18 Mud pumping mechanism (Raymond, 1999)

2.6.2 Development of pore water pressure

Soil mechanics theories consider soil as a simple three phase system that includes soil particles, air trapped between pores and pore water (Figure 2.19). The three-phase system is not observed in compacted clays (Wan et al., 1995). The soil structure is instead made up of a complex of aggregations of clay particles. The clay particles are curved flaky structures and will strongly attract the water molecules and so the voids between the particles will become saturated.

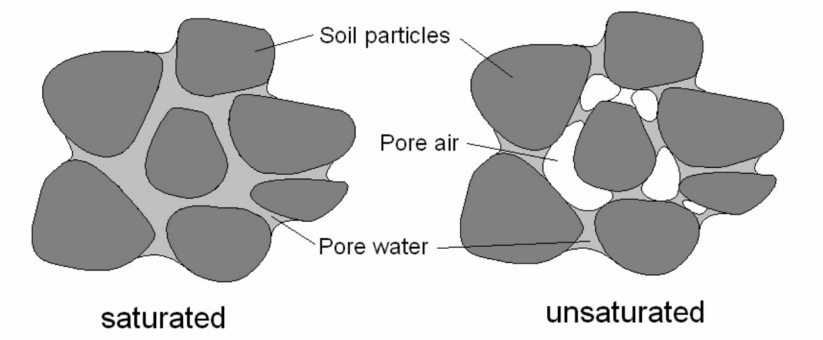


Figure 2.19 Saturated and unsaturated soil particles

Two conditions are essential for development of pore water pressure: repeated loading and subgrade soil in saturated condition. Migrated fine particles block ballast and reduce the drainage characteristics. Thus, the effect of ballast fouling must be taken into account.

Reduction in ballast permeability is a major cause of hydraulic erosion, subgrade attrition, reduced railway track stability, and ballast degradation. Therefore, it is important to have an efficient and well-operated drainage system that could effectively drain rainwater from the track. According to Parson (1990), who conducted experiments investigating the change in hydraulic conductivity with an increase of ballast fouling, the hydraulic conductivity of a ballast layer reduces significantly with an increase of fouling materials. The results show that the value of hydraulic conductivity drops dramatically from 2.54-5.08 cm/sec for clean ballast to 0.0005 cm/sec for highly fouled ballast. Based on the research of Selig and Waters (1994), the difference in the permeability between clean and moderately fouled ballast is 10-15%. The results of their investigation showed that the permeability values of clean ballast might be as much as two times those of moderately fouled ballast. A similar conclusion was made by Tennakoon et al. (2012), who stated that permeability and drainage conditions of the ballast layer decrease with an increase of the fouling level.

Standing water is a cause of many railway problems such as subgrade attrition, swelling volume change, and slurry formation under repeated loading. Because of the standing water on the subgrade interface, the strength of the subgrade soil and its stiffness decrease with time. Field observations show that the number of mud pumping cases increases sharply during high rainfall periods (Reynold, 1994; Sussman et al., 2012). Laboratory tests have indicated that the standing water directly affects the amount of mud pumping. At the state close to a saturated condition, subgrade fine particles rose rapidly; which was not the case when the conditions were unsaturated (Alobaidi et al., 1994; Selig et al., 1994; Duong et al., 2013; Chawla et al., 2016).

Accumulated water on railway tracks has different sources; it could come from precipitation falling directly on the track, upward subsurface seepage and surface flow (Selig and Waters, 1994). Duong et al. (2014) investigated old railway tracks and studied the effect of intermixing when a granular layer is directly placed on the top of a cohesive subgrade layer. They pointed out the main factors of this effect: such as the sub-base layer being open graded, with cyclic loading and free water standing at the interface level. The reason for this mixing is the local failure of the subgrade soil under the sub-base particles; upward movement of plastic soil into the sub-base layer; and penetration of the sub-base particles into the sub-base layer.

It was assumed by several researchers (Alobaidi, 1994; Duong, 2014) that if pore water pressure occurs on the surface of cohesive subgrade soil, then it should be in the thin layer below the surface because that layer has low permeability characteristics. It was also expected that in this case the main force that pushes fine particles will be created by dissipation of pore water pressure at a high hydraulic gradient. The researchers found it difficult to prove the assumption experimentally because of difficulties in measuring the pore water pressure at the contact point of the ballast and the subgrade layers. Important experimental works investigating the development of pore water pressure on a pavement surface were conducted at the University of Birmingham (Hoare, 1982; Alobaidi, 1994). The particular focus was to find a correlation between the amount of pumped fines and the development of pore water pressure. The research was conducted using cyclic triaxle tests and different combinations of geotextiles. Although pavements and railways are different models where the applied load and its frequency are not the same, the mud pumping phenomenon should have a similar genesis. In the study the applied load was in a range between 10 and 30 kPa with a frequency of 2.0 Hz. The transducer to measure the pore water pressure was placed at a depth of 7 mm from the contact point of the geotextile and the subgrade. Alobaidi (1994) investigated the same mechanism in

pavements and proposed a method to measure the amount of pumped soil by measuring the change of thickness through Equation 2.14.

$$\Delta h \text{ (pump)} = \frac{w_f}{A_f \times \gamma_d}$$

Equation 2.14

where:

w_f - mass of soil passing through the geotextile (kg)

A_f - loaded area (m^2)

γ_d - unit weight of the soil (kg/m^3)

Comparing and combining the empirical and numerical results, Alobaidi (1996) concluded that under dynamic loading the amount of pumping is affected by the rate of pore water pressure dissipation and the key for solving the mud pumping problem lies in understanding the soil behaviour at the subgrade–subbase interface. As there is a common practice of placing a transition layer between them, it is essential to take into consideration the way in which geotextiles or any other transition layers such as a sand blanket affect the overall condition. In another publication Alobaidi et al. (1998) stated that with an increase of standing water the amount of mud pumping increases and with an increase of water amount the role of load frequency increases, but that was not the case when there was no water, or the water amount was not significant. The author also considered the effect of moisture content on the pavement subgrade strength and its erodibility. In the experiment, initially 200 kPa of consolidation load was applied on the fully saturated soil sample with the following unloading stage to 10 kPa. After the test the moisture content was measured at the various depths. After visual observation, it was found that surface soil particles were in a very loose condition and were susceptible to erosion by flowing water.

Aw (2007) reported that pore water pressure increases gradually when the subgrade soil is normally consolidated cohesive soil. In the case of over-consolidated soil, it decreases due to dilation at the initial stage, and after that there is an increase in excessive pore water pressure. A correlation between the critical stress application ratio was found by Aw, (2007), which is the application of shear stress over the undrained strength of the soil ($\tau c/S_u$). It was stated that if the stress is applied below the τ_c/S_u, then the subgrade layer could carry a large amount of cyclic loading without accumulating plastic deformation.

2.6.3 Soil strength in cyclic loading

Soil strength changes under repeated dynamic loading. It depends on soil characteristics such as the level of saturation, void ratio, the level of compaction (loose or dense soil). In the case of saturated subgrade soil, pore water pressure develops and does not dissipate quickly under cyclic loading. Compared with monotonic stress, less cyclic stress is required to reach the point where the soil may fail due to an increase of pore water pressure, because after each cycle it does not return to the initial level and continues development. According to Lambe et al. (1969), under cyclic load the soil particles are continuously rearranging, and that leads to a decrease of soil volume and an increase of pore water pressure. Lefebvre (1986) conducted several experiments on a consolidated and over-consolidated Grande Baleine clay that was highly sensitive to cyclic loading, investigating correlations between pore water pressure and soil strain. He identified that the axial strain was developing progressively until a sudden decrease just before the failure. The pore water pressure continued to remain stable, as well as the axial strain curve that also stayed almost flat and stable. Some researchers (Waters, 1968; Sangrey, 1969; Procter, 1984; Lefebvre, 1986) studied the influence of a critical level of stress and arrived at a similar conclusion: a critical level of stress exists below the monotonic peak

strength level. Below that level, the strain of the soil stayed the same. Shear deformation occurs above the critical level of stress. The observations of Selig (1994) showed that materials tend to be compacted with an increase of soil stiffness and strength, and the permanent strain increases after a large number of cycles. According to Gidel et al. (2002) and Ekblad (2006), water has a significant effect on permanent deformation and resilient modulus, that decreases with an increase in the amount of water.

2.6.4 Mud pumping enhanced by localised concentration of cyclic stress/strain

In some sections of rail lines such as switches and crossings, rail/expansion joints and transition zones, the stress and strain under the rail can be exacerbated and thus accelerate the degradation of ballast and subgrade to trigger mud pumping (Ito, 1984; Woodward et al., 2009; Powrie, 2014; Li et al., 2016; Yang et al., 2018). For example, the discontinuity and uneven contact surface between the wheels and the rail at the rail joints leads to a larger concentration of cyclic stress and strain under the sleepers, as shown schematically in Figure 2.20, based on the peak wheel-rail contact force measured in previous studies (Yang et al., 2018). In a similar mechanism, Coelho et al. (2011) pointed out an abrupt change in foundation stiffness when trains move through a transition zone (e.g. between ballasted and concrete slabs at bridges and tunnels). These abnormal responses can result in more severe degradation of the underlying foundation, with 4 to 5 times larger displacement than normal tracks. At switches and crossings, trains usually change speed abruptly and move transversely over different jointed rail lines, leading to significantly larger impact loads (Powrie, 2014). Note that higher cyclic load (i.e. cyclic deviator stress) is a key factor that accelerates ballast breakage and abrasion. Furthermore, the fluidisation and infiltration of subgrade/filter layers can increase as the cyclic stress increases (Ito, 1984; Liu and Xiao, 2010; Duong et al., 2014). This explains why track problems (including mud pumping) are significant in these sections of rail lines, and the

maintenance costs are higher than for normal sections (Selig and Waters, 1994; Powrie, 2014; Hudson et al., 2016). The same issue also occurs at the expansion joints which connect different panels of slab tracks and/or railway bridges (Muramoto et al., 2006; Huang et al., 2018).

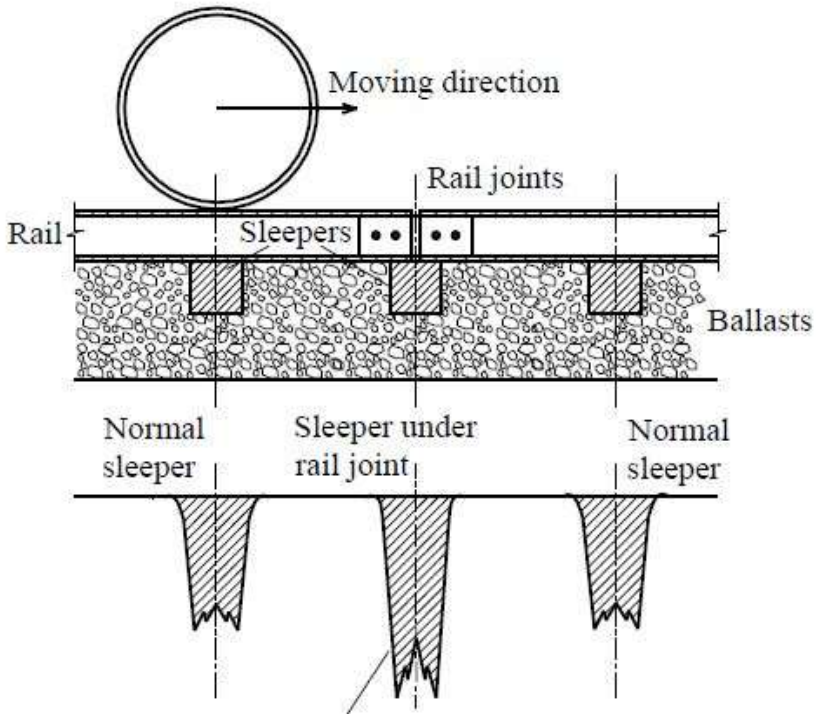


Figure 2.20 Stress/strain concentration under sleepers at rail joints (Thanh et al., 2019)

2.7 Remediation solutions

Early railway tracks were built on cohesive subgrade soils with direct placing of an angular ballast layer on them; and in many cases, intermixing between the two layers occurred. The chances of intermixing increase if the applied dynamic load is high, there is a presence of freestanding water, and the sub-base is open graded (Tang, 2014; Duong, 2014). The mixing happens because of the local failures of the subgrade soil under the sub-base particles. The soil plastically flows into the upper sub-base layer, while the sub-base penetrates into the subgrade soil. The local shear failure and mixing could be prevented by separating the subgrade and

ballast layers. There are several approaches to address the mud pumping problem; all of them have advantages and disadvantages. Firstly, to clean and/or completely replace fouled materials at muddy sites. This is a common method used in practice due to its simplicity and long-life effectiveness; however, this solution is expensive and time consuming. Alternatively, a separator layer between the subgrade and ballast could be installed. In the case of geotextiles, soil particles are pushed upwards because of the quick dissipation of the excess pore pressure. Geotextiles work as a barrier, whereas the sand layer provides a drainage pathway and collects and holds the pumped fine particles. Finally, chemical stabilisation can be used, where engineering properties or original materials are improved by adding chemical composites that create the bonds between the soil/ballast particles; and/or voids are minimised by using chemical/biological products (Blacklock, 1978; Kayes et al., 2000; Karol, 2003). The sand layer and geotextiles are common solutions and will be discussed in the following section.

2.7.1 Sand layer

A layer of sand has been the conventional transition layer used between the subgrade and sub-base layers. It was proved by experiments and throughout field observations that a layer of granular material such as sand is a good preventer of fines' migration (Ayers, 1986; Bell et al., 1982; Alobaidi, 1994; Ghataora, 2006). When using a sand layer, in order to select the thickness and particle size characteristics, it is important to consider the sand based on filtration criteria (Friedi and Anderson, 1982). The disadvantages of using this method are the high cost of the works and the question of whether there is local availability of the materials; therefore, the method is considered as unsuitable. Ayers (1986) concluded that the best prevention method of slurry rise is a sand blanket layer. If the railway track has a layer of the correct sand across the whole width of the rail track, then there is no possibility of the rise of the slurry. He also revealed different types of failures such as: erosion pumping failure (EPF), dirty ballast

pumping failure (DBPF), and bearing capacity failure (BCF). His conclusion was that the pumping problem is not related to the strength of the subgrade soil, which was later disproved by other researchers (Alobaidi, 1994; Ghataora, 2006; Nguyen, 2019).

2.7.2 Geotextiles

Geotextiles as an alternative solution to a layer of sand has advantages such as their high tensile strength, being lightweight, their availability, installation time and a wide range of design properties. If the load is applied on the granular layer that is placed on top of a soft subgrade, local shear failure is likely to occur. The granular material will penetrate the soft subgrade layer and results in extensive rutting. Initially, the idea of using geotextiles was for separation of the coarse aggregate of the sub-base layer from penetration into the subgrade layer. The research conducted by Barenberg et al. (1975) tested loading on a model footing, resting on a stone aggregate, a soft subgrade system with and without geotextiles. In that experiment a non-woven geotextile of low tensile modulus was used. The outcome of the tests was that applying a geotextile increases the bearing capacity factor by two times from 3.3 (without) to 6.0 (with). When the geotextile was used, the local shear failure did not occur, and the system showed high deformation only at general shear failure. High tensile modulus geotextiles change the mode of failure and increase the bearing capacity by membrane action as well (Barenberg, 1980; Giroud, 1981). The geotextile restrains the lateral deformation of the sub-base layer due to an imposed load. As a result, the confining stress of the sub-base layer increases and the load distribution ability of the layer improves. In the case of a soft subgrade under dynamic loading, the geotextiles stretch and develop tension and act as a membrane reducing pressure on the ballast and subgrade, thus mitigating their degradation (Ghataora, 2006; Chawla, 2016). The vertical component of the tensile stress counteracts the applied stress, reducing the stress acting on the subgrade surface. The amount of tension developed in the geotextile is determined by

the tensile modulus, the anchorage length outside the loaded area and the rutting depth (Alobaidi, 1994). Thick geotextiles can offer some cushioning, but the benefits would probably soon be lost as the ballast abrades the geotextile.

Another sub-ballast function is to drain water from below, compensating for any excess pore water pressure in the subgrade caused by the repeated load. This is a permeability function, which the geotextile can initially perform well. However, if the subgrade is clay, or a material comprising clay as an abrasion product, then the pores can get clogged up by the fines and the permeability decreases or even ceases to exist (Sharpe and Caddick, 2015; Yee, 2016). As technologies have been advanced, geotextiles are utilized as preventers of subgrade fines' migration. However, the number of research works related to detailed analysis of using remediation materials are limited. This fact seems improbable considering the scale of the problem and the potential benefits of finding an efficient solution (Ito, 1984; Ayres, 1986; Alobaidi, 1994; Ghataora et al., 2006; Chawla, 2016).

Geotextiles reduce the average stress level because of their wide distribution of surface loads and also proportionally reduce the contact stresses with a following decrease of the rate of pumping. Dawson (1986) stated that the amount of pumping is reduced because the geotextiles decrease the contact stress. It was stated that the total stresses may be considered as a combination of two types of stresses: the static and the cyclic. The author suggested that although the placed geotextile can reduce the static stress, it could also reduce the cyclic stresses. Alobaidi (1994) tested different remediation solutions such as a layer of sand, geotextiles and geocomposites, which is a sandwich combination of a textile and a sand layer. The conclusion was that the type of geotextile has a significant effect on the migration of fines from the subgrade layer. It was found that with the use of geotextiles the amount of mud

pumping was at a minimum level and in general, it prevented the migration of fines better because it functions as a filter and separation layer. In his research, Ayers (1986) stated that although some geotextiles could be useful in tracked water control, no geotextiles have been found that could fully prevent the passage of clay slurry under dynamic loading. However, thermally bonded non-woven geotextiles were identified as the most efficient solution, compared to mechanically bonded geotextiles or geomembranes. Saxena (1986) tested a range of geotextiles under dynamic loading with fully saturated clay. The author also observed the development of pore water pressure and a decrease of the soil strength. Under high pressure and an undrained condition, soil deforms quicker and more significantly. The way it deforms is through penetration into geotextiles. According to Saxena (1986), at the early stage of geotextile development, the materials were not able to fully protect the track structure. Chawla (2016) investigated the reinforcement, separation, filtration and drainage effects of applying geotextiles. The study investigated the degradation of subgrade cohesive soils named Dhanaury clay and Delhi silt under dynamic loading. The combination of the cyclic loading and the subgrade soil's characteristics, such as high permeability of silty soil, led to a rapid rise of pore water pressure, which was the main factor for slurry formation. The author mentioned that the pore water pressure increases faster when the subgrade soil has low plasticity. The subgrade gets softer under the influence of slurry water that leads to penetration of granular particles into the subgrade with a following increase of the settlement.

Although various geosynthetics have been examined over the years, conclusions about their efficiency vary widely. Many conventional investigations show that using geosynthetics to mitigate mud pumping has limited efficiency (Ayres, 1986; Sharpe, 1988; Yang and Yu, 1989). Furthermore, geotextiles suffer from severe tension and abrasion induced by ballast, which significantly reduces their capacity for separation. Other researchers indicate that geosynthetics

play a large part in stabilising subgrade and reducing mud pumping. Geotextiles reduce the migration of fines and quickly dissipate excess pore pressure, but they don't decrease the magnitude of cyclic excess pore pressure (Alobaidi and Hoare, 1996, Sharpe, 2014; Chawla, 2016; Lenart, 2018). The difference between opinions could be explained by the time when the particular research was conducted. For example, the early research works in 80s discussed the limited efficiency of the tested materials, probably because the technologies then were still developing; whereas the latest works were satisfied with the geotextiles' performances, because of advanced manufacturing technologies and accumulated knowledge.

2.8 Previously investigated soils

The way the entire railway structure behaves under dynamic loading depends on the physical characteristics of the subgrade layer. The soil's characteristics determine the state of the foundation base. The mud pumping phenomenon is directly related to the physical characteristics of cohesive subgrade soils (Selig and Waters, 1994) and it only occurs for certain types of cohesive soils. Therefore, it was essential to gather all available information about mud pumping cases and analyse them. Table 4. summarises the information about previously tested soils. It includes the type of the soil and its physical characteristics (LL, PI, Gs, moisture content, if applicable), as well as the country of origin and the names of the researchers. A plasticity chart of soils used in the previous investigations on subgrade mud pumping is presented in Figure 2.21. Subgrade soils can be divided into three groups, with the largest cluster of data in the medium plasticity soils, where the liquid limit lies between 35 and 55% and the plasticity index between 15 and 30%. A few studies have been conducted on both low and high plasticity soils. Most soils that are susceptible to mud pumping are fine-grained, inorganic clayey soils, silts and clays with medium to low plasticity.

Table 4. Laboratory-based studies on migration of fines

Compilation of soil characteristics						
Researchers	Country	Soil	Moisture content, %	Specific gravity, Gs	LL (%)	PI (%)
Ayers et al., 1986	UK	Over-consolidated marine deposit clay			44	24
Saxena, 1986	US	Artificial soil, Ottawa sand 45% kaolinite 50%, bentonite 5%	16.4	2.66	40	27.6
Raymond, 1986	US	El Dorado plastic clay	18		48	30
Raymond, 1986	US	Copan plastic clay	19		48	30
Raymond, 1986	US	Valley Falls plastic clay	23		45	22
Alobaidi, 1994, 1996 and 1998	UK	Kauper marl, silty clay, medium plasticity	19	2.735	49	26
Mattson, 2003	UK	London clay	22		76	50
Voottipruex et al., 2003	Thailand	Inorganic clay, low and medium plasticity			43	21
Bahmani, 2004	UK	Oxford clay	21		69	39
Jeyabalamoorthy, 2005	UK	Kaolinite, boulder clay	17		42	20
Ghataora et al., 2006	UK	Etruria marl	18	2.64	34	16
Muramoto et al., 2006	Japan	Arakida clay			49.4	21.7
Aw, 2007	US	Silty sand, low plasticity				
Ciu et al., 2012	US	Medium plasticity clay	19		57.8	24.1
Trinh et al., 2012	France	Finely grained soil	16		58	24
Duong 2014, 2016	France	Kaolinite and crushed sand	16		27	11
Ebrahimi et al., 2014	US	Sauk Country clays, low and high plasticity			36	19
					64	42
		Wisconsin clays, low and high plasticity			28.6	6
					38	22
Chawla et al., 2016	India	Dhanauru clay	16.7		36	15
Chawla et al., 2016	India	Delhi clay	15.4		22.5	5
Chen et al., 2016	China	Red clay			40	15
Kermani et al., 2017	US	Non-plastic silt	11	2.79	17	1
Indraratna et al., 2019	Australia	Low plasticity clay			26	15

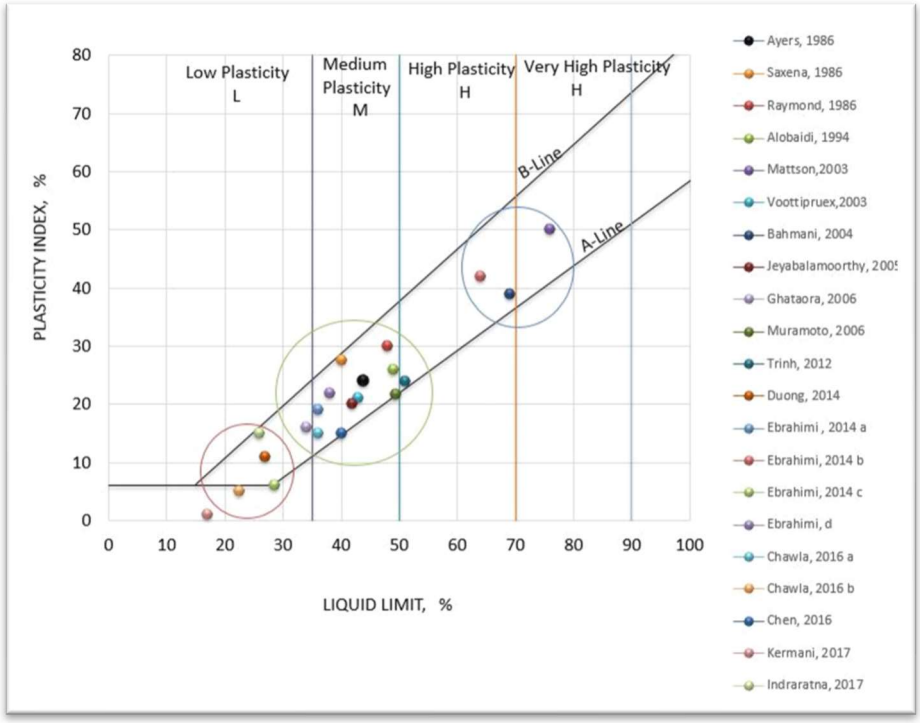


Figure 2.21 Plasticity chart of previously investigated soils

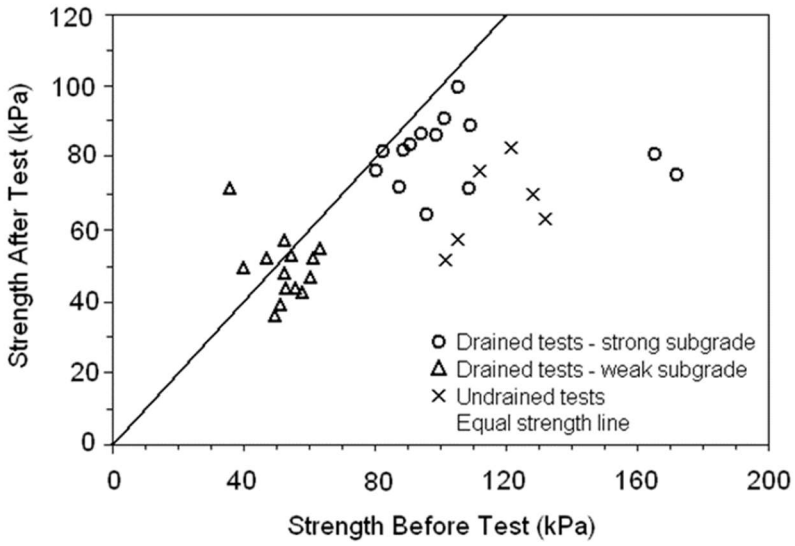


Figure 2.22 Plasticity chart of previously investigated soils (Ghataora, Burns, Evdorides, 2006)

(Note: "Drained test relates to load test where no water was added to the soil and for undrained test 500 ml of water was added, but not allowed to drain simulating the worst-case scenario, where the ballast is not free draining").

2.9 Summary

This chapter presented a critical literature review on the subject of railway subgrade and the mud pumping problem. The following conclusions were made:

- The main factors of subgrade degradation and the mud pumping phenomenon are cyclic loading, excess water, excess of fine particles.
- Mud pumping can be accelerated by a stress concentration; improper contact between the sleepers and the ballast (i.e. under-sleeper voids); the freeze and thaw cycles in cold regions; and an increasing water table during high rainfall periods, increasing the excess of pore water pressure being the main mechanism.
- Mud pumping can be evaluated through ballast fouling indices such as the fouling index (FI), percentage void contamination (PVC), $R_{b\text{-}f}$ and other theoretical approaches.
- Several groups of solutions for mud pumping can be summarised: (1) clean, modify and completely replace fouled materials at muddy sites; (2) enhance drainage at the foundation; (3) geotextiles reduce ballast degradation and subgrade softening.
- The USPs were reported as an efficient solution to reduce vibrations, improve track stability and stresses on all track components and substructure due to a better load distribution; information about the effect of the USPs on subgrade soil is limited.

The experimental research method was chosen as a scientific approach of the thesis, where the quantitative data was obtained through experimental procedure and it was related to similar previous works. Variables such as with USP/without USP were used and applied to more dependent variables (saturated/unsaturated subgrade soil) to measure their effect on the railway track. The effect was observed and recorded over a period of time (Chapter 4). The comparison was made between different groups from the test (bs, bsw, bsusp, bswusp). Conclusions regarding were drawn (Chapter 5).

Chapter 3 METHODOLOGY

3.1 Introduction

Many studies that have previously investigated railway problems (Alobaidi, 1995, Ghataora, 2006; Chawla, 2014) were conducted in laboratories rather than in the field; since this approach has been proved as an efficient method to study track problems, due to the relatively low cost and the ability to quickly change the tested parameters and materials. The test apparatuses could be reasonably quickly designed and built in the laboratory at any scale, even in close proximity to the original scale of real railway tracks. Therefore, this research study was also chosen to be conducted in the laboratory. The main objective of the work was to study behaviour of subgrade soils (i.e. permanent deformation, stiffness, erodability) under repeated loading with different variables such as saturation condition, and initial moisture content, and also tests with and without USPs. The main question was how these parameters affect the properties of subgrade soil and how they influence its performance. This chapter provides data about the tested materials including information about the geotechnical characteristics of the tested soils, the ballast and the under-sleeper pads. The testing programme is explained in detail, providing a description of the procedure and the experimental set-ups. It gives information about the small and the large-scale apparatuses, where railway track loading conditions with similar ranges of maximum and minimum applied load and frequency were simulated.

3.2 The laboratory work programme

To achieve the research objectives, a systematic literature review was undertaken to identify the current knowledge about the response of cohesive soils to dynamic loading, specifically in the railway environment (Chapter 2). The study also encompassed a review of modes of failure and their treatment, particularly relating to the erosion of subgrade soils. Based on the information obtained from the literature review, two investigation approaches were developed: the small-scale cyclic test; and the large-scale cyclic test. Findings were used to design the small-scale test apparatus and procedures. Also included was a large-scale test in a 2.0 m x 1.65 m chamber to validate the smaller scale of 230 mm diameter, the most used test. These developments enabled the programme of study to be undertaken. The programme of the study has defined three main stages. An overview of the conducted tests is given in Table 5.

1. Analysis of soil characteristics

This stage includes the following steps to determine the basic soil properties and assess the erodibility of the tested subgrade soils. The selection of cohesive soils includes those which are common as a subgrade soil and susceptible to mud pumping. Then to investigate the erodibility of the selected subgrade soils experimental work was carried out to assess the behaviour of the subgrade soils at different moisture conditions that will be used during analysis stage (the details of the tests used are given in Chapter Three). The list of conducted tests included: the Atterberg limits, the compaction test, the unconfined undrained test, the specific gravity test (*Gs*), the particle size distribution (the hydrometer test), the consolidation and permeability tests, and the organic and soil content. The investigation of the soils' erodibility and their susceptibility to erosion mechanisms was completed using the hole erosion

test (HET) and the crumb test. The tests were conducted in accordance with British Standard 1377:1990 (Parts 1-5).

2. Detailed investigation of the behaviour of subgrade soil under cyclic loading

This stage included the small-scale test to experimentally investigate the effect of the under-sleeper pads as a material that could improve the performance of railway tracks. This type of test has been previously used by most researchers who investigated similar subgrade problems (Alobaidi 1994; Ghataora 2006, Duong 2011, Chawla 2014). The small-scale test was assembled to study the performance of the subgrade layer with and without the USPs. It allowed direct measurements of following parameters:

1. The cyclic pore water pressure at the subgrade/ballast interface.
2. The permanent subgrade deformation.
3. The stiffness of the subgrade soil.
4. The amount of loosened soil.

These parameters have been selected based on the previously conducted works (Alobaidi, 1994; Ghataora, 2006), as they would have a direct influence on the behaviour of subgrade soil, its deterioration and the migration of fine particles. The test was modified with a pressure transducer which allowed the measurement of the development of the pore-water pressure on the contact point between the ballast and the subgrade layer. The amount of loosened soil was used in previously conducted research works to study the performance of different remediation solutions and was examined at the end of each test. The parameters that gave data during the test and after the test enabled a clearer picture about the behaviour of subgrade soil, and the amount of pumping during and after the test to be seen.

3. The large-scale test

The behaviour of ballast should ideally be studied through tests conducted on a real track under actual loading conditions. However, these tests are not only costly and time consuming but also disrupt traffic schedules. Therefore, laboratory experiments simulating field load and boundary conditions are usually carried out on ballast specimens. To attain this, the large-scale test apparatus was assembled enabling a realistic simulation of railway track behaviour under cyclic loading. The purpose was to validate the small-scale test results, comparing the data received from both apparatuses. The test enabled the measurement of the permanent deformation and soil stiffness.

Table 5. The laboratory work programme

Laboratory study	Description of the study	Investigation apparatus
1	Soil classification tests	BS 1377, part 1, 2,3,4: 1990
	Erodibility tests	BS 1377, 5: 1990 Hole erosion test, crumb test
2	Mud pumping investigation; permanent and cyclic deformation of subgrade soil; soil stiffness and strength; development of pore water pressure	The small-scale tests
3	Verification of the small-scale tests' results, comparing them with results obtained from the large-scale test.	The large-scale test

3.3 Tested materials

3.3.1 Ballast

The role of the ballast layer is to carry the load of the track superstructure, reduce the amount of stress distributing to the subgrade layers, and to provide a clear drainage path. Firm, angular, uniformly graded rocks and stones free of dirt and dust are used as a ballast material (Selig and Waters, 1994). A wide variety of materials have been used for ballast; igneous rocks of granite and basalt are often used as a source of ballast material. The size and gradation are two main design characteristics of the ballast. The Network Rail Standard (RT/CE/S/006,2019) provides the limitations of the size of the ballast material; in the UK the size of the selected ballast should be in the range between 31.5 mm and 63 mm (Table 6).

Table 6. Ballast particle size distribution limits

Sieve size (mm)	Percentage weight passing (%)
63	100
50	70-100
40	30-65
31.5	0-25
22.4	0-3
32-50	> 50

The selected ballast material used in this research was in the range of the industry requirements provided by Network Rail and the size was measured using a dry sieve analysis method (BS1377: Part 2, 1990). The particle size distribution curve is presented in Figure 3.1. In the case of the small-scale tests about 3 kg of ballast was used in each test, forming a height of approximately 75 mm.

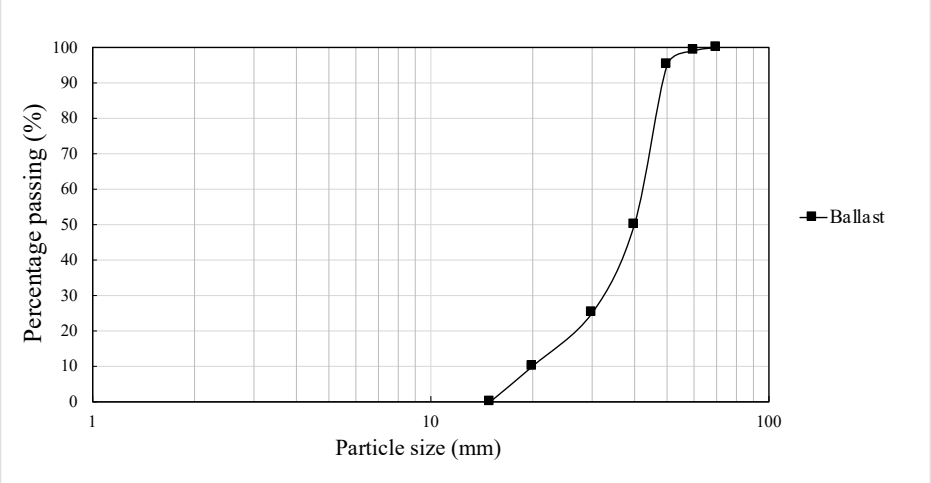


Figure 3.1 Ballast particle size distribution, (BS1377: Part 2, 1990)

3.3.2 Under sleeper pad (the USP)

The USPs are the highly elastic pads made of Sylomer and were used as a layer between the sleeper and the ballast layers. The main application of the USP is improvement of track geometry quality. The SLB-type elastoplastic pads are used to reduce the load on the ballast. The optimised material properties of these types permit a particularly stable embedding of the ballast. The high damping of these pad types has a positive effect on the vibration behaviour of the sleeper. Based on discussions with Getzner Werkstoffe GmbH, the static bedding modulus of the USP was selected at 0.36 N/mm3. This corresponds to resultant static spring stiffness 70 MN/m when applied to half the bottom surface area of the sleeper. The bedding modulus was chosen as it represents typical values for a USP with medium stiffness. The technical data is presented in the Appendix.

3.3.3 Geotextile

The Geotextile (geocomposite), specifically designed to reduce the migration of fines from the subgrade soils, was placed between the subgrade and ballast layers. It was a bonded three-layer

sandwich of geotextile materials designed to permit the passage of water through the composite and filter out the bulk of the soil fraction finer than 0.002 mm. The material was provided by the manufacturer for research purposes and for reasons of confidentiality no further technical details can be revealed here. The description of material and its key properties are listed below, and further information cannot be given for confidential reasons.

Unit weight (g/m2)	1375
Thickness (mm)	5.7
Tensile strength (kN/m)	44
CBR puncture resistance (N)	8750

(https://www.terramgeosynthetics.com/market-sector/railways/?aaopen=preventing-clay-pumping).

3.3.4 Subgrade soil

Cohesive soils may have unpredictable behaviour such as shrinking and swelling (Dasog et al., 1987). According to Thomas et al. (2000) clayey soils, with clay contents exceeding 60% have high or very high shrink–swell potential. After a thorough literature review, it was found that the previously published research works usually investigated one type soil with one moisture content (Table 4). To better understand the behaviour of cohesive soil subjected to cyclic loading it was decided to test a broader range of cohesive materials, medium and high plasticity clays were tested, each of them with three different moisture contents.

Considering the number of tests, it was not practical to use undisturbed *in situ* clay in this research, instead it was decided to use some bulk soils, which are common in the UK (London clay, Etruria marl) and some manufactured soils (china clay, bentonite). These naturally cohesive soils can be found as a selected subgrade material in the railway industry. It was also decided to test one synthesized soil (a mixed soil of china clay and 5% bentonite). The moisture

content could affect the behaviour of the cohesive soil (Craig, 1997); therefore, each soil was tested with three different moisture contents. All tested soils are commercially available in the UK. The advantage of the manufactured clay was the standard and the high quality of the provided material, guaranteed by the manufacturer. It gave a consistency to the soil samples, which allowed the same high-quality subgrade soil specimens for the laboratory investigations to be repeatedly made. The supplier of the English china clay was the Tolsa Company. The Berkbent 163 bentonite, a sodium carbonate activated type with a percentage of weight retained on 150 μm of 5%, was chosen for the mixed soil. The London clay and Etruria marl soils were taken from the Civil Engineering laboratory of the University of Birmingham, the materials were stored in a bulk condition. The London clay was supplied by Potclays Ltd, UK and Etruria marl was supplied by Wienerberger Ltd, Sandown Works, Aldridge, Walsall, UK.

3.4 Soil classification tests

Soil characteristics are highly variable and complex; they depend on several factors such as particle size distribution, plasticity and liquidity limits, unit weight, specific gravity, compaction, organic and salt contents. The main tests that were considered for the analysis are soil classification, identification of their strength and compressibility (soil stiffness), and the soils' permeability. The range of the preliminary classification tests, the Atterberg limits, the index test, hydrometer analysis, specific gravity (Gs), compressibility and permeability were done in accordance with BS 1377-2:1990.

3.4.1 Atterberg limits

According to Vardanega and Haigh (2014) Atterberg limits describe changes in the behaviour of cohesive soils with varying water content. They are widely used as index parameters to compute the plasticity index, which can be empirically correlated against many soil properties in geotechnical design. Perhaps the most famous of these correlations is Casagrande's A-line which classifies soils into clays and silts based on a correlation between soil type and a combination of liquid limit and plasticity index (Casagrande, 1947). The plasticity index has been used to predict undrained shear strength (Skempton, 1954 and 1957); the ratio of strength to Standard Penetration Test (SPT) blow count (Stroud, 1974). The bearing capacity of cohesive soils depends on soil plasticity (Das, 1997); thus, it was important to identify the Atterberg limits as they show the upper plastic limit when the soil is plastic and the lower plastic limit when the soil changes its state to liquid. The plasticity index (PI) is also known as the main determinant of soil plasticity. It is a difference between the liquid limit (LL) and the plastic limit (PL): PI = LL – PL. These characteristics were obtained according to the British Standard specifications (BS 1377- 2:1990). Another key soil parameter is the liquidity index (LI), which gives information about the soil state and the soil's behaviour (plastic, brittle or liquid). Equation 3.1 shows how the LI could be measured.

$$LI = (w - PL) / (LL - PL) \qquad \text{Equation 3.1}$$

When LI > 1 the condition of the soil is liquid; and when LI < 0 the behaviour of the soil is bitter soil (dry and firm). The soil behaviour is plastic when 0 < LI < 1. The summary of the Atterberg limits including the liquidity index and the optimum moisture content (%) is given in Table 7. The values of the LL and PL of each investigated soil were plotted on the Casagrande plasticity chart (Figure 3.2). According to the Casagrande chart, the tested soils

could be identified as inorganic clays with intermediate plasticity. The data is presented in Appendix.

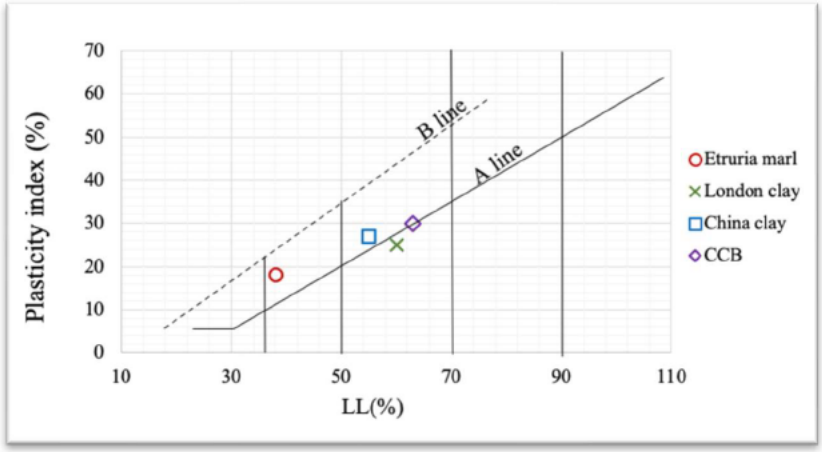


Figure 3.2 Casagrande plasticity chart (after Barnes, 2016)

Table 7. Summary of Atterberg limits of investigated soils

Soil	OMC %	w %	Liquidity Limit %	Plasticity Limit %	Plasticity Index %	Liquidity Index
Etruria marl	80	14	38	18	20	-0.2
	100	17	38	18	20	-0.05
	120	21	38	18	20	0.15
London clay	80	17	60	25	35	-0.22
	100	21	60	25	35	-0.11
	120	25	60	25	35	0.1
china clay	80	25	55	27	28	-0.7
	100	30	55	27	28	0.11
	120	35	55	27	28	0.28
CCB 5%	80	26	63	30	33	-0.12
	100	32	63	30	33	0.06
	120	38	63	30	33	0.24

The tested soils had different plasticity characteristics. Where Etruria marl is medium plasticity clay, English china clay, London clay and the mix of kaolinite and 5% bentonite correspond to high plasticity clays.

3.4.2 Particles' size distribution

Based on the size of the soil particles, their gradation, and the proportion between different sizes of particles, a tested soil could be identified as uniformly graded, well graded or poorly graded. Das (1997) stated that from the nature of the particle size distribution the permeability of soil could be estimated. Hydrometer analysis was conducted to determine the particle size distribution of the cohesive soils (BS 1377-2:1990). A measured amount of dry soil powder was mixed with distilled water and sodium hexametaphosphate (the dispersant solution) in a 1-litre glass measuring cylinder. The dispersant component was used to split the cohesion of the individual particles. The glass cylinder was placed in a warm water bath with a constant temperature (24-26 °C) for a period of 24 hours. The readings were taken with the following time intervals: 0, 0.5, 2, 4, 8, 30 minutes and 1, 2, 8, 24 hours. According to BS 5930: (1999) the investigated soils could be characterised as medium plastic clays. The results show that about 70% of the tested materials was larger than 0.005 mm (the range representing the fine silt materials) and about 30% was in a range of clay materials (Figure 3.3). Results showed that about 50 % of the material was in the fine silt range and 50 % was clay (less than 0.002 mm).

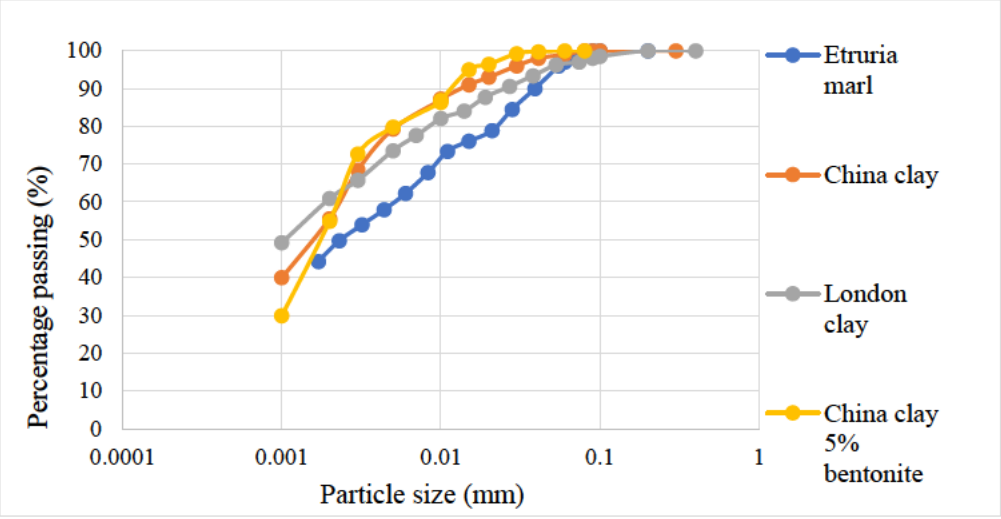


Figure 3.3 Particle size distribution

3.4.3. Specific gravity

Specific gravity (Gs) was measured according to BS1377-2: 1990. The found values of the Gs of the tested soils were in a range between 2.61 and 2.79, which corresponds to the usual values for cohesive soils. They are presented in Table 8.

Table 8. Specific gravity (Gs)

Tested Soil	Specific Gravity (Gs)
Etruria marl	2.79
London clay	2.68
china clay (kaolinite)	2.61
china clay (95%) + bentonite (5%)	2.64

3.4.4. Compaction test (y_d/OMC)

One of the objectives of the research was to study the behaviour of subgrade soils under dynamic loading with different moisture contents. With an increase of moisture the density of the soil changes; the compaction curve enables the identification of the density of the soil at any moisture content. It illustrates the correlation between dry density and moisture content. A precise amount of water was added to dry, pre-sieved clay and mixed to receive the required moisture content. The range of the moisture content was chosen starting from a low value and gradually increasing by 5% up to the liquid limit (the Appendix). At the beginning of each test, the mass of the mould was measured with and without the extension. Following that, the soil was compacted by a 2.5-kg hammer in three equal layers. To compact each layer 27 blows of the hammer were completed. The tests were conducted following BS1377-4: 1990 and were repeated three times to confirm that the results were repeatable. The compaction curves of Etruria marl and London clay are presented in Figure 3.4 and 3.5 respectively, and Figure 3.6

shows the compaction curves of china clay and the mixed soil of 5% bentonite and china clay. The compaction curves of the two soils were combined in order to indicate the difference in the characteristics between two similar soils. Data of the maximum dry density and OMC of all tested soils is presented in the Appendix.

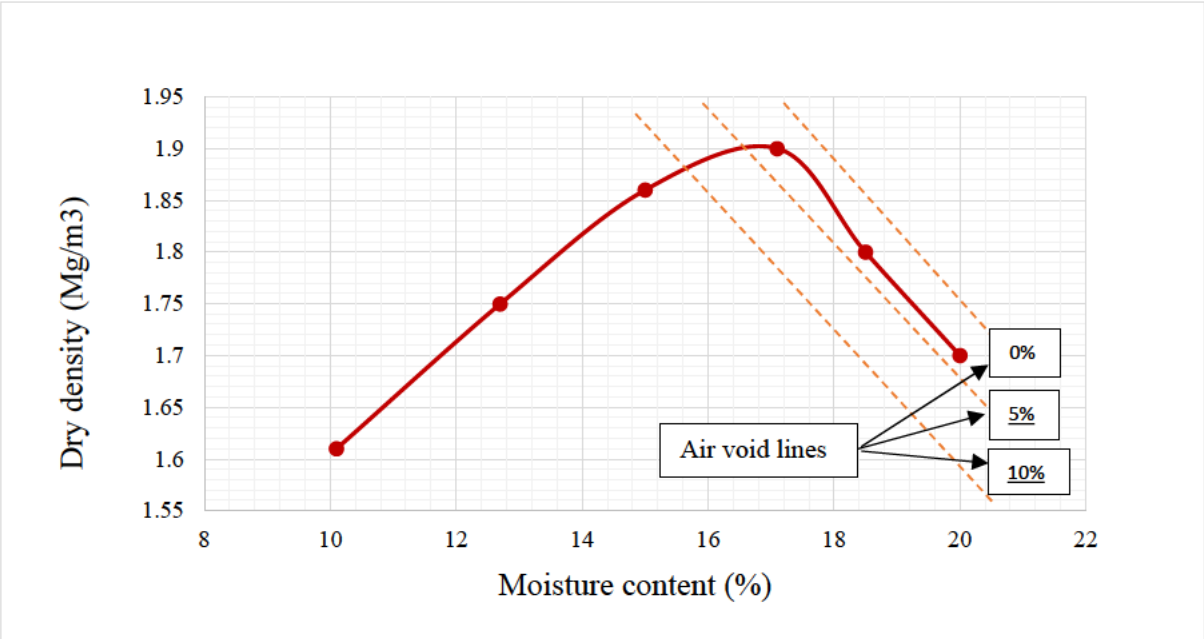


Figure 3.4 Compaction curve of Etruria marl

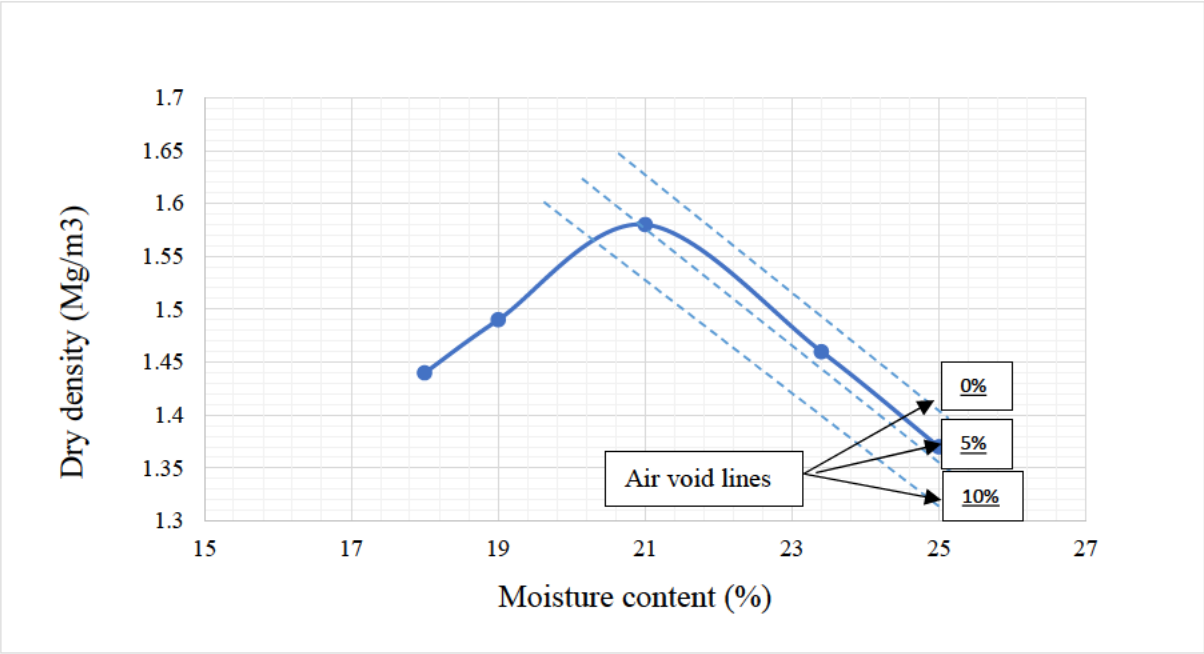


Figure 3.5 Compaction curve of London clay

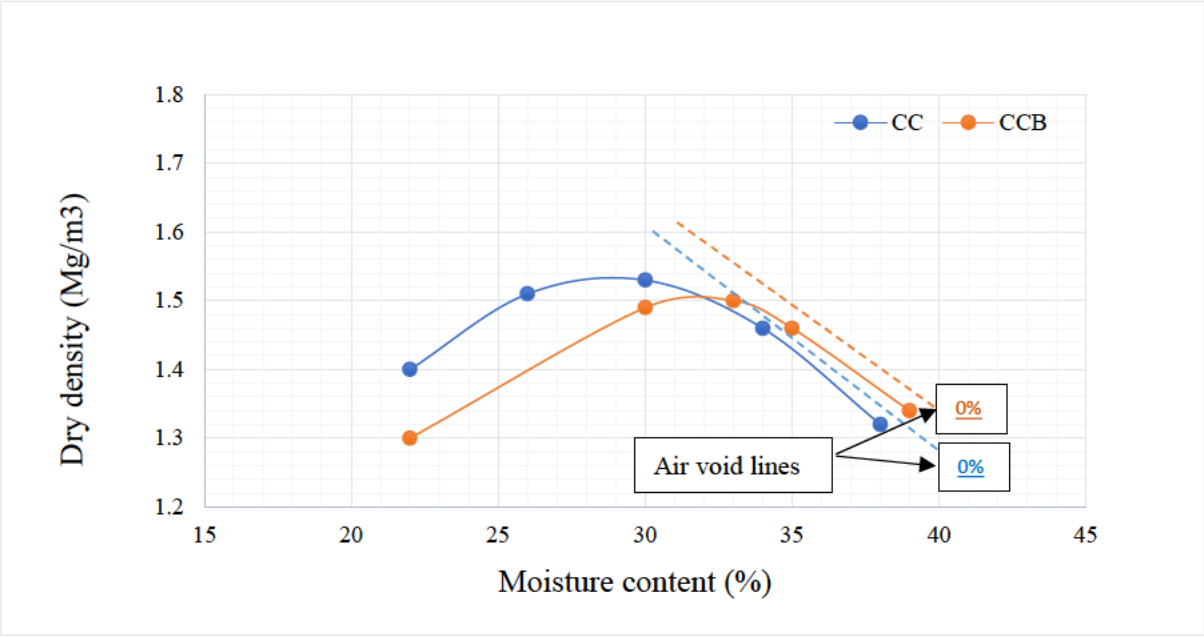


Figure 3.6 Compaction curves of china clay and 5% bentonite mix

3.4.5 Shear strength of the tested soils

According to Poulos (1989) basic soil characteristics such as its minerology, particle size distribution, the shape of particles, the void ratio and pore water greatly affect the ability of a

soil to sustain shear stress. The strength of the soil depends on its structure, the arrangement of the particles (consolidated or over consolidated soil) and the state of the soil (undisturbed or disturbed). Other conditions such as the magnitude, the rate and the time of the loading (static or dynamic, monotonic or cyclic) also affect the strength of the soil. The undrained shear strength of cohesive soils can lie in a range from extremely low to extremely high (Table 9). The shear strength in this study was determined using the shear vane test (BS1377: Part 7: 1990). The strength of the soil was measured at different depths before conducting the small-scale test. It was done to control the quality of the prepared clay bed. During soil installation the clay was tested at different positions and depths with a 12.7-mm hand vane. The strength of the subgrade soil was measured before and after each test in different locations to gather data for further analysis of the changes. The soil strength was also measured by a soil penetrometer in order to cross-check the obtained values. A penetrometer allows the quick measurement of unconfined compressive strength, and shows values ranging from 0 to 4.5 tsf, which is equal to a range from 0-450 kPa. The readings were taken under contact points of the subgrade and the ballast, as well as between the ballast rocks, at different points in order to achieve accuracy and obtain the correct value. The equipment gave the value of the soil strength in kg/cm^2, which was converted to kN/m^2.

Table 9. Undrained shear strength of clays (BS EN ISO14688-2:2004)

Undrained shear strength of clays	Undrained shear strength, Cu (kPa)
Extremely low	<10
Very low	10-20
Low	20-40
Medium	40-75
High	75-150
Very high	150-300
Extremely high	>300

The values of the undrained shear strength of the tested soil are given the Appendix and will be used and discussed later in Chapter 4. The measurements were taken at least three times, they had a variation of ± 1 kPa, the average undrained shear strength was taken. Figures 3.7-3.10 show the undrained shear strength values of four tested clays and obtained before conducting the main investigation. The results demonstrate the trends where the undrained shear strength declines with an increase of moisture content in all the tested soils; the data will be later used in the analysis in Chapter 4.

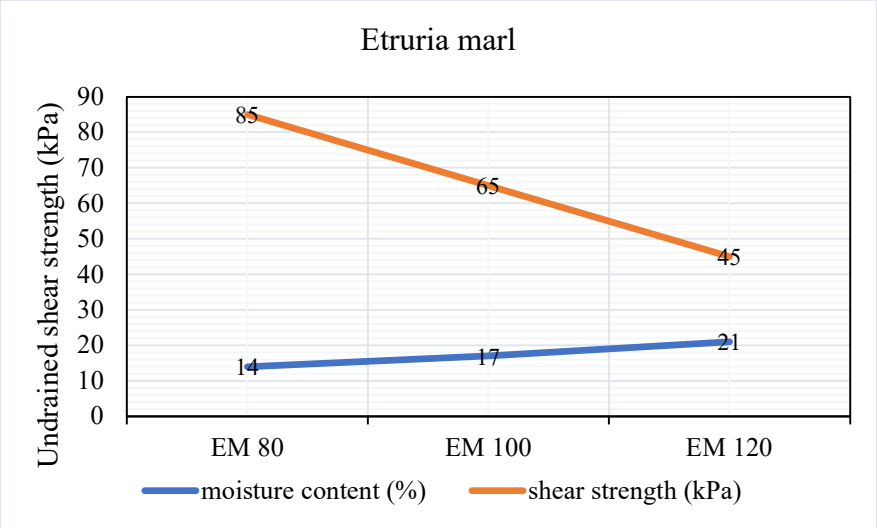


Figure 3.7 Relationship between moisture content/undrained shear strength, EM

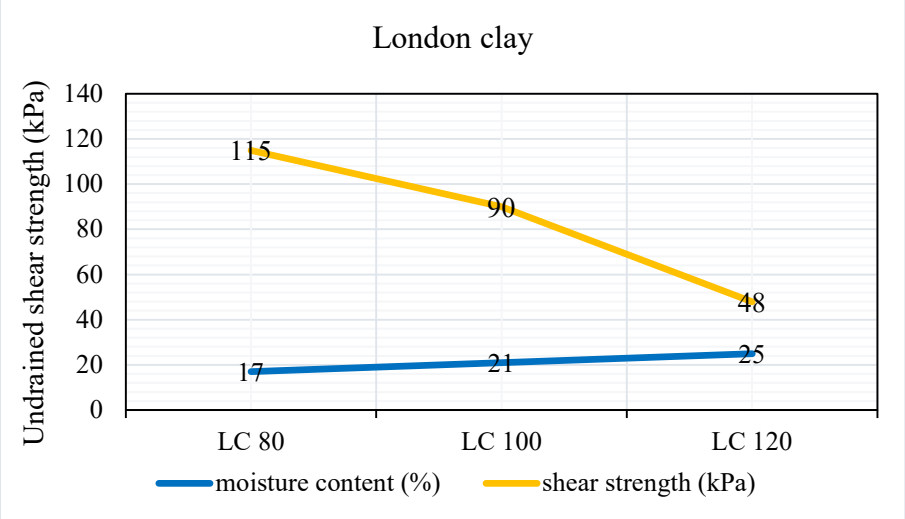


Figure 3.8 Relationship between moisture content/undrained shear strength, LC

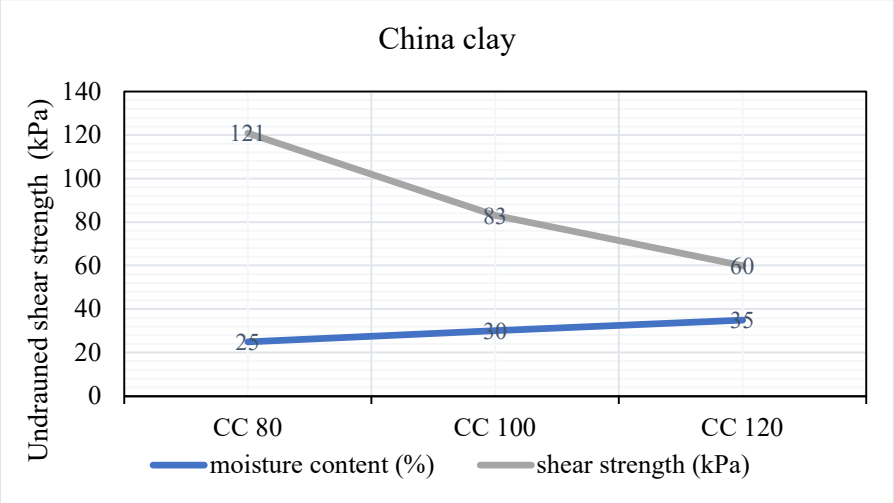


Figure 3.9 Relationship between moisture content/undrained shear strength, CC

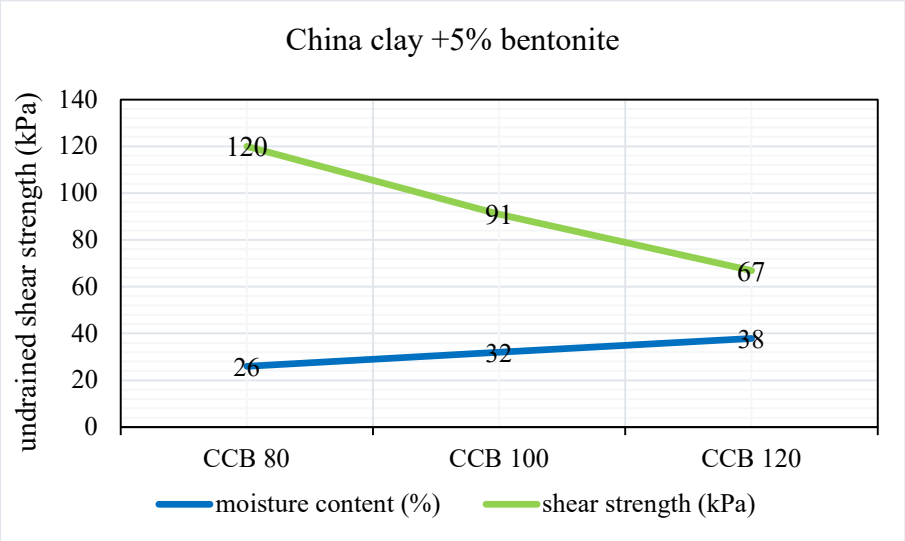


Figure 3.10 Relationship between moisture content/undrained shear strength, CCB

3.4.6 Consolidation test

The susceptibility of the tested soils to compression under loading conditions was measured using a one-dimensional consolidation test (the odometer apparatus). The apparatus enables the study of the compression behaviour of the soil under different loads and also assists in

finding the coefficient of soil permeability. The test was completed following British Standard requirements and explained in BS 1377-5:1990. Three physical parameters were measured c_v, m_v and k, they will be described in the following section.

The coefficient of consolidation (cv) is the rate of volume change (m^2) per unit of time (year) and is found using Equation 3.2:

$$c_v = \frac{T_{v90} {h_d}^2}{t_{90}}$$ Equation 3.2

where T_{v90} is the time factor of 90% consolidation and equals 0.848; h_d is the path of drainage and t_{90} is 90% of the consolidation time. The coefficient of volume compressibility (m_v) is obtained from Equation 3.2. The unit m_v is (m^2/kN), where the effective stress increment is:

$$m_v = \frac{\Delta h}{h_0} \frac{1}{\Delta \sigma'}$$ Equation 3.3

$$c_v = \frac{k}{m_v \gamma_w}$$ Equation 3.4

The soil samples were prepared in a ratio of 1.5*LL (Head, 1996; Sivakumar et al., 2004b). The saturated soil sample was left for 24 hours under the load (5 kPa). Following that, the load was gradually increased in the following steps 25 kPa, 50 kPa, 100 kPa, 200 kPa and 400 kPa (BS 1377-5:1990). After each load, the soil sample was reloaded and the reading of the settlement value of the recovered soil was taken. The settlement readings were taken at a certain time period as described in the BS.

Table 10. General values of m_v (Barnes, 2001)

Type of clay	m_v (m2/MN)
Very stiff, heavily over-consolidated clay	< 0.05
Stiff over-consolidated clay	0.05–0.1
Firm over-consolidated clay, laminated clay, weathered clay	0.1–0.3
Soft normally consolidated clay	0.30–1.0
Soft organic clay, sensitive clay	0.5–2.0
Peat	> 1.5

3.4.7 Permeability test

In general, cohesive soil clays and silts have low permeability. It depends on the particle size distribution and the viscosity of the water. Well graded materials give a lower permeability value; whereas the value is higher if the soil contains more voids. An assumption was made that each soil was fully saturated and homogeneous. When the compression and flow are one-dimensional, m_v, c_v and the coefficient of permeability are directly related to each other (Craig, 1997). Table 11 presents the values of the coefficient of permeability of different soils (Aysen, 2002). In this research, the coefficient of permeability (k) of each of the soils was determined as specified by BS 1377-5:1990. One of the methods to find the soil permeability is from Equation 3.5; where, y_w is the unit weight of the water (Craig, 1997). The coefficient of permeability k (m/s) is measured based on the c_v and m_v results.

$$k = c_v * m_v y_w * 3.17*10^{-11} = c_v m_v * 3.17*10^{-10}. \quad \text{Equation 3.5}$$

Table 11. Coefficient of permeability values

Types of soil	Coefficient of Permeability (m/s)
Clean gravels	$1- 10^{-2}$
Clean gravels, clean sand and gravel	10^{-2}-10^{-5}
Very fine sands, organic and inorganic silts, mixtures of sand, silt and clay	10^{-5}-10^{-9}
Clays	10^{-9}-10^{-11}
Well drained soils	1-10^{-6}
Poorly drained soils	10^{-6}-10^{-8}
Practically impervious	10^{-8}-10^{-11}

The settlement curve was plotted and the values of c_v, m_v and k were found (Appendix). The results of compressibility, consolidation coefficients and permeability are presented in Table 12. The obtained values are similar to values of typical normally consolidated clays. The average value of permeability obtained is 1.83 x 10^{-8} cm/s. This value is within the range of values in the literature (Barnes, 2016).

Table 12. Results of consolidation test

Soil	c_v (mm^2/min)	m_v (m^2/MN)	k
Etruria marl	19.4	0.71	$2.2*10^{-9}$
London clay	13.2	0.79	$1.55*10^{-9}$
china clay	27.2	1.13	$7.65*10^{-9}$
china clay 5% bentonite	24.6	1.04	$5.71*10^{-9}$

3.4.8 Organic content test

The presence of organic materials significantly affects the characteristics of cohesive soils. It increases clay plasticity, compressibility, hydraulic conductivity (Odell et al., 1960), and decreases the value of specific gravity (Puppala et al., 2007). It reduces soil strength and makes soil more susceptible to swelling and shrinkage (Franklin et al., 1972; Santagata et al., 2008).

According to Edil (1997), the behaviour of cohesive soils(clay/silt) varies depending on the percentage of organic matter. For instance, if it lies in a range 6-20% then the soil behaves as a mineral soil, however the behaviour changes significantly once the percentage of organic content exceeds 20%. According to BS EN ISO 14688 – 2:2004, soils are classified based on the organic content (Table 13).

Table 13. Classification of soils with organic content

Soil	Organic content (< 2 mm) % of dry mass
Low organic	2-6
Medium organic	6-20
High organic	> 20

In order to measure organic content (OC), firstly the samples of tested soils were taken to obtain the moisture content. The weight of the dry soil was taken after placing the specimen at 105 ^{0}C and another at 440 ^{0}C. Equation 3.6 enables the determination of the OC of tested soils; W_{105} is the weight of the dry soil specimen after 24 hours at 105 ^{0}C; W_{440} is the weight of the dry soil specimen after 24 hours at 440 0C. The obtained results are presented in Table 14.

$$\%OC = \frac{w_{105} - w_{440}}{w_{105}} X100$$

Equation 3.6

Table 14. Organic content

Soil	Organic content (< 2 mm) % of dry mass
Etruria marl	3
London clay	2
china clay	<1
China clay +5% bentonite	<1

3.4.9 Void ratio

The void ratio characterises the compactness of soils. The value of the void ratio depends on the volumetric changes of the soils (the void ratio of loose soils is higher than that of dense soils). According to Das (2009), the range of the void ratio between 0.9 to 1.4 corresponds to soft clay and stiff clays have a ratio of 0.4 to 0.6.

Table 15. Combined data of Specific Gravity and void ratio

Soil	*w (%)*	*Gs*	*e*
Etruria marl	14	2.79	0.39
	17		0.47
	21		0.58
London clay	17	2.68	0.45
	21		0.56
	25		0.67
China clay	25	2.61	0.65
	30		0.78
	35		0.91
5% mix	26	2.64	0.68
	32		0.84
	38		0.98

3.4.10 Discussion

To understand the behaviour of the subgrade subjected to cyclic loading it was necessary to test a broader range of cohesive soils. Four soils were tested to determine their properties, which then were input into an analysis of the subgrade's performance. A range of laboratory tests was completed, and an explanation of the conducted tests and procedures was given in Section 3.2. All soils have been tested for their index properties. The liquid and plastic limit tests were performed, and the details have been presented in Table 7. Plasticity tests indicate the cohesive units of the soil EM to be medium plasticity , CC, CCB and LC to be of high

plasticity typically, with plasticity generally between 50 to 60% (Figure 3.2). Compaction tests were carried out to determine the optimum moisture content (OMC) and maximum dry density (MDD). The maximum dry density and optimum moisture content tabulated in Table7 show that adding 5% of bentonite does not have a significant impact on the MDD; however, there is a small increase in the OMC. The maximum dry density of CC and CCB were in the range of 1.51 to 1.53 kg/m^3, with the optimum moisture content at 30 to 32%. The maximum dry density of LC and EM were in 1.58 and 1.88 kg/m^3, with the optimum moisture content at 21and 17% respectively. The results were used as guides for preparing subgrade soils for the hole erosion test, the small-scale test and the large-scale test, where the specimens were prepared at OMC and ± 20% of OMC. As later was seen , the EM and LC soil could be generally compacted to higher dry densities than the CC and CCB soils

Figure 3.3 shows the particle size distribution (PSD) of the soils used in this study. The PSD analysis showed high silt and clay content, the tested soils could be described as silty clays.

The results of the specific gravity tests were shown in Table 15, which was reported in the range 2.61-2.79 that is in the typical range mentioned for clays (Head, 2006). This value was used in the calculations of the degree of saturation and void ratio of the clays, which later is used in Chapter 4 in the discussion of the results of the small-scale test. Void ratio characterises the compactness of soils. The value of the void ratio depends on volumetric changes of soils (the void ratio of loose soils is higher than that of dense soils). According to Das (2009) the range of the void ratio between 0.9 and1.4 corresponds to soft clay and for stiff clays is 0.4-0.6. As can be seen from Table 15 the void ratio of soils CC and CCB was generally higher in contrast to EM and LC; that could explain the higher rate of permanent deformation of the CC and CCB soils, which will be discussed later in Chapter 4.

Permeability of cohesive soils depends on the particle-size distribution and the viscosity of the water. In general, cohesive soil have low permeability. Well-graded materials give a lower permeability value; whereas the value is higher if the soil contains more voids. The obtained results of all four soils were in the range of 1.5 to 7.5 *10-9 which is described as low permeable (Table12).

The presence of organic materials significantly affects the characteristics of cohesive soils. It increases soil plasticity, compressibility, and hydraulic conductivity (Odell et al., 1960); and decreases the value of specific gravity (Puppala et al., 2007). It reduces soil strength and makes soil more susceptible to swelling and shrinkage (Franklin et al., 1972; Santagata et al., 2008). According to Edil (1997), the behaviour of cohesive soils varies depending on the percentage of organic matter. For instance, if it lies in the range of 6 to 20% then the soil behaves as a mineral soil; however, its behaviour changes significantly once the percentage of organic content exceeds 20%: when the initial void ratio (e_0), optimum moisture content (OMC), and compression index (Cc) increase. According to BS EN ISO 14688 – 2:2004, soils are classified based on their organic content (Table 14). The results show all four tested soils have low organic content.

The susceptibility of the tested soils to compression was measured using a one-dimensional consolidation test (the odometer apparatus). Three parameters were measured c_v, m_v and k; and described in the following Section 3.4.7. As can be seen from Table 10, the compressibility of the soils CC and CCB was higher compared to the soils EM and LC, the result will be used later in discussion of subgrade permanent deformation.

The shear strength in this study was determined using the shear vane test (BS1377: Part 7: 1990). The test was carried out to assess the sensitivity of different soil types to moisture changes. The test is also used to develop correlations with other properties of the tested

subgrade soils for design purposes. The results demonstrate the trends where the undrained shear strength declines with an increase of moisture content in all the tested soils. The results show the sensitivity of soils with high proportions of sand and silt to moisture changes. Soil CC, while it is weaker than the other two soils with the optimum dry and optimum moisture contents, shows a higher compressive strength at the optimum wet condition. This is shown not only for strength but also for a higher resistance to axial deformation, where it undergoes 2.5% axial strain. This trend is demonstrated in Chapter 4 more clearly through the permanent deformation test results. The values of the undrained shear strength of the tested soil were given and will be used later in Chapter 4.

This section presented the characteristics of materials used in the research. The required procedures for different tests carried out were described in detail. The details of the measurements and calculations have been presented in the Appendix. It was important to understand the aspects of the results which can assist in interpretation of the behaviour of the subgrade soil under cyclic loading. A comparison of the materials used in this research with each other was possible using obtained data. The next stage is to analyse these materials in the context of applying cyclic loading, which has been discussed in Chapter 4.

3.5 Determination of soil erodibility

Some types of cohesive soils are more susceptible to erosion and this erosion process takes less time. This is especially true for dispersive soils, where the force required to remove the soil particles is usually very low. According to Sherard et al. (1976a), dispersion is a process when clay particles go into suspension practically in still water. Mitchell (1993) stated that the dispersion of cohesive soils depends on factors such as clay mineralogy, salt, and sodium content. Therefore, identifying the dispersibility of the tested soils was an important step before

conducting the main experiments. Conventional soil classification tests cannot give information about the soil's susceptibility to dispersion; therefore, special tests are required such as the hole erosion test (HET) and the crumb method (BS 1377-5:1990). A simple classification test based on visual observation of soil coherence in water was introduced by Emerson (1967) and is called the 'crumb test'; it was later modified by Atkinson et al. (1990). The improvement of the crumb test meant could evaluate the soil's behaviour at zero effective stress. When the sample is put under a fully saturated condition in water, and this is called a 'cylinder dispersion test'. Sherard et al. (1976b) developed a laboratory test called the pinhole test to directly assess the dispersivity (colloidal erosion) of compacted clay soils. It involved the flow of distilled water through a 1.0-mm diameter hole of a compacted specimen. Dispersive clays were identified when the outflow was cloudy. The interparticle forces and shear strength decrease when the surface of cohesive soil is swollen, which increases the erodibility process. Dispersive soils (those clays where the fine surface particles could disassociate without any water flow) behave differently. The relationship between the plasticity index, the clay content and the soil erodibility is presented in Figure 3.11 (Reséndiz, 1977). It shows the area, marked between A= 0.3 and 1.0 as a zone of soil featuring potential susceptibility to piping.

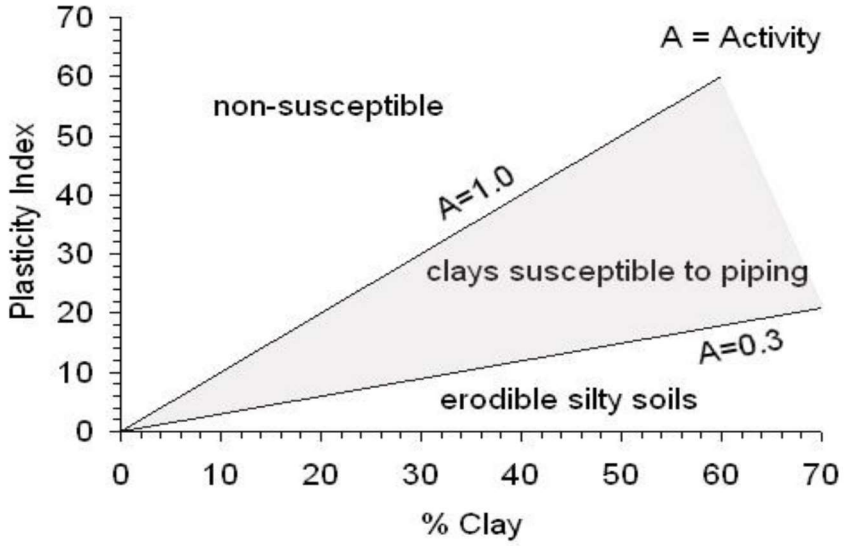


Figure 3.11 Clay activity in embankments failed by piping (Reséndiz, 1977)

Clay dispersion also depends on its salt content. Perry and Postol (1977) studied the relationship between sodium salts and total salt content, the sodium absorption ratio (SAR); and found that clays containing a high sodium content compared to the total dissolved salts are dispersive. According to Anandarajah and Zhao (2000), the presence of cations in terms of both the type and concentration of ions in the pore water significantly affects the susceptibility of clays to dispersion. The erosive effect of water increases with a decrease of the level of ion concentration. The total salt content in the water also has an important effect on the dispersity of soils. Figure 3.12 illustrates the correlation between the level of sodium and salt and their influence on the interparticle structure that holds clay particles together. The clays with low salt concentration could become more dispersive if the lower sodium (%) content increases.

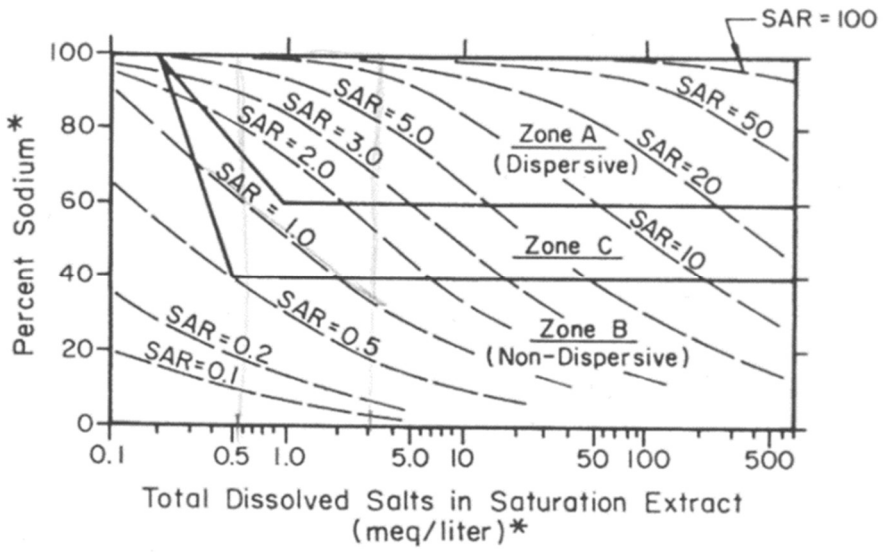


Figure 3.12 Soil dispersion chart (Perry and Postol, 1977)

3.5.1 Crumb test

Dispersive characteristics of clay soil depend on its initial moisture content, the intrinsic properties of the soil's materials and water chemistry. One of the methods that is often used to quickly identify dispersive clays is the crumb test; where dispersibility is decided depending on their performance in a sodium hydroxide solution. The sample should be kept at the field moisture content and the sample's behaviour will identified according to the classification stated in the BS code 1377-5:1990. Four mechanisms contribute to the disruption of soil crumbs (Emerson, 1964). These are hydration, de-aeration, osmotic swelling and dispersion.

1. Hydration and de-aeration are the primary mechanisms causing the disintegration of dry soils' crumbs. These dry soils are disrupted violently as water molecules return to their energetically favoured site on the particle surface. As the hydra front penetrates the soil, air is pushed ahead and collects within the interior under positive pressure. This pressure acts to further disturb the integrity of the crumb. This process of hydration and de-aeration continues

until the fragment is wetted completely and all air bubbles have escaped. The result is a residual pile of soil materials with no trace of its original structure. This process is very rapid and completes within a short time.

2. Osmotic swelling and fracturing: osmotic swelling pressure arises when iron concentrations within the soil phase are greater than in the ambient solution. Water moves into the soil to reduce the concentration difference and the soil consequently expands. It may occur in relation to two distinct sources of iron concentration: (a) free salts of the pore water; or (b) the ion swarms neutralized by charges located within the soil particles. Osmotic pressure can be relieved by the streaming of the solution out of the soil mass and by diffusion of salt from the soil into the solution. Streaming is sometimes accompanied by dispersive soil particles, forming a deltaic dispersion pattern. Streaming or diffusion of the irons cannot relieve the osmotic potential developed by the bound ion swarms. The soil consequently retains the imbibed water and swells. As swelling proceeds, the soil particles are progressively separated, and the attractive forces weakened. Dispersion occurs when swelling pressure is high enough to cause fracture between individual soil particles. Generally, dispersive conditions are evidence that sodium is present in the system and the other factors influencing the dispersive soils are salt concentration, soil PH and the initial moisture content.

3. Sodium: the effectiveness of sodium as a dispersive agent is related to ionic charges of plus one, calcium and magnesium ions with charges of plus two and aluminium ion charges of plus three. The reason for this sensitivity of dispersion to salt concentration is that the thickness of the ion swarms about the soil particles is controlled by this variable. As salt concentration increases ion swarm thickness decreases, until at some concentration, the repulsive interaction

between swarms occurs only at a distance within the range of stronger attractive forces. Above this salt concentration, attractive forces dominate, and particles do not disperse. High salt content inhibits dispersion by collapsing the ion swarm. Diffusion of salt out of the crumb will also increase the external salt concentration sufficiently to prevent dispersion, unless the ratio of water to soil is large enough.

The specimens used in these tests are: (i) compacted to get the maximum dry density at the optimum moisture content and with different moisture contents; (ii) have a moisture content and dry density taken according to the data from a previously conducted compaction test and compaction curve. The response of the soil is classified into four types (BS 1377-5:1990):

Grade 1. No response: remoulded crumb retains original size and shape.

Grade 2. Slumping: remoulded crumb disintegrates to form a structure pile with serrated edges.

Grade 3. Fracturing: crumb breaks into fragments, which retain their straight edges and create irregular shaped patterns.

Grade 4. Dispersion: dispersion crumb edges become diffused in initial stages. As it continues, crescents develop near the dish edge where shadow and colloid combine to provide enough contrast for the film to detect.

3.5.2 Hole erosion test

The hole erosion test (HET) is used to measure erosion with respect to the diameter of the specimen, the soil's friction factor, the shear stress and the rate of erosion (Figure. 3.13). In this test, some assumptions were made: the soil samples have a hole with a uniform cross section along the length; and the friction factor varies linearly with time between its initial and final value. In general, the non-plastic and low plastic soils are very susceptible to erosion and the erosion rate lies in a range between extremely to moderately; while plastic soils erode much

more slowly. Erosion is influenced strongly by the compaction parameter; the materials' compacted higher density has a low rate of erosion. Coarse-grained materials have low shear stress and the soils with fine grain materials have a low rate of erosion (Van C.F et al., 2002). Moisture content and the degree of compaction highly influence the erosion rate. The diameter is thought to be uniform after erosion takes place, but erosion normally takes place in the initial portion of the slot where the flow expands and imposes friction on the surface of the slot. The erosion increases from the inlet to a certain distance and thereafter decreases depending on the rate of flow and velocity. The development of tunnel erosion is associated with the presence of dispersive materials. Soils contain exchangeable sodium which causes them to break down when wet and release fine particles into the solution. Therefore, the dispersive clays rapidly erode producing turbid water; and non-dispersive clay soils produce little change in pinhole diameter size and clean water.

The boulder clay was oven-dried for 24 hours to prepare the laboratory specimens for the hole erosion test. The dried clay was sieved through a 425-μm sieve, and measured and mixed with distilled water in the required ratio, in order to get the exact moisture content (BS 1377-2:1990). Based on the initial aim to test different clays at a range of moisture contents, all four clays were tested at 80%, 100% and 120% of the optimum moisture content (OMC). Based on the data of the compaction curve, the calculated amount of distilled water was added to the dry clay and then mixed thoroughly and stirred until it became an homogeneous mixture. It was kept for 24 hours to attain the uniform moisture contents for the clay specimen. A 38-mm diameter mould was used for specimen preparation. The compaction curve data gave information about the required soil density; the volume of the mould was calculated as well as the recurred soil mass for that specific moisture content. Following that stage, the correct amount of material was placed inside the mould and the soil was compacted using a hand jack until it achieved the required density. Then it was wrapped in cellophane and stored for a

minimum of 24 hours inside the refrigerator to achieve soil saturation before being subjected to the erosion test. The sample's diameter was 38 mm, and the length was 80 mm; 60 mm of the length of the sample was taken for the erosion test and the balance of 20 mm was taken for moisture contents and other related tests. Each sample was taken for a moisture content test. For each specimen a brass cone was pushed into the specimen to align the specimen's longitudinal axis and subsequently a 1-mm diameter pinhole was made using a 1-mm hypodermic needle. Once the pinhole was made, the weight of the sample was measured. Figure 3.13 illustrates a schematic diagram of the HET. Upstream and downstream of the tested sample were pressure transducers and the flowmeter to measure the parameters at a predetermined time interval (Figure 3.14). At the upstream side was a gate valve that controlled the applied pressure. The dimensions of the specimen were 52 x 100-110 mm, the diameter of the made hole was 3 mm. In order to prevent leaks, rubber washers were placed on both sides of the transparent acrylic tube, which allowed visual observation of the erosion process. Prior to the test, the pipe system was de-aired by filling water under low pressure into the pipe system (1–3 kPa), with a flow rate of < 0.9 l/min and the air was released. The pump produces a maximum pressure of 350 kPa that generates the maximum flow rate of 30 l/min.

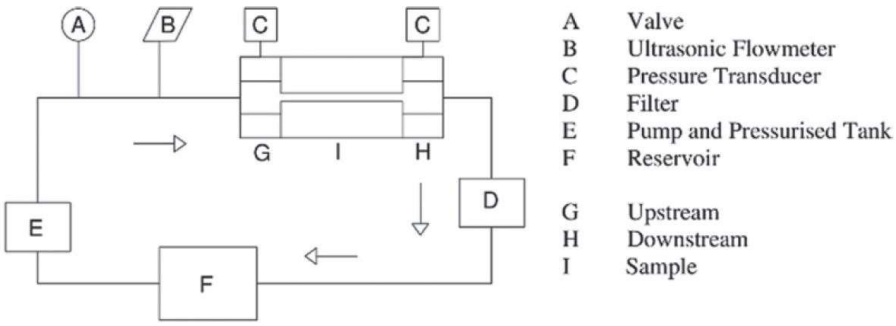


Figure 3.13 Schematic diagram of hole erosion test (Walenna et al., 2019)

Slowly opening the valve upstream and downstream allowed a deferential pressure of 5 kPa to be achieved. The recording intervals were set to per second, both for pressure and water flow rate. Depending on the clearness of the out flow with respect to the water head, the degree of dispersion is determined. To achieve accuracy, the test was repeated three times for each soil profile. After the test, the pipe system was dewatered and disassembled, and the carefully extruded specimen was air dried, cast by melted paraffin and left for approximately 10 minutes until it hardened.

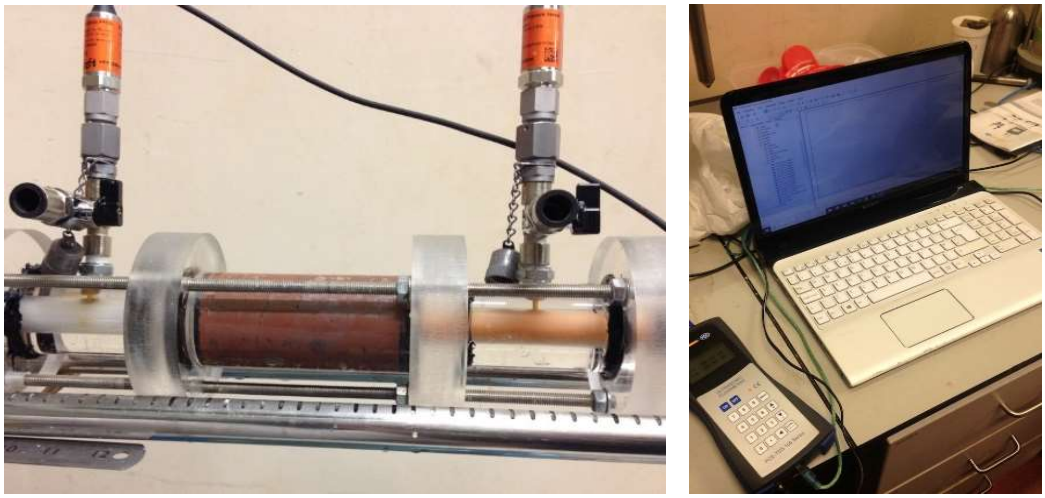


Figure 3.14 Hole erosion test apparatus (tested specimen and control station)

The cast paraffin was taken out (Figure 3.15) and its diameter was measured at five points. Following that, the volume of the eroded material was calculated as area (A) of the cross section multiplied by the length (l) of the specimen, V = A*l. The following calculation of the erosion rate was based on the known time and volume, E = V/t.

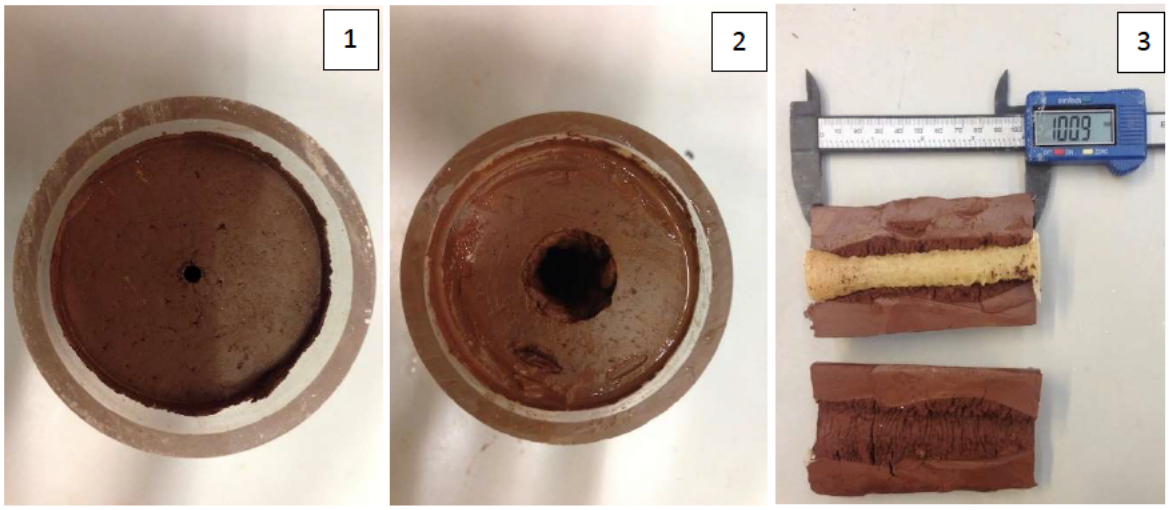


Figure 3.15 Specimen of Etruria marl during HET, before the test (1); after (2); cast (3)

The importance of the HET is that it gives information about the erosion rate of the tested soil with different moisture contents. The 1-mm hole was made with pin apparatus. The initial length of the specimen was 100 mm. The volume of the hole was measured knowing the area, and the length: $V_1 = A*l$ (where r – radius of the hole; A- calculated area; l- length of the sample). The test was run for 10 minutes. Following that, the specimen was cast with melted wax and the volume was calculated (V_2). The eroded volume V_{er} was calculated as V_2-V_1. The objective was to measure the amount of eroded soil after 10 minutes of running the test and compare the erodibility of the tested cohesive soils.

3.5.3 Results and Discussion

After placing the specimens into a dilute solution of sodium hydroxide and observing the reaction of the behaviour of the crumbs, the results indicated that all four clays showed no reaction (there were no signs of cloudiness caused by colloids in the suspension) or a slight reaction (a very slight cloudiness was seen). Figure 3.16 shows the specimens under the testing.

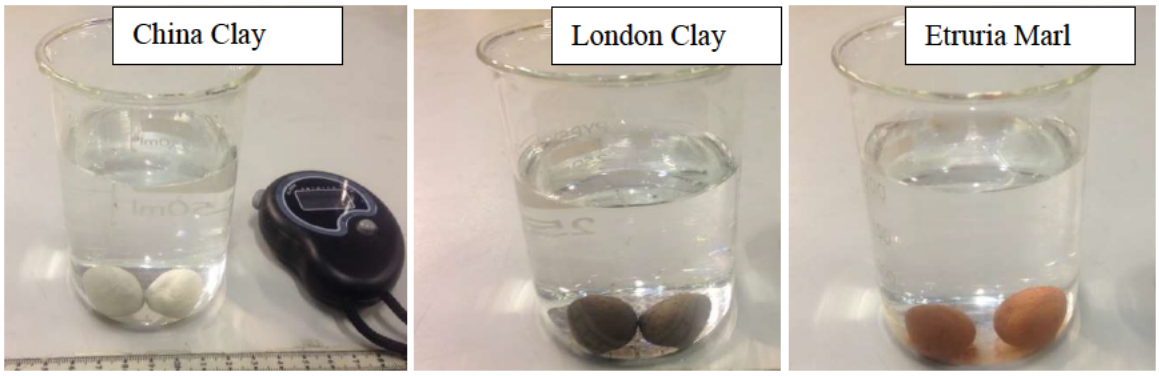


Figure 3.16 Crumb test, specimens of tested soils

All four tested soils showed non-dispersive behaviour (Grade 2) in a dilute solution of sodium hydroxide. However, Etruria marl and London clay exhibited non-dispersive behaviour (Grade 1) in distilled water. The soils of china clay and a mix of china clay and 5% bentonite showed non-dispersive behaviour (Grade 2) in both tap and distilled water (Table 16).

Table 16. Crumb test dispersion results, BS 1377-5:1990

	Etruria marl	London clay	China clay	China clay and 5% bentonite mix
Distilled water	Grade 1	Grade 1	Grade 2	Grade 2
Dilute solution of sodium hydroxide	Grade 2	Grade 2	Grade 2	Grade 2

Erodibility of the cohesive soil was tested using the hole erosion test (HET). Each soil was tested in a range of different moisture contents, 80%, 100% and 120% of OMC respectively. To gain accuracy each test profile was repeated three times. In total thirty-six tests were conducted. Overall, London clay showed the lowest rate of erodibility at different moisture contents (Table 17). The highest level of erosion was seen in china clay at 120% of OMC. A more detailed discussion will be given in Section 4.5.2.

Table 17. Results of hole erosion test

Soil	London clay			Etruria marl			China clay			5% bentonite mix, CC		
w (%)	OMC 80%	OMC 100%	OMC 120%	OMC 80%	OMC 100%	OMC 120%	OMC 80%	OMC 100%	OMC 120%	OMC 80%	OMC 100%	OMC 120%
Average diameter (mm)	7.35	7.97	9.1	13.2	13.5	14.2	10.14	11.26	15.17	10.01	11.10	14.72
V_1 (mm^3)	79.00											
V_2 (mm^3)	4241	4986	6501	13681	14310	15828	8071	9952	18065	7850	9672	17009
Eroded volume V_{er} (mm^3)	4162	4907	6422	13602	14231	15749	7992	9873	17986	7771	9593	16930
Eroded mass (g)	79	97	115	265	298	274	109	176	320	135	168	297
Erosion rate (g/min)	7.9	9.7	11.5	26.5	29.8	27.4	10.9	17.6	32	13.5	16.8	29.7

3.6 Small-scale test

Previously, researchers have tried to understand the problem by studying it in the laboratories and in the field. There were monitoring works and research studies conducted in the field (Raymond, 1986; Aw, 2007; Hudson et al., 2016, for example), which were useful to gather *in situ* data; however, there are obvious drawbacks of that method, such as the cost of the tests, the time consumed and the scale of the research. Alternatively, the railway track condition could be reconstructed in the laboratory, where, although the parameters are still the same as in industry itself (load, frequency etc.), the scale of the test rig is compact, which saves time and enables the testing of more conditions within the same period of time at a much more affordable budget. Previously, numerous research works have been conducted at the University of Birmingham investigating mud pumping phenomenon using the one-dimensional loading apparatus (Hoare, 1982; Alobaidi,1994; Ghataora, 2006). The choice of the same test apparatus was done deliberately. Firstly, it allows a comparison of the results of previously conducted

investigation works with current results (Mattsson, 2005; Ghataora, 2006). Secondly, a range of studies of mud pumping have been done at the University of Birmingham (Alobaidi, 1994), therefore the facility can be used along with the instrumentation, adding new test modifications which will be discussed further in this chapter.

3.6.1 Determination criteria of remediation solutions

The behaviour of subgrade soil with and without the USPs was investigated using existing test apparatus and modified test procedures (Figure 3.17). The following parameters were studied: permanent deformations, subgrade stiffness, development of pore water pressure and amount of eroded soil. The selection of these parameters could be explained because of their direct and indirect influence on the behaviour of subgrade soils. These parameters were constantly monitored during the test and the dynamic changes were investigated. The received data was later used for further analysis, finding the correlation between these parameters.

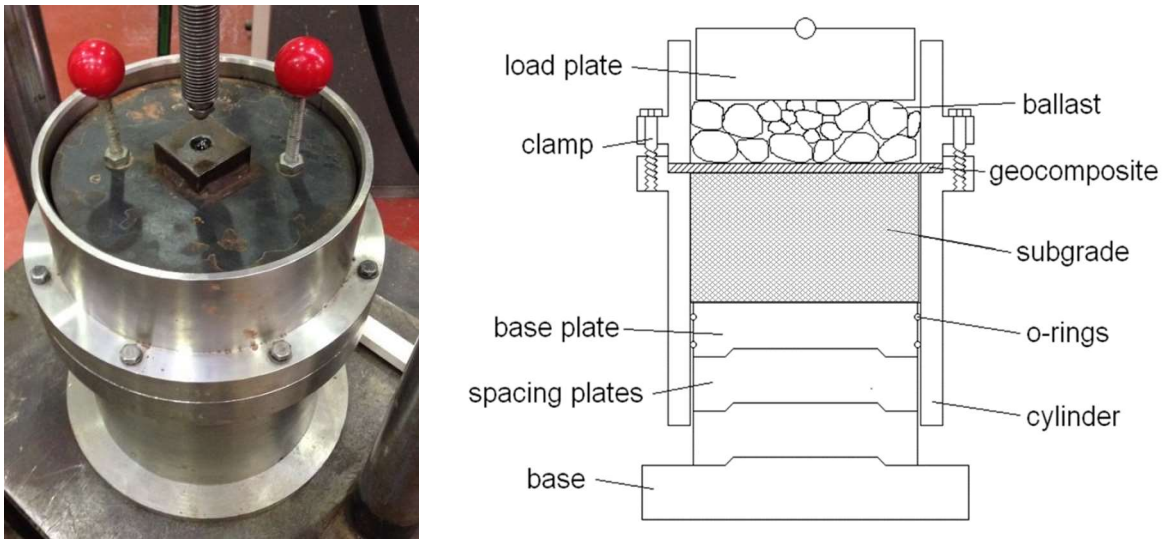


Figure 3.17 Layout of the small-scale test (Ghataora et. al. 2006)

3.6.2 Cyclic loading machine

Much of the developmental work was undertaken using a prototype test apparatus that was developed from the apparatus used by other researchers who previously conducted studies at the University of Birmingham (Snaith and Bell, 1978; Hoare, 1982; Alobaidi, 1994).

Using a hydraulic loading ram of 50 kN capacity, cyclic load was applied to the soil sample by a plunger to the rigid load plate, which allows the application of a static and dynamic load of a chosen frequency and amplitude. The machine contains three main parts, namely the control unit, the hydraulic components and the loading frame. The apparatus with a fitted digital/analogue board collects the data from the tests, a full description of the apparatus is provided in Figure 3.18.

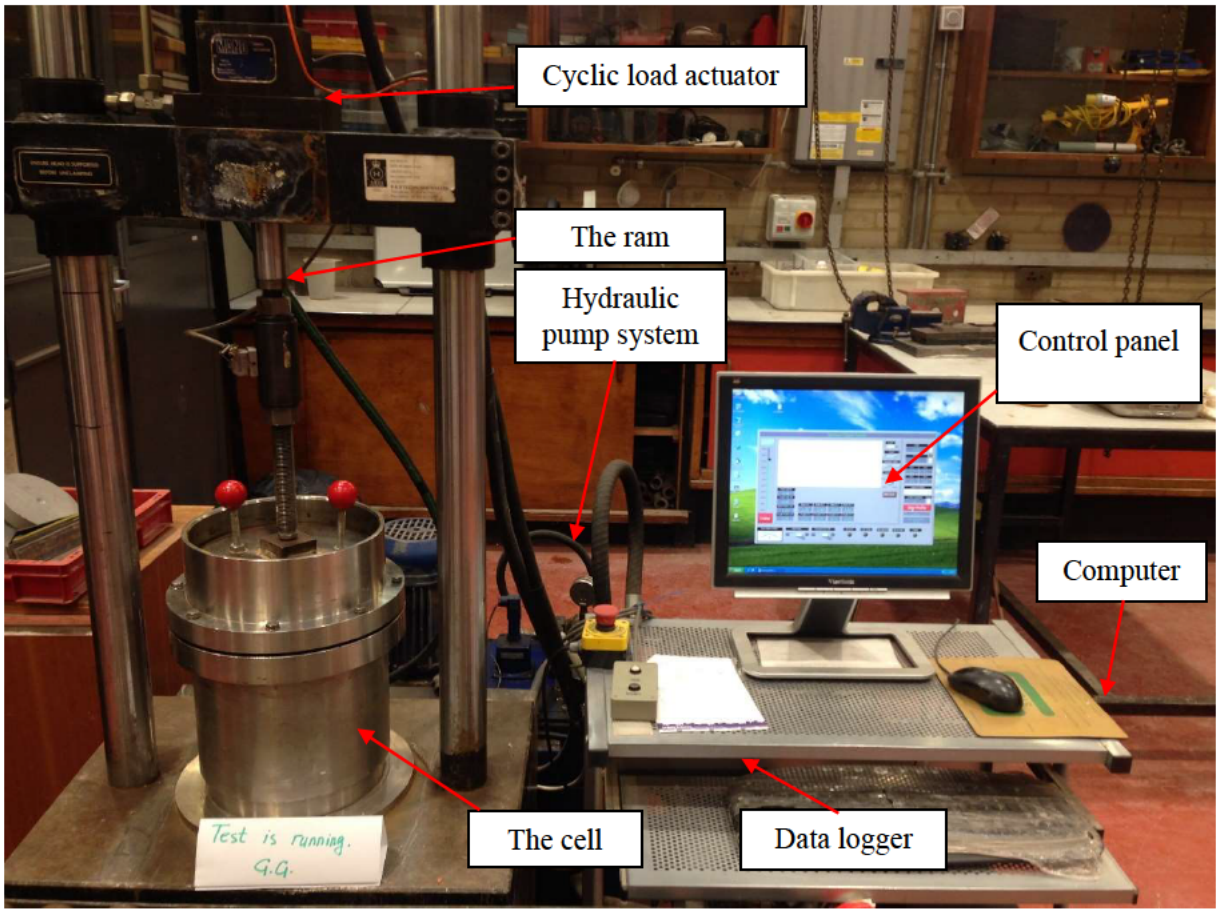


Figure 3.18 The small-scale test apparatus

The load is applied to the ram using the servo hydraulic pump and the ram applies the dynamic load directly to the cell. The electronical controlling unit of the servo hydraulic pump controls different load parameters (frequency of the load, amplitude of the load, the type of cyclic load, etc.). The panel controls the position of the rod at any stage; it also helps to set the mean amount of cyclic load at the beginning of the test. (Mean load in this test was 2.8 kN.) It controls the amount of load and the amount of amplitude (6.1 kN and 0.5 kN). There are three parts: load, strain and position; this helps us to adjust the range of output voltage. The frequency adjustment panel is set to 3 Hz. The unit receives the output voltage from the control unit and converts the voltage to data that is recorded on the PC.

3.6.3 Instrumentation

The control unit enables the application of cyclic loading at different conditions. The position level, stress basis were controlled through machine settings. Three types of wave shape are available: triangular, rectangular and sinusoidal. The number of applied cycles is controlled and could be chosen at any range. The frequency of the cycling ranges from 0.0001-100 Hz. The maximum limit of the applied load could be set so that if the limits are exceeded the machine stops and gives a warning signal. During the test, the load, strain, position, and pore water pressure readings were taken from the digital unit. The maximum and minimum values of them are constantly recorded by the machine software. The unit transfers data to a logger and a computer unit and is collected there.

The apparatus components are described is the following section:

- Hydraulic components- These are composed of the hydraulic pump and the other units that control the operation of the pump. The hydraulic pump is a single-stage positive

displacement gear type. The machine has two settings: 10 kN and 50 kN. In this research a 10-kN load cell was used.

- Loading element- A one-dimensional type of loading applied onto an area and equal to the total cross-sectional area of the mould was chosen in this research. This type of loading was used previously in other research works investigating mud pumping (Alobaidi, 1994; Ghataora, 2006). The servo-controlled valve and actuator are placed at the top of the leading frame. The main task of the unit is to convert the hydraulic power into mechanical power for application to the specimen, which is done by the actuator. The actuator itself is controlled by a servo-hydraulic valve. The elements of the loading frame include the base, two stiff vertical columns and the upper crosshead that can be positioned at any level of the columns. The vertical columns have a diameter of 64 mm. The test specimen is placed on the base. The load and displacement are measured directly by the load cell and the linear variable differential transducer, which are fitted to the actuator. The manufacturer calibrated the load cells before the research work began. All regular checks and maintenance works have been done according to the specifications and requirements. Prior to the test the machine was calibrated using SANS electromechanical universal testing machine (CMT 5000 series). A dynamic test was run with this cell three times for both compression and tension, in order to ascertain margins of error (Alobaidi, 1994).

- Pore-water pressure measurement- Pore water pressure (PWP) transducer was installed prior to each new test set-up. Transducer was installed at the surface of the subgrade and was aimed to measure the change in pore pressure at the contact point of the ballast and the subgrade soil. The membrane filter was attached to both devices to prevent the blockage of the pipe system. The data was recorded on Channel 1 and Channel 2 and

was stored on the computer. All required calibrations were done before the test was run. Before launching the test and measuring the pore water pressure, all necessary calibration tests were conducted. The calibration was done by comparison to a known head of mercury using a self-compensating mercury pressure system. For small heads of up to 30 kPa it was calibrated against known heads of water. The calibration curve is shown in Figure 3.19. After calibration, the known pressure was applied, and the output voltage of the transducers taken after suitable amplification. The data acquisition computer programme took 30 readings per cycle per channel. The response of the transducer was checked, applying PWP output gathered from the transducers against the time within a cycle, and the response of the transducers was always quick; there was no time lag between the applied load and the PWP response.

- Displacement measurements- This study was carried out based on the previously obtained test results with improvements covering the gaps in knowledge. The testing machine and the data acquisition system were similar to those previously used at the University of Birmingham (Hoare et al., 1982; Alobaidi et al., 1994, Ghataora, 2006). Servocon Digital Control Ltd supplied the logging system that was used to monitor the load and pressure transducers' readings. For static loading the readings were taken at an interval of 0.1 seconds; this provided the large quantity of data that was essential to define the specimen behaviour under loading conditions. In terms of cyclic loading, the readings were taken every 10 cycles. The collected test data was stored on the computer. The data gave information about the change in pore pressure, permanent and cyclic deformations. The objectives of the research consist of measuring the permanent and cyclic deformations. The deformations were measured by a deflectometer installed on the actuator of the loading machine. The range of movement of the transducer is 100

mm. Although the permanent deformation was measured in a wide range from 1 mm to up to 30 mm, the cyclic deformation on the other hand was insignificant and measured in some tests as small as 0.05 mm, which is very small compared to the range of the transducer.

- Data acquisition system- To monitor and control the load and pressure transducers a logging system supplied by Servocon Digital Control Ltd was used. The signals were read with up to 0.001 accuracy. For the cyclic loading test the data was recorded every 100 cycles. Data from the test had been transferred directly to a personal computer and the computer proceeded the received information through a data acquisition and control interface board. A computer programme was required to collect data using a specific pattern of such factors as: cyclic frequency; numbers of the channel used; numbers of readings to be taken during each cycle; number and time of readings to be taken during each test; and name of file in which the collected data will be kept (Alobaidi, 1994).

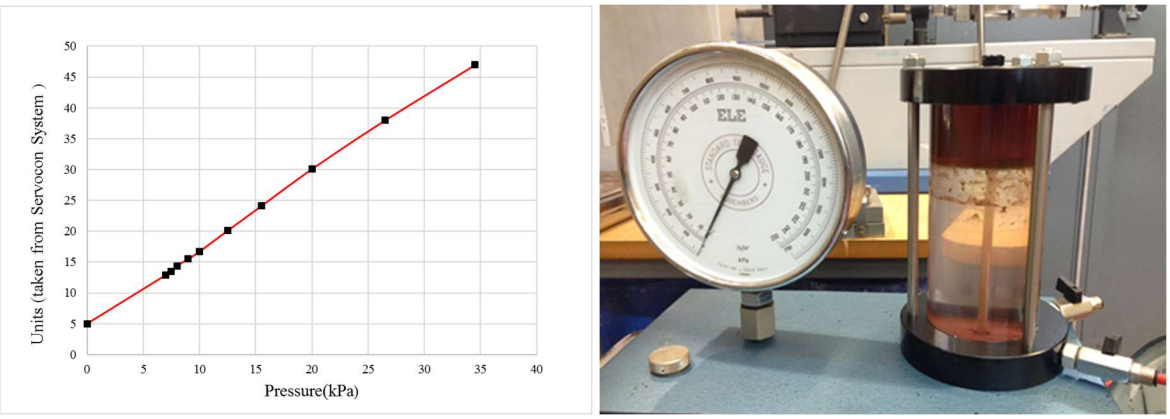


Figure 3.19 Pressure calibration curve and self-compensating mercury pressure system

3.6.4 Test variables

Frequency dynamic stress wave- The sine shape pulse represents the same stress pulse as in the applied stress in railways (Ghataora, 2006; Duong et al., 2014). The frequency of the cycles represents the speed of the train $f=V/3.6$, where V is the speed of the train and L is the length of the carriage. Earlier work has shown that within a range of 1-5 Hz, the frequency of loading has no significant effect on the mud pumping action (Peacock and Bolton, 1968; Brown and Hyde, 1975). Other works proved that the frequency affects the amount of pumping in the case of soft cohesive subgrade soil (Brown et al., 1975; Duong, 2014). In previous studies, researchers chose a frequency of 3 Hz in a pumping test (Alobaidi, 1994; Ghataora, 2006). Although the above frequency values represent the time of a traffic pulse at subgrade level, the rest period between two successive pulses was not simulated (Dawson, 1986). For a more realistic simulation, one 5-Hz pulse should be followed by a rest period (around 2 seconds). Because of the fact that the laboratory machine used in this research does not allow the cyclic loading to be broken up with pauses, it was decided to decrease the frequency of the loading to make some allowance for the rest periods between loading pulses (Alobaidi, 1994). Therefore, the 3Hz frequency was chosen in this research. Based on Equation 3.1, the sinusoidal wave of 3 Hz represents the train velocity of 225 km/h for a standard 20-metre carriage (Network Rail, 2007). Previous research works studied a wide range of applied numbers of cycles, from 500 and 1,000,000. Due to time limitations the number of cycles was chosen as 200,000, which represents one working week in the laboratory: 50,000 cycles per day. One day was dedicated to the test settings and instrumentation.

Dynamic stress- The pressure at the subgrade level is found using one of the theoretical approaches. Selig and Waters (1994) proposed an approach where subgrade pressure (P_c) is the ratio of the stress applied on the ballast (P_m) to the ballast depth (h), given in inches ($P_c = 16.8 P_m/h^{1.25}$). A relatively similar approach to measure the subgrade stresses was introduced by the

Japanese National Railway ($P_c = 50P_m/10+h^{1.35}$). Yoo and Selig (1979) studied dynamic stresses, conducting investigations in the field, and found that the subgrade stress generated by four-axle hopper cars each weighing 131 tons ranged between 80 and 110 kPa. They explained the cyclic stress ratio (CSR), which is the ratio of the cyclic deviator stress over the static deviator stress of reinforced soil at failure. This research investigated a maximum cyclic stress of 150 kPa and mean stress of 70 kPa that is equivalent to CSR = 0.8.

3.6.5 Investigation procedure

In this investigation, the wide range of cohesive soils was tested under different conditions such as: different moisture contents, state of subgrade soil saturation, and the effect of applying remediation solutions (with and without USPs). The test programme was purposefully chosen to study the influence of factors affecting mud pumping. This section describes the investigation procedure, and the way the results were analyzed. The steel plate has two holes each of 7 mm diameter, which allows the insertion of two pipes to measure the pore water pressure changes. To place the pressure transducer inside the sample a vertical hole of 10 mm diameter was made through the soil sample. After drilling the hole the transducer was installed 7 mm below the surface of the subgrade soil and the hole was refilled using the soil removed during the drilling. The second transducer was placed to measure the pore water pressure on the subgrade interface.

Undertaken steps:

1. Soil preparation was the initial step of the test. Commercially available English china clay supplied by Sibelco, and bentonite, supplied by Tolsa were delivered in powder condition ready for the test. London clay and Etruria marl came to the laboratory in bulk condition. To prepare the clays for the test, soil was taken from the bag, cut into

small pieces and left to dry in a 105-°C oven for 24 hours to remove any water content. After that, the dried soil was powdered in a soil crushing machine to a state of powder and sieved through 2-mm mesh to remove large particles that were not crushed previously (BS 1377-1:1990). The dried soil was then pulverised and mixed with a predetermined amount of water to obtain the desired moisture content. In the first tests this was the optimum moisture content, though in later tests, the desired moisture content was increased in order to create a subgrade of lower strength. The dry density was chosen to correspond with the moisture content on the compaction curve.

2. The small-scale test involved a steel cylinder with an inside diameter of 230 mm and a height of 200 mm; therefore, the target volume was measured and known as $V = (\pi r2)*l$ (Figure 3.20). For each test set-up the information about target soil density and moisture content was taken from a previously conducted compaction test (BS 1377-4:1990). The dry clay powder was measured and mixed using an automatic mixer with added distilled water for about 12 minutes. The added amount of water corresponded to the target moisture content. Following this step, a sample of soil was taken for moisture content measurement. The remaining soil was put in the refrigerator for 24 hours to create a homogeneous moisture content.



Figure 3.20 The small-scale test (conducted steps from top left to bottom right)

3. The prepared soil was placed in the cell in four parts and compacted to a depth of approximately 140 mm, using a static compaction technique. The moisture content of each one was taken to ensure it was constant throughout the sample. The clay was then compacted by a static load. Each of the three layers was compacted under approximately 500 kPa of static load with subsequent unloading and loading steps until there was no visually observed settlement.

   The target density of the subgrade soil was determined from the compaction/ moisture content and strength determinations (Figures 3.4 - 3.6.). Since the volume into which this material was to be compacted was determined by the size of the space for subgrade soils in the text apparatus, then the target density could be achieved by compacting a predetermined dry weight of soil mixed with a predetermined quantity of water (from

compaction tests) into the given volume in the test apparatus. Soil compacted in the test mould was allowed to stand for 24 hours before undertaking any load tests.

4. After this stage, the clay soil was carefully levelled (Figure 3.20). The soil strength was checked by a hand penetrometer before and after each test. The readings were done at the contact points of the ballast and subgrade, as well as at the point of no contact; in each case a minimum of 10 readings was taken with the following calculation of the average value. Using a penetrometer under the contact point of the ballast and the subgrade soil, as well as between the two ballast particles, readings were taken both prior to and after each test. In order to measure accurate data at least 10 penetrometer readings were measured before and after each test. The soil strength could be found from the bearing capacity equation: $c_u = q/Nc$ (the unit is given in kg/cm2). The undrained shear strength (c_u) is a ratio of a soil's bearing capacity to the constant value (N_c); which depends on the shape of the equipment ($\pi + 2$) in this research.

Calculation of the cone resistance

Cone res. (N/cm^2) = Total force (pressure(cm) * spring compression (N/cm) / cone surface area (cm^2). With a chosen combination and cone, the factor will remain constant (= constant factor). Spring compression (N/cm)/cone surface area (cm^2). Only the compression of the spring, indicated by the indicator ring, outside the penetrometer is variable. This compression calculated together with the constant factor gives the cone resistance. The strength of the spring, as indicated, applies to the maximum compression of 10 cm. Therefore, this reduces by a value of 10 cm. For example, with a spring pressure of 150 N and a cone of 0.25 cm^2 the constant factor will be 15.0/0.25 = 60.0 The constant factors applicable to the various spring-pressures and cones are indicated in Figure 3.21. The manual is provided in the Appendix.

Cone	0.25 cm^2	0.5 cm^2
Spring pressure		
50 N (5 kgf)	20	10
100 N (10 kgf)	40	20
150 N (15 kgf)	60	30

Example: Spring pressure 50 N; cone 0.5 cm^2; reading 8.2 cm.
Cone resistance = 8.2 x constant factor = 8.2 x 10 = 82 N/cm^2.

To convert into kg/cm^2: 10 N/cm^2 = 1 kg/cm^2, than 82 N/cm^2 = 8.2 kg/cm^2

Figure 3.21 Calculation of cone resistance (from the manufacturer manual)

5. A 75-mm thick layer of ballast was placed on the subgrade. The base ballast rocks were numbered, and each position was recorded to make sure that in next test the contact area of the ballast and soil would be identical. In the case when the under-sleeper pad was tested, it was placed above the ballast layer. The shape of the cut material was almost identical to the diameter of the cylinder, but just slightly smaller, to allow the placing of the material above the soil.

6. Two different types of tests were performed, referred to as “unsaturated” and “saturated”. In the saturated test, before applying the cyclic load, 500 ml of distilled water was poured onto the ballast; that amount of water was chosen as a sufficient amount to cover the subgrade layer. The cell did not enable any water to drain and furthermore the mould was covered with cling film to seal the sample. In the case of the china clay, two different amounts of standing water were tested: 500 ml and 1000 ml were applied in order to investigate the influence of water. The data and results will be presented in Chapter 4.

7. One ballast rock was specifically modified to measure the pore water pressure at the contact point of the subgrade and the ballast. To do this a hole was drilled in the ballast

and a pipe was passed through. The pipe was 100% filled with water. The adapter was installed at the other end of the pipe. On the other side the adapter was connected to a transducer and the recorded data was transferred through Channel 1 and 2 to the connected Servocon Digital System.

8. Following that, 500 ml of water was added, and the sample was left for approximately 24 hours for saturation. After soaking the top subbase, a 30-mm thick steel plate (225 mm diameter) was positioned on the top of the ballast and an initial load of 1 kN was applied. The procedure was similar to that conducted previously by Ghataora (2006). After approximately 5 minutes, the cyclic load was added to the whole cross-sectional area of the sample.

9. To record static loading as well as cyclic loading, the programme was launched prior to the main test. It allowed the recording of the settlement under static one-dimensional loading as well as pore water pressure. The cyclic load was applied to the sample by a plunger to the rigid load plate using hydraulic loading ram apparatus (Figure 3.18), which allows the application of static and dynamic loads of a chosen frequency and amplitude. The load on the surface of the sample varied sinusoidally between set limits. The upper and lower load limits in this study were chosen to be 6.1 kN and 0.5 kN respectively, to result in a pressure approximately between 10 kPa and 150 kPa, following on from an earlier specification of work. The frequency and duration had to be specified at the start of every test and were kept constant throughout this study at values of 3 Hz and 95400 seconds respectively. Connected to the MAND machine was a computer in which a logging program was installed to record data. Initially, the time interval was small, but this was increased by the factor of 1.5 for each subsequent

recording throughout the test. Thus, a typical recording interval sequence could be 8, 12, 18, 27, 41 etc. Each recording contained a set of 30 readings forming one cycle. At the end of each set of recordings the logging program summarised these 30 data points by showing the average of the variables recorded. These consisted of maximum and minimum values of load and position, together with the time at which the recording was taken. The numbers of the raw data from the logging program were given in bits but could be transformed into kN and mm respectively by using a table provided by the manufacturers of the cyclic load equipment.

10. After completion of the test the ballast and the USPs (in some cases) were accurately removed, the slurry was collected, oven-dried and measured. The reading of the subgrade soil strength under the ballast and between the ballast was measured by a hand vane. The moisture content of the subgrade was taken before and after each test. Two samples were taken every time in order to obtain a reliable value, from the average. The samples were taken from the very top of the subgrade and weighed (m) before being left to dry in the oven at 105 °C for 24 hours; after which the samples were weighed again (md). On the basis of the weights obtained, the moisture content was calculated in accordance with BS 1377-2: 1990.The soil moisture content was recorded. Soil samples were taken from three different depths to measure the moisture content.

3.6.6 Data analysis

Upon test completion, the test data was sent by the data acquisition program to the computer and stored on the hard disk. The programme allowed the recording of data from four channels.

A computer-controlled load frame with specifically designed data logging system was used in this study. Maximum and minimum load, cyclic and permanent deformation, and position of load plunger were recorded every 100 cycles together with the time.

The data was processed in the following sequences:

1. The minimum and maximum readings after each cycle, with the corresponding time record from all channels were summarised in the summary file. A typical set of recordings as seen on the logging computer screen is shown in Table 18. The first column displays the load, the second the position and the last the time in seconds.

Table 18 The raw data of a cyclic load test

Date	Time	Cycles	Load Pk	Load Trgh		Posn Pk	Posn Trgh		Disp Pk	Disp Trgh		Ext Pk	Ext Trgh		Ch 1 Pk	Ch 1 Trgh		Ch 2 Pk	Ch 2 Trgh
09/12/2019		0.109	0.000	0.492	0.000	0.455	0.000	-0.000	0.000	-0.000	0.000	1.556	0.000	0.058	0.000	-0.113	0.000	0.002	0.000
09/12/2019		0.219	0.000	0.491	0.000	0.458	0.000	-0.000	0.000	-0.000	0.000	1.557	0.000	0.066	0.000	-0.103	0.000	0.003	0.000
09/12/2019		0.328	0.000	0.494	0.000	0.457	0.000	-0.000	0.000	-0.000	0.000	1.544	0.000	0.077	0.000	-0.077	0.000	0.002	0.000
09/12/2019		0.437	0.000	0.505	0.000	0.458	0.000	-0.000	0.000	-0.000	0.000	1.586	0.000	0.059	0.000	-0.095	0.000	0.002	0.000
09/12/2019		0.547	0.000	0.508	0.000	0.456	0.000	-0.000	0.000	-0.000	0.000	1.568	0.000	0.076	0.000	-0.086	0.000	0.004	0.000
09/12/2019		0.656	0.000	0.521	0.000	0.461	0.000	-0.000	0.000	-0.000	0.000	1.572	0.000	0.077	0.000	-0.112	0.000	0.002	0.000
09/12/2019		0.766	0.000	0.545	0.000	0.463	0.000	-0.000	0.000	-0.000	0.000	1.541	0.000	0.071	0.000	-0.098	0.000	0.002	0.000
09/12/2019		0.875	0.000	0.559	0.000	0.469	0.000	-0.000	0.000	-0.000	0.000	1.562	0.000	0.050	0.000	-0.099	0.000	0.003	0.000
09/12/2019		0.984	0.000	0.561	0.000	0.471	0.000	-0.000	0.000	-0.000	0.000	1.559	0.000	0.065	0.000	-0.077	0.000	0.002	0.000
09/12/2019		1.094	0.000	0.575	0.000	0.473	0.000	-0.000	0.000	-0.000	0.000	1.535	0.000	0.069	0.000	-0.095	0.000	0.003	0.000
09/12/2019		1.203	0.000	0.588	0.000	0.478	0.000	-0.000	0.000	-0.000	0.000	1.535	0.000	0.078	0.000	-0.083	0.000	0.003	0.000
09/12/2019		1.312	0.000	0.588	0.000	0.479	0.000	-0.000	0.000	-0.000	0.000	1.558	0.000	0.073	0.000	-0.140	0.000	0.003	0.000
09/12/2019		1.422	0.000	0.601	0.000	0.483	0.000	-0.000	0.000	-0.000	0.000	1.557	0.000	0.075	0.000	-0.092	0.000	0.002	0.000
09/12/2019		1.531	0.000	0.612	0.000	0.487	0.000	-0.000	0.000	-0.000	0.000	1.558	0.000	0.052	0.000	-0.105	0.000	0.003	0.000
09/12/2019		1.641	0.000	0.622	0.000	0.492	0.000	-0.000	0.000	-0.000	0.000	1.567	0.000	0.062	0.000	-0.079	0.000	0.002	0.000
09/12/2019		1.750	0.000	0.630	0.000	0.491	0.000	-0.000	0.000	-0.000	0.000	1.541	0.000	0.050	0.000	-0.105	0.000	0.002	0.000

2. The data was summarised and plotted using Microsoft Excel programme. The summaries at the end of each cycle were put together (Table 19). The third column displays the number of cycles. The last three columns show permanent deformation, cyclic deformation and the stiffness, respectively. The values were calculated for every 100 cycles. The permanent deformation was calculated as the difference between the current position and the initial position (the programme gave the current position for each 100 cycles and the initial position

was already known). It was found as the difference between Position Trgh- initial Position Pk. The applied load was calculated as the difference between the Load Peak and Load Trgh. Once the permanent deformation for every 100 cycles was known, then the calculation of the stiffness was done as a ratio between the applied load over the permanent deformation (Crawford et al., 2001). Finally, the data was plotted as "permanent deformation against the number of cycles" and "the subgrade stiffness against the number of cycles".

Table 19 Compilation of data

DATE	TIME	CYCLES	CUMMULATIVE CYCLES	LOAD		POSITION		PERMANENT DEF.		CYCLIC DEF.		STIFFNESS
				Load Pk	Load Trgh	Posn Pk	Posn Trgh					
12/02/2019	0.016	0		0.773	0	0.809	0					
12/02/2019	32.078	0		3.376	0	0.967	0					
12/02/2019	08:45:57	1		3.405	-1.676	5.737	-0.014					
12/02/2019	08:46:30	100	150100	5.943	0.398	1.121	0.905	0.096	0.10533	0.216	0.22883	25.6713
12/02/2019	08:47:03	200	150200	6.124	0.487	1.135	0.903	0.094	0.10967	0.232	0.23333	24.2974
12/02/2019	08:47:36	300	150300	6.19	0.514	1.138	0.918	0.109	0.114	0.22	0.235	25.8
12/02/2019	08:48:09	400	150400	6.212	0.521	1.162	0.907	0.098	0.11833	0.255	0.23517	22.3176
12/02/2019	08:48:43	500	150500	6.217	0.524	1.15	0.914	0.105	0.12433	0.236	0.2315	24.1229
12/02/2019	08:49:16	600	150600	6.202	0.514	1.153	0.939	0.13	0.13	0.214	0.22667	26.5794
12/02/2019	08:49:49	700	150700	6.211	0.519	1.174	0.931	0.122	0.12983	0.243	0.22817	23.4239
12/02/2019	08:50:23	800	150800	6.248	0.553	1.171	0.929	0.12	0.13383	0.242	0.22567	23.5331
12/02/2019	08:50:56	900	150900	6.258	0.551	1.165	0.944	0.135	0.13567	0.221	0.22333	25.8235
12/02/2019	08:51:29	1000	151000	6.231	0.534	1.176	0.943	0.134	0.1375	0.233	0.22133	24.4506
12/02/2019	08:52:03	1100	151100	6.235	0.529	1.155	0.948	0.139	0.13833	0.207	0.22033	27.5652
12/02/2019	08:52:36	1200	151200	6.221	0.528	1.161	0.938	0.129	0.13717	0.223	0.22233	25.5291
12/02/2019	08:53:09	1300	151300	6.213	0.524	1.183	0.955	0.146	0.14033	0.228	0.223	24.9518
12/02/2019	08:53:42	1400	151400	6.229	0.494	1.168	0.94	0.131	0.1395	0.228	0.22217	25.1535
12/02/2019	08:54:16	1500	151500	6.228	0.515	1.164	0.955	0.146	0.14383	0.209	0.2155	27.3349
12/02/2019	08:54:49	1600	151600	6.219	0.527	1.175	0.948	0.139	0.14267	0.227	0.21767	25.0749
12/02/2019	08:55:22	1700	151700	6.234	0.527	1.16	0.941	0.132	0.143	0.219	0.21867	26.0594

3. The stiffness is the ratio of the applied load to the deflection of the subgrade layer. The Winkler method (Crawford et al., 2001) was used where a vertical force (P) applied by a wheel produces a vertical rail deflection (w). The track stiffness (k), at a point directly underneath the wheel as it passes is defined as: $k = P/w$. The track modulus (u) is then defined by: $u = k^{4/3}/(64EI)^{1/3}$; where E is the Young's modulus of the rail steel and I is the rail moment of inertia. Crawford et al. (2001) suggested that track moduli determined with different methods do not vary excessively. A method for obtaining the track stiffness was discussed by Crawford et al. (2001), in which the slope of a secant to the load/deflection curve represented the stiffness. The

same method has been used in this work, but for the whole system. For every cycle of a test the stiffness in terms of kN/mm could thereby be calculated by plotting load against position.

The procedure was repeated for all the recordings throughout a test and the values summarised as in Chapter 4.

3.7 Large-scale test

3.7.1 General information

To assess the closeness of the results of the small-scale cyclic load tests to a real railway track, a larger scale test was conducted in a box made of concrete chambers that could accommodate three half sleepers. Considering the scope of the project and the number of tests conducted with different variables (four types of subgrade soils, saturated/unsaturated condition, with and without under-sleeper pads) it would be difficult to study the problem on site in the industry. The large-scale test represents an intermediate approach between conventional laboratory ballast testing and railway track field trials. The test simulated real railway track conditions, with an actual load applied on the real track section. It was conducted at the Civil Engineering laboratory of the University of Birmingham (Figure 3.22). Only one test was conducted as it took a long time to set up and run. Nonetheless, since the larger test was about 82 times the area of the smaller tests, it was considered to give a good indication of closeness of the small tests to the track.

3.7.2. Tested Materials

Etruria marl (EM) was used as the subgrade soil as it was also used in the small-scale tests. The EM had a moisture content of 17%, its natural moisture content when delivered (section 3.4). The prepared soil was placed in the cell in four parts and compacted to a depth of approximately 220 mm, using a dynamic compaction machine (Figure 3.22). The moisture content of each one was taken to ensure it was constant throughout the sample.

Ballast for both the large and small tests complied with the Network Rail (RT/CE/S/006 (2000) standard. The ballast material used in the large-scale test was the same as the one used in the small-scale test with materials ranging between 35 and 55 mm. A prototype geotextile material designed to prevent migration of fines was tested in both apparatuses. Details of the geotextile cannot be disclosed for confidentiality reasons. However, tests with both apparatuses were conducted in the same conditions.

3.7.3. Test set up and procedure

The large-scale test was assembled in a concrete pit with the following dimensions: 2 m deep x 4.1 m long x 2.5 m wide. The large-scale test facility was made of a track section constructed within a concrete frame 1.65 m wide x 2.0 m long x 1.15 m high, constructed from three concrete sections and reinforced by 25 mm steel tie rods. The concrete sections were installed into the pit lifted by the cranes under the loading actuator. A 220-mm thick layer of Etruria marl formed the subgrade layer.

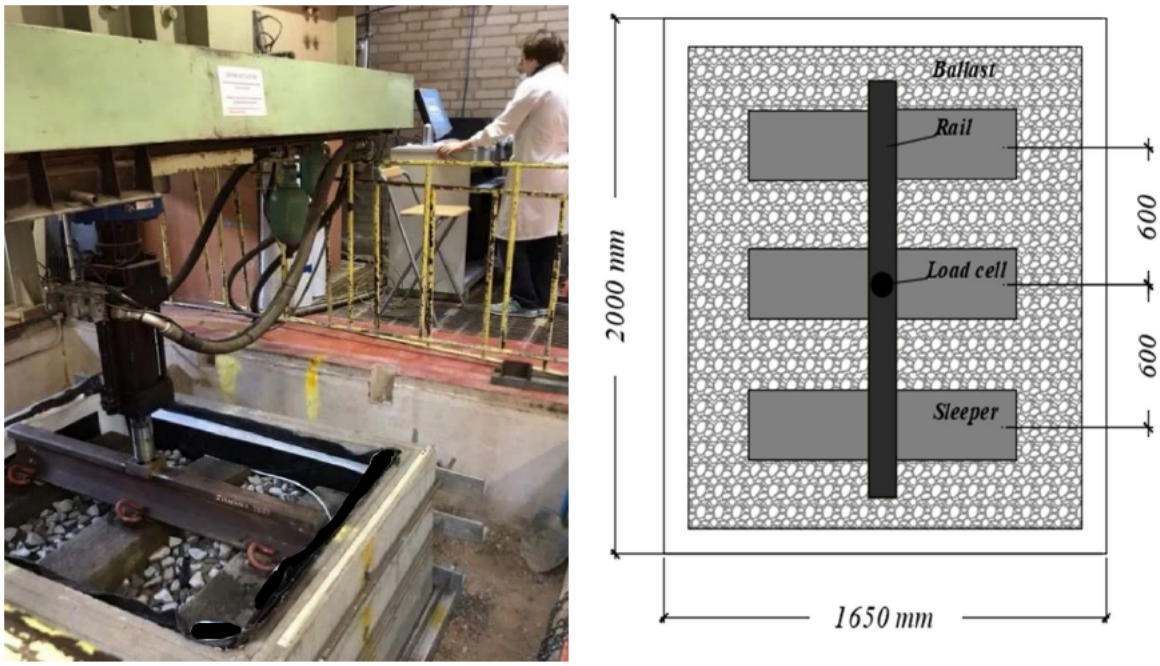


Figure 3.22 The large-scale test, subgrade permanent deformation investigation

The subgrade soil (Etruria marl) was dried, pulverised and mixed in a large mixer with a predetermined amount of water to obtain the desired moisture content of 17%, which corresponds to the OMC. The prepared subgrade soil was placed in the assembled concrete frame in four parts and compacted using compaction apparatus (Figure 3.23). A sample to measure the moisture content of each one was taken to ensure it was constant throughout the test preparation. After compaction, the EM had a density of 1770kg/m^3 and a moisture content of 18.2%. The shear strength was measured by hand-vane test and was recorded as 63 kPa. The subgrade stiffness was measured using a plate load test (PLT) in accordance with BS EN1997-2: 2007. The geotextile material was placed on top of the subgrade and folded over the vertical sides of the tank. Vertical steel plates were glued on to the geotextile before adding three 100-mm thick layers of ballast, each compacted to the maximum using a plate compactor; giving a final ballast layer thickness of 300 mm. Three concrete half sleepers were placed on the ballast at a spacing of 600 mm and connected by a rail. Load was then applied to the rail at the centre sleeper. The complete set-up and plan of the layout are shown in Figure 3.25. Load

was applied at 3 Hz in a cyclic sinusoidal loading form, with a minimum and maximum of 10 to 125 kN respectively, to result in a pressure approximately between 12 kPa and 150 kPa. The frequency of loading was in the range1 to 3 Hz as suggested by Ghataora et al. (2004). The instrument arrangement for the large-scale test was similar to that in previous tests (Ghataora, 2006), and the instrumentation included an actuator load cell to measure the load applied to the sleepers. Systems Services Ltd calibrated the apparatus. The assembled railway section of three sleepers and a rail was installed on the centre of the ballast bed after the compaction was completed. To prevent sleeper rotation and give stability to the railway section more ballast material was placed between and around the sleeper. Overall a quarter of a million cyclic loadings were applied, with a daily target of 50,000 cycles. Prior to the start of the test, water was added to give a 30-mm head of water above the subgrade, simulating the worst-case scenario. Every 100 cycles, load (maximum and minimum values) together with both cyclic and permanent deformation at the top of the rail were recorded. The results are provided and discussed in Section 4.2.5.

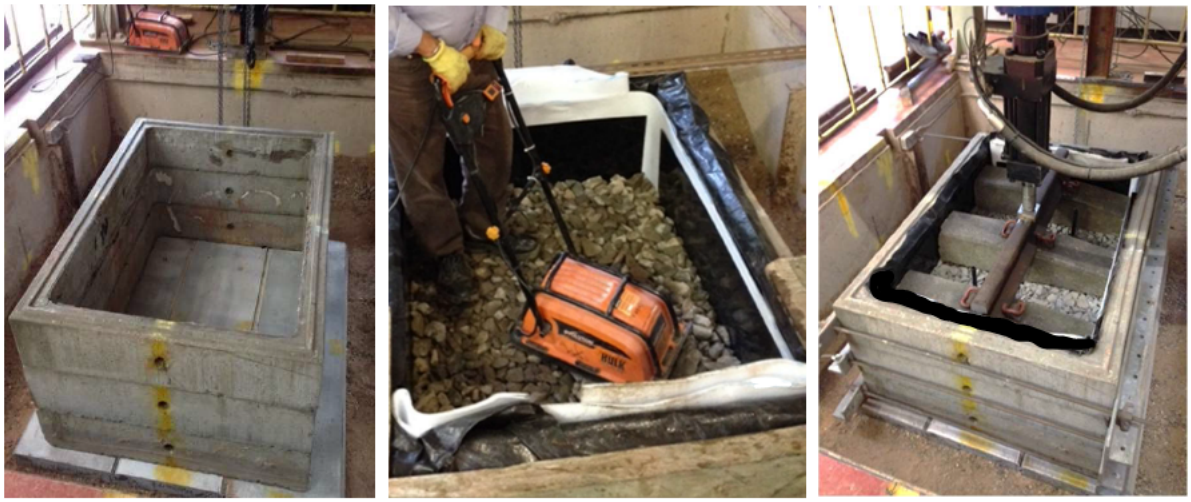


Figure 3.23 The large-scale test, the University of Birmingham

3.8 Contact area between ballast and a sleeper

The contact area of the USP was measured (Table 20). The following measurements were taken: the diameter of the unit cell = 230 mm; the area of the USP ≈ 0.0415 m^2; A = πr^2 = $\pi \cdot 0.1152 \approx 0.0415$ m^2. The average contact point between the ballast and the sleeper with the USP ≈ 0.012 m^2 (which is 28.9% of total area A= 0.0415 m^2). Whereas the average contact point between the ballast and the sleeper without the USP ≈ 0.0008 m^2 (which is 1.9 % of total area A = 0.0415 m^2). As can be seen, after conducting 250,000 cyclic loadings the contact area of the sleepers without pads was the lowest (1.9%). The results of the test using a sleeper with a USP showed a much higher contact area (28.9 %). This is an essential parameter that influences the contact pressure, which provides more uniform load distributions and reduces contact pressure on the ballast. The results correspond to the industry research results from Getzner in 2014, when after remaining in service for nine years in a track with an annual load of around 12–15 million tonnes, individual concrete sleepers with pads were removed. The measurements made on the sleepers with pads in a railway track confirm the results obtained from other measurements (Lay and Steger, 2015). The contact area of sleepers with pads is around four times higher than that of sleepers without pads, 30% and less than 5 % respectively (in this research the results were 28.9% and 1.9% correspondingly). The degradation rate of the railway track section with USPs was significantly low. The results showed that applying the USP doubles the tamping interval and prevents the breakage of the ballast. This is primarily explained by increasing the contact area between the underside of the sleeper and the top layer of ballast (Figure 3.24). The higher the load on the track, the more efficient the effect of the pads. A higher contact area leads to a better assimilation of the load into the ballast and a reduction in the load acting on the subgrade (Musgrave and Wehbi, 2016).



Figure 3.24 The contact area between ballast and the USP, the print

Table 20. Measured contact area between ballast and sleeper (with/without USP)

Contact area with USP		Contact area without USP	
Test number	m2	Test number	m2
1	0.015	1	0.0007
2	0.01	2	0.0009
3	0.013	3	0.0006
4	0.009	4	0.0009
5	0.015	5	0.0007
6	0.011	6	0.0006
7	0.017	7	0.0008
8	0.009	8	0.0011
9	0.01	9	0.0009
10	0.01	10	0.0011
11	0.01	11	0.0011
12	0.012	12	0.0007
13	0.001	13	0.0006
14	0.013	14	0.0009
Average	0.012 m2	Average	0.0008m2

3.9 Summary

Since the focus of the study was to investigate the effect of repeated loading on cohesive soils, and to study the deterioration process of the subgrade layer, the structure of these tests suggested herein was chosen. For permanent deformation tests it is important to set a detailed test configuration that should include information about tested materials, load, and frequency. Information about the conducted tests and the materials used was presented in this chapter. The physical characteristics of the cohesive soils tested in this study were obtained in accordance with BS 1377-4:1990; the small-scale test and the large-scale test were described and later conducted in accordance with a procedure that was developed at the University of Birmingham. The chapter gives a detailed description of the apparatus used in this research, the required procedures, as well as an explanation of the steps conducted for each test. These test results are presented in the Appendix and are used in Chapter 4 for analysis.

Chapter 4 RESULTS AND DISCUSSION

4.1 Introduction

The results and analysis of the conducted tests along with some discussions are presented in this chapter. The laboratory investigation was carried out in accordance with the research methodology explained in Chapter 3. The work has been divided into three parts. The aim of the first part was to obtain the soil characteristics of some subgrade soils, in accordance with BS 1377-4:1990, and evaluate the susceptibility of those soils to erosion and dispersion processes (Sections 3.4-3.5). The second part of the laboratory tests included investigation of subgrade soil behaviour under dynamic loading using the small-scale test, in particular to investigate the deformation od subgrade soil. One of the main objectives of the study was to investigate the effect of using the USPs on the response of subgrade soil when subjected to dynamic loading, through experimental work. The idea was to look into the USPs' use as a potential remediation solution to minimise and prevent the effect of the mud pumping phenomenon. Much of the developmental work was undertaken using a prototype small-scale test that was based on and developed from the apparatus used by Snaith and Bell (1978), Hoare (1982), Alobaidi (1994) and Ghataora (2006).

This laboratory scale investigation focused mainly on the fundamental mechanical behaviour of subgrade layer under repeated loading. Overall, 96 tests were completed. At each test 200,000 cycles were applied. Tests with and without under sleeper pads (USP) have been carried out. The whole system has been subjected to cyclic loading and measurements have been taken before, during and after the tests. The design of the apparatus is given and described in Section 3.6.

A steel cylinder with inside dimensions of 230 mm diameter and 200 mm height was used. The subgrade material was compacted to a depth of 140 mm. The ballast was then placed on top of the subgrade to a thickness of about 75 mm. The cyclic tests were carried out on cohesive soils: Etruria marl, London clay, china clay and a mix of china clay and 5% of bentonite (CCB). Dynamic stress ranging between 10 and 150 kPa was applied in a frequency of 3 Hz. A comparison was made between the behaviour of the subgrade soils with moisture contents representing 80%, 100% and 120% of the optimum moisture content (OMC). All subgrade soils were tested in unsaturated and saturated conditions. Another objective was to measure the behaviour of the subgrade soil. The parameters such as permanent deformation, cyclic deformation, amount of loosened soil and the change in subgrade stiffness were studied. To see their effect, the tests were run with and without the USPs. Finally, the development of pore water pressure (PWP) with the number of cycles was also observed and examined.

The third part of the laboratory investigations was the validation of the results obtained using the small-scale test. The objective was to compare the outcomes of the large-scale test with the results of the small-scale test. To achieve this the large-scale test was assembled and run. The test simulates the railway track conditions that include the dimension of the track structure (1:1), the applying load, and the frequency (Section 3.7). Laboratory testing using the large-scale apparatus has been carried out employing a set-up resembling a railway cross-section.

4.2 Permanent deformation, the small-scale test

According to Selig and Waters (1995), the subgrade layer has a major influence on the track's performance. Its main function is to provide a stable platform. With time and repeated loading from traffic, vertical plastic strain accumulates in all layers of a railway track which leads to its total deformation. Permanent deformation of the track depends on many factors, such as loading condition, number of cycles, type of subgrade soil, its moisture content and dry density (Shenton, 1985).

4.2.1 Subgrade permanent deformation, saturated/unsaturated conditions

Although the focus of the research was to test the effect of the USPs on saturated subgrade soil (when 500 ml of distilled water was added prior to the test), it was necessary to run some tests in an unsaturated condition to compare the effect of the water. Figures 4.1 to 4.4 show the permanent deformation of different cohesive soils under saturated and unsaturated conditions. Each graph illustrates the trends of subgrade deformation in different initial moisture contents. The tests were divided into categories of with and without the USPs. All soils were tested with three different moisture contents representing 80%, 100% and 120% of OMC (e.g. LC 80 is interpreted as London clay, OMC 80%). Each test profile had its own abbreviation such as ballast-subgrade (bs); ballast-subgrade-the USP (bsusp); ballast-subgrade-water (bsw); ballast-subgrade-water-the USP (bswusp).

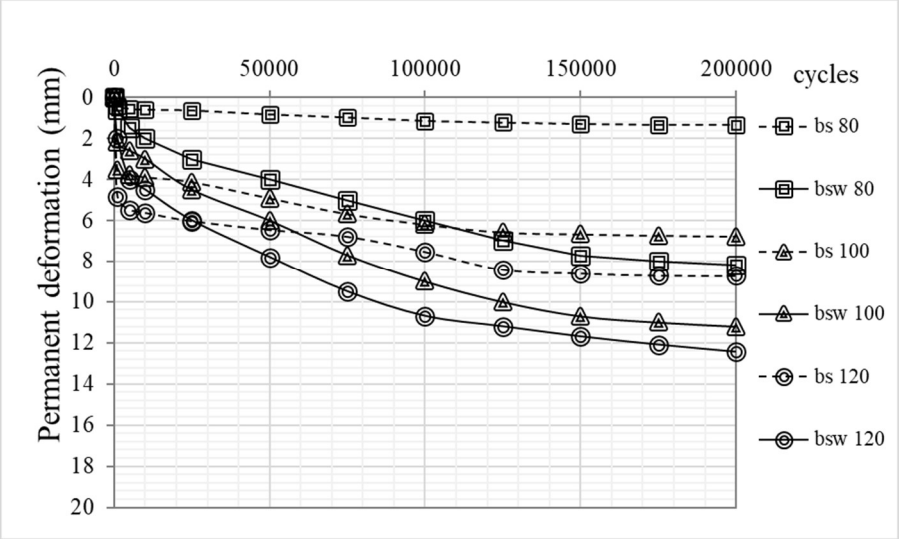


Figure 4.1 Permanent deformation, saturated/unsaturated condition, EM

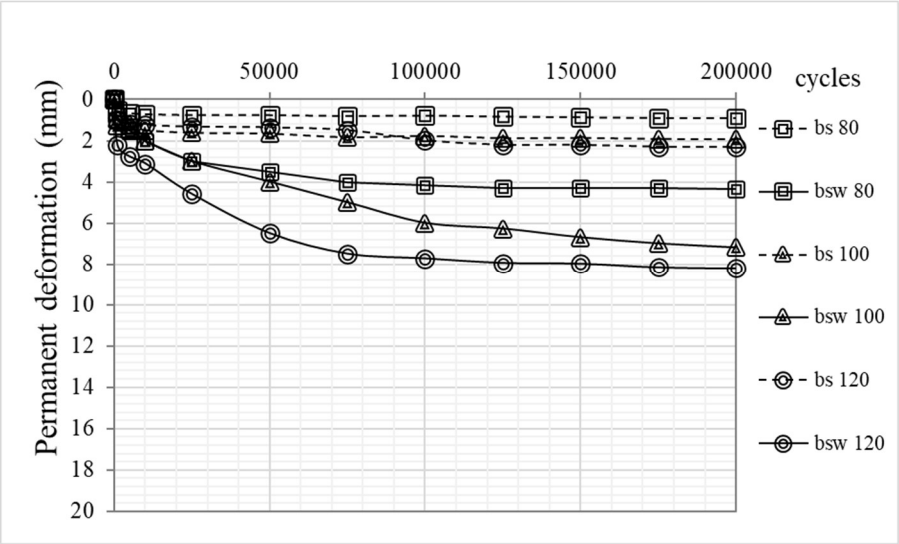


Figure 4.2 Permanent deformation, saturated/unsaturated condition, LC

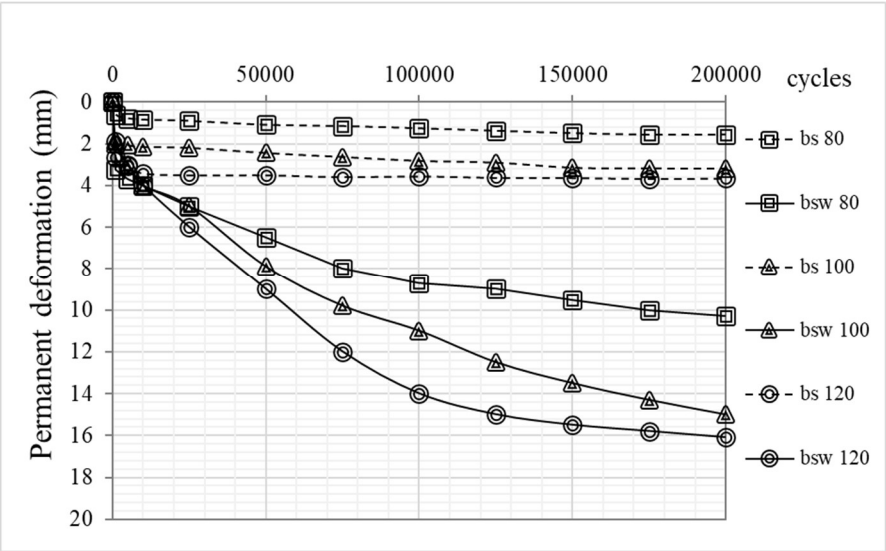


Figure 4.3 Permanent deformation, saturated/unsaturated condition, CC

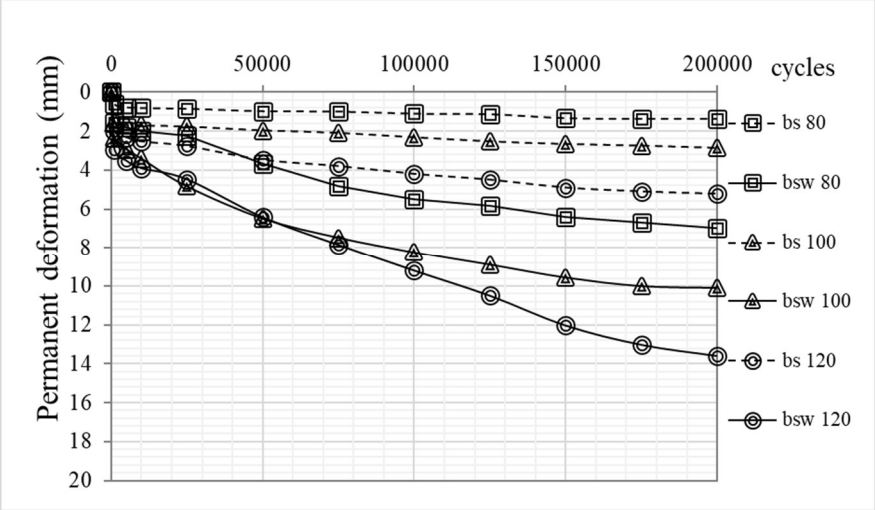


Figure 4.4 Permanent deformation, saturated/unsaturated condition, CC

It could be seen that free-standing water significantly affects the rate of permanent deformation. All soils tested regardless of their initial moisture content showed a significant difference in permanent deformation with and without free-standing water. After applying 200,000 cycles the difference between saturated and unsaturated tests was approximately 2 mm. However, in some cases the difference was higher. For example, in the case of EM 80 the difference was

almost 6 mm (Figure. 4.1). These outcomes were expected which is in agreement with previously conduced works (Alobaidi and Hoare, 1994). In the case of the unsaturated test, the difference between permanent deformation in the test with different moisture contents was not significant: approximately 1-2 mm, and all four cohesive soils showed a similar trend. The only exception was the difference between EM 80 and EM 100 (5mm).

4.2.2 Subgrade permanent deformation, effect of soil type

Figures 4.5-4.7 show how cohesive soils with different physical characteristics (Chapter 3) are susceptible to permanent deformation. The fact that the applied conditions were the same in all cases allows a comparison of the results. According to Rasul (2016), permanent deformation of cohesive soils with a high proportion of sand and silt should be higher than in soil with clay contents, at different moisture contents ranging from 80% OMC to 120% OMC. As can be seen china clay had highest permanent deformation regardless of initial moisture content. The least susceptible to deformation was London clay, which showed the smallest amount of permanent deformation with all moisture contents. Etruria marl and a mix of china clay and 5% bentonite showed similar trends. It can be seen, again, that the increase of the moisture content significantly increased the permanent deformation.

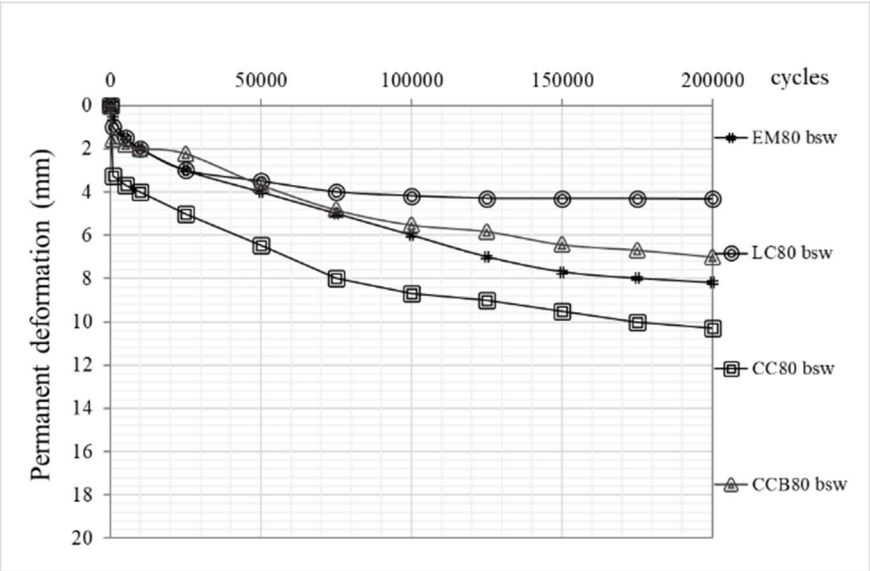


Figure 4.5 Permanent deformation, effect of soil type, OMC 80%

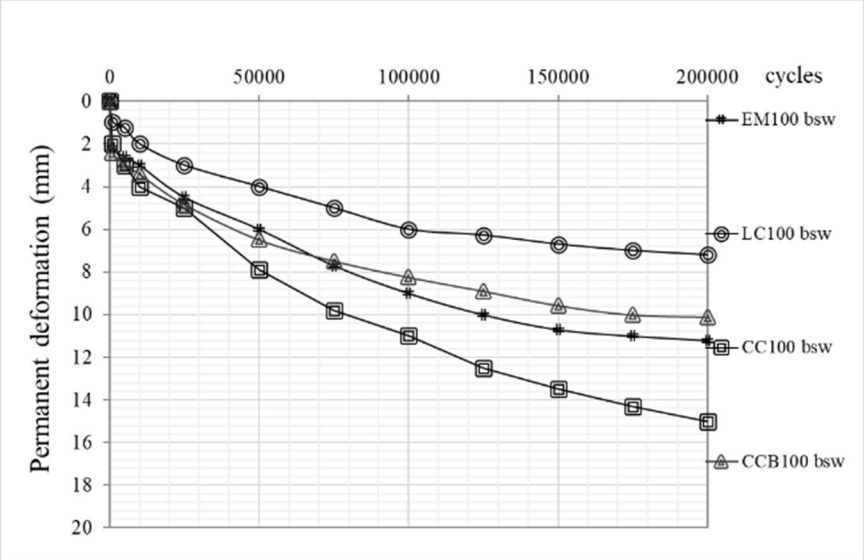


Figure 4.6 Permanent deformation, effect of soil type, OMC 100%

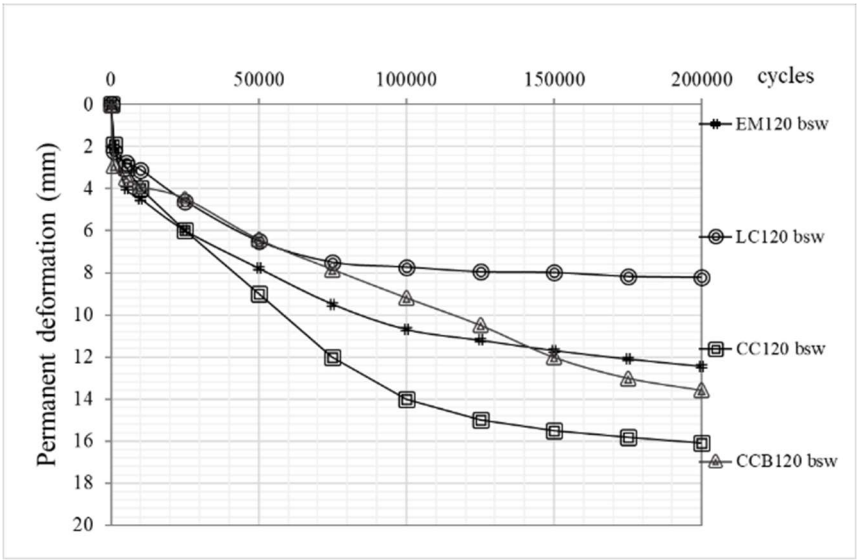


Figure 4.7 Permanent deformation, effect of soil type, OMC 120%

The results could be explained in that London clay has a lower permanent deformation because of its physical characteristics (a lower proportion of sand and silt) compared to Etruria marl. On the other hand, the high level of deformation of china clay and the mixed clay could be explained in the following way. After applying 200,000 load cycles, the ratio of final moisture content versus the initial moisture content was slightly higher in the case of CC and CCB rather than in EM and LC. One of the reasons could be the compaction at the preparation stage which left some tiny voids in the soil. Those voids were filled with the added 500 ml water and eventually gave a higher permeability, and the actual moisture content was higher.

4.2.3 Subgrade permanent deformation, with/without the USP

From the soil mechanics theory explained by Karl Terzaghi, it is well known that the moisture content affects the soil's characteristics, and with an increase of moisture the effective stress decreases. Lekarp et al. (2000a) stated that although the stress level remains the same, the permanent deformation development changes with an increase of moisture content. Therefore,

it was expected similar trends would be seen in the behaviour of the subgrade soil. The measurements of the undrained shear strength were taken before the test; the results showed a decrease of values of undrained shear strength with the increase of the moisture content (Section 3.4.5). The response of the soil to applied repeated loading is nonlinear. The progression of permanent deformation depends on the number of applied loads. The rate of the cumulative permanent deformation increases with an increase in the number; however, the rate of permanent deformation decreases. As can be seen, all four tested soils showed similar trends when, with an increase of moisture content from OMC 80% to OMC 120%, permanent deformation increased. The tendency was the same with and without USPs. All soils tested without USPs and with a moisture content corresponding to OMC 120% showed the large permanent deformation. While soils CC120 (bsw) and CCB120 (bsw) had the largest deformation of 16 mm and 14 mm respectively. On the other hand, the same soils with USPs deformed less when USP was applied. For example, in the case of CCB there was a significant improvement in the permanent deformation, which changed from 14 mm to 6 mm. The deformation of EM and LC was increasing slowly until approximately 100,000 cycles and then it stabilized, whereas in case of CC and CCB the deformation was increasing gradually during the entire test of 200,000 cycles. All tested soils demonstrated better results in permanent deformation when the USP was installed; the increase was steady and didn't exceed the results of the test without the USP.

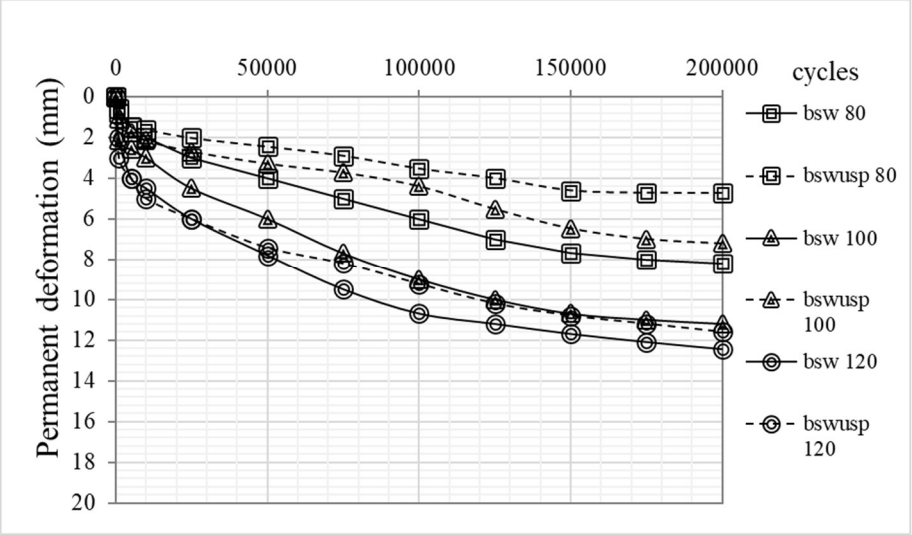


Figure 4.8 Permanent deformation, with/without the USP, EM

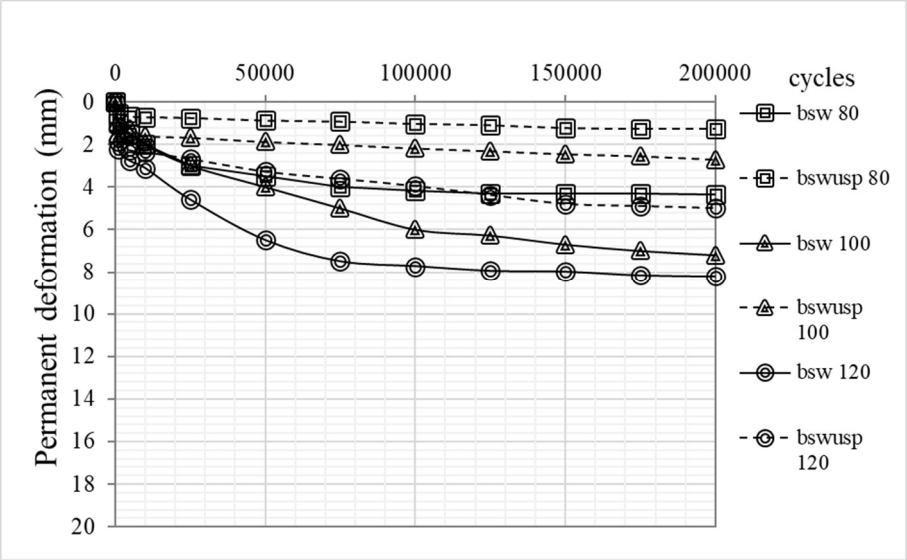


Figure 4.9 Permanent deformation, with/without the USP, LC

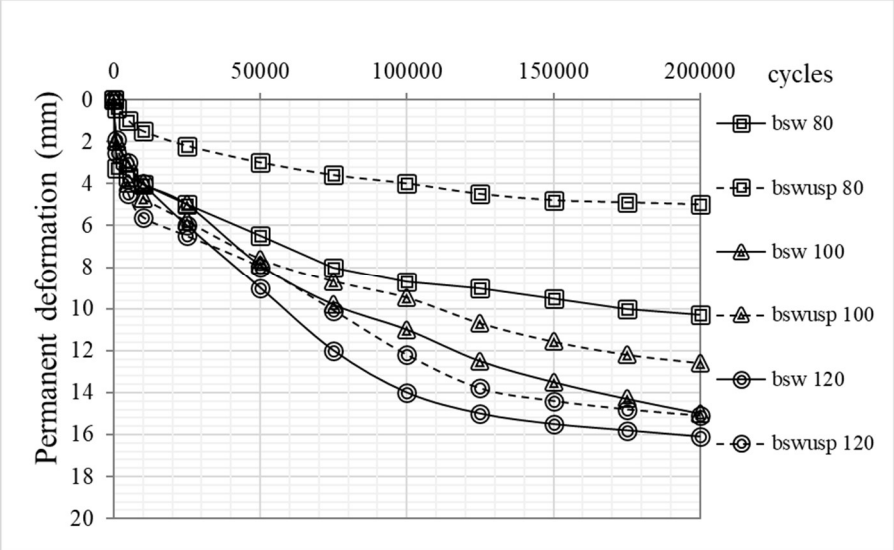


Figure 4.10 Permanent deformation, with/without the USP, CC

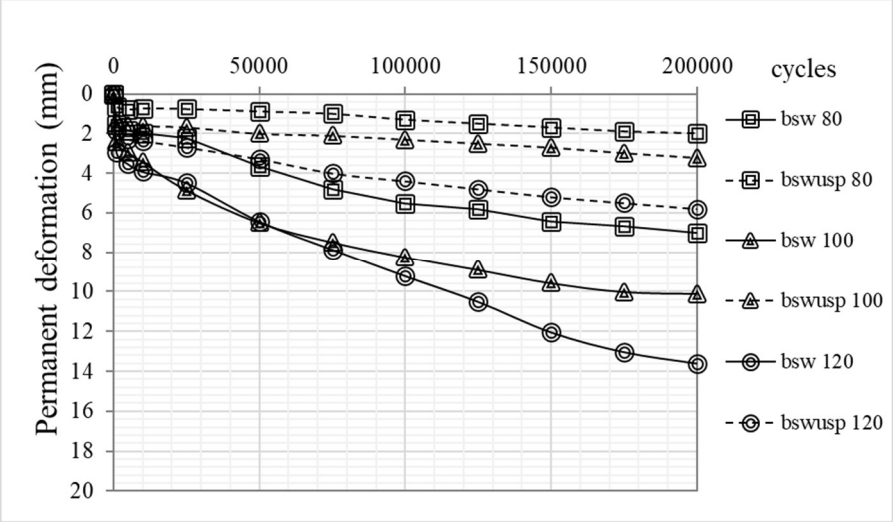


Figure 4.11 Permanent deformation, with/without the USP, CCB

The test results of all four soils show rapid deformation up to around 10,000 cycles, which could be due to its initial densification and further packing after the corners of the sharp angular aggregates began to break. However, once the ballast started to stabilise, the rate of deformation gradually decreased and then remained relatively constant after 100,000 cycles.

This indicates that during the initial stage there is a time when the ballast underwent considerable particle rearrangement and densification, which after reaching a threshold compression, resisted further deformation during any subsequent load cycles. A similar observation was recorded previously by Indraratna et al. (2013). In this study, for the unsaturated tests, most of the stabilisation of the permanent deformation was completed by approximately 50000 cycles. However, for most tests with USPs, slight deformation continued to about 100000 cycles. Overall, the results of this research show less permanent deformation in tests with USPs compared to the test without the USPs. The reason for this is provided below.

The previous studies reported that the contact area between the ballast aggregates and the sleeper increases from 1-5% (without the USP) to up to 30 % when the USP is used (Potocan and Dorfner, 2013; Lay and Steger, 2015; Musgrave and Wehbi, 2016). In this study the use of the USP increased the contact area up to 28.9 % (section 3.6.8). Due to this factor the highly concentrated stresses at the sleeper–ballast interface (from a hard concrete sleeper) are distributed over a wider area, which reduces the magnitude of the vertical stress at the sleeper–ballast interface and within the ballast mass at particle–particle contacts (Figure 3.26). Eventually, the uniform distribution of stress helps to reduce the permanent deformation of the subgrade soil. Several researchers reported that the percentage reduction of stress at the sleeper– ballast interface varied between 8 and 12% (Dahlberg, 2010; Le et al., 1999; Indraratna et al., 2013). In the dynamic test, the introduction of the USP increased the contact area, reducing the applied stresses. At the end of 200000 cycles the sleeper without the USP settled lower in contrast to the tests with the USP. The difference represents 10-25% reduction in settlement as a result of the installation of the USP. As a compressible material the USP was expected to be compressed to some extent and contribute to the settlement. On the other hand, clays with high dry density and high undrained shear strength (especially with low moisture content) are relatively incompressible. Therefore, the USP would be compressed and be a factor

in the settlement. Figures 4.8 and 4.9 show evidence of small settlements for tests with London clay and Etruria marl; whereas the tests with china clay and china clay and 5% bentonite show much higher deformation (Figures 4.10 and 4.11 respectively). London clay showed minor deformation, which could be explained by the fact that it has a high dry density and high undrained shear strength (Section 3.4.4); which was one of the highest (120 kPa). On the contrary, china clay showed the highest permanent deformation. These results were expected, as the undrained shear strength before and after the test dropped from 120 kPa to 65 kPa. One of the reasons for this big drop might be the voids left during compaction, which were saturated with added water in a higher proportion than was expected. High deformation of CC and CCB could be because of the value of the void ratio (section 3.4.9), which characterises the compactness of soils. The value depends on the volumetric changes of soils (the void ratio of loose soils is higher than that of dense soils). As can be seen from the Table 15 the void ratio of CC and CCB was generally higher in contrast to EM and LC, that could explain the higher rate of deformation of CC and CCB. The results show that with an increase of moisture content (100% OMC to 120% OMC) the permanent deformation gradually increases by approximately 15-20%. This is in agreement with previously conducted studies (Alobaidi and Hoare, 1994; Duong et al., 2014, 2016) and shows the negative effect of water content on subgrade strength. The tests with the USPs show better results compared to the reference test in terms of permanent deformation.

4.2.4 The large-scale test, subgrade permanent deformation investigation

The behaviour of subgrade should ideally be studied through tests conducted on a real track under actual loading conditions. However, these tests are not only costly and time consuming but also could disrupt traffic schedules. Therefore, laboratory experiments simulating field load and boundary conditions are usually carried out on ballast specimens. To attain this, the large-

scale test apparatus was assembled to enable the realistic simulation of railway track behaviour under cyclic loading. The purpose was to validate the small-scale test results, comparing the data received from both apparatuses. The relationships between the number of cycles and settlement are shown in Figure 4.12, which shows two curves representing the permanent deformation of subgrade soil after applying 250,000 cycles of loading using the small-scale and the large-scale tests. Both show a similar trend of deformation where there was initial rapid deformation, which during the first 20,000 cycles stabilised to give steady state settlement following the trend observed by Indraratna et al. (2004) and Ghataora et al. (2006). At the end of the test, the permanent settlement of the small-scale and the large-scale tests was 8.5 mm and 9.1 mm respectively; a difference of only 7%. This demonstrated that the small-scale test may reasonably well represent field settlement for the same conditions.

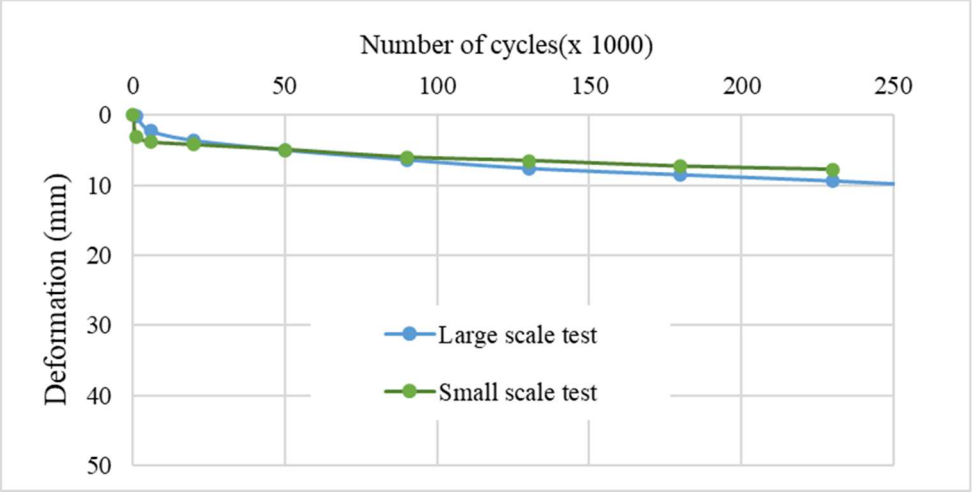


Figure 4.12 Permanent deformation of subgrade layer, the large-scale test

4.2.5 Subgrade permanent deformation. Summary

Permanent deformation of the subgrade is one of the key criteria that must be considered; with the negative outcomes being presented in the literature review. One of the factors affecting

permanent deformation of subgrade soil is moisture content, and the susceptibility of soils to moisture content was presented. Etruria marl and china clay were found to be more susceptible to permanent deformation and the rate increased with the increase of moisture content, affecting it to a higher degree. This indicates the sensitivity of this type of soil and the necessity of improving it. After thorough investigation and testing of different cohesive soils under repeated loading, it was found that applying the USPs has a positive effect on subgrade permanent deformation; the difference was in a range between 5 to 20%. The results from this section combined with the results of the following sections will be used in further analysis.

The permanent deformation of the cohesive subgrade soils was considerably larger in the case of the tests with free-standing water. In this case, the average permanent deformation was almost twice that in the unsaturated tests. The difference could be explained by the earlier observations on moisture content and moved soil: when higher moisture content causes slurry initiation and the presence of water promotes slurry to move. Subsequently, the moved slurry leaves space for the ballast particles to sink in (Dawson, 1986), causing settlement. The correlation between the moved soils has become obvious from the results of this study and is in agreement with results from previously conducted works (Alobaidi and Hoare,1994; Ghataora, 2006; Duong, 2014). Those studies showed a direct correlation between migration of soil and subgrade settlement. Both of those parameters followed the same pattern with time. Subgrade soil with high moisture content (120% OMC) and USPs could still be expected to show large permanent deformation if ballast particles sink into it, by pushing the clay into the voids of the ballast. However, this does not seem to have happened to a great extent, according to both the settlement results and inspection of the sample tests. The fact that clay demonstrates small settlements is in agreement with earlier discussed results, which suggests that the small settlements are a consequence of small changes in moisture content and a small amount of soil which has moved. The smallest deformation was in the case of the unsaturated (dry) soil

condition for all four tested soils; the stronger the subgrade soil, the lower the settlement, which was in accordance with previous research works (Alobaidi and Hoare, 1994). The curve of the largest settlement corresponds to soil CC 120, which is the weakest soil (67 kPa) and at the same time of relatively low unit weight, implying that it possesses high potential compressibility. The second largest settlement corresponds to material CCB 120, which is stronger (70 kPa) than CC 120 but has approximately the same unit weight. The soil LC 80 showed the smallest settlement. The fact that it showed the highest value of strength (115 kPa) explains why it did not settle much.

4.3 Stiffness

The Guide to Track Stiffness (2016) explains the term spring stiffness (S), which indicates a stiffness in terms of the point load needed to cause a unit deflection; S has units of force divided by deflection (kN/mm). Its value depends on the effective stiffnesses of all the individual elements of the track system combined. The term modulus, denoted k, indicates the line load needed to cause a unit deflection. The line load is quantified in units of force divided by length, for example MN/m, giving k in units of force divided by length squared, e.g. MN/m2. Spring stiffness or the modulus may relate to the track-bed (i.e. below the sleeper and including any USPs), the rail pad, or the complete support system. A detailed theoretical explanation of stiffness was given in Section 2.4.4 and Section 3.6.6.

Different theoretical models have been developed for the calculation of a track modulus based on load versus deflection relationships. Although there is no consensus on the most accurate method, the most commonly used is the Winkler method (Crawford et al., 2001).

A vertical force (P) applied by a wheel produces a vertical rail deflection (w). The track stiffness (k), at a point directly underneath the wheel as it passes is defined as the ratio of vertical force to vertical rail deflection, in which the slope of a secant to the load/deflection curve represents the stiffness. The same method has been used in this work, but for the whole system. For every cycle of a test the stiffness in terms of MN/m could thereby be calculated by plotting load against position for the 100 cycles. The procedure was repeated for all the recordings throughout the test and the values summarised.

In this study, the stiffness of the tested subgrade was plotted against the number of cycles. For each test the stiffness was registered at a point where the settlement curve had stabilised. These values for all tests are listed in Table 21 and used for later plots. Parameters such as liquidity index and the stiffness were examined. The general trend of all tests shows a gradual increase of stiffness during the first 50,000 cycles followed by a slower increase until 100,000 cycles. After that point, usually the stiffness remained the same or slightly decreased. The results correlate well to previous research works. For example, Dehlen (1969) explained that due to the progressive densification of the saturated soil with a number of applied cycles, the stiffness increases. Other authors explained that the stiffness changes because of the development of strain (Thom et al., 2008; 2013; Sivakumar et al., 2013). On the other hand, Ng et al. (2013) reported a slight reduction in stiffness due to dilation, in the case of unsaturated soil samples.

At the beginning of the main research investigation, it was necessary to measure the stiffness of the materials used: the USPs and a combination of the ballast and USPs. The results showed that the stiffness of the USP was in a range of 35 to 37 kN/mm (Figure 4.13).

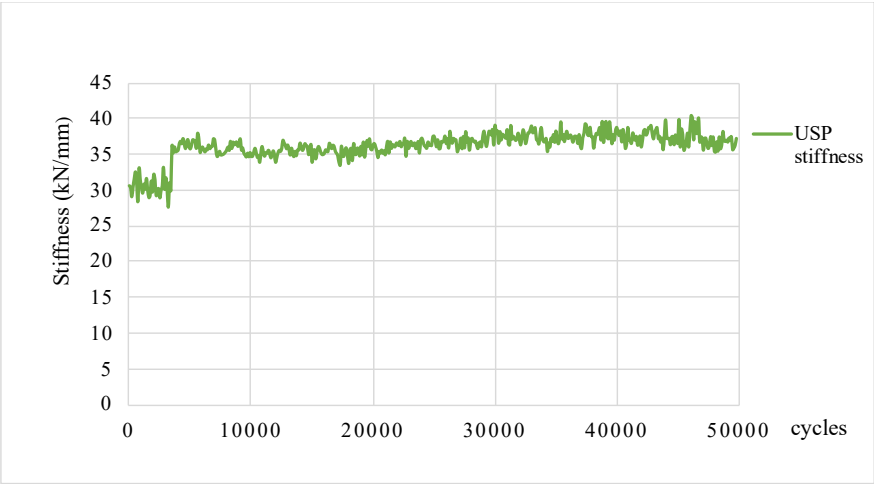


Figure 4.13 Stiffness of the under-sleeper pads (USP)

Figure 4.14 illustrates raw fluctuating data of subgrade stiffness. It represents a typical response of loading stiffness. The test data was giving an unclear picture due to an overlap of data. It was therefore decided to select a salient point such that smother graphs showing trends could be drawn without compromising the overall trends (Table 21). The aim of the rolling average was to reduce the fluctuation, but still show the trends of results, in order to better compare results of different tests. This procedure was adopted for all the tests.

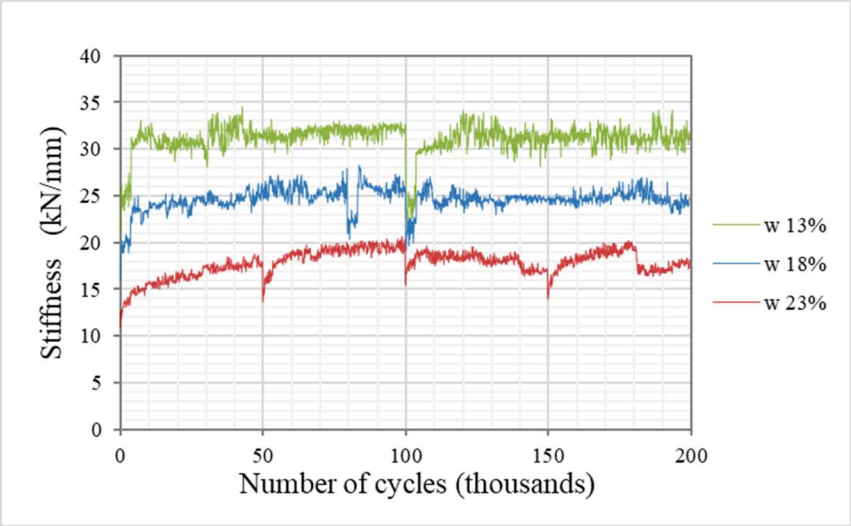


Figure 4.14 An example of fluctuation of stiffness (Etruria marl, raw data)

Table 21. Stiffness at the end of the tests

	Stiffness (KN/mm)			
Soil	EM	LC	CC	CCB
bs80	31.5	37.02	29.5	33.8
bs100	28.5	31.9	27.5	31.5
bs120	27.2	27.12	26.4	30.35
bsusp80	22.63	31.48	25.71	27.1
bsusp100	21.3	24.91	23.01	26.89
bsusp120	20.4	22.04	22.33	25.2
bsw80	30.28	33.8	25.76	30.28
bsw100	26.05	30.28	25.11	27.11
bsw120	23.11	23.05	22.98	25.2
bswusp80	22.93	25.95	23.08	23.65
bswusp100	22.42	22.63	22.88	23.12
bswusp120	22.03	22.52	21.12	23.02

4.3.1 Stiffness of subgrade soil, Etruria marl

Figure 4.15 illustrates the stiffness of different tests that were run on saturated and unsaturated subgrade soil, represented by Etruria marl. The tests had different moisture contents corresponding to 80%, 100% and 120% OMC. As can be seen from the diagram, the stiffness of all test variations increases quickly during the first 10,000 cycles until approaching approximately 50,000 cycles when the trends stabilize, and after 100,000 cycles they reach a plateau and remain the same until 200,000, with some deviations. The results of tests that were run on saturated subgrade with and without the USPs are presented in Figure 4.14; as can be seen, the trends are similar. The results are summarised in Figure 4.15, which shows the stiffness after reaching the stabilisation point.

In the case of the unsaturated tests (bs 100, bs 120), the stiffness of the subgrade decreases slightly with an increase of moisture content. This occurs as the density decreases after reaching the maximum at optimum moisture content. It could be also explained as soil dilation, as was previously reported by Ng et al. (2013) who presented the dilation of unsaturated specimens

under cyclic loading in contrast to the compression of the equivalent saturated specimens. In the research the values of the unsaturated soil stiffness increased steadily before reaching a plateau, and after a number of cycles indicated a slight reduction due to dilation.

In the case of the saturated test without USPs (bsw 80, bsw 100 and bsw 120) after adding 500 ml of distilled water to the subgrade, the stiffness decreased: approximately by 15% from bsw 80 to bsw 100, and by 13% from bsw 100 to bsw 120. This sharp decline by almost 30% showed the negative effect of free-standing water. The saturated tests with the USPs showed similar tendencies, although with a smoother gradient, where the overall decrease of subgrade stiffness from bswusp 80 to bswusp 120 was approximately 17%. Under saturated conditions, the test with USPs showed almost slightly less reduction of subgrade stiffness.

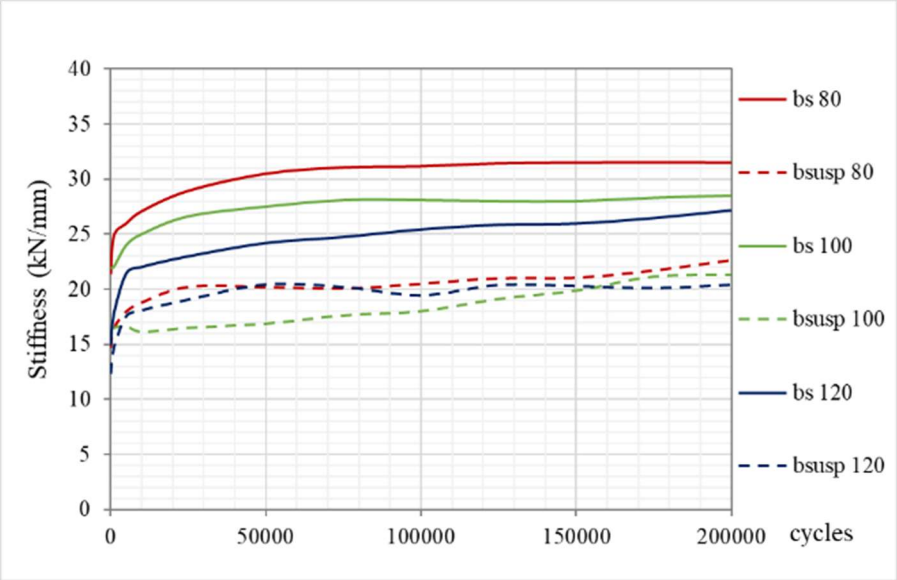


Figure 4.15 Stiffness of unsaturated subgrade, EM with/without the USP

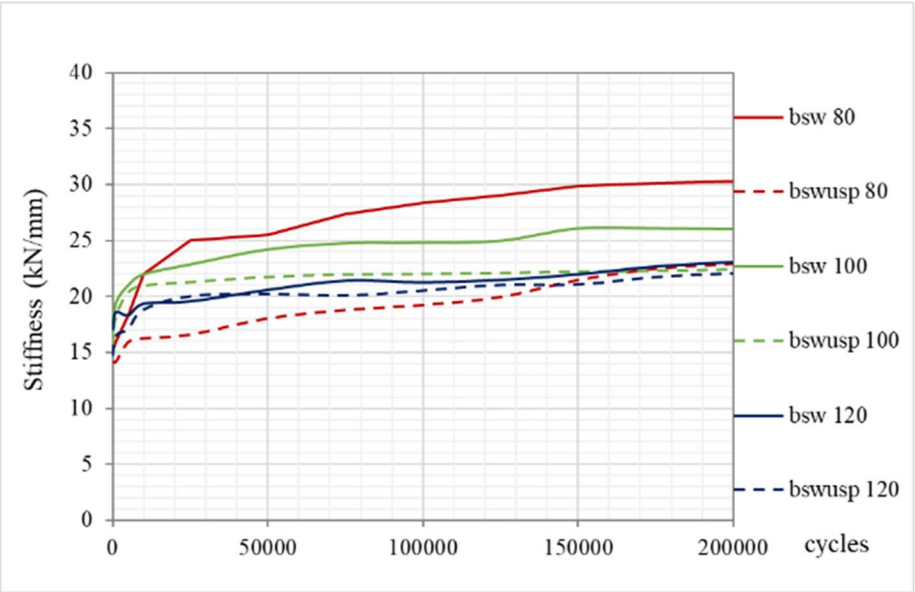


Figure 4.16 Stiffness of saturated subgrade, EM with/without the USP

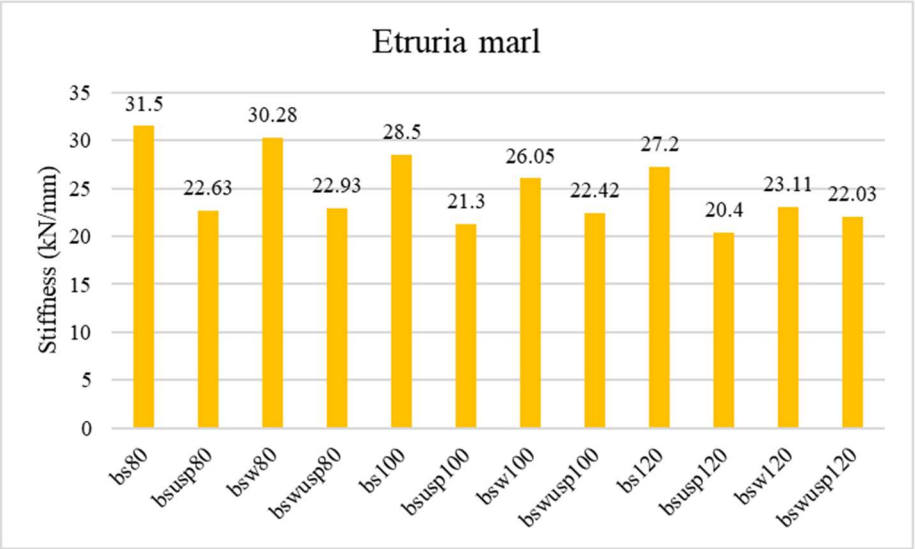


Figure 4.17 Stiffness at stabilization point, Etruria marl

Figure 4.17 combines and shows the trends, how the subgrade stiffness changes. As can be seen, free-standing water affects the stiffness of subgrade soil, reducing it. The tests with different initial moisture contents (bsw 80, bsw100 and bsw 120) showed decrease of stiffness

values with increase of moisture content. The graph illustrates that with time and after running 200,000 cycles, repeated loading affected the saturated subgrade soil.

4.3.2 Stiffness, subgrade soil, London clay

Figures 4.18-4.20 summarize the results of subgrade stiffness represented by London clay. There was a similar tendency when during the first 10,000 cycles the results showed a rapid increase of stiffness values for all test variations until approaching approximately 50,000 cycles, then it stabilized. Unsaturated soils showed higher stiffness in contrast with the saturated tests (Figure 4.19), which proves the effect of degree of saturation on softening of subgrade soil.

The results correlate well with previous research works (Dehlen, 1969; Thom et al., 2008; Ng et al., 2013; Sivakumar et al., 2013). For example, Dehlen (1969) explained that due to the progressive densification of the saturated soil with a number of applied cycles, the stiffness increases. Other authors explained the stiffness changes because of the development of strain (Thom et al., 2008; Ng et al., 2013; Sivakumar et al., 2013). On the other hand, Ng et al. (2013) reported a slight reduction in stiffness due to dilation, in the case of the unsaturated soil samples.

The tests bs 80, bs 100 and bs 120 showed a level of stiffness in a range, approximately 25-35kN/mm. A sharp decline by almost 30% was detected after adding 500ml of water to the unsaturated subgrade without the USPs, which confirmed the negative effect of free-standing water. The effect of USPs on the saturated subgrade soil can be seen from Figure 4.20. It shows that after applying 200,000 load cycles the stiffness of London clay with the USPs was higher compared to the saturated test without the USPs.

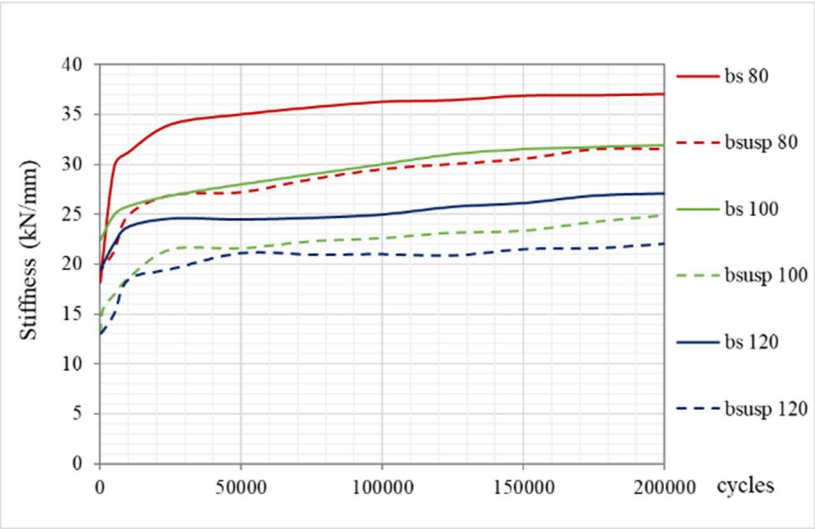


Figure 4.18 Stiffness of unsaturated subgrade, LC with/without the USP

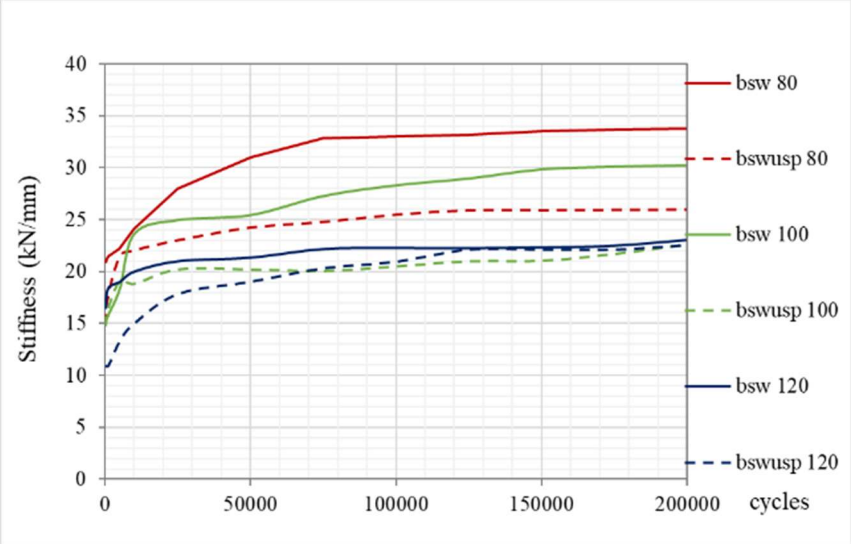


Figure 4.19 Stiffness of saturated subgrade, LC with/without the USP

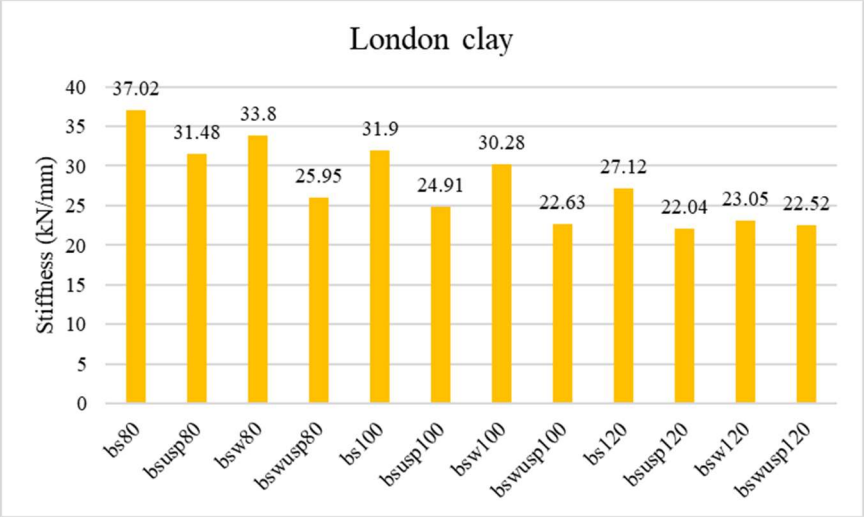


Figure 4.20 Stiffness at stabilization point, London Clay

4.3.3 Stiffness, subgrade soil, china clay

Figures 4.21- 4.22 show the trends of the tests run on china clay. They are similar to the trends that have been seen in the cases of Etruria marl and London clay, such as where the stiffnesses of all test variations increased slightly with the number of cyclic loads. As can be seen from Figure 4.23 although the stiffness of the unsaturated test was higher, the difference was not significant (i.e. about 10-20%).

The saturated tests without the USPs, bsw 80, bsw 100 and bsw 120, showed similar results. Again, this might be explained by the use of free-standing water, when after certain period of time the combination of water and repeated loading softens the top layer of the soil, creating slurry. As a result, the change of initial moisture content does not show a significant difference, which may be because the upper layer of the soils softens and dominate the response to loading. An example of change in strength of the upper parts of the soils before and after testing was demonstrated by Ghataora (2006 et. al.) and presented in Figure 2.22. The observations of this study correspond to previous studies. For example, Seed et al. (1962) discussed the sensitivity of stiffness to small changes in water content and density for material on the wet side of OMC,

while material on the dry side of OMC is less sensitive. The increase in density until reaching OMC resulted in an increase of stiffness, while the stiffness reduced as the density decreases for the wet side of optimum conditions. The results of testing saturated china clay with applied the USPs showed a slightly higher level of stiffness at the end of the test, approximately 10%.

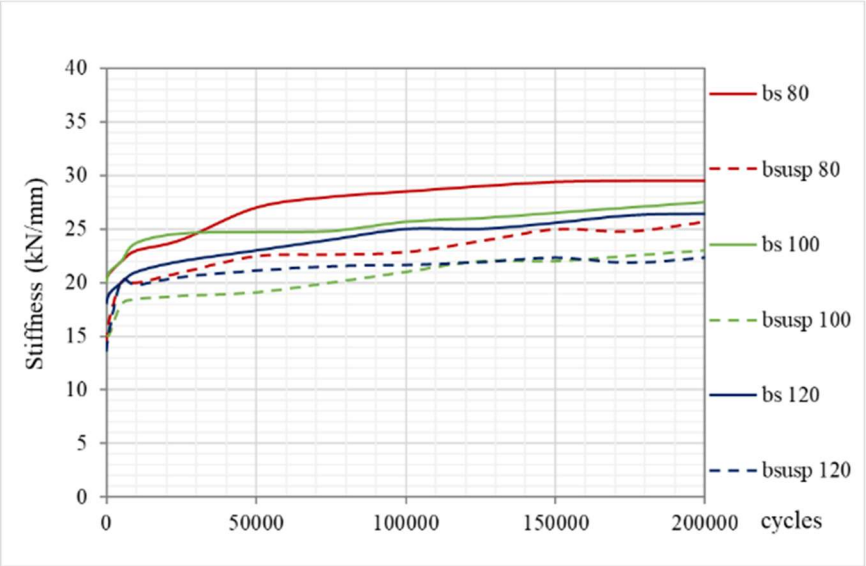


Figure 4.21 Stiffness of unsaturated subgrade, China clay with/without the USP

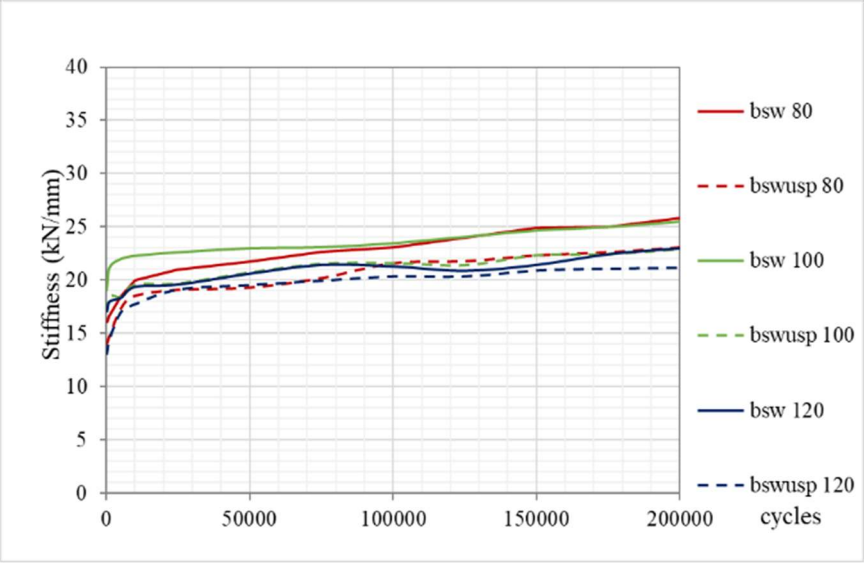


Figure 4.22 Stiffness of saturated subgrade, China clay with/without the USP

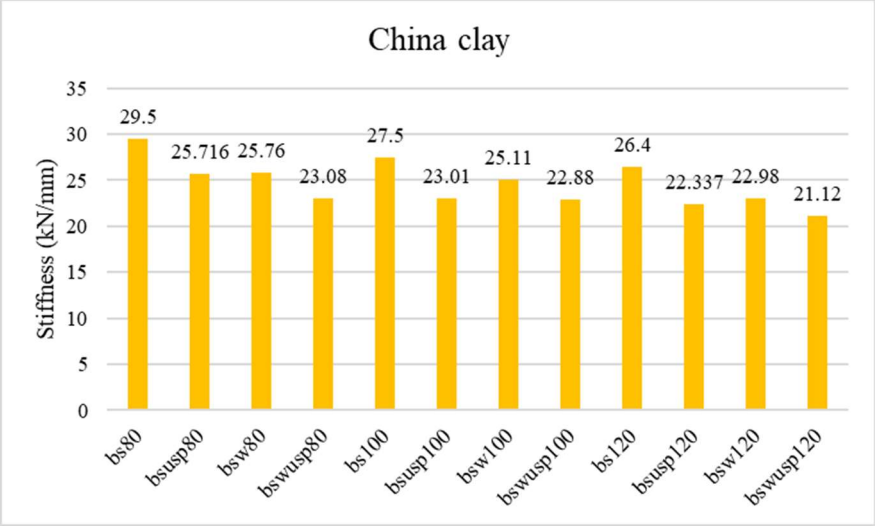


Figure 4.23 Stiffness at stabilization point, China clay

4.3.4 Stiffness, subgrade soil, a mix of china clay and 5%bentonite

The trends of the stiffness changes are presented in Figure 4.24, which are similar to the previously discussed soils and gradually increase from the start of the test. After adding 500 ml of water the stiffness was expectedly lower, and the trend was decreasing with the increase of moisture content from 80% OMC to 120% OMC. It shows that with time and after running 200,000 cycles, repeated loading affected the saturated subgrade soil.

The effect of USPs on the saturated subgrade soil can be seen from Figure 4.25. It shows that at the end of the test and after applying 200,000 load cycles the stiffness of CCB without USPs was slightly higher; however, in the case of OMC 80% the difference was significant (approximately 20-25%). It is difficult to say precisely what causes this result. One reason could be the movement of ballast causing it lock into the test cell wall, forming some arching action, and giving an impression of an increase in stiffness.

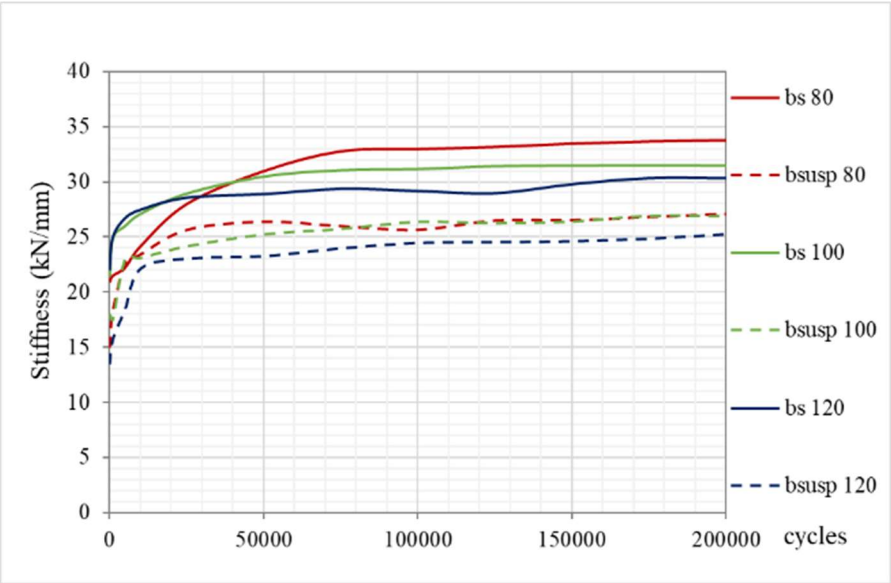


Figure 4.24 Stiffness of unsaturated subgrade, CCB with/ without the USP

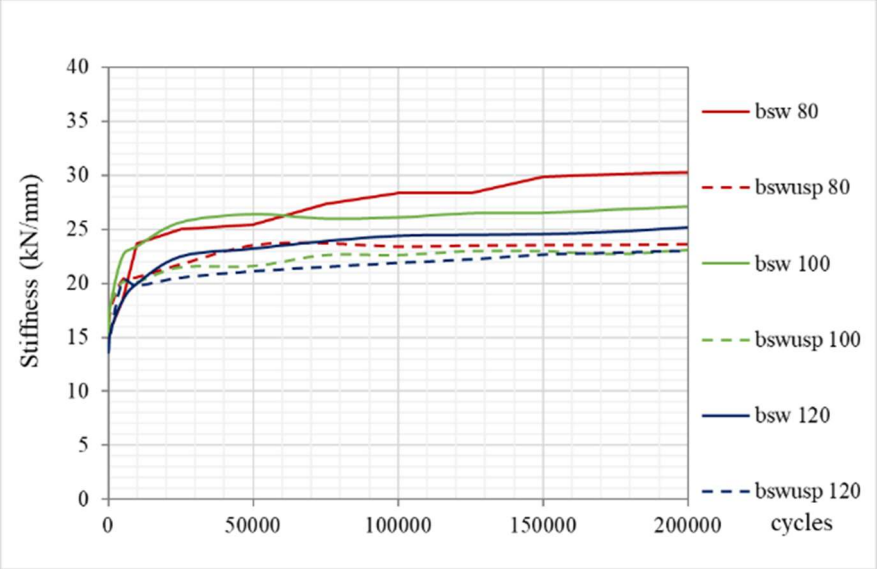


Figure 4.25 Stiffness of saturated subgrade, CCB with/without the USP

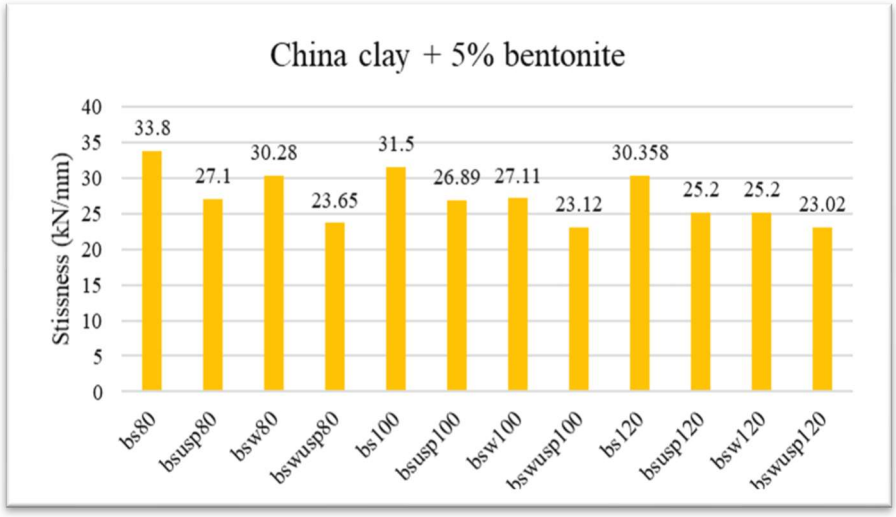


Figure 4.26 Stiffness at stabilization point, CCB

4.3.5 Discussion

As a resilient railway component, the USPs provide an elastic layer between sleepers and ballast particles (Potocan and Dorfner, 2013). As a result, the highly concentrated stresses at the sleeper–ballast interface (from a hard concrete sleeper) are distributed over a wider area, which reduces the magnitude of the vertical stress, allowing for a more uniform distribution and decreases overall deformation. The increased contact area of ballast by the USPs at the sleeper–ballast interface reduced the induced stresses at the interface and at particle–particle contact. In this research the contact area increased from approximately 2% to 29% (section 3.6.8). The attachment of the USPs reduced the value of the stiffness at a given number of loading cycles, and the stiffness gradually increased with the number of loading cycles.

The results show an initial unstable phase, leading onto stabilisation, where some curves display a continued increase in stiffness throughout the test and others start to stabilise or decrease after approximately 100,000 cycles. The initial unstable phase could be represented by the reorganisation of ballast particles. Crawford et al. (2001) explains that the force from

the sleeper is transferred through the contact points of the ballast. The deformation of the stones leads to an increased contact area between the stones, steadily increasing the stiffness of the ballast mass. There was a strong indication suggesting that the density of the subgrade material may have a significant influence on the subgrade's performance. Li and Selig (1994) who reported that the soil's physical state (water content and dry density) influences the behaviour of the railway foundation. Other factors that may influence the performance of the subgrade soil are the percentage of fines, plasticity index, and the liquid limit, which was previously concluded by several authors (Yau and Von Quintus, 2004; Soliman and Shalaby, 2013). The void spaces could influence the stiffness as the development of matric suction relates to the pore sizes and the ability to retain water in capillary tension. Void spaces in a soil body relate to particle size distribution. Seed et al. (1962) reported the sensitivity of stiffness to small changes in water content and density for wet material, while material on the dry side of optimum is less sensitive. As the stiffness was measured at the end of the test, it was observed that the water significantly influences the level of settlement (subgrade permanent deformation), and stiffness when the moisture content of saturated subgrade soil was 80% OMC and OMC100%, however, it does not affect stiffness at the same level in case of OMC 120%. Instead, the stiffness of the saturated tests with and without the USPs was relatively similar. This could be because at 120% OMC the soil stiffness is lesser than that of the USP. Thus when load is applied the subgrade deformation dominates behaviour. Hence the test results of stiffness with and without the USP are similar.

In terms of stiffness values, higher stiffness was expected in the case of the strong subgrade soils; for example, London clay in all cases showed higher stiffness. China clay (CC) and the mixed soil (CCB) showed lower values of stiffness and the largest settlement, which could be explained by their relatively low unit weights. When soft subgrades showed an overall higher stiffness of the system (CCB80 bsw), that could be explained by the movement of ballast

causing it lock into the test cell wall, forming some arching action and giving an impression of an increase in stiffness. As another example, the high stiffness of the tests on the weaker subgrade can be explained by the load being carried by the pore water to a greater extent than in the tests with the stronger subgrade with lower moisture content. The high stiffness can in fact give a false picture by implying that the weakest subgrade is more stable when the truth is probably the opposite. Applying the USPs was beneficial in giving a much smoother and more uniform development of stiffness as the number of loading cycles increased.

4.4 Pore water pressure

Development of pore water pressure (PWP) due to repeated loading was named as a main reason of migration of fine particles and mud pumping phenomenon along (Alobaidi and Hoare 1996, 1998; Ghataora et al. 2006; Trinh et al. 2012; Duong et al. 2014, Chawla 2016). Therefore, it was important to record and analyse the dynamic of PWP and to analyse the effect under sleeper pads (the USPs). This analysis was essential for further investigations of correlations between development of pore water pressure and the amount of permanent deformation, subgrade stiffness and the amount of loosened soil. Pore water pressure corresponded to the cyclic deviator stress at the loading frequency of 3 Hz; the maximum applied cyclic load was 150 kPa. It was measured for both test set-ups: ballast-subgrade-water, and ballast-subgrade-water-the USP, at the contact point between the ballast and the subgrade soil. Figures 4.27-4.38 show the development of pore water pressure in the subgrade soils (Etruria marl, London clay, China clay and a mix of China clay with 5% bentonite), placed at different moisture contents 80%, 100% and 120% of the optimum moisture content (OMC) tested with and without the USPs. Pore water pressure transducer PT1 was accurately placed on the surface of subgrade in the centre of the small-scale test.

4.4.1 Development of pore water pressure at OMC 80%

As can be seen from Figures 4.27-4.30 that all four soils showed similar trends and there was not a significant difference between the test results: pore water pressure developed with USP was slightly lower comparing with tests conducted without the USP. Overall, the tests without USPs showed a higher excess of PWP and a high range of fluctuation of cyclic PWP (approximately between 6-12 kPa); whereas in the tests with USPs, the PWP was almost half the maximum value, approximately 5 kPa and the fluctuation was not that significant (in a range of 1-2 kPa). It remained the same during 100000 cycles of the test. All four subgrade soils showed similar trends. In the case of London clay and China clay there was not a significant difference between the test results with and without the USPs, where the results showed similar values of PWP between 5-6 kPa. The PWP in tests without the UPSs was about 7 kPa, which could be explained because of the strength and stiffness of the London clay and China clay which was high when the moisture content is low. It could be said that for subgrade soils with low initial moisture content (80% OMC), the effect of the USPs was not significant.

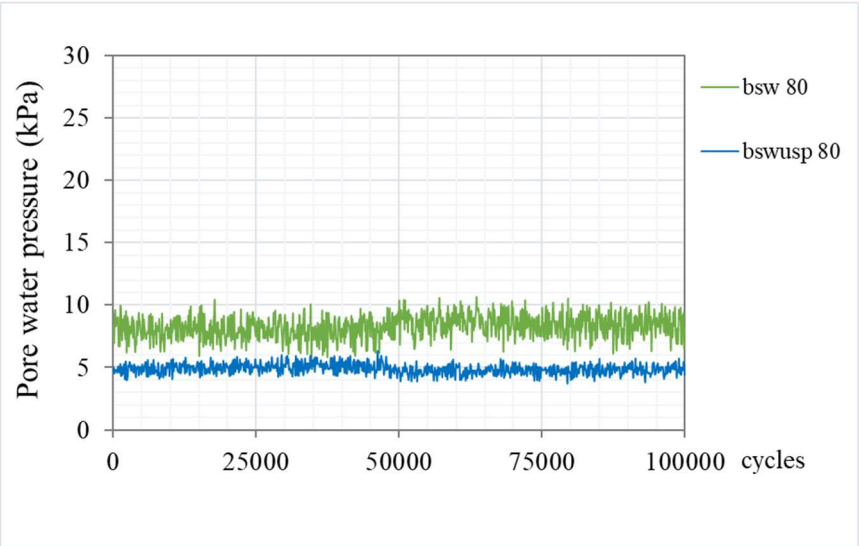


Figure 4.27 Development of pore water pressure/ EM, OMC 80%

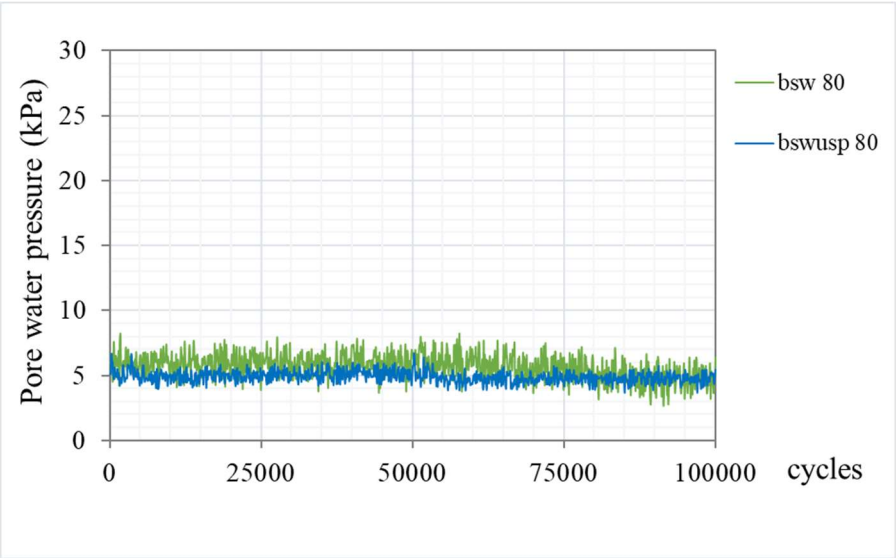


Figure 4.28 Development of pore water pressure/ LC, OMC 80%

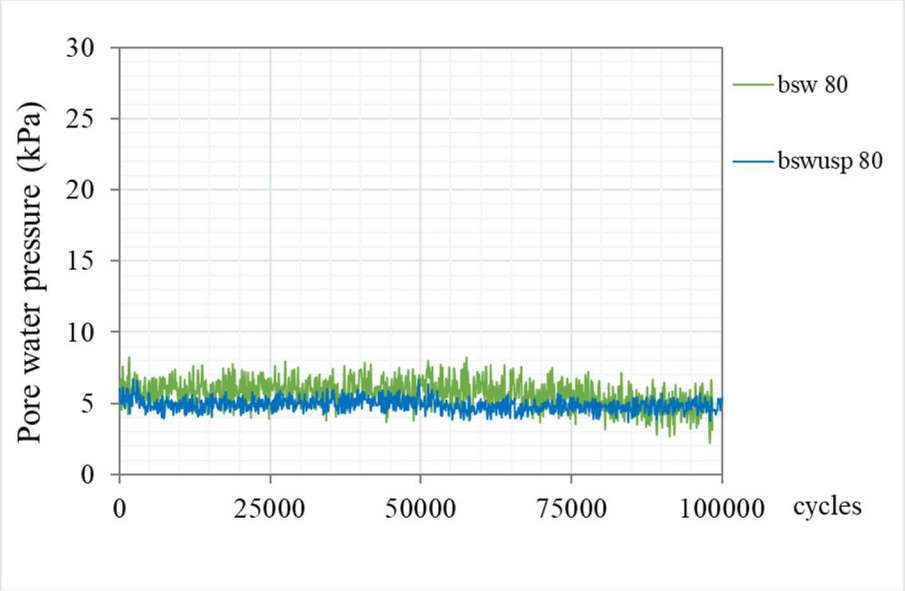


Figure 4.29 Development of pore water pressure/ CC, OMC 80%

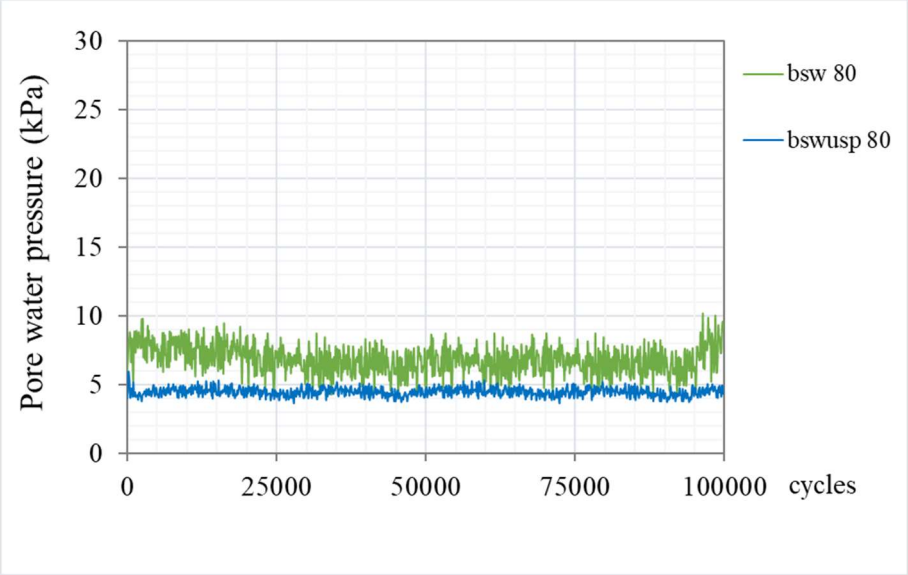


Figure 4.30 Development of pore water pressure/ CCB, OMC 80%

4.4.2 Development of pore water pressure, OMC 100%

Figures 4.31-4.34 illustrate changes of pore water pressure corresponding to the cyclic deviator stress at the OMC 100% for subgrade soils with and without the USPs. The pore pressure changes that occurred in tests with the USPs can be seen from the figures. The pore water pressure was initially built up rapidly before it started to decrease. With an increase of the initial moisture content, the effect of under sleeper pads could be seen; all figures show that pore water pressure slightly decreases from the initial 8 -10 kPa to 4-6 kPa. In the test without the USPs, under continued application of cyclic loading, excess pore water pressure gradually built up over each cycle. The tests without USPs showed a rise of pressure to 12-16 kPa and a high fluctuation of cyclic pressure in a range of 5 kPa. This could explain the high amount of loosened soil in the tests without USPs, when the high fluctuation of cyclic pressure works as a suction mechanism, explained previously in other works (Alobaidi, 1994; Ghataora, 2006; Duong et al., 2014). On the other hand, the insignificant fluctuation in the case of the USPs and the lower amount of loosened soil could be explained by the USPs reducing the cyclic pressure and suction.

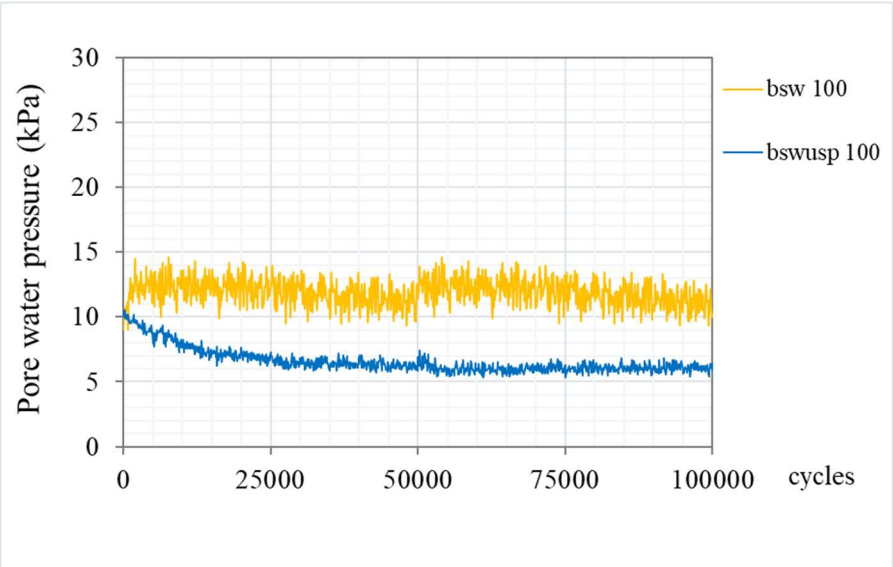


Figure 4.31 Development of pore water pressure/ EM, OMC 100%

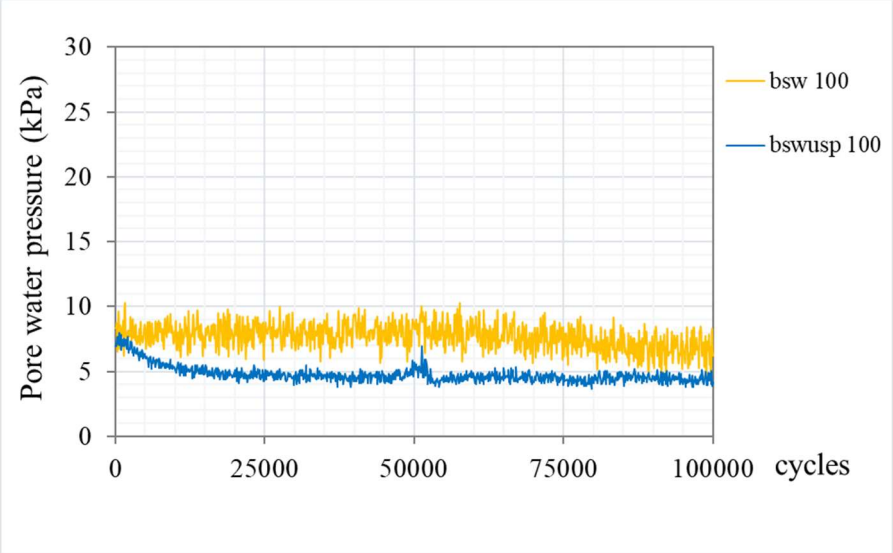


Figure 4.32 Development of pore water pressure/ LC, OMC 100%

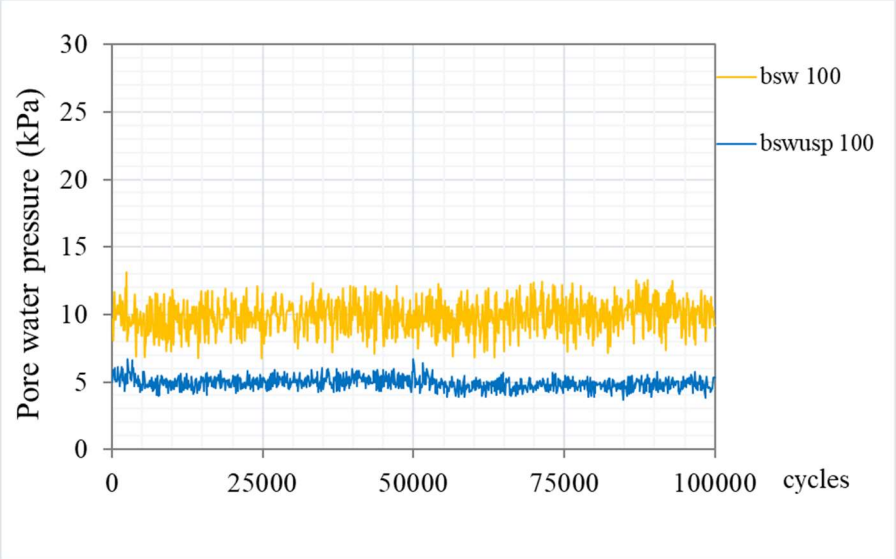


Figure 4.33 Development of pore water pressure/ CC, OMC 100%

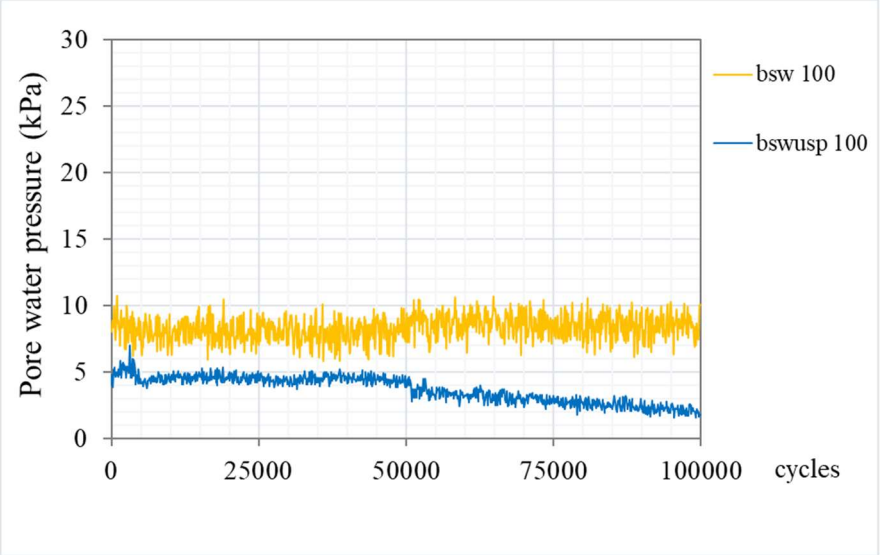


Figure 4.34 Development of pore water pressure/ CCB, OMC 100%

4.4.3 Development of pore water pressure, OMC 120%

As can be seen from Figures 4.35-4.38, when saturated subgrade soil was tested without USPs the development of the pore water pressure grew during the test and built up rapidly from the initial 12 kPa to 18-20 kPa. All subgrade soils showed similar trends except the London clay. As London clay is a stiff clay it meant the trend only grew slightly. When the subgrade soils

were tested without USPs, the cyclic pore water pressure fluctuated significantly; it could be observed that the difference between maximum and minimum values was up to 8 kPa. On the other hand, when the USP was installed, the changes in pore pressure were not so sharp and were maintained at a lower level compared to the tests without USPs during the applied cyclic loading. The cyclic fluctuation was in a range 1-2 kPa; the trend remained stable during the tests. Although the test with the USP showed increases in values of PWP compared with OMC 80% and 100%, it was much less compared with the test where the USP was not installed. The difference was up to two times.

To sum up, a comparison between the development of pore water pressure in the tests with and without USPs under the application of cyclic loading was proposed in this analysis. The results show that using under sleeper pads reduces fluctuation and level of pore water pressure. As expected, without the USPs the excess of pore water pressure increased with cyclic deviator stress at OMC 100% and 120%. Results show that in the case of most specimens, the pore water pressure increased significantly at the initial stage of the loading application.

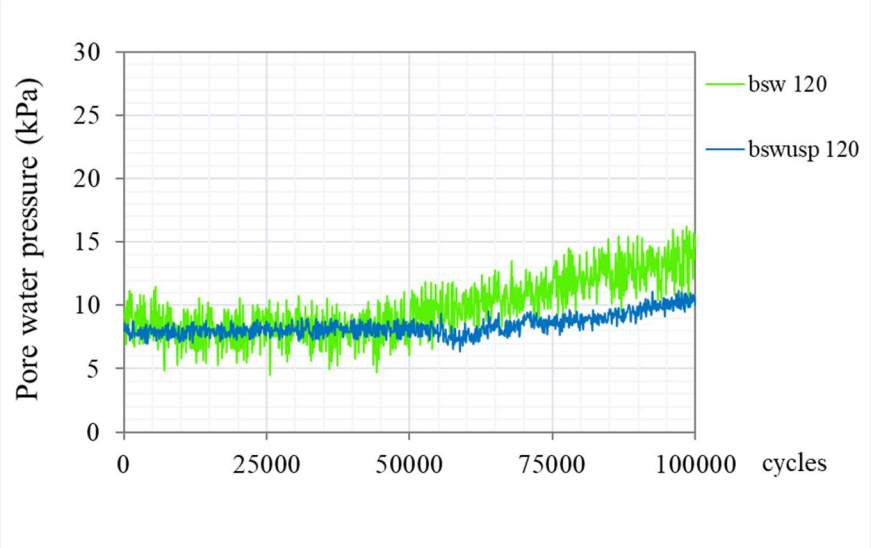


Figure 4.35 Development of pore water pressure/ EM, OMC 120%

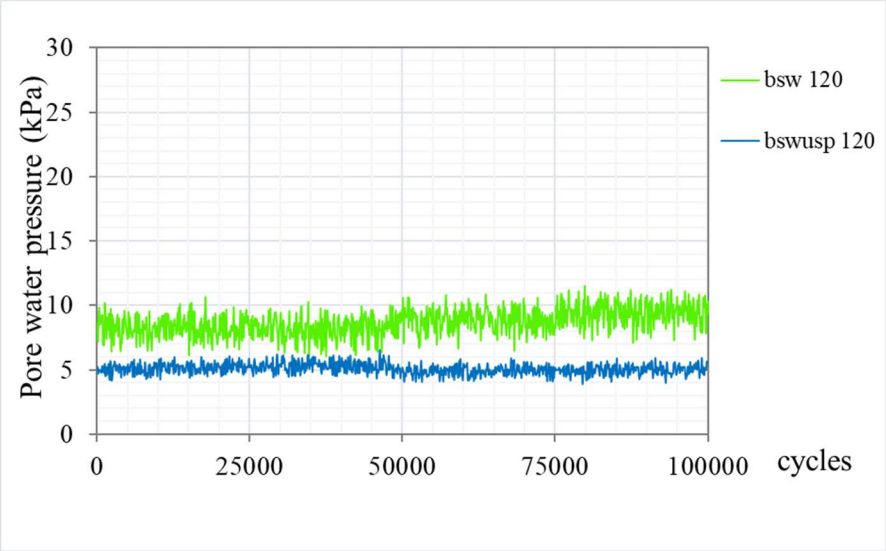


Figure 4.36 Development of pore water pressure/ LC, OMC 120%

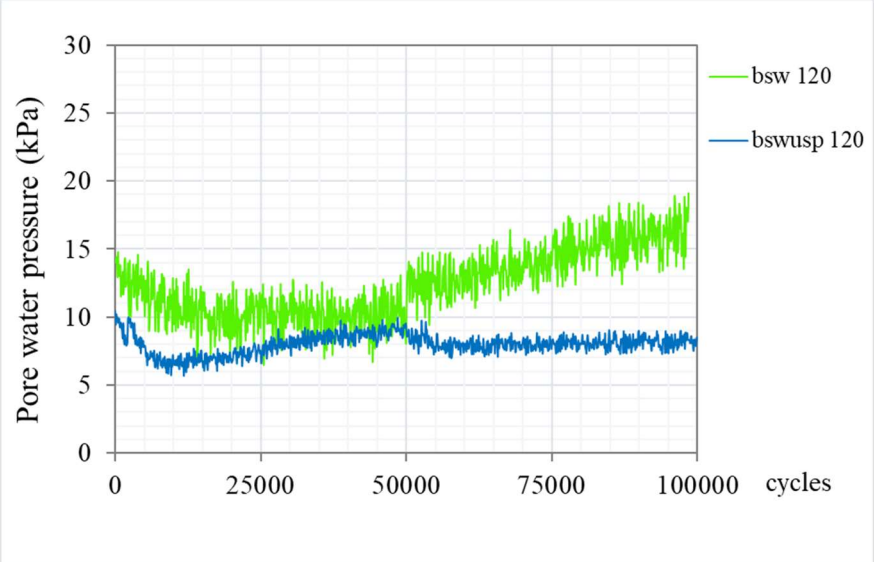


Figure 4.37 Development of pore water pressure/ CC, OMC 120%

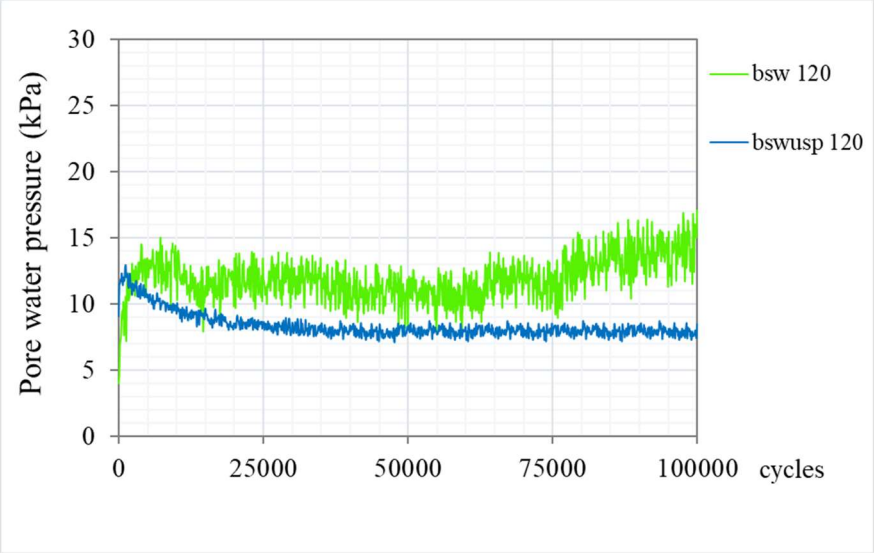


Figure 4.38 Development of pore water pressure/ CCB, OMC 120%

4.4.4 Summary

A series of cyclic tests were carried out to investigate the effect of the USP on development of pore water pressure at the subgrade/ballast interface. The tests were conducted on the range of subgrade soils with different dry density and initial moisture content, corresponding to 80%, 100% and 120% of OMC. In case of 80% OMC no significant changes in pore water pressure development were measured during the loading. The tests with and without the USP showed similar trends with slightly higher level of pore water pressure in case of tests without the USP. In case of 100% and 120% OMC the level of pore water pressure and its fluctuation was higher in the tests conducted without the USP, as can be seen in case of Etruria marl and English china clay. On the other hand, in case of 100% and 120%OMC the level of pore water pressure was lower in the tests with USP, there was a considerable improvement in reduction of pore water pressure development, examples of EM100, CC100, CCB 100, CC120, CCB120. This could be explained as the USP reduce vibrations from the repeated load, decreases stresses and transmits the load into subgrade in the smoothest way, which affecting the development of pore water pressure. As a result, test with USP showed lower pore water pressure.

4.5 Analysis of results of the small-scale tests

Factors affecting the creation of mud pumping are repeated loading and the saturated condition of the soil (Alobaidi and Hoare, 1994; Selig et al., 1994). The objective of this study was to identify the effect of the applied USPs on the subgrade soil: such as undrained shear strength, stiffness and erodibility of saturated subgrade soil. The main focus was to investigate the behaviour of subgrade soil in a saturated condition with free-standing water. Two soils used in this study were from natural deposits: Etruria marl and London clay; another two were commercially produced china clay and a mix of china clay and bentonite.

4.5.1 Relationship between liquidity index and subgrade strength

The undrained strength of clays has been widely related to the liquidity index (Vardanega and Haigh, 2014). The density of soil increases with the increase in moisture content until it reaches the maximum (at optimum moisture content) then it decreases after that. As soil density decreases with increasing water content (a case of OMC 120%) a soil with a high LL will exhibit a lower strength at the liquid limit than those soils with lower liquid limits (Haigh, 2012).

The liquidity index before and after the cyclic test was calculated according to BS 1377-4:1990 and is presented in Table 20. The relationship between undrained shear strength and the liquidity index is shown in Figure 4.39. The results show that the strength of the subgrade soil decreases with the increase of the liquidity index. The graph compares the strength of the subgrade, with and without the USPs. As can be seen, both trends are decreasing with the increase of the liquidity index. It is important to note that the lower values correspond to stiffer cohesive characteristics of soils. The trends give a clear picture: with an increase of the liquidity index the subgrade soils with the USP show a higher level of undrained shear strength,

comparing to the tests without the USP. In other words, applying the USP could be efficient in the case of weak subgrade soils.

Table 22. Moisture content/ liquidity index

Soil	w (%) before	w (%) after		IL before	IL after	
	before	bsw	bswusp	before	bsw	bswusp
Etruria marl	14	20.4	19.5	-0.2	0.12	0.075
	17	24.2	23.1	-0.05	0.31	0.255
	21	27.2	26.9	0.15	0.46	0.445
London clay	17	22.4	21.7	-0.22	-0.07	-0.095
	21	25.6	24.5	-0.11	0.017	-0.01
	25	29.5	28.5	0.1	0.128	0.1
China clay	25	28.2	27.5	-0.3	0.04	0.017
	30	31.2	30	0.1	0.15	0.1
	35	37.2	35	0.28	0.36	0.28
5% mix	26	29.4	28.5	-0.12	-0.01	-0.04
	32	37	35.9	0.06	0.2	0.17
	38	41.3	39.7	0.24	0.34	0.3

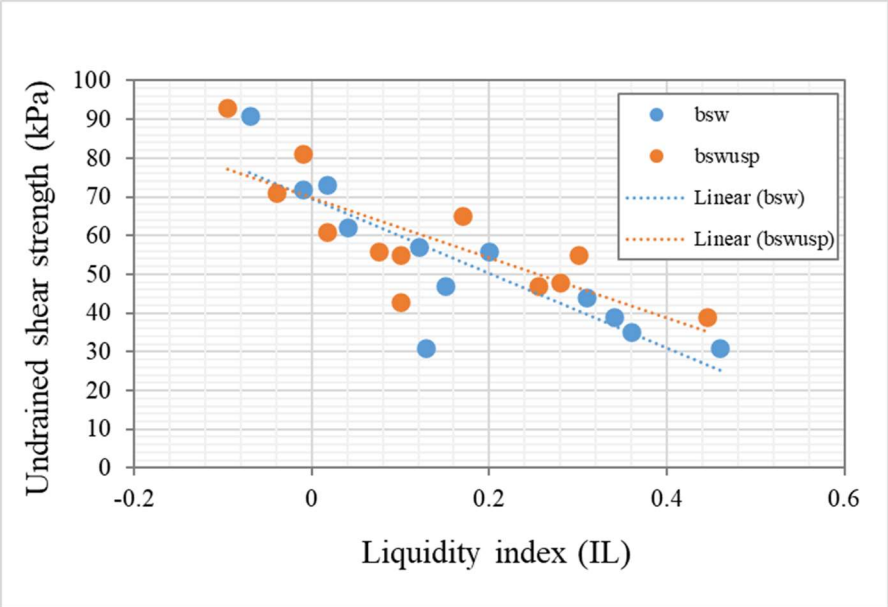


Figure 4.39 Relationship between shear strength and liquidity index

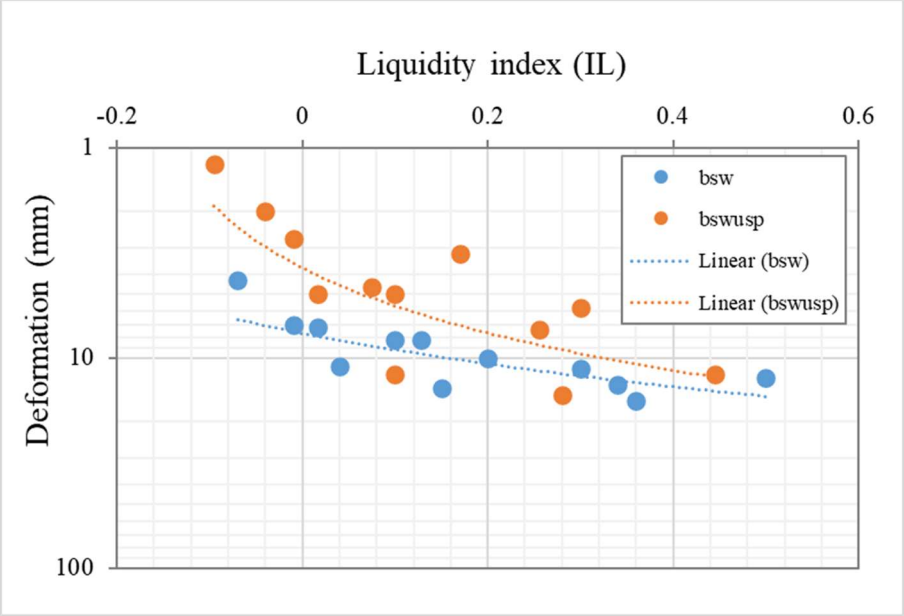


Figure 4.40 Relationship between liquidity index and subgrade deformation

The graph in Figure 4.40 demonstrates how the level of subgrade deformation depends on the liquidity index. It is clear from the graph that the deformation of subgrade soil is lower in cases when the USP is applied, regardless of initial moisture content. The difference in deformation was bigger when the liquidity index was negative, but even with increase of subgrade moisture content the deformation was lower in tests with USP.

The correlation between moisture content and the strength of the soil has been shown in Figures 4.41- 4.44. Four variables were compared in this graph: the moisture content; the strength of the subgrade before the test; and after the test; with and without under sleeper pads. After running the cyclic test, the strength of the saturated soil reduced significantly, which was expected. There was a significant difference in soil strength with the USP compared to without the USP; the b/s/w tests showed the largest weakening of the clay. This implies that the under-sleeper pads efficiently reduce the softening of the subgrade and provide good protection, which is promoted by high moisture content. All four tested cohesive soils showed similar tendencies.

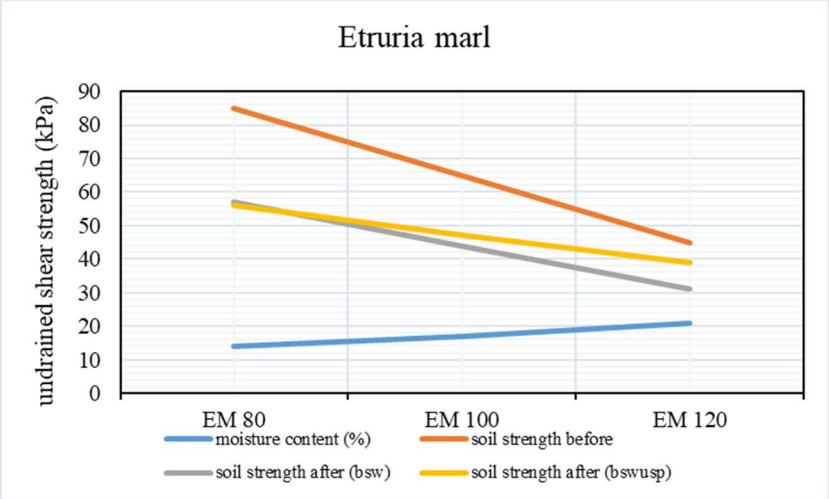


Figure 4.41 Undrained shear strength /moisture content, EM

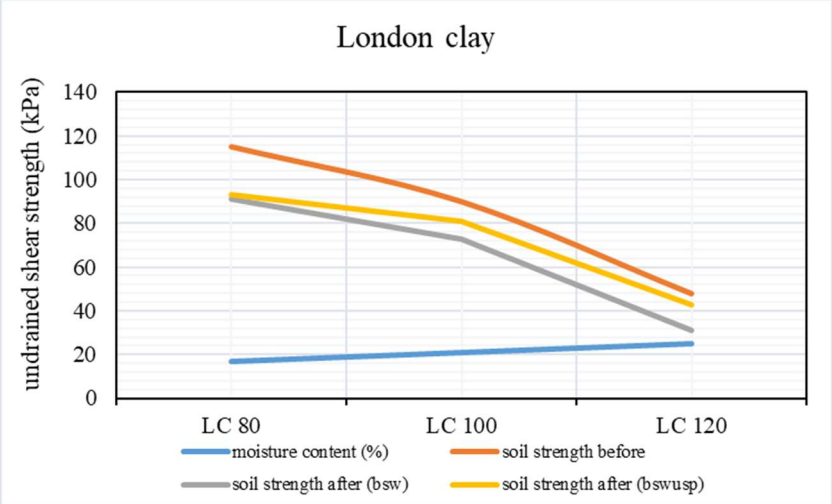


Figure 4.42 Undrained shear strength / moisture content, LC

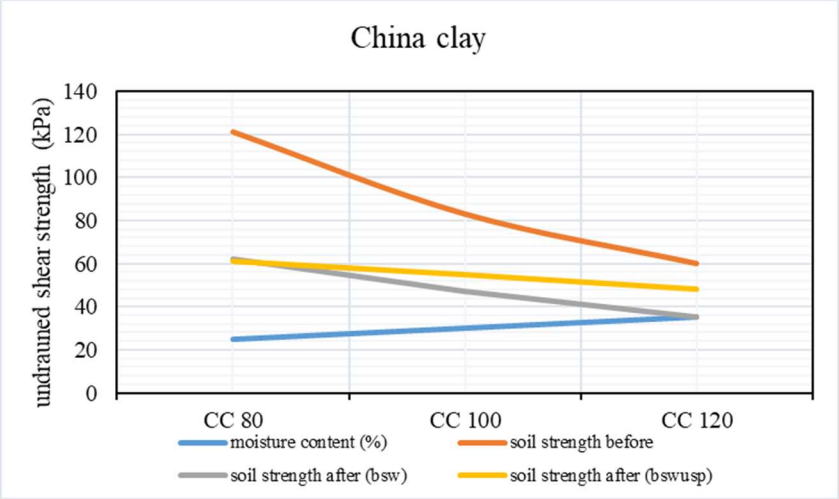


Figure 4.43 Undrained shear strength / moisture content, CC

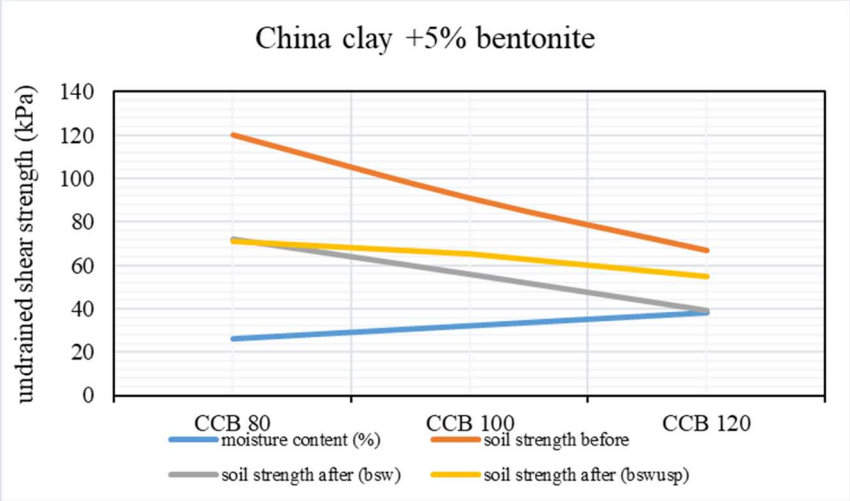


Figure 4.44 Undrained shear strength / moisture content, CCB

4.5.2 Relationship between liquidity index and eroded soil

The behaviour of the ballast changes when it is fouled with migrated fine particles from the subgrade layer. The presence of clay has a detrimental effect on the performance of a railway track; leading to problems such as excessive plastic deformation, massive shear failure and progressive shear failure (Selig and Waters, 1994). One of the objectives of this study was to

identify the effects of using the USPs on the soil subgrade. One such effect could be that the soil subgrade erosion may be reduced with the USPs, and hence, migration of fines into the overlying ballast may be reduced.

Previous studies (Alobaidi and Hoare, 1994; Selig and Waters, 1994) have shown that the amount of soil that becomes mobile (eroded) increases with the increase of the subgrade's moisture content. The results of this investigation also showed a similar trend. Figure 4.45 illustrates the amount of eroded soil increases with the increase of the liquidity index, which is directly related to moisture content. The trend suggests that the amounts of eroded soil increase at a higher rate in the case of the subgrade soil without the USP; under the same conditions the USP efficiently reduces erodibility of the subgrade soil.

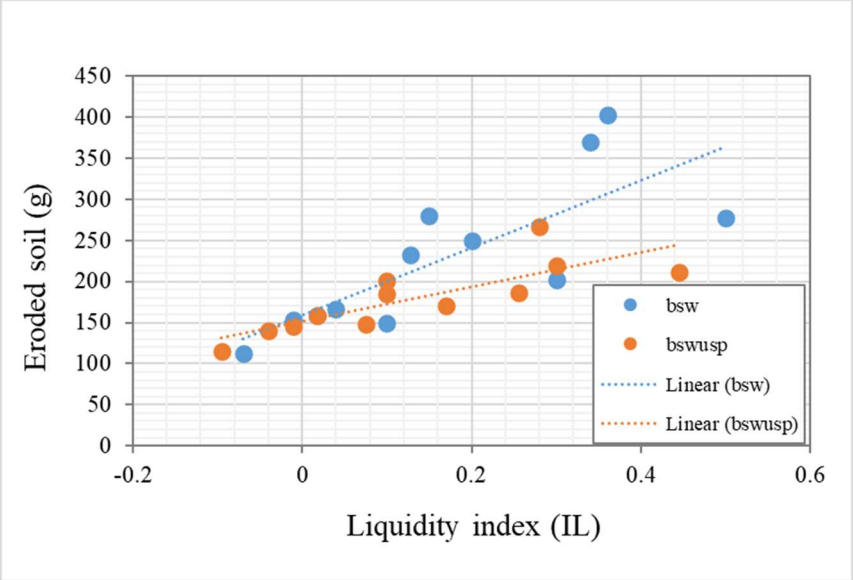


Figure 4.45 Relationship between liquidity index and eroded soil after the test

The difference between the amount of eroded soil in the tests with and without the USPs is presented in Figures 4.46- 4.49. The graphs show similar trends when the rate of erosion increases with increases of soil moisture content. All four soils showed a similar level of

erosion at 80% OMC; however, with an increase of moisture content the erosion rate accelerates. As can be seen from the graphs, applying the USP slows down erosion.

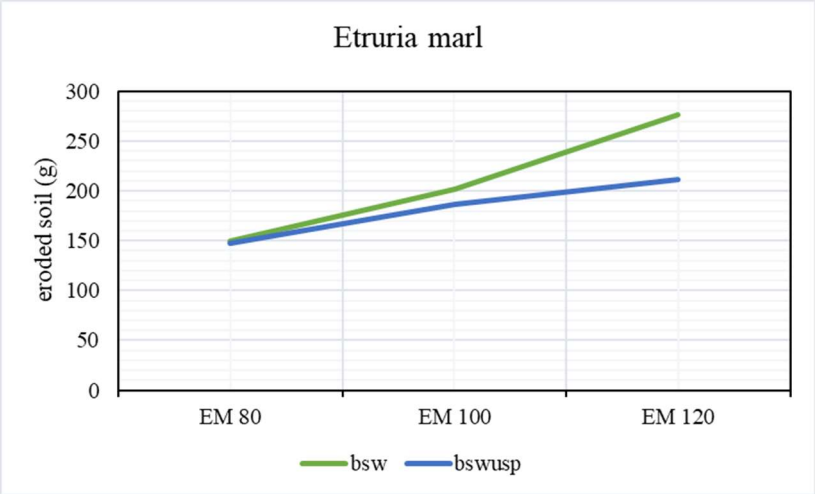


Figure 4.46 Erodability of Etruria marl

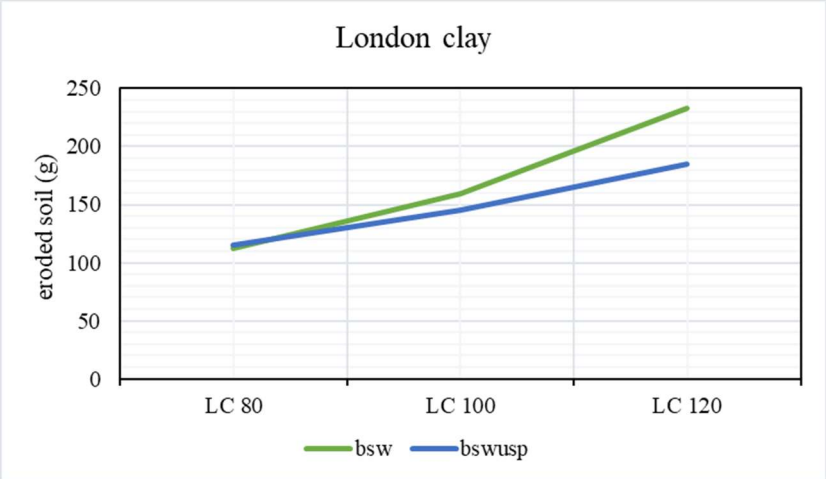


Figure 4.47 Erodability of London clay

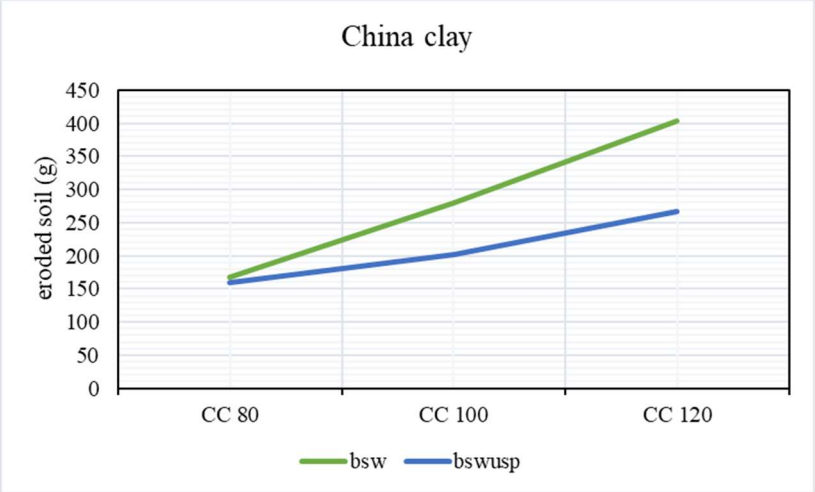


Figure 4.48 Erodability of China clay

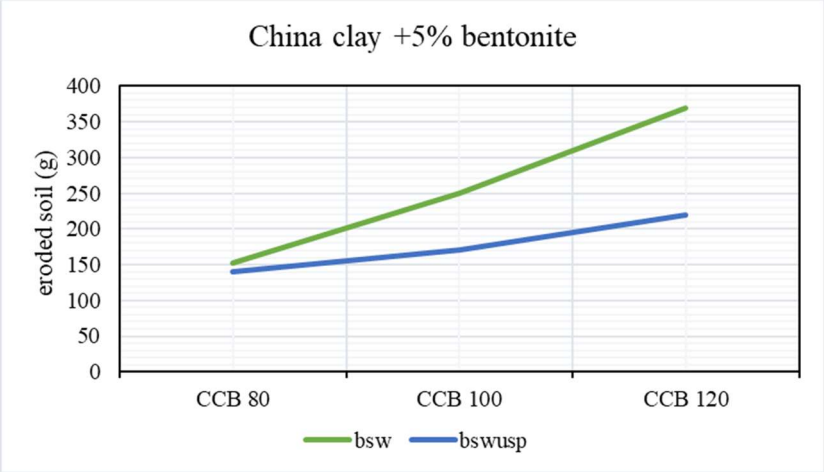


Figure 4.49 Erodability of CCB

Table 23. Amount of eroded soil

Soil	w (%)	w (%) after		IL	IL after		Eroded soil	
	before	bsw	bswusp	before	bsw	bswusp	bsw	bswusp
Etruria marl	14	20.4	19.5	-0.2	0.12	0.075	150	148
	17	24.2	23.1	-0.05	0.31	0.255	202	187
	21	27.2	26.9	0.15	0.46	0.445	277	211
London clay	17	22.4	21.7	-0.22	-0.07	-0.095	112	115
	21	25.6	24.5	-0.11	0.017	-0.01	159	145
	25	29.5	28.5	0.1	0.128	0.1	233	185
China clay	25	28.2	27.5	-0.3	0.04	0.017	167	159
	30	31.2	30	0.1	0.15	0.1	280	201
	35	37.2	35	0.28	0.36	0.28	403	267
5% mix	26	29.4	28.5	-0.12	-0.01	-0.04	153	140
	32	37	35.9	0.06	0.2	0.17	250	170
	38	41.3	39.7	0.24	0.34	0.3	370	220

Table 21 provides information about the type of the soil, moisture content, liquidity index and amount of eroded soil. The results show significant differences in the amount of loosened soil between the stronger and weaker subgrades, which was expected and corresponds to other research works (Ghataora, 2006; Duong, 2014; Chawla, 2016). It was expected that the weak subgrade and high moisture content would show the results of larger amounts of mobilised clay. The results illustrate the amount of clay collected after applying 200,000 cycles. The total amount of clay was presented as a combined amount of all fines collected from the ballast surface, from freestanding water, plus the amount of slurry from the subgrade surface. Note that in each case 500 ml water was added to the ballast at the start of the test. Notably larger amounts of loosened soil have been collected in tests without the USPs. Throughout the tests, those with USPs show the best results in terms of total amounts of eroded subgrade soil. It can be observed that the tests without the USPs represented the worst case (with the exception of two tests, EM 80 and LC 80, where the results were very similar with and without the USPs). It was observed with all four clays under different moisture contents, which provides reassurance that the USPs in general could help prevent the contamination of the ballast layer. The tests performed with the USPs showed the amount of moved soil to be just 75% of that

seen in the same test without the USPs. The EM and LC also performed better with the USPs and showed an improvement, but in contrast with CC and CCB the difference was not that significant (10-20%). The results also illustrate that the amount of moved material was smaller in the case of LC under all moisture conditions, 80%, 100%, 120%. The test of CC 120 and CCB 120 without the USPs overall showed the worst results and were particularly bad in terms of the large amount of moved material (403 and 370 grams respectively). In comparison, using USPs for the same soils indicated a significant reduction in the amount of loose soil (66% and 60% respectively).

Considering that the soils CC and CCB had the highest value of void ratio as well as lowest unit weight, it could be concluded that the use of the USP shows more efficiency when the subgrade soils are soft, as they are more susceptible to compression and deformation.

Figures 4.50- 4.52 show how the amount of eroded soil relates to other characteristics. It shows that the amount of eroded soil increases with the decrease of the soil's undrained shear strength and the decrease of subgrade stiffness. This was similar to the outcomes of other research works (Ghataora, 2006, Duong et.al.,2014).

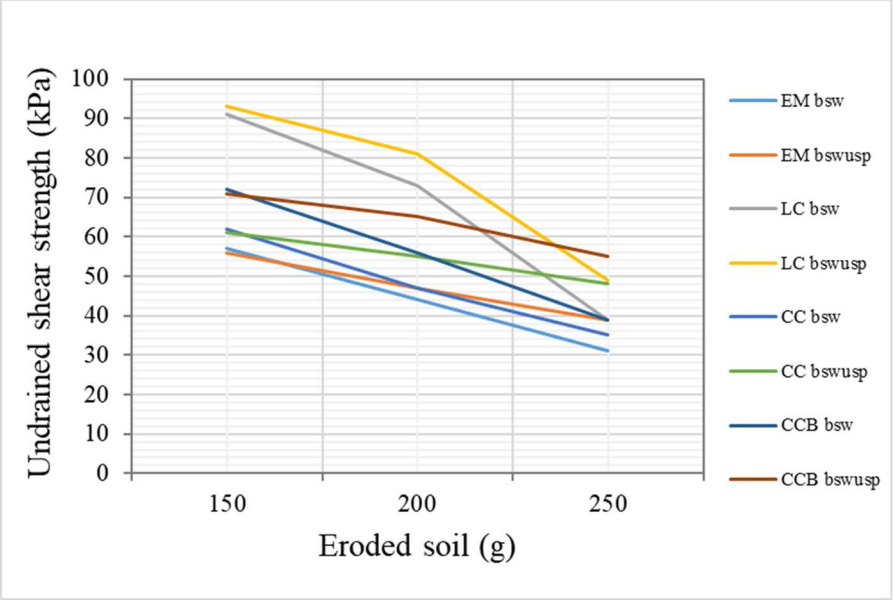


Figure 4.50 Relationship between loosened soil and subgrade strength

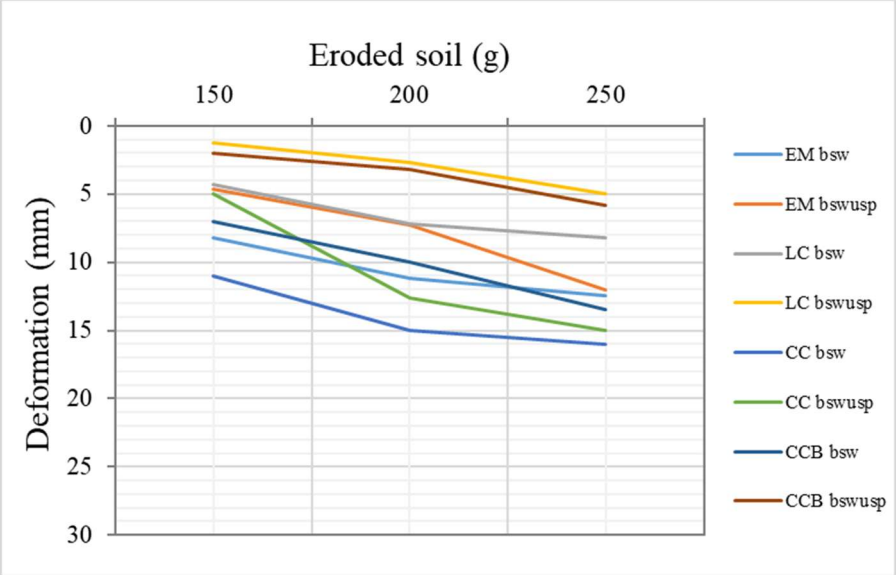


Figure 4.51 Relationship between loosened soil and subgrade settlement

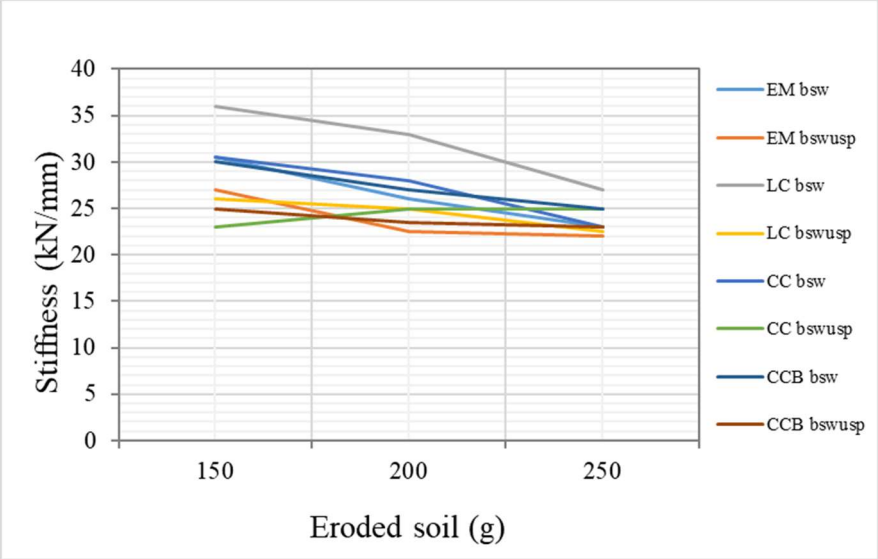


Figure 4.52 Relationship between eroded soil and subgrade stiffness

4.5.3 Relationships between stiffness and deformation

Figure 4.53 shows the relationship between the stiffness and subgrade deformation. The tests showed a lower value of stiffness at the end of the experiment and less permanent deformation. As was discussed previously (Section 4.3) the attachment of the USP material modifies elastic deflection and subgrade permanent deformation by increasing the contact area and reducing contact stresses. This is due to the indentation of ballast into the softer material on the soffit, providing more stable contacts for load distribution and increasing the contact area. The permanent deformation was higher in the case of tests without USPs. Over the range of 200,000 loading cycles, the USPs represent an effective intervention for reducing settlement by 20-30%; while the tests without the USPs showed deterioration in performance. Adding water showed significant effects on the settlement. However, on the stiffness there were no such signs. The notably lower stiffness of the test with the USP corresponds to the earlier trend, showing that a thick and relatively soft USP results in a decrease in stiffness.

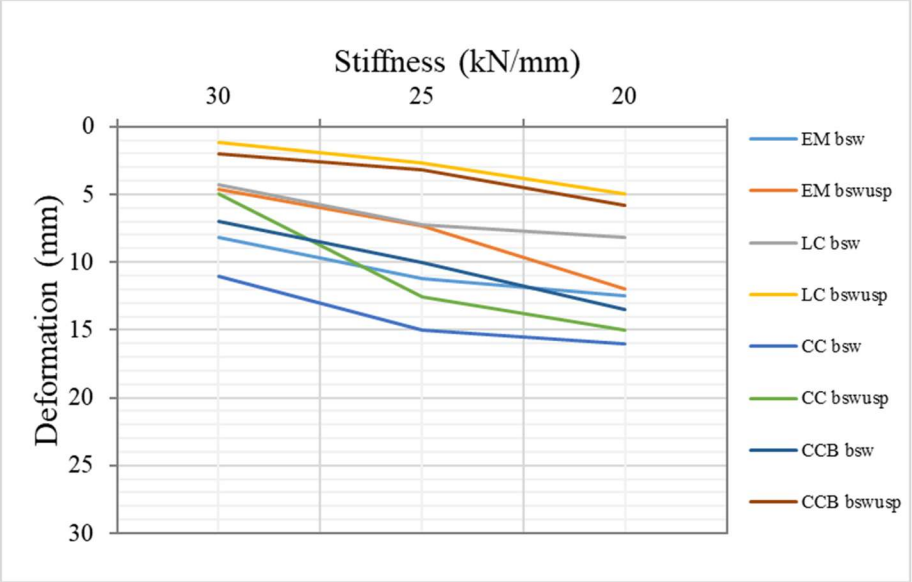


Figure 4.53 Relationship between soil stiffness and subgrade deformation

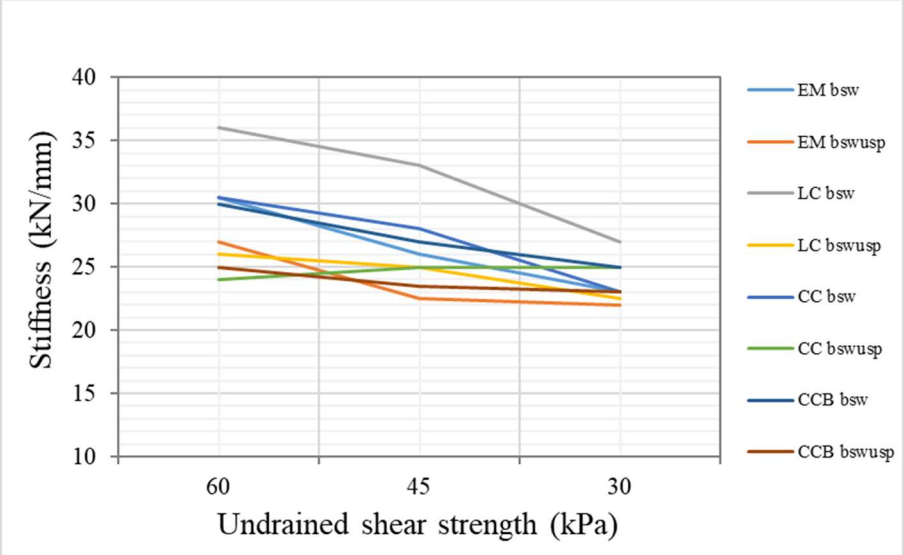


Figure 4.54 Relationship between soil strength and subgrade stiffness

4.5.4 Discussion

The effectiveness of applying the USPs is noticeable. The contact areas in the tests with the USPs were greater in the corresponding zones than in the tests on the same sleeper without USPs. Because the contact area increases, and the contact stresses decrease, the USP could reduce the permanent settlement and potentially the ballast damage. The greatest permanent deformation was in the case of the subgrade soils under saturated conditions and the highest moisture content, OMC 120%. These correspond to the result of the moved material rather than the moisture content, which suggests that the deformation is directly related to the amount of moved material. The results show again the major influence that water has on the detrimental effects on a railway structure. The correlation between the amount of eroded soil and deformation have become obvious from the results of this study; which is in agreement with results of previously conducted works (Yang and Yu, 1985; Ghataora, 2006), when the curves of the contamination variation with the number of cycles followed the same pattern as the curves of settlement with time. Results show that the settlements follow to a great extent the amounts of moved clay (Figure 4.51). The tests with the USPs show better results compared to the tests without them. The deformation also follows the loss of material from the subgrade, but there is less settlement compared to the tests with no USP.

The Figure 4.40 illustrates that the settlement is increasing with the increase of the liquidity index. In other words, there is a direct link between the increase of moisture content and the increase in settlement. All four soils representing 80% of OMC showed little difference between the values of soil strength after the test. However, with the increase of moisture content, the difference between the soils' strength after the test with /without the USPs also increases.

When the OMC was 100%, the subgrade with under sleeper pads (USPs) showed an increase of soil strength by 7-15%. The biggest difference in soil strength (with and without USPs) was in case of LC 120, CC 120 and CCB 120, where applying USPs improved the strength of the soil by 30%. The tests of EM 120 showed the lower difference, around 20%. This could be because of the way how the ballast was placed in that test. If the contact area between the ballast and the USP in that particular test was lower than average , then the contact stresses were higher. If so the difference between the test with and without the USP would be less significant.

The results show that applying the USPs does influence the subgrade soil strength and the difference depends on the moisture content. For instance, the smallest changes in strength are found in tests when the moisture content was lower than OMC, where the changes are of only a few percent. The difference between subgrade soil strength with and without the USPs increases with the increase of the subgrade soil's moisture content. When it is equal to OMC the difference was approximately 10%; whereas when the moisture content was equal to 120% OMC then the difference was 15%. The strength test results show an apparent trend that moisture content affects the strength of the soil. The trend was similar for all four tested soils.

Chapter 5 CONCLUSIONS AND RECOMMENDATIONS

5.1 Summary

To quantify the general long-term effect of sleepers with pads, laboratory investigations have been carried out to measure the rate of track deterioration. The research provide impressive evidence of the positive influences of the USPs on the subgrade soil. The USPs constitute a yielding springy layer underneath the sleepers and increase the contact areas, which leads to a better assimilation of the load into the ballast and a reduction in the load acting on the subgrade. The results are both a better distribution of the loads in the track and a reduction in the contact pressures between the sleeper and the top layer of ballast. There is also a positive impact on the lessening of subgrade soil erodibility and formation of mud pumping. This leads to a reduction in settlement in combination with an improved quality of track geometry. The benefits for the Railway industry are reduced maintenance outlay and the higher availability of the railway lines. The design of the classical ballasted superstructure benefits from lasting improvements through such innovative developments (Loy et.al.,2018).

This chapter presents conclusions of the current study and its practical implications, followed by the scope for further research. The study investigated the effect on subgrade behaviour of applying USPs and reducing the mud pumping of the ballasted rail tracks. The USPs are used to reduce attrition between the sleeper and the ballast. It results in an increase in contact area between the two materials and thus reduces contact stresses. It was envisaged that the inclusion of the USPs may also have an impact on the response of subgrade soils to loading, as the USPs are made of a relatively stiff, but compressible material. Thus, the aim of the laboratory test programme was to investigate the effect of using the USPs on the subgrade deformation, stiffness, and erodibility. A laboratory-based investigation that simulated railway track support

layers including the USPs was conducted using four soils (Etruria marl, London clay, china clay and a mix of china clay with 5% bentonite) as the subgrade at three moisture contents subjected to repeated stresses equivalent to those found in railway tracks in the UK. The bulk of the testing was conducted on small-scale apparatus measuring about 230 mm diameter and 200 mm high. The findings of the small tests were compared and verified using a large-scale test conducted in a 2.0 m x 1.65 m concrete chamber. During the tests, both permanent and cyclic deformations were measured together with soil erosion, and in some cases pore water pressure developed at the ballast subgrade interface. The following conclusions are drawn from this study. They are grouped into key theme areas of the research.

5.2 Conclusions

Contact area

- This is an essential parameter that influences the contact pressure. Measurements after the test conducted with the USPs showed a significant increase of contact area from 1.9% (without the USP) to 28.9% (with the USP). The results closely correspond to previous industry tests and research works (Getzner, 2014; Lay and Steger, 2015).

Permanent deformation

- The use of USPs showed a 5 to 60% reduction in permanent deformation for all subgrade soils(saturated condition) compared to tests conducted without the USPs at the three moisture contents (80% OMC, OMC and 120% OMC) examined. The largest reductions (40 to 60%) were noted for high plasticity soils LC and CCB at 120% OMC.

- The results showed less permanent deformation in the long tests conducted with the USPs, especially in cases of high initial moisture content (100% OMC, 120% OMC). This is most likely because the USPs increase the contact area at the sleeper/ballast interface and hence reduce the vertical stress.

- The results show that with an increase of moisture content (100% OMC to 120% OMC) the permanent deformation gradually increases with the number of load cycles by approximately 15-20%. This is in agreement with Abolaidi, (1995) and Indraratna et al. (2011).

- For stiffer soil (unsaturated condition), inclusion of the USPs in the track, has the effect of reducing permanent deformation and the amount of eroded soil. Whereas for softer soils with moisture content higher than the optimum, the deformation of the subgrade dominated and the USPs do not have a beneficial effect.

Development of pore water pressure and amount of loosened soil

- All four tested soils showed no significant changes in pore water pressure development when the initial moisture content was lower than OMC in both cases with/without the USPs. Tests on the subgrade without the USPs at OMC 100% and 120% showed that there was a significant build-up of excess pore pressure under cyclic loading. All four cohesive soils tested with the USPs showed a lesser increase in PWP compared to tests without the USPs. The difference was in a range between 15-30%. Soils CC and CCB showed the largest increase of PWP.

- Under cyclic loading with an increase of PWP the amount of loosened/eroded soil increases. This observation is in agreement with previous research works (Alobaidi 1994; Selig and Davis, 1995). In general, all subgrade soils examined with the USP performed better in terms of loosening of soil (i.e. erosion) compared to tests without the USPs. The amount of loosened soil with the USPs was 25-30% less. The amount of soil loosened in the tests without the USP was worse at high initial moisture contents.

- The tests with the USPs showed a reduced amount of eroded soil and PWP while there was higher undrained shear strength, indicating that the USPs have an overall beneficial effect for the soils examined.

Subgrade stiffness

- The subgrade soil with USPs showed a reduction in stiffness by approximately 20-30% and a reduction of settlement by around 15-25% after 200,000 cycles, compared to tests without the USPs.
- Stiffness and settlement both showed a non-linear relationship with the number of load cycles. The results show an initial high rate of change - an unstable phase, leading onto a stable phase where either there was little change with the load cycles or there was a steady increase or decrease after approximately 100,000 cycles.

The large-scale test

- Both the small- and large-scale tests were undertaken with a composite to prevent migration of fines. In both cases the stress at the subgrade level was the same. Both the tests showed similar loading cycles/settlement profile with similar amounts of permanent deformation, the difference between the two being only 7%. This shows that the small-scale test closely represented full-scale conditions.

5.3 Recommendations for further research works

The laboratory tests in this research program have provided a good insight into the effects of using the USP on railway subgrade. The work provides a good starting point for better understanding of the PWP/mud pumping interconnection. As was highlighted in the literature review, the available information on the effect of the USPs is limited. Although the primary objective of this study, the effect of the USP on subgrade, was achieved, there are aspects that need to be addressed and further investigations are necessary until the contribution made by this thesis may be extended into engineering practice. All of this work raises additional questions that could be addressed through some of these suggestions for future research:

- Only one USP of medium stiffness was investigated in this study. However, the USP pads are made of a range of materials with different stiffnesses. It is suggested that the effect of the USPs of different stiffness values on subgrade should be investigated to optimise their use in railway track.
- However, the USP pads are made of a range of materials with different stiffnesses. It is suggested that the effect of the USPs of different stiffness values on subgrade should be investigated to optimise their use in railway track.

- This study looked at the effect of USPs on subgrade with a range of initial moisture contents, with no additional water during testing and with water added at the start of the test to represent the worst-case scenario for three soil types. It is recommended that these tests are conducted on a wide range of soil types with different plasticity, strength and permeability etc. to develop an envelope for the USPs.

- Future work is also needed to be carried out to investigate the effectiveness of the USPs under the condition of a fluctuating water table. In this case, the design of the apparatus should allow the drainage of water. As an alternative solution, a cyclic triaxial test could be used. The drained condition could be tested there, when the cohesive soil has relatively low permeability, for example, a mix of sand and clay. This could be modelled during a cyclic triaxial test by keeping the drainage lines to the test specimen open (i.e. by maintaining fully drained conditions).

- This study was undertaken at one set of stresses – maximum and minimum. It is recommended that tests may be undertaken at larger maximum stress to represent deteriorating ballast and or increased train loads.

- The study considered only clean ballast, and without any fouling materials. The implications of ballast fouling for the USPs may be investigated.

- Geotextile composites are sometimes used to prevent migration of fines. It is suggested that the effectiveness of these composites should be investigated for the inclusion of USPs in track construction.

REFERENCE LIST

Alobaidi, I. and Hoare, D.J., (1994). Factors affecting the pumping of fines at the subgrade–subbase interface of highway pavements: a laboratory study. Geosynth. Int. 1 (2), 221–259.

Alobaidi, I. and Hoare, D.J. (1996). The development of pore water pressure at the subgrade-subbase interface of a highway pavement and its effect on pumping of fines. Geotextiles and Geomembranes, 14: 111-135.

Alobaidi, I. and Hoare, D.J. (1998). Quantitative criteria for anti-mud pumping geocomposites. Geotextiles and Geomembranes, 16: 221-245.

Aw, E.S. (2007). Low cost monitoring system to diagnose problematic rail bed: case study at a mud pumping site. PhD thesis, Massachusetts Institute of Technology.

Ayres, D.J. (1986). Geotextiles or geomembranes in track? British railways' experience. Geotextiles and Geomembranes, 3(2): 129-142.

British Standards Institution (1990). BS ISO 1377-1-7:1990 Methods of Test for soils for civil engineering purposes — Part 1-7: Shear strength tests (total stress).

British Standards Institution (2009). BS ISO 11277:2009, Soil quality. Determination of particle size distribution in mineral soil material. Method by sieving and sedimentation. London: BSI.

Brown, S.F. and Selig, E.T. (1991). The design of pavement and rail track foundations. In Cyclic loading of soils: from theory to design. Edited by M. P. O'Reilly & Brown, S. F. Van Nostrand Reinhold, Glasgow. pp. 249-305.

Cai, X., Liu, K., Wang, H. and Guo, L. (2015). Study on mud pumping mechanism of subgrade surface layer in slab ballastless track zone. Sensors & Transducers, 186(3): 154-160.

Chawla, S. and Shahu, J.T. (2016). Reinforcement and mud-pumping benefits of geosynthetics in railway tracks: Model tests. Geotextiles and Geomembranes, 44(3): 366-380.

Danquah, W., Ghataora, G. and Burrow, M. (2014). The effect of fouling on hydraulic conductivity of the rail track substructure. In: European Conference on Geotechnical Engineering. Vienna, Austria, p.225.

Duong, T.V., Tang, A.M., Cui, et al., (2013). Effects of fines and water contents on the mechanical behaviour of interlayer soil in ancient railway sub-structure. Soils and Foundations, 53(6): 868-878.

Duong, T.V., Cui, Y.-J., Tang, A.M., et al., (2014). Investigating the mud pumping and interlayer creation phenomena in railway sub-structure. Engineering Geology, 171: 45-58.

Ghataora, G.S., Burns, B., Burrow, M.P.N. (2006). Development of an index test for assessing anti-mud pumping materials in railway track foundations. The University of Birmingham.

Ghataora, G. and Rushton, K. (2012). Movement of water through ballast and sub-ballast for Dual-Line railway track. Transportation Research Record: Journal of the Transportation Research Board, 2289, pp.78-86.

Hayashi, S. and Shahu, J.T. (2000). Mud pumping problem in tunnels on erosive soil deposits. Géotechnique, 50(4): 393- 408.

Hoare, D.J. (1982). A Laboratory study into pumping clay through geotextiles under dynamic loading. 2nd Int. Conf. on Geotextiles, Las Vegas.

Hudson, A., Watson, G., (2016). Remediation of mud pumping on a ballasted railway track. Procedia Engineering, 143:1043-1050.

Indraratna, B., Attya, A. and Rujikiatkamjorn, C. (2009) Experimental Investigation on Effectiveness of a Vertical Drain under Cyclic Loads. Journal of Geotechnical and Geoenvironmental Engineering, 135: 835-839.

Indraratna, B., Nimbalkar, S., et al., (2010). Field Assessment of the Performance of a Ballasted Rail Track with and without Geosynthetics. Journal of Geotechnical and Geoenvironmental Engineering, 136(7): 907-917.

Indraratna, B., Nimbalkar, S. and Tennakoon, N. (2010). The Behaviour of Ballasted Track Foundations: Track Drainage and Geosynthetic Reinforcement. Geo-Florida, American Society of Civil Engineers, pp.2378-2387.

Indraratna, B., Su, L. and Rujikiatkamjorn, C. (2011). A new parameter for classification and evaluation of railway ballast fouling. Canadian Geotechnical Journal, 48(2), pp.322- 326.

Indraratna, B., Tennakoon, N., et al., (2013). Behaviour of clay-fouled ballast under drained triaxial testing. Géotechnique, 63(5): 410-419.

Ito, T. (1984). Actual situation of mud pumping and its countermeasures. Quarterly Reports of the Railway Technical Research Institute, 25(4): 117-123.

Li, D. and Selig, E. (1998). Method for Railroad Track Foundation Design. I: Development. Journal of Geotechnical and Geoenvironmental Engineering, 124(4), pp.316-322.

Li, D. and Selig, E. (1998). Method for Railroad Track Foundation Design. II: Applications. Journal of Geotechnical and Geoenvironmental Engineering, 124(4), pp.323-329.

Li, D. (2018). 25 years of heavy axle load railway subgrade research at the Facility for Accelerated Service Testing (FAST). Transportation Geotechnics, 17: 51-60.

Liu, J. and Xiao, J. (2010). Experimental Study on the Stability of Railroad Silt Subgrade with Increasing Train Speed. Journal of Geotechnical and Geoenvironmental Engineering, 136(6): 833-841.

Liu, D., Fu, H., Zhu, X., Liu, Y. and Rao, J. (2013). Study on the remediation of mud pumping. Applied Mechanics and Materials, 275-277: 1560-1563.

Liu, S., Huang, H., Qiu, T. and Kerchof, B. (2019). Characterization of Ballast Particle Movement at Mud Spot. Journal of Materials in Civil Engineering, 31(1): 04018339.

Lim, W. (2004). Mechanics of railway ballast behaviour. PhD thesis. The University of Nottingham.

Muramoto, K., Sekine, E. and Nakamura, T. (2006). Roadbed degradation mechanism under ballastless track and its countermeasures. Quarter Report of Railway Technical Research Institute (RTRI), 47(4).

Muramoto, K. and Nakamura, T. (2011). Development of the countermeasure against roadbed degradation under ballastless tracks for existing lines. In Proceedings of the 9th World Congress on Railway Research, Lille. pp. 1-10.

Network Rail (1998). Rail Track Line Specification: NR/SP/TRK/ 033 Track Blanketing Sand. London, UK. Network Rail.

Network Rail (2005). Specification: RT/CE/C/9039 'Formation Treatments', Issue 1. London, UK: Network Rail.

Rushton, K. and Ghataora, G. (2009). Understanding and modelling drainage of railway ballast. Proceedings of the Institution of Civil Engineers - Transport, 162(4), pp.227- 236.

Rushton, K. and Ghataora, G. (2014). Design for efficient drainage of railway track foundations. Proceedings of the Institution of Civil Engineers - Transport, 167(1), pp.3- 14.

Raymond, G.P. (1986). Geotextiles Application for a branch line upgrading. Geotextiles and Geomembranes 3, pp 91-104

Raymond, G.P. (1999). Railway rehabilitation geotextiles. Geotextiles and Geomembranes 17, pp. 213-230.

Selig, E. and V, D. (1991). Sources and causes of ballast fouling. Bulletin No. 731. American Railway Engineering Association, pp.145-457 vol.92.

Selig, E. and Waters, J. (2007). Track geotechnology and substructure management. London: Thomas Telford.

Sussmann, T., Ruel, M. and Chrismer, S. (2012). Source of Ballast Fouling and Influence Considerations for Condition Assessment Criteria. Transportation Research Record: Journal of the Transportation Research Board, 2289, pp.87-94.

Takatoshi, I. (1997). Measure for the stabilization of railway earth structure. In Japan Railway Technical Service, Tokyo.

Tennakoon, N. and Indraratna, B., e (2012). The Role of Ballast-Fouling Characteristics on the Drainage Capacity of Rail Substructure. Geotechnical Testing Journal, 35(4), p.104-107.

Trinh, V.N., Tang, A.M., Cui, et al., (2012). Mechanical characterisation of the fouled ballast in ancient railway track substructure by large-scale triaxial tests. Soils and Foundations, 52(3): 511-523.

Wong, R.C. and Thomson, P.R. (2006). In Situ Pore Pressure Responses of Native Peat and Soil under Train Load: A Case Study. Journal of Geotechnical and Geoenvironmental Engineering, 132(10): 1360-1369.

Voottipruex, P. and Roongthanee, J. (2003). Preventation of mud pumping in railway embankment: a case study from Baeng Pra-Pitsanuloke, Thailand. International Journal of Applied Science and Technology, 13(1): 20-25.

Yang, C. and Yu, X. (1985). Mud-pumping prevention of railway subgrade by using geotextile. Research report on Railway Formation Mud-pumping Prevention with Geopolymer Material, China Academy of Railway Sciences.

Yu, S., Wu-ming, L., Ji-dong, T., et al., (2016). Analysis of subgrade soil mud pumping model. Electric Journal of Geotechnical Engineering, 21(24): 7729-7740.

APPENDIX

Compaction test

BS 1377:1990	Test NO.:	Location: Civil Engineering Lab
No. of layers: 3	Rammer: 2.5 kg	
Blow per layer : 25	Drop: 300mm	Soil description: English china clay
Compacted by:	Sample preparation:	Sample type:
Proctor cylinder NO.: 1	No. of separate batches	

Soil	**Etruria Marl**					
Test number	A	B	C	D	E	F
m_2 (g)	5401	5535	5643	5691	6292	6315
m_1 (g)	3785	3785	3785	3785	4476	4576
m_2-m_1 (g)	1616	1750	1858	1906	1816	1739
ρ (g/cm3)	1.61	1.75	1.86	1.9	1.8	1.7
ω (%)	10.1	12.7	15	17.1	18.5	20
ρ_d	1.45	1.56	1.61	1.62	1.52	1.41
Vane shear strength	over 120	119	70	59	41	31

Moisture content							
Container number	A	B	C	D	E	F	G
Mass of wet soil and container (g)	52.01	79.61	50.01	74.45	10.02	12.2	19.02
Mass of container (g)	48.7	72.6	44.4	66.1	9.01	10.83	16.5
Mass of moisture (g)	3.3	7	4.6	8.35	1	1.37	2.5
Mass of soil (g)	31.7	54.9	30.8	48.35	5.4	7.43	12.4
Moisture content (%)	10	12.7	15	17	18.5	18.5	20

Soil	**London Clay**				
Test number	O	A	B	C	D
m_2 (g)	4994	5074	5154	5034	4944
m_1 (g)	3574	3574	3574	3574	3574
m_2-m_1 (g)	1420	1500	1580	1460	1370
ρ (g/cm3)	1.44	1.49	1.58	1.46	1.37
ω (%)	18	19	21	23.4	25
ρ_d	1.2	1.26	1.3	1.18	1.09

Moisture content						
Container number	O	A	B	C	D	E
Mass of wet soil and container (g)	42.53	42.98	60.2	49.1	86.34	121.3
Mass of container (g)	17	17	17.7	17.8	14.6	17.55
Mass of wet soil (g)	25.53	25.98	42.5	31.3	71.74	103.8
Mass of dry soil and container (g)	38.84	38.84	52.57	43.2	71.6	98.85
Mass of moisture (g)	3.69	4.14	7.63	5.9	14.74	22.45
Mass of soil (g)	21.84	21.84	34.87	25.4	57	81.3
Moisture content (%)	0.169	0.19	0.219	0.232	0.259	0.276

Soil	**China Clay**				
Test number	1	2	3	4	5
m2 (g)	6680	6786	6802	6739	6678
m1 (g)	4979.5	4979.5	4979.5	4979.5	4979.5
m2-m1 (g)	1450	1510	1530	1460	1320
ρ (g/cm3)	1.4	1.51	1.53	1.46	1.32
ω (%)	22	26	30	34	38
ρd	1.14	1.19	1.17	1.09	
Vane shear strength	120+	120	53	23	14
	1.3	1.49	1.5	1.46	1.34
bentonite mix	22	30	33	35	39

Moisture content					
Container number	A	B	C	D	E
Mass of wet soil and container (g)	8.54	12.05	17.36	8.55	12.11
Mass of dry soil and container (g)	7.71	10.65	14.41	7.18	9.64
Mass of container (g)	3.92	5.32	4.7	3.18	3.5
Mass of moisture (g)	0.83	1.4	2.95	1.37	2.47
Mass of dry soil (g)	3.8	5.34	9.73	4.01	6.15
Moisture content (%)	22	26	30	34	38

Atterberg limits

BS 1377-2:1990	Mass of wet soil and container (g)	Mass of dry soil and container (g)	Mass of container (g)	Mass of moisture (g)	Mass of dry soil (g)	Moisture content %	
Etruria marl	21 19	20 27	17 74	0 92	2 53	36	LL 38 (%)
	21 37	20 43	17 72	0 94	2 71	39	
	26 62	23 91	16 93	2 71	6 98	39	
	21 61	19 7	14 62	1 91	5 08	37	
	5 31	5 1	4 04	0 21	1 06	19	PL 18 (%)
	4 8	4 64	3 7	0 16	0 94	17	
	4 9	4 68	3 33	0 22	1 35	17	
	4 15	4 1	3 22	0 05	0 88	18	
London clay	68 26	46 84	17 04	21 42	35 7	60	LL 60 2 (%)
	78 96	57 02	17 7	21 94	39 32	56	
	69 5	50 37	17 8	19 3	32 57	60	
	60 28	42 26	14 6	18 02	27 66	65	
	21 21	20 46	17 55	0 75	2 91	25 7	PL 25(%)
	20 78	20 14	17 53	0 64	2 61	24 5	
	81 06	80 42	77 81	60 92	62 89	24 6	
	81 49	80 74	77 83	61 03	63 19	25 75	
China clay	20 29	15 07	3 99	5 22	9 85	53 02	LL 55 4(%)
	28 73	21 2	5 49	7 53	13 67	55 11	
	20 06	14 77	3 39	5 29	9 48	55 78	
	32 51	23 81	4 76	8 7	15 11	57 62	
	3 98	3 81	3 19	0 17	0 62	27 12	PL 27 1 (%)
	4 49	4 24	3 29	0 25	0 95	27 09	
	4 97	4 85	4 38	0 12	0 47	27 14	
	4 83	4 64	3 88	0 19	0 76	27 08	
5% bentonite and China clay	14 87	11 15	4 82	3 72	6 33	58 78	LL 63 1 (%)
	14 55	10 72	4 48	3 83	6 24	61 39	
	15 34	11 46	5 34	3 88	6 12	63 41	
	14 59	10 48	4 55	4 11	5 93	69 31	
	16 7	13 2	4 82	2 97	8 5	30 5	PL 30 (%)
	14 6	12 5	5 5	2 1	7	30	
	16 26	13 58	4 48	2 68	9 1	29 51	
	16 12	13 45	4 55	2 67	8 9	30 1	

Consolidation test

London C	Load kpa						Etruria M	Load kpa					
time	beam	25	50	100	200	400	time	beam	25	50	100	200	400
0	21	31.35	40.85	44.81	48.56	52.63	0	0.2	6.64	18.55	22.15	25.82	29.48
10	24.51	32.41	41.09	44.9	49.05	53.01	10	0.5	7.52	18.72	22.42	26.16	29.91
20	24.61	32.78	41.19	45.06	49.15	53.11	20	0.51	7.67	18.76	22.49	26.26	29.99
30	24.71	33.03	41.27	45.16	49.24	53.19	30	0.52	7.8	18.8	22.55	26.32	30.05
40	24.84	33.26	41.34	45.24	49.32	53.25	40	0.53	7.91	18.83	22.6	26.36	30.11
50	24.99	33.46	41.4	45.31	49.38	53.31	50	0.54	8.02	18.85	22.64	26.41	30.16
1	25.11	33.65	41.45	45.36	49.45	53.36	1	0.56	8.09	18.87	22.67	26.45	30.21
2	25.71	34.46	41.71	45.65	49.73	53.62	2	0.62	8.47	18.98	22.82	26.64	30.43
4	26.56	35.66	42.08	46.02	50.11	53.98	4	0.76	8.97	19.18	23.03	26.91	30.74
8	27.88	37.18	42.57	46.53	50.61	54.45	8	0.93	9.68	19.42	23.33	27.32	31.16
15	29.36	38.62	43.06	47.07	51.16	54.95	15	1.13	10.57	19.71	23.71	27.74	31.67
30	30.55	39.69	43.58	47.69	51.83	55.55	30	1.44	11.97	20.13	24.27	28.37	32.28
1	30.99	40.21	43.95	48.11	52.26	56.01	1	1.87	13.81	20.75	24.96	29.01	32.75
2		40.49		48.37	52.53	56.25	2		16.1			29.43	33.01
4		40.65	44.38				4		18.11	21.88			
8	31.3	40.78	44.58				8	5.91	18.39	22.11			
24	31.35	40.85	44.81	48.75	52.81	57.51	24	6.64	18.55	22.31	26.05	29.81	33.41
		47.71	48.56	52.63	57.43				22.15	25.82	29.48	33.03	
China C	Load kpa						5% mix	Load kpa					
time	beam	25	50	100	200	400	time	beam	25	50	100	200	400
0	14.18	26.63	36.6	40.15	43.55	47.05	0	20	30.45	0	8.85	12.81	16.95
10	18.3	28.63	37.4	41.15	44.8	48.01	10	21	32	2.01	9.35	13.41	17.51
20	18.8	30.63	37.8	41.71	45.35	48.81	20	21.1	32.45	4.01	9.51	13.61	17.75
30	19.1		38.05	41.95	45.65	49.11	30	21.18	32.65	4.31	9.63	13.81	17.95
40	19.6		38.25	42.12	45.85	49.26	40	21.25	32.9	4.51	9.73	13.91	18.11
50	19.8	31	38.42	42.3	45.95	49.37	50	21.3	33.1	4.75	9.82	14	18.21
1	20	31.3	38.6	42.41	46.05	49.42	1	21.35	33.3	4.81	9.91	14.11	18.31
2	21.7	33.5	39.11	42.77	46.31	49.65	2	21.65	34.2	5.31	10.28	14.55	19.35
4	23.88	35.4	39.41	42.95	46.49	49.75	4	22.1	35.5	6.05	10.79	15.15	19.77
8	25	35.85	39.59	43.08	46.61	49.84	8	22.85	37.2	6.82	11.211	15.76	19.98
15	25.38	36.1	39.81	43.16	46.68	49.97	15	23.82	39.3	7.55	11.7	16.13	20.08
30	25.48	36.2	39.92	43.22	46.75	50.05	30	25.82	40.5	8.05	11.74	16.37	20.2
1	25.53	36.26	40.02	43.29	46.81	50.11	1	27.48		8.35		16.52	20.3
2		36.31	40.04	43.34			2			8.52	12.1		
4		36.35	40.09	43.4	46.95	50.16	4			8.64	12.45	16.72	20.37
8		36.4	40.1	43.44		50.2	8			8.74	12.65		20.42
24	26.63	36.52	40.15	43.5	47.05	50.3	24	30.45		8.85	12.81	16.93	20.54
		40.03	43.34	46.83	50.01				8.63	12,51	16.53	20.11	

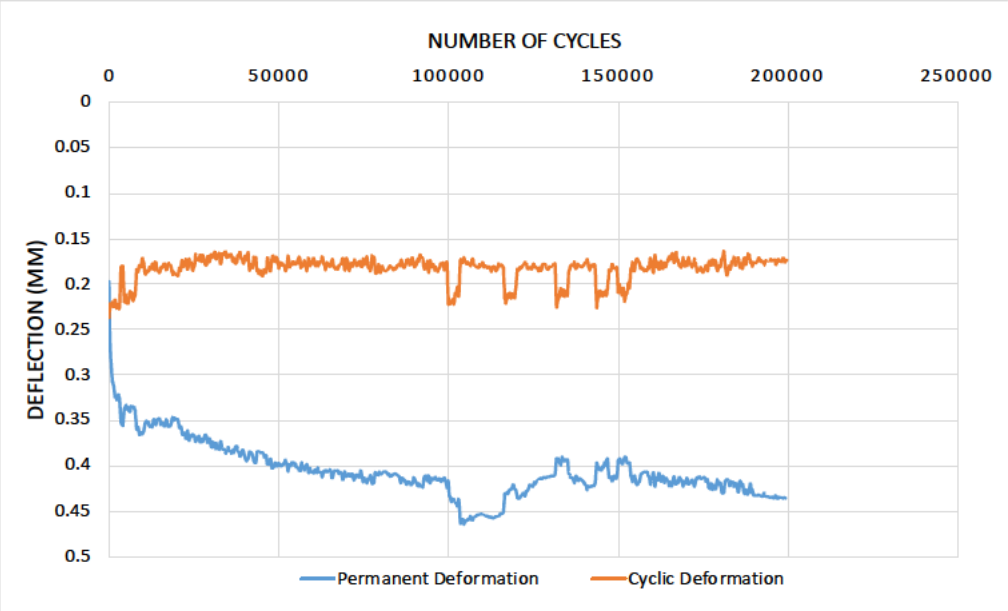
Hydrometer analysis

Etruria Marl							
Elapsed time, (min)	Temperature C°	Reading Rh'	Rh' + Cm =Rh	Effective depth Hr (mm)	Particle diameter D (mm)	Rh' - Ro' =Rd	Percentage finer (%)
0	24	24	24 35	126 75			
0 5	24	19 5	19 85	128 75	0 07	18 5	99
1	24	19	19 35	130 75	0 05	18	98
2	24	18 5	18 85	132 75	0 035	17 5	95 2
4	24	18 5	18 85	133 75	0 025	17 5	95 2
8	24	17 5	17 85	136 75	0 018	16 5	89 76
15	24	16 8	17 15	139 75	0 013	15 8	83 23
30	24	16 3	16 66	141 55	0 009	15 3	76 1
60	24	15	15 35	146 55	0 006	14	71 8
120	24	14 2	14 55	149 95	0 005	13 2	68 1
240	24	13	13 35	154 75	0 003	12	65 28
480	24	12 1	12 45	158 35	0 002	11 1	60 4
1440	24	10 2	10 55	165 95	0 001	9 2	52 2
London Clay							
Elapsed time, (min)	Temperature C°	Reading Rh'	Rh' + Cm =Rh	Effective depth Hr (mm)	Particle diameter D (mm)	Rh' - Ro' =Rd	Percentage finer (%)
0	24	24	24 35				
0 5	24	19	19 35	130 75	0 074	18	99
1	24	18	18 35	134 75	0 053	17	96 22
2	24	17 5	17 85	136 75	0 38	16 5	93 39
4	24	17	17 35	138 75	0 27	16	90 56
8	24	16 5	16 85	140 75	0 019	15 5	87 73
15	24	16	16 35	142 75	0 014	15	84 07
30	24	15 5	15 85	144 75	0 01	14 5	82 07
60	24	14 9	15 25	147 75	0 007	13 9	77 6
120	24	14 01	14 36	150 75	0 005	13	73 58
240	24	13 5	13 85	152 75	0 003	12 5	70 75
480	24	13	13 35	154 75	0 002	12	67 92
1440	24	12	12 35	158 75	0 001	11	62 26
China Clay							
Elapsed time, (min)	Temperature C°	Reading Rh'	Rh' + Cm =Rh	Effective depth Hr (mm)	Particle diameter D (mm)	Rh' - Ro' =Rd	Percentage finer (%)
0	24	13 5	13 85	144 75			
0 5	24	11 5	11 85	152 75	0 08	10 85	61 28
1	24	11 5	11 85	152 75	0 06	10 85	61 28
2	24	11 5	11 85	152 75	0 041	10 85	61 28
4	24	11 5	11 85	152 75	0 03	10 85	61 28
8	24	11 5	11 85	152 75	0 02	10 85	61 28
15	24	11 5	11 85	152 75	0 015	10 85	61 28
30	24	11 5	11 85	152 75	0 01	10 85	61 28
60	24	11 5	11 85	152 75	0 01	10 85	61 28
120	24	11 5	11 85	152 75	0 005	10 85	61 28
240	24	11 3	11 65	153 55	0 003	10 35	58 47
480	24	10 5	10 85	156 75	0 002	9 85	55 65
1440	24	8 5	8 85	164 75	0 001	7 75	43 78

Combined data

Soil	w (%)	w (%) after		IL	IL after		Strength (kPa)	Strength aft		Loose soil aft		Settlement (mm)		Stiffness aft (kN/mm)	
	before	bsw	bswusp	before	bsw	bswusp	before	bsw	bswusp	bws	bswusp	bsw	bswusp	bsw	bswusp
Etruria marl	14	20.4	19.5	-0.2	0.12	0.075	85	57	56	150	148	8.2	4.6	30.5	27
	17	24.2	23.1	-0.05	0.31	0.255	65	44	47	202	187	11.2	7.3	26	22.5
	21	27.2	26.9	0.15	0.46	0.445	45	31	39	277	211	12.45	12	23	22
London clay	17	22.4	21.7	-0.22	-0.07	-0.095	115	91	93	112	115	4.3	1.2	36	26
	21	25.6	24.5	-0.11	0.017	-0.01	90	73	81	159	145	7.2	2.7	35	25
	25	29.5	28.5	0.1	0.128	0.1	48	31	43	233	185	8.2	5	27	22.5
China clay	25	28.2	27.5	-0.3	0.04	0.017	121	62	61	167	159	11	5	30.5	23
	30	31.2	30	0.1	0.15	0.1	83	47	55	280	201	15	12.6	28	25
	35	37.2	35	0.28	0.36	0.28	60	35	48	403	267	16	15	23	25
5% mix	26	29.4	28.5	-0.12	-0.01	-0.04	120	72	71	153	140	7	2	30	25
	32	37	35.9	0.06	0.2	0.17	91	56	65	250	170	10	3.2	27	23.5
	38	41.3	39.7	0.24	0.34	0.3	67	39	55	370	220	13.5	5.8	25	23

Ballast, permanent and cyclic deformation



Compilation of raw data

Date	Time	Cycles		Load Pk	Load Trgh	Posn Pk	Posn Trgh	Ch 1 Pk	Ch 1 Trgh	Ch 2 Pk	Ch 2 Trgh	Permanent deformation		Cyclic deformation	Soil stiffness
09/12/2019	0.109	0		0.492	0	0.455	0	1.556	0	0.058	0				
09/12/2019	34.344	0		3.372	0	2.269	0	1.646	0	0.07	0				
09/12/2019	08:46:53	1	1	3.385	0	2.269	0	0	0	0	0				
09/12/2019	13:18:52	49000	49000	6.196	0.527	4.939	4.559	3.545	4 597	1.769	2.882	4.104	4.11	0.38	14.91842
09/12/2019	13:19:26	49100	49100	6.246	0.532	4.934	4.567	3.423	4.751	1.758	2.904	4.112	4.11	0.367	15.56948
09/12/2019	13:19:59	49200	49200	6.249	0 52	4.935	4.559	3.517	4.683	1.95	3.084	4.104	4.11	0.376	15.2367
09/12/2019	13:20:32	49300	49300	6.211	0.518	4.953	4.562	3.522	4.633	1.762	2.882	4.107	4.11	0.391	14.5601
09/12/2019	13:21:06	49400	49400	6.222	0.533	4.932	4.565	3.51	4 549	1.742	2.902	4.11	4.11	0.367	15.50136
09/12/2019	13:21:39	49500	49500	6.225	0.518	4.941	4.568	3.498	4 568	1.846	2.978	4.113	4.11	0.373	15.30027
09/12/2019	13:22:12	49600	49600	6.225	0.525	4.941	4.563	3.534	4.409	1.904	3.028	4.108	4.11	0.378	15.07937
09/12/2019	13:22:46	49700	49700	6.235	0 52	4.948	4.558	3.355	4.676	1.821	2.671	4.103	4.11	0.39	14.65385
09/12/2019	13:23:19	49800	49800	6.243	0.523	4.954	4.566	3.437	4.668	1.813	2.819	4.111	4.11	0.388	14.74227
09/12/2019	13:23:52	49900	49900	6.228	0.531	4.939	4.571	3.511	4.748	1.733	2.918	4.116	4.12	0.368	15.48098

Development of pore water pressure, extracted and combined data

	CC 100		CC 80		CC 120		mix		LC		EM	
	bsw	usp	bsw	usp	bsw	usp	bsw	usp	bsw	usp	bsw	usp
0	9	5	6	6.0488	14	10.4568	8	4	8	6	9	15
100	9 619091	5.5464	6.35	5.16	14	9.4216	8.84	4.728	8.35	6.968	9.883636	15 2512
200	8.07	5.8704	6.687273	5.0176	14.41182	10 2056	8.324545	3.856	8.687273	7.1416	10.56636	14 3648
300	10.77545	5.7296	4.555455	5.2192	14.09818	9 8584	8.811818	5.1816	6.555455	7.6696	10.36727	15 0856
400	11.66182	6.0488	5.269091	5.0088	12.92364	9 9704	9.91	5.0504	7.269091	7.1296	10.72	14 2056
500	9 821818	5.16	7.602727	6.14	14.76909	9 5704	8.807273	5.2952	9.602727	7.1248	10.82	14 2432
600	9.59	5.0176	6.289091	5 944	13.02636	9 6744	7.4	5.0016	8.289091	7.012	10.53636	13 8648
700	10.20545	5.2192	4.767273	5.1672	13.17273	9 8744	8.106364	4.5912	6.767273	7.976	11.07455	14 6544
800	10.35	5.0088	6.542727	5.0504	13.82364	9.232	9.353636	4.8696	8.542727	7.3032	9.021818	12 9288
900	10.70545	6.14	6.408182	4.6736	13.78636	9.4584	10 68909	4.9552	8.408182	7.8464	11.31273	13.1992
1000	10.01727	5.944	5.898182	5.6144	11.51727	9 5792	8.632727	4.7296	7.898182	6.676	11.86909	13 2816
1100	10.46182	5.1672	5.714545	5.496	13.01364	9 2168	8.848182	4.6376	7.714545	7.4408	11.42909	13 2784
1200	10.03727	5.0504	5.736364	6.0928	11.68091	8.92	8.14	5.1576	7.736364	6.9104	13.00545	12.4144
1300	11.43636	4.6736	6.881818	5.1024	13.32273	8.428	8.395455	4.7288	8.881818	7.2288	11.39727	12.472
1400	11.03182	5.6144	4.217273	5.9936	11.68818	9 5424	6.955455	4.7712	6.217273	7.5208	12.04636	12.4168
1500	9.164545	5.496	7.701818	5.1368	12.28091	8 3504	9.024545	5.8232	9.701818	6.952	12.52909	12.4464
1600	10.10818	6.0928	8.239091	4.7512	14.06909	7 9736	9.614545	4.9632	10.23909	7.212	11.12273	11.844
1700	10.98364	5.1024	5.806364	4.3168	14.29	8 6616	8.318182	4.5728	7.806364	7.4504	12.36909	11.4048
1800	10.55909	5.9936	5.855455	5.6488	12.22818	8 2704	8.544545	5.4704	7.855455	7.08	12.32818	13.616
1900	8 832727	5.1368	5.035455	4.8536	12.33545	7 8976	8.969091	5.7072	7.035455	6.7128	11.98273	13.1168
2000	9 385455	4.7512	5.859091	5.3216	12.58	7.936	8.91	5.1512	7.859091	6.7496	14.51273	12.4344
2100	8 868182	4.3168	6.133636	4.8736	12.52636	8.1304	9.036364	5.5464	8.133636	7.66	12.54364	12.212
2200	11.90545	5.6488	6.152727	6.7224	13.93091	9 8584	6.728182	5.1016	8.152727	6.4216	13.08091	12 5896
2300	11.08273	4.8536	5.692727	5.8216	11.39636	9 9704	7.945455	5.3632	7.692727	6.8328	13.16182	12.1176
2400	13.07273	5.3216	6.010909	5.6512	10.17636	9 5704	6.732727	4.6944	8.010909	6.6224	11.55545	10.952
2500	8 042727	4.8736	7.191818	5.7672	14.15	9 6744	9.935455	4.5072	9.191818	6.844	11.87727	11.4496
2600	8.36	6.7224	6.097273	5 544	10.56091	9 8744	9.664545	5.4136	8.097273	7.2888	12.46818	11.184
2700	8.7	5.8216	5.394545	5.26	10.05455	9.232	8.316364	5.2256	7.394545	7.2248	11.01545	10 3376
2800	9 808182	5.6512	6.339091	5.0976	12.14818	9.4584	7.183636	5.2256	8.339091	6.4128	12.75727	9 9936
2900	9 603636	5.7672	7.01	6.612	12.72636	9 5792	8.453636	4.9296	9.01	6.644	12.01727	10 5632
3000	9 213636	5.544	5.631818	6.0776	12.57091	9 2168	8.859091	4.876	7.631818	6.564	13.50909	10.4032
3100	9.118182	5.26	5.965455	6.0696	13.84364	8.92	7.917273	6.9736	7.965455	6.2384	12.58818	9 8432
3200	9.194545	5.0976	6.460909	5.1336	11.45727	8.428	9.147273	4.892	8.460909	6.9048	11.78273	10 0424
3300	9 613636	6.612	5.409091	4.7112	11.63091	9 5424	7.85	4.5344	7.409091	6.5288	12.02909	10 2016
3400	9 982727	6.0776	6.616364	5.6072	12.40182	8 3504	7.32	5.5	8.616364	6.4888	11.71	9.808
3500	9 292727	6.0696	5.312727	5.2912	13.55727	7 9736	9.502727	4.5424	7.312727	6.3328	12.54636	9.7984
3600	9.5	5.1336	5.107273	5.0344	13.82727	8 6616	6.200909	5.9392	7.107273	6.792	11.39	10.148
3700	10.74273	4.7112	5.512727	4.8776	10.93545	8 2704	9.029091	4.6792	7.512727	6.7288	11.80364	9 5528
3800	11.40364	5.6072	5.746364	5.0104	10.56091	7 8976	8.768182	5.8984	7.746364	6.232	11.94364	9 8384
3900	8 650909	5.2912	5.283636	5.504	14.57636	7.936	8.596364	5.5592	7.283636	6.3984	13.88909	9.4936
4000	6 884545	5.0344	6.279091	4.7096	11.68909	8.1304	6.673636	4.9104	8.279091	5.8808	12.68636	9.4848
4100	10.36273	4.8776	5.056364	5.1984	12.35727	8 3912	8.251818	4.0296	7.056364	6.4352	13.04	9.4744
4200	9 837273	5.0104	6.834545	4.768	12.41182	7.7224	7.846364	4.5608	8.834545	6.4816	12.44273	9.7128
4300	8 620909	5.504	5.779091	4.2304	13.03545	8 5144	7.714545	4.7176	7.779091	6.136	12.76182	9.46
4400	9.61	4.7096	5.709091	4.8304	12.09	7 3224	8.287273	4.62	7.709091	6.6248	11.87182	9.1184
4500	9 207273	5.1984	5.23	4.76	13.55364	8.4448	8.756364	4.1184	7.23	6.6168	12.73545	9.1512
4600	9.715455	4.768	5.365455	4.42	11.22727	7 8024	9.032727	5.1664	7.365455	6.3304	13.22364	9.4144
4700	10.21182	4.2304	5.815455	4.8448	11.57727	7.996	7.385455	4.3688	7.815455	6.0096	13.56091	9.1776
4800	9.405455	4.8304	6.456364	5.756	12.55818	8 2552	8.778182	4.136	8.456364	6.1992	12.65455	9 2472
4900	8 390909	4.76	6.595455	5.7664	12.97727	7.7792	8.350909	4.4392	8.595455	6.3288	11.06182	9.04
5000	9 524545	4.42	6.061818	5.072	11.33727	7.804	7.108182	4.1112	8.061818	6.2176	12.64545	9 0632
5100	9 232727	4.8448	4.746364	4.5272	10.05727	7 8872	6.237273	4.1672	6.746364	5.9584	13.16091	9.7568
5200	10.08455	5.756	5.650909	4.672	12.56545	7 6648	6.988182	4.1232	7.650909	6.1608	13.40091	9.4376
5300	9 872727	5.7664	6.380909	4.836	12.68455	7 0544	6.842727	4.2352	8.380909	6.032	10.80818	8 6512
5400	6 891818	5.072	6.749091	4.7952	11.08727	7 3624	8.704545	3.8888	8.749091	5.964	13.48	9.1024
5500	7 594545	4.5272	5.324545	4.7728	12.66818	6.4336	7.582727	4.3128	7.324545	5.3448	11.91273	9.4912
5600	7.99	4.672	5.037273	4.5808	14.09364	7 2944	8.035455	4.4328	7.037273	5.6568	12.74364	8.872
5700	9 801818	4.836	6.817273	4.828	13.03273	6 8616	9.353636	4.3952	8.817273	5.9872	11.95182	8 6136
5800	10.64727	4.7952	5.084545	5.1088	9.01	6 8648	8.827273	4.124	7.084545	6.0592	12.16455	8.7312
5900	8.430909	4.7728	4.911818	4.6528	9.404545	6 9248	8.641818	4.0984	6.911818	6.168	11.36182	8.844
6000	9.46	4.5808	6.095455	5.0832	10.72909	7.012	7.987273	3.7864	8.095455	5.2016	12.42636	8 8672
6100	8 528182	4.828	6.708182	4.5688	10.98909	7.4856	7.626364	4.1768	8.708182	5.5464	13.33545	8 8816
6200	10.87636	5.1088	5.713636	5.2936	13.24364	7.1168	7.18	4.2976	7.713636	5.6472	10.78455	8 9776
6300	11.29182	4.6528	5.131818	4.3152	11.78727	7 2256	7.367273	4.3056	7.131818	6.0456	13.72	9.1224
6400	8.718182	5.0832	5.125455	5.0592	11.30364	7 0224	9.278182	4.4152	7.125455	5.8152	9.998182	8.824
6500	10.65545	4.5688	5.741818	4.3888	12.07545	7 3512	7.312727	4.5232	7.741818	5.8808	12.56909	8 9544
6600	11.09636	5.2936	6.018182	4.948	12.96	6.7632	8.819091	4.3792	8.018182	5.8144	12.32545	9 3264
6700	9.780909	4.3152	6.855455	4.5256	13.40182	7 5272	8.245455	4.14	8.855455	5.2968	14.16	8 6576
6800	8 995455	5.0592	5.801818	5.2776	11.05636	6 3384	7.920909	4.6664	7.801818	5.7168	10.96545	8.728
6900	8.136364	4.3888	5.389091	4.66	8.968182	6.28	7.481818	4.32	7.389091	5.9104	11.24636	7 9296
7000	7.768182	4.948	6.716364	4.0584	11.08273	6.752	7.274545	4.2512	8.716364	5.7368	12.47364	8.7624
7100	9 893636	4.5256	5.290909	5.4976	10.47364	6 8248	7.553636	4.2432	7.290909	5.7624	11.73364	7.7144
7200	11.54091	5.2776	6.854545	5.312	11.43	7.272	7.796364	4.696	8.854545	5.9328	13.91727	8 6792
7300	8.3	4.66	6.553636	3 972	11.78364	6.1976	7.907273	4.2344	8.553636	5.272	12.02091	8.7912
7400	8 336364	4.0584	6.046364	4.0712	8.938182	7 0296	7.76	4.4568	8.046364	6.0128	11.71545	8.1312
7500	11.48273	5.4976	6.738182	4.4672	9.171818	7.1312	9.149091	4.5144	8.738182	5.7	12.70273	8.636
7600	9 973636	5.312	6.040909	5.1944	12.32636	6.828	8.041818	4.148	8.040909	5.6472	12.61818	8 9776
7700	9 267273	3.972	5.970909	5.0712	12.39364	7.4216	6.552727	4.2592	7.970909	5.2784	14.61091	8.484
7800	7.708182	4.0712	5.350909	5.4592	12.19545	6.44	9.252727	4.4648	7.350909	5.42	13.25182	8 6584
7900	10.51636	4.4672	6.270909	5.3432	10.33818	6.756	8.156364	4.8632	8.270909	5.4456	11.54364	8.44

Properties of the USP, provided by the manufacturer “Getzner”

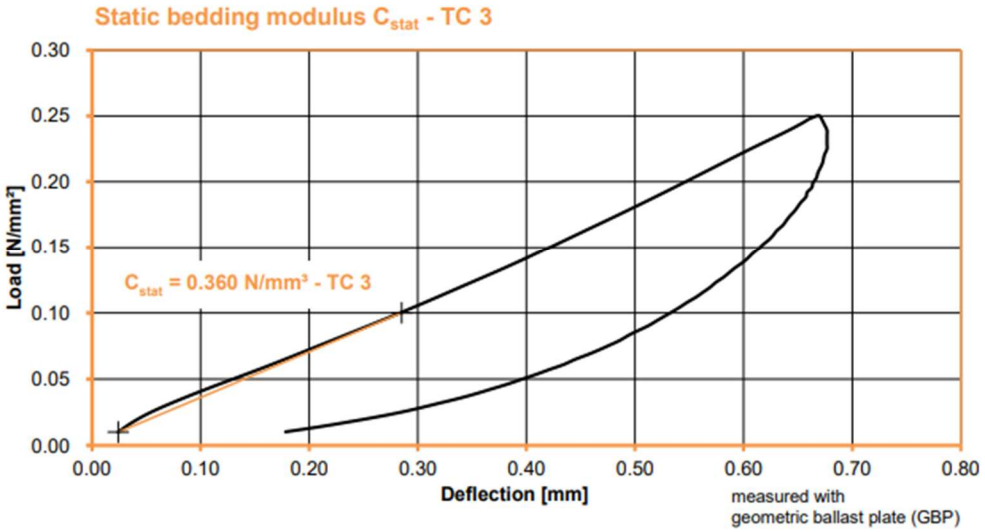
Product key data	
Static bedding modulus	C_{stat} = 0.360 N/mm³ (EN 16730 TC 3) C_{stat} = 0.380 N/mm³ (EN 16730 TC 4)
Main range of application	TC 3: main lines, high speed lines TC 4: heavy haul lines



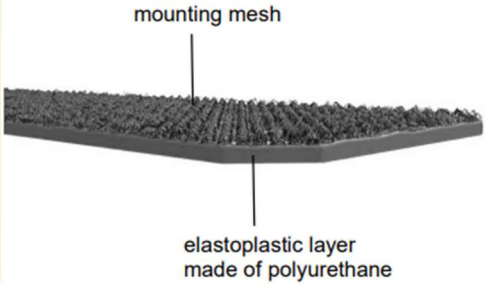
Product properties	
Material	elastoplastic Under Sleeper Pad (USP) made of mixed cellular polyurethane (PUR) elastomer with mounting mesh for concrete sleepers
Colour	resilient layer: black, mounting mesh: black
Thickness	approx. 12 mm including mounting mesh, approx. 7 mm without mounting mesh
Specific mass	approx. 3.0 kg/m²
Fixation on the sleeper	full surface connection provided by the mounting mesh which is directly embedded into the wet concrete during the production process of the sleeper
Bond strength by pull-out of USP on sleeper	σ_{min} = 0.40 N/mm², σ_{av} = 0.50 N/mm² (measured according to EN 16730)
Range of application	– in ballasted track – for ballast protection – track stabilisation and improvement of track quality
Fatigue test of USP on concrete block	test report acc. to EN 16730 no. 3519-2017 of Technical University of Munich (TUM)
Approvals	approvals from numerous railway operators in different countries

Material properties measured according to track category TC 3

Material properties	Characteristic data	Test method	Remark
Static bedding modulus C_{stat} between 0.01 and 0.10 N/mm²	0.360 N/mm³	EN 16730 TC 3	USP on concrete block (approval)
Static bedding modulus C_{stat} between 0.01 and 0.10 N/mm²	0.360 N/mm³	EN 16730 TC 3	USP alone (quality control)
Low frequency dynamic bedding modulus $C_{dyn}(f)$ for determination of track dynamics $C_{dyn,5Hz}$ $C_{dyn,10Hz}$	 0.540 N/mm³ 0.580 N/mm³	 EN 16730 TC 3 EN 16730 TC 3	 USP on concrete block (approval)
Low frequency dynamic bedding modulus $C_{dyn}(f)$ for determination of track dynamics $C_{dyn,5Hz}$ $C_{dyn,10Hz}$	 0.550N/mm³ 0.610 N/mm³	 EN 16730 TC 3 EN 16730 TC 3	 USP alone (quality control)



Product design	
Design	2 layers
Geometry	adjusted to the shape of the sleeper; a distance ≥ 10 mm between the sleeper edge and the used USP is recommended; 2 pieces per sleeper
Delivery form	stacked on palettes



Material properties	Characteristic data	Test method	Remark
Tensile strength σ	2.50 N/mm²	ISO 527-3	
Fatigue test	passed	EN 16730 TC 3	in ballast box test report no. 3519-2017/TUM
Capability for stacked stocking of sleepers with USP max. number of sleepers max. load	 15 pcs. 0.80 N/mm²	 EN 16730 TC 3	
Effect of severe environmental conditions max. increase of C_{stat} σ_{min} σ_{av}	 15% 0.40 N/mm² 0.50 N/mm²	 EN 16730 TC 3	 typical value bond strength by pull-out of USP on sleeper
Resistance to water	excellent resistance	based on DIN 53428	refer to chemical resistance data sheet
Resistance to chemical agents	good resistance	based on DIN 53428	refer to chemical resistance data sheet
Resistance to fire	B2 class E	DIN 4102 EN ISO 11925-2	normally inflammable EN 13501-1
Resistance to hydrocarbons	good resistance	based on DIN 53428	refer to chemical resistance data sheet
Resistance to ozone	excellent resistance	based on DIN 53428	refer to chemical resistance data sheet

DB SLB 3007 EN © Copyright by Getzner Werkstoffe GmbH | 10-2018

All information and data is based on our current knowledge. Further information can be found in the download area of our website. The data can be applied for calculations and as guidelines, are subject to typical manufacturing tolerances and are not guaranteed. We reserve the right to amend the data.

Hand penetrometer, Calculation of the cone resistance

2. Calculation of the cone resistance

Calculation of the cone resistance is as follows:

$$\text{Cone res. (N/cm}^2\text{)} = \frac{\text{Total force (pressure(cm) x spring compression (N/cm)}}{\text{cone surface area (cm}^2\text{)}}$$

With a chosen combination and cone, the factor:

$$\frac{\text{spring compression (N/cm)}}{\text{cone surface area (cm}^2\text{)}}$$

will remain constant (= constant factor).

Only the compression of the spring, indicated by the indicator ring, outside the penetrometer is variable. This compression, calculated together with the constant factor gives the cone resistance. The strength of the spring, as indicated, applies to the maximum compression of 10 cm. Therefore this reduces by a value of 10 cm. E.g. with a spring pressure of 150 N and a cone of 0.25 cm² the constant factor will be 15.0 / 0.25 = 60.0

The constant factors applicable to the various spring-pressures and cones are indicated in the following table:

Cone	0.25 cm²	0.5 cm²
Spring pressure		
50 N (5 kgf)	20	10
100 N (10 kgf)	40	20
150 N (15 kgf)	60	30

Example: Spring pressure 50 N; cone 0.5 cm²; reading 8.2 cm.
Cone resistance = 8.2 x constant factor = 8.2 x 10 = 82 N/cm².

To convert into kg/cm²: 10 N/cm² = 1 kg/cm², than 82 N/cm² = 8.2 kg/cm²

3. Maintenance

☞ **Keep the equipment clean and dry.**

☞ **Wear of the cones is unadvoidable with constant use. The diameters of the cones must be: 0.5 cm² = 8 mm and 0.25 cm² = 5.6 mm.**
A reduction of 5 %, i.e. with a diameter of 7.6 and 5.3 mm, means that the cones must be replaced

☞ **The compression springs must be replaced, if it is suspected that false values are indicated. An indicative check of the springs can be done by pushing the springs to the maximum on a appropriate balance and compare the value with the original values as stated above (resp. 5, 10 and 15 kgf).**

RESEARCH DEGREE THESES - Third Party Editor Declaration Form

ID		**Name (capital letters)**	**RAFAEL KAMALOV**
College	**College of Engineering and Physical Science**		
Programme	**PhD in Civil Engineering**		

Name of Third Party Editor	**Janet Hingley** **Janet's Proofreading Service**
Address	**8 Lord Nelson Drive, Dartmouth, Devon TQ6 9QW.** **Email:** **Telephone:**

I can confirm that the above named was used as a third-party editor for part of my thesis in accordance with the guidelines set out in the Statement on Editorial help for Postgraduate Research Theses and that I have recorded the contribution made in the acknowledgement page of my thesis.

Signature: .... Date: 30/06/2020

Postgraduate Researcher

I can confirm that in acting as a third-party editor for part of the thesis submitted by the above named, I have complied with the Statement of Editorial Help for Postgraduate Research Theses.

Signature: Date:30/06/2020

Third Party Editor

The completed form **must** accompany your thesis when you submit it for examination to the Research Student Administration Team, Registry – Academic Services, University of Birmingham, Edgbaston, Birmingham B15 2TT.

This form will be made available to the examiners. You are advised to keep a copy for yourself.